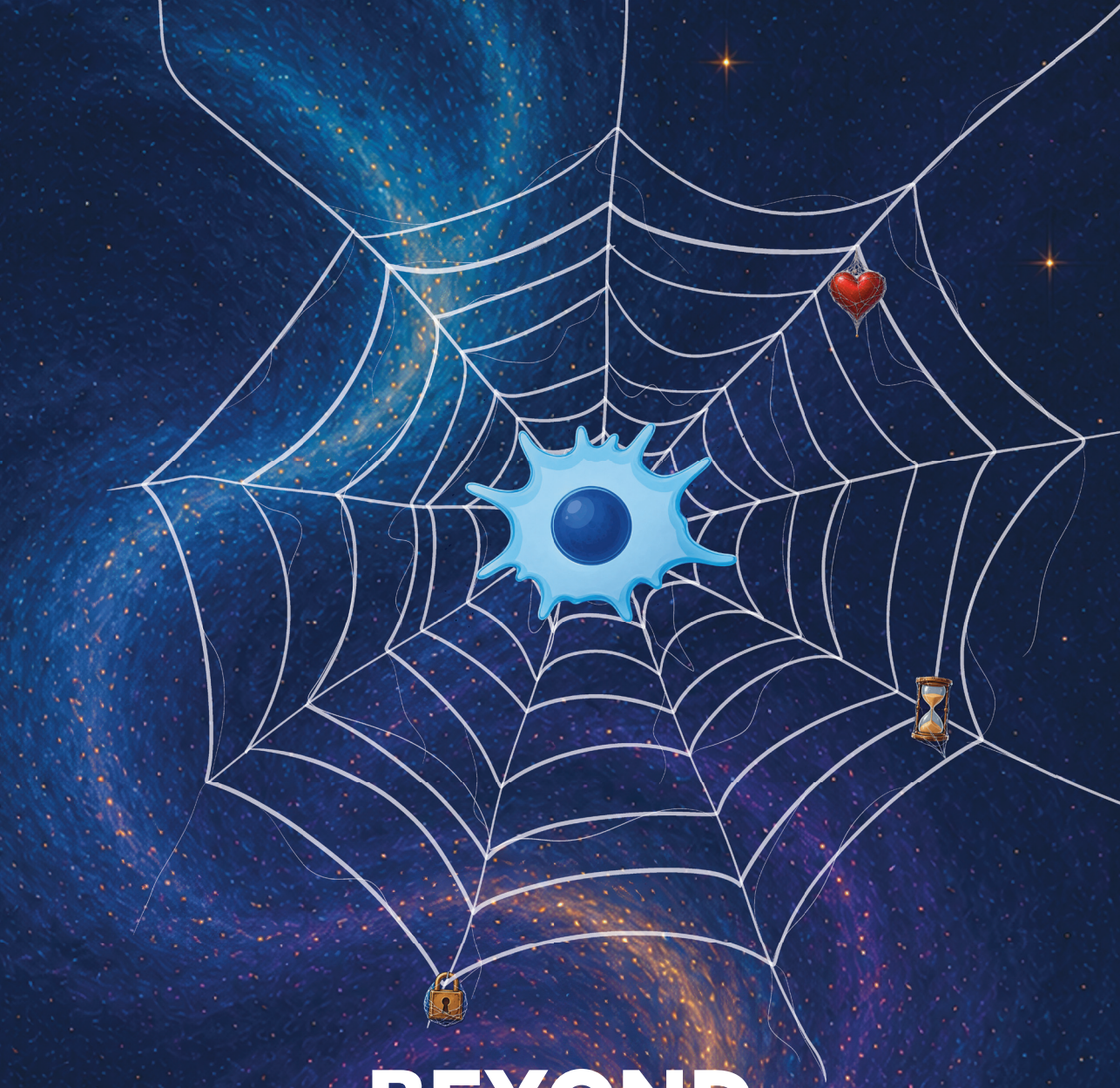

BEYOND BIOENERGETICS

UNVEILING INFLAMMATORY MACROPHAGE IMMUNOMETABOLIC NETWORKS

KARL JORGEN HARBER

Beyond Bioenergetics

Unveiling Inflammatory Macrophage Immunometabolic Networks

Karl J. Harber

The studies described in this thesis were carried out at the department of Molecular Cell Biology and Immunology and the department of Medical Biochemistry, both located at the Amsterdam UMC.

Title:	Beyond Bioenergetics: Unveiling Inflammatory Macrophage Immunometabolic Networks
Author:	Karl J. Harber
Cover:	Stefanie van den Herik | www.herikmedia.nl
Lay-out:	Karl J. Harber
DOI:	https://doi.org/10.5463/thesis.1708
Printed by:	ProefschriftMaken

Printing of this thesis was financially supported by: Vrije Universiteit Amsterdam.



© 2026, Karl J. Harber
All right reserved. No part of this publication may be reproduced, stored or transmitted in any form or by any means, without prior permission from the author. Copyright of the publications remains with the publishers.

VRIJE UNIVERSITEIT

Beyond Bioenergetics

Unveiling Inflammatory Macrophage
Immunometabolic Networks

ACADEMISCH PROEFSCHRIFT

ter verkrijging van de graad Doctor of Philosophy
aan de Vrije Universiteit Amsterdam,
op gezag van de rector magnificus
prof.dr. J.J.G. Geurts,
volgens besluit van de decaan
van de Faculteit der Geneeskunde
in het openbaar te verdedigen
op donderdag 10 september 2026 om 13.45 uur
in de universiteit

door

Karl Jorgen Harber

geboren te Romford, Verenigd Koninkrijk

promotoren:	dr.ir. J. Van den Bossche
	prof.dr. M.P.J. de Winther
	prof.dr. H.E. de Vries
copromotor:	dr. M. van Weeghel
promotiecommissie:	dr. G. Kooij
	prof.dr. C.J.M. de Vries
	prof.dr. I. Bot
	prof.dr. N.P. Riksen
	dr. J. Kroon
	dr. I.P. Foskolou

Table of contents

Chapter 1 **General Introduction** **6**
- Inflammatory diseases
- Inflammation: the driving factor of atherosclerosis
- The origin of immunometabolism
- Methods of unravelling immunometabolic networks
- Validating immunometabolism: lessons from existing therapies
- Immunometabolism as a potential target to control atherosclerosis progression
- Aim and outline of the thesis

Chapter 2 **Let's Enter the Wonderful World of Immunometabolites** **28**
Trends in Endocrinology & Metabolism (2019)

Chapter 3 **Adenine is an Anti-inflammatory Metabolite Found to be More Abundant in M-CSF Over GM-CSF-Differentiated Human Macrophages** **36**
Immunology Letters (2024)

Chapter 4 **D-2-Hydroxyglutarate is an Anti-Inflammatory Immunometabolite that Accumulates in Macrophages After TLR4 Activation** **58**
Biochimica et Biophysica Acta (BBA) - Molecular Basis of Disease (2022)

Chapter 5 **Succinate is an Inflammation-Induced Immunoregulatory Metabolite in Macrophages** **88**
Metabolites (2020)

Chapter 6 **Targeting the ACOD1-Itaconate Axis Stabilizes Atherosclerotic Plaques** **112**
Redox Biology (2024)

Chapter 7 **General Discussion** **150**
- Main outcomes of this thesis
- An evolutionary view on immunometabolism
- Context is key
- Navigating mechanistic heterogeneity in atherogenic mouse models
- The ACOD1-itaconate axis in atherosclerosis
- Future directions: advancing clinical translation of atherosclerosis immunometabolism
- Concluding remarks

Appendices English summary **168**
Nederlandse samenvatting
List of publications
Portfolio of education
Acknowledgments
About the author

1



General Introduction

Inflammatory diseases

Inflammatory diseases make up a substantial portion of global disease burden, causing symptoms that range in severity, of which some contribute to mortality. Inflammatory diseases encompass a wide range of diseases, including autoimmune, allergy, neurodegenerative, cancer, cardiovascular and respiratory diseases; the latter 4 appear in the top-10 causes of death worldwide [1]. An intact immune system is a necessity to fight pathogens and maintain tissue homeostasis. Disrupted, or chronically persistent, inflammatory responses result in substantial accumulation of inflammatory cells and secretion of large quantities of inflammatory mediators in the affected area, which severely damage tissue and cause numerous complications [2, 3]. Immunomodulating drugs have been proven to help dampen inflammatory responses and improve patient outcomes, however this method of systemic immune cell suppression is often accompanied by side effects due to the opportunistic environment for pathogens to emerge [4-6]. Therefore, there is a demand for generating novel treatments that specifically target immune cells associated with the inflammatory disease, whilst retaining the activity and viability of the rest of the immune system [7].

Central to cell activity is metabolism. Immune cells are highly dependent on metabolism to function during immune responses, and cells such as macrophages are no exception [8, 9]. As such, the aim of this thesis is to understand the metabolic networks and metabolites that govern the inflammatory phenotype of macrophages, investigating how intervening with such pathways alters macrophage function, and in turn the progression of inflammatory disease.

The immune system and innate immunity

The immune system is made up of two lines of defence. Innate immunity orchestrates the primary immune response upon pathogen recognition, whilst the adaptive immune response, following activation from the innate immune system, responds with a highly target-specific inflammatory response [10]. Together these fight off incoming pathogens that break through external barriers or remove aberrant cells that drive disease. However, improper regulation of the immune systems can lead to disease initiation and progression.

The innate immune system is a group of mononuclear cells, mainly derived from myeloid progenitor cells in the bone marrow [11, 12]. Monocyte derived macrophages are phagocytic cells capable of engulfing and degrading pathogens or cell debris by means of lysosomal degradation [13, 14]. Degraded protein fragments, called peptides, are subsequently displayed on major histocompatibility complex (MHC) receptors [15]. Cell surface MHC class II receptors present 10 – 15 amino acid long peptide epitopes to

the adaptive immune system, binding to T cells or B cell receptors [16]. The activated T cells proliferate by cellular division to generate specialized T cell, whilst B cells synthesise large quantities of epitope specific antibodies that specifically target pathogens [17, 18]. Granulocytes, other innate immune cells present within the circulation, release enzyme- or toxin- containing lysosomes in inflamed areas that help counter pathogens and cytokines [19]. Within inflammatory diseases, any of these cell types can be involved in the pathogenesis of disease.

Inflammation: the driving factor of atherosclerosis

Atherosclerosis is a chronic inflammatory condition and the most prevalent cause of cardiovascular disease (CVD). It is characterized by an invasion of myeloid and lymphoid immune cells as well as low-density lipoprotein (LDL) deposition in the innermost layer of the blood vessel, the intima, often causing the affected area to grow over time (Figure 1) [20-22]. At initial stages, vessel endothelial cells are activated and upregulate adhesion molecules in response to LDL infiltration; predominantly occurring in regions with disturbed blood flow, for which the risk is heightened in individuals who smoke [23-25]. Circulating innate and adaptive immune cells bind to the vessel wall adhesion molecules and migrate across the endothelial barrier, occasionally bringing LDL molecules with them [23, 26]. LDL molecules within the intimal lining are exposed to oxidative reactions that convert LDL into highly reactive oxidised LDL (oxLDL) molecules [27, 28]. Phagocytosis of oxLDL activates migrated monocytes and macrophages, stimulating the secretion of inflammatory mediating cytokines, such as tumour necrosis factor alpha (TNFα), IL-10, IL-1β and IL-6 [26]. This initial activation of immune cells triggers a vicious cycle: newly activated cells release signals that drive recruitment, migration and activation of additional immune cells, whilst the growing accumulation of oxLDL further fuels this inflammatory response, driving plaque progression.

It is widely accepted that macrophages heavily burdened with phagocytosed oxLDL, named foam cells, are key drivers of atherosclerosis development [29, 30]. Foam cells in mice mediate plaque progression in an inflammatory-independent manner however, expressing inflammatory genes at a substantially lower level than non-foamy macrophages [31]. Whether this is the same circumstance in human plaques is still under scrutiny [32-35]. Regardless, foam cells experience alternative challenges in the form of oxidative stress and cellular hypertrophy, rendering them prone to cell death [36, 37]. Apoptosis, an organised and regulated method of cell death, often triggers minimal inflammation. This is because the intracellular contents are contained within an intact cell membrane, preventing their exposure to the extracellular environment [38]. Failure to complete apoptosis, clear apoptotic cells or occurrence of necrosis, is a subsequent strain on atherosclerosis progression [26]. Continuous build-up of cell debris leads to the generation of a necrotic core, which is exceptionally challenging for macrophages

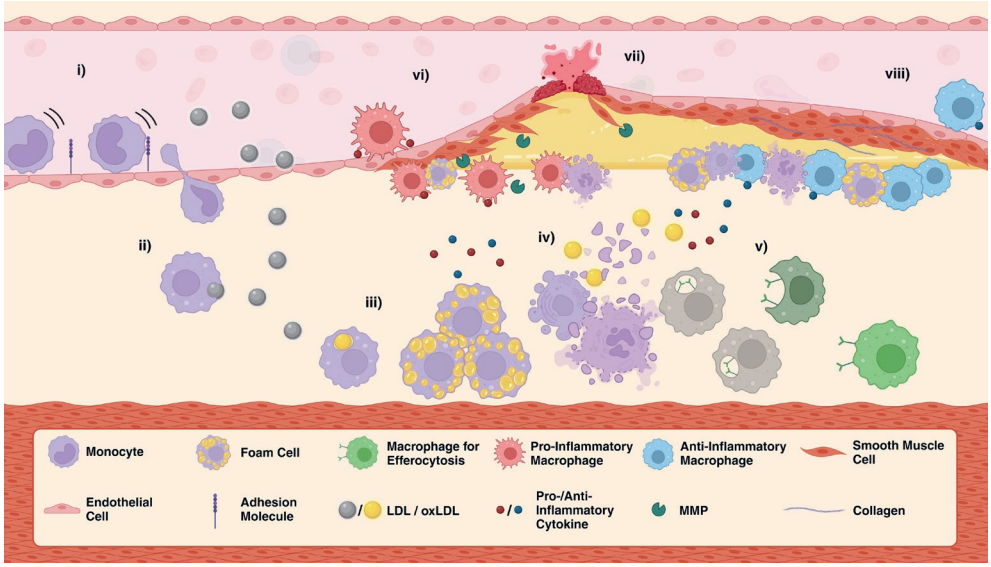

Figure 1. Myeloid driven atherosclerosis progression. Monocytes are key players in the initiation and development of atherosclerosis, up to the point of plaque rupture. i) Monocytes roll along the endothelial wall of vessels until encountering adhesion molecules, such as ICAM and VCAM, which facilitate transendothelial migration of monocytes into the vessel intimal lining. LDL particles migrate into the vessel wall which are then ii) phagocytosed by monocytes and subsequently iii) oxidised to form oxLDL. Monocytes containing oxLDL, iv) otherwise known as foam cells, fail to undergo apoptosis in a controlled manner with an intact membrane, releasing oxLDL back into the vessel wall as well as an array of proteins and cytokines. v) Expression of efferocytosis receptors on migrated macrophages are internalised in the plaque in response to oxLDL particles and release pro-inflammatory cytokines, preventing the clearing of cell debris. Cytokines released during failed apoptosis promote the migration of additional monocytes and subsequently differentiate into vi) pro-inflammatory macrophages. These macrophages secrete MMPs that degrade the extracellular matrix around smooth muscle cells of the plaques fibrous cap, making it thinner and more prone to vii) rupture. Encouraging the recruitment and migration of viii) anti-inflammatory macrophages promotes fibrous cap thickening and thus generates atherosclerotic plaques that are less rupture prone.

to degrade, and pushes plaques into a vulnerable state whereby the smooth muscle cell (SMC) fibrous cap thins [37]. Ultimately, vulnerable plaques are prone to vessel rupture and subsequent thrombogenesis, resulting in myocardial infarctions and strokes.

Some plaques, depending on the balance of macrophage subsets, are slower in growth and at a lower risk of rupture due to maintaining a thick fibrous cap. Independently of changes in plaque size, fibrous cap integrity can undergo modification by local clonal expansion of SMCs or secretion of matrix metalloproteinases (MMPs) [39, 40]. Whilst it is still under scrutiny whether SMC clonal expansion occurs in human atheromas, MMP-driven fibrous cap degradation is a clear determining factor of plaque instability [40, 41]. Secretion of MMPs by the heterogenic macrophage population within the plaque degrades extracellular matrix proteins, reducing fibrous cap thickness [42]. Although macrophages expressing either pro- or anti-inflammatory markers both contribute

to MMP secretion, anti-inflammatory macrophages orchestrate tissue repair and remodelling and therefore are more beneficial to plaque stability at later stages and may even facilitate plaque regression [42-46]. Considering that macrophages are present at all stages of plaque progression, skewing the balance of the heterogeneous macrophage population within plaques towards an anti-inflammatory profile would likely support the development of more stable plaques [47]. Unfortunately, macrophages fail to switch from a pro-inflammatory state by anti-inflammatory mediator stimulation, highlighting the unmet need to develop an alternative method to steer pro-inflammatory macrophages towards an anti-inflammatory phenotype [48].

The origin of immunometabolism

The production of energy is at the core of survival; without it, organisms from a unicellular level to the largest animals on earth would cease to exist. Yet, even during favourable conditions, external factors threaten organism survival, making it essential to have an arsenal of protective mechanisms. The demand for vital survival mechanisms resulted in the emergence of metabolism and the immune system billions of years ago, with adaptive immunity likely existing 450 million years ago [49, 50]. The metabolic and immune systems have therefore been long standing partners in the history of the biotic era, and it is not implausible that one system could influence the other [50]. We only assigned a word to this phenomenon in the last 10 years; immunometabolism. On a fundamental level, this field outlines the profound metabolic changes that occur in immune cells, that drive immune cell function and activity [51].

Before the term immunometabolism was established, Otto Heinrich Warburg demonstrated that starvation of tumour cells from oxygen and glucose, thereby limiting the cell's capability to undergo respiration and fermentation, affected tumour cell viability [52]. Through this, Warburg discovered that tumour cells have a preference for fermentation and only switch to respiration upon glucose deprivation. In other words, cells rewire their basic metabolic flux from the highly efficient oxidative phosphorylation (OXPHOS) to a dependence on anaerobic glycolysis, generating ATP at a faster, yet less efficient manner. By switching to faster ATP generation, tumour cells generate sufficient energy to fuel the production of biosynthetic precursors required for rapid proliferation [53]. This phenomenon is named the Warburg effect [54].

2-Hydroxyglutarate and the establishment of the term immunometabolite

More recently, the term oncometabolite described any metabolite that accumulated in malignant cells, as a result of genetic mutations, whose presence supported tumour growth [55]. The first oncometabolite to be reported, D-2-hydroxyglutarate (D-2HG, also known as R-2HG), forms as a result of mutations in the enzymes isocitrate dehydrogenase

1 and 2 (IDH1 and IDH2), with α-ketoglutarate as their substrate [56, 57]. These mutations are often found in human gliomas and acute myeloid leukaemia (AML). D-2HG is a competitive inhibitor of dioxygenases, preventing the substrate α-ketoglutarate from binding. By inhibiting dioxygenase activity, D-2HG alters DNA and histone methylation in these malignant cells, supporting tumour development [58, 59].

Unlike D-2HG, the stereoisomer L-2-hydroxyglutarate (L-2HG, also known as S-2HG) is not a product of genetic mutations and is not described as an oncometabolite. L-2HG is detectable in healthy individuals, and is produced by enzymes MDH1, MDH2 and LDHA in hypoxic conditions [60]. L-2HG accumulates In CD8+ T cells in response to T-cell receptor binding by stabilisation of the transcriptional regulator hypoxia-inducible factor 1 alpha (HIF-1α) which in turn induces LDHA [61]. Similarly, L-2HG accumulation in CD8+ T cells alters DNA and histone methylation and consequently steer CD8+ T cell fate towards an enhanced proliferative and anti-tumoral state. This observation that L-2HG accumulation could reprogram T cell function established the first use of the term immunometabolite; the term has since expanded to encompass any endogenous metabolite that functions as a signalling molecule that influences the immune response [61].

The underlying mechanisms that govern metabolic rewiring from OXPHOS to anaerobic glycolysis is highly present during macrophage inflammation. Activity of the TCA cycle enzymes IDH and succinate dehydrogenase (SDH) are suppressed during inflammation (Figure 2) [62]. Suppression of SDH, complex 2 of the electron transport chain, slows OXPHOS and therefore macrophages switch to alternative methods of generating energy [63]. Macrophages undergoing inflammatory stimulation shift their energy production towards glycolysis to meet energetic demands. This metabolic strategy, however, is problematic in the context of inflammatory diseases since it commits the macrophage to a highly glycolytic state, restricting its ability to transition towards an anti-inflammatory phenotype [48]. Inflammatory diseases such as atherosclerosis consist of an imbalance of macrophage phenotypes in the lesion area, in favour of pro-inflammatory macrophages, driving this vicious cycle that exacerbate the disease as mentioned earlier [47]. Phenotypically switching macrophages in this setting is key to dampening the progression of this disease. Elucidating the immune-modulating properties of metabolites from central metabolism pathways glycolysis, OXPHOS and the TCA cycle, as well as surrounding metabolic pathways, such as beta oxidation, fatty acid metabolism and the pentose phosphate pathway, has consequently become a major research focus [64-67]. Full comprehension of the modulating properties of metabolic components within these pathways, could reveal novel methods to control the activation or inactivation of aberrant immune cells that drive inflammatory diseases, without the need for drugs that come with severe side effects, such as immunotherapies that deplete the patients' immune cells.

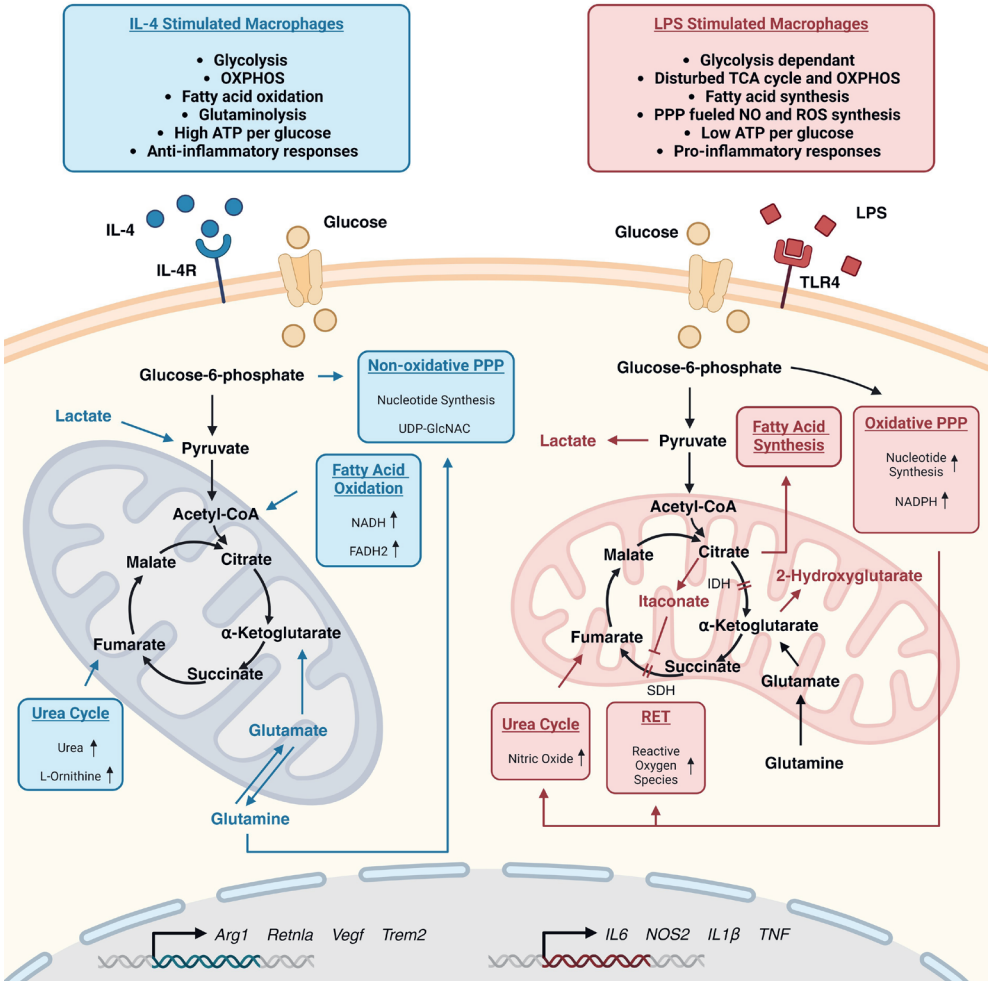

Figure 2. Intracellular metabolic changes in pro- and anti-inflammatory macrophages. Myeloid driven atherosclerosis progression. Macrophages stimulated with either IL-4 (left) or lipopolysaccharide (LPS) (right) and their subsequent metabolic changes. Altered abundance of metabolites in core metabolism is highlighted in coloured text, whilst changes to specific metabolic pathways are depicted in coloured boxes. Genes are in italic text. Breaks in metabolic flux of the TCA cycle are shown by two red lines, where the effected enzymes are labelled.

Succinate is context dependently pro- or anti-inflammatory

One of the most studied immunometabolites in the context of immune-modulation and inflammatory diseases is succinate, the substrate of the TCA cycle enzyme SDH [68-71]. Upon TLR4 activation, macrophages metabolise large quantities of glucose and glutamine into downstream intermediates of glycolysis and the TCA cycle. During inflammation, SDH is inhibited, resulting in diminished oxidation of succinate into fumarate and an accumulation of succinate [72, 73]. Simultaneous suppression of IDH in

inflammatory macrophages prevents the TCA cycle generation of succinate, indicating that succinate's continued accumulation is derived from anaplerotic processes such as glutaminolysis and the γ-aminobutyric acid (GABA) shunt [62, 70]. The extracellular G protein-coupled receptor (GPCR) succinate receptor 1 (SUCNR1) binds succinate which activates transcription factor HIF-1α, resulting in secretion of pro-inflammatory cytokine IL-1β [68, 74]. Additionally, succinate drives the generation of mitochondrial reactive oxygen species (ROS) and is instrumental to the ensuing inflammatory response. These signalling pathways highlight the pro-inflammatory nature of succinate accumulation in macrophages, however succinate is also able to drive anti-inflammatory responses in the context of obesity, cancer and neuroinflammation [71, 75, 76]. Macrophage SUCNR1 deficiency in obesity, which is associated with chronic inflammation, leads to a heightened inflammatory response, suggesting an anti-inflammatory role for the succinate-SUCNR1 axis. Whilst this anti-inflammatory response is also observed in macrophages from lean patients, obesity in patients prevents this anti-inflammatory effect of succinate [75]. Similar effects of the succinate-SUCNR1 axis occurs in neural stem cells, where binding of SUCNR1 activates production and subsequent release of prostaglandin E2, dampening neighbouring macrophage inflammation [76]. Cancer cell-derived succinate released into the tumour microenvironment also suppresses the anti-tumour activity of macrophages, promoting their tumour associated macrophage phenotype [71]. These observations highlight the complexity of immunometabolites and how their role in immunomodulation is highly context dependent.

Itaconate is a potent anti-inflammatory immunometabolite

In addition to immunometabolites succinate and 2-hydroxyglutarate, the metabolite itaconate was revealed to be among the most accumulated metabolites in inflammatory macrophages [72]. In fact, itaconate was shown to be a partial inhibitor of SDH, one of the canonical mechanisms of metabolic rewiring that occur during macrophage stimulation [72]. The enzyme ACOD1 (also known as IRG1), encoded by *Acod1*, is the only known synthesizer of itaconate, and upon deletion, inflammatory macrophages contain only a negligible amount of measurable itaconate [72, 77]. Consequently, the metabolic rewiring of *Acod1* deficient macrophages is unlike that of wild type (WT) inflammatory macrophages, due to the lack of itaconate-driven SDH suppression [72, 73]. Succinate fails to accumulate in these cells, whilst succeeding TCA cycle intermediates fumarate and malate accumulate to a higher degree compared with WT macrophages. These macrophages display an enhanced inflammatory response in the absence of succinate accumulation, regardless of succinate being described as a pro-inflammatory immunometabolite in certain macrophage inflammatory settings.

Conversely, when itaconate is added exogenously to macrophages prior to initiating an inflammatory response, succinate accumulates to a greater extent than without

exogenous itaconate, resulting in macrophages with significantly less inflammatory potential [72, 78, 79]. These findings establish itaconate's dual role as both an integral component of canonical metabolic rewiring observed in inflammatory macrophages and as a potent anti-inflammatory immunometabolite.

Additional investigation into the mechanisms behind itaconates' anti-inflammatory effects shows that exogenous itaconate reduces inflammatory gene expression and secretion of pro-inflammatory mediators IL-6, TNFα, IL-12p70 and IL-1β [72, 80, 81]. Derivatives of itaconate that contain structural modifications to allow for passive transport of itaconate across the cell surface have been used to demonstrate this suppression. Dimethyl itaconate (DMI), a derivative of itaconate that suppresses ROS generation, reduces ischemic reperfusion injury when administered intravenously during ischemia [72]. DMI has electrophilic properties that are unlike that of natural itaconate, causing Michael reactions that induce anti-inflammatory signalling through the IκBζ-ATF3 axis [80]. 4-octyl itaconate (4-OI), another itaconate derivative, has lower electrophilic properties; to a similar degree as present in natural itaconate. 4-OI induces anti-inflammatory effects through nuclear factor erythroid 2-related factor 2 (NRF2) and Kelch-like ECH-associated protein 1 (KEAP1) signalling pathways by means of itaconate driven alkylation of cysteine residues [81]. An analogue of 4-OI, itaconate-alkyne (ITalk), identified 1926 proteins in inflammatory macrophages that are the target of itaconation, a post-translational modification (PTM) carried out by itaconate-derived Michael reactions [82]. How itaconation affects activity of these proteins, however, still requires investigation. A series of comparative experiments with itaconate derivatives highlighted that the signalling induced in inflammatory macrophages by itaconate derivates are a result of the derivatives' structural modifications; unmodified itaconate fails to induce responses through the same NRF2 and ATF3 signalling pathways [83]. Unmodified itaconate instead promotes secretion of interferon beta (IFN-β) and suppresses mature IL-1β secretion. This stark difference in signalling pathways between endogenous itaconate and its derivatives emphasises the importance of model selection, particularly if the fundamental mechanisms of immunometabolism are to be fully understood.

Methods of unravelling immunometabolic networks

Metabolism is a vastly intertwined network of pathways where a single enzyme can facilitate singular or bi-directional reactions, as well as catalysing multiple different reactions that can take place in both intracellular and extracellular compartments. Consequently, understanding the entire metabolic state of a cell requires multiple techniques that measure enzymatic activity, metabolic flux and metabolite content. Fortunately, we are now in an era of scientific research where complex techniques that yield large quantities of data are at our disposal, giving us access to methods beyond simple metabolic assays.

Genomics and transcriptomics

The term omics describes the technique of measuring the entire contents of a cell or extracellular fluid in the context of a specific compartment. At the most fundamental level, the genome defines a cells metabolic and immune potential. Genomics, which maps out the complete DNA sequence, is essential for identifying genetic mutations that could permanently alter a cells metabolic wiring, such as the mutations found in IDH1 and IDH2 described earlier [56, 57, 84]. DNA is isolated from a sample, fragmented into readable sizes, amplified by polymerase chain reaction to increase the signal to a readable level, and then finally sequenced [85]. This however, does not provide information on whether a gene is active within the sample. To determine how a gene or genetic mutation translates into cellular function, other complimentary omics approaches can be used [86]. Transcriptomics measures all RNA transcripts in a sample to provide an overview of which genes are actively expressed at a specific time point. The process of transcriptomics is similar to genomics, however the isolated RNA fraction must be first be enriched for mRNA and then stabilised by forming complimentary DNA with reverse transcriptase [87]. Transcriptomics is essential for observing the upregulation of genes that encode key metabolic enzymes, receptors and transporters during macrophage activation. However, changes in gene expression do not always directly correlate with protein abundance or activity, making it crucial to observe changes within a cell at a protein level.

Proteomics, metabolomics and lipidomics

Proteomics is a mass spectrometry technique that can measure the full protein content of a sample through degradation into peptides; peptide abundance is measured, and their sequence is identified [88, 89]. Since transcription-based techniques provide genetic expression that doesn't always directly translate into protein content, proteomics is a highly informative method of measuring enzymes, better illustrating the current cellular metabolic status. Moreover, when protein lysates are enriched for proteins with PTMs, proteomics has the potential to detect PTMs such as phosphorylation, glycosylation and ubiquitination, which have significant consequences on enzyme activity or function [90, 91]. In contrast to the standard proteomics approach, native proteomics offers an alternative, more complex technique, which extracts and measures proteins in their intact state, preserving non-covalent protein complexes [92]. This method not only preserves information about protein-protein interactions but is also essential for determining which proteins are being targeted by metabolites or drugs within the cell.

Metabolomics and lipidomics refers to the identification of the entire metabolome and lipidome, respectively. Such data can reveal shifts in the metabolome and lipidome during different stages of inflammatory activation [93]. This technique forms the basis of identifying new immunometabolite candidates that may facilitate inflammatory

responses. Recent developments also provide these omics approaches at a single cell level, an application that is becoming more relevant due to the heterogenic nature of immune cell environments in inflammatory diseases [66]. However, the resulting data of these omics approaches are static and only provide information at a single timepoint. Unlike secretion of cytokines in *in vitro* experiments that often accumulate and are not reabsorbed, the proteome, metabolome and lipidome of cells are frequently changing, therefore, taking a static reading of these compartments may not be the most informative to fully observe the metabolic activity of a cell. Whilst it is possible to make samples with multiple time points to generate kinetic data, this quickly becomes expensive and thus finding an alternative technique is a better option.

Tracer-based metabolomics, fluxomics and extracellular flux

Tracer-based metabolomics and fluxomics can identify which energy sources a cell is most dependent on to generate specific compounds and highlights the direction and magnitude of metabolic activity within a cell, respectively. Stable isotope tracers like glucose, glutamine or oleic acid, most frequently labelled with either 13C or 15N, replace their unlabelled counterparts in cell cultures, or are administered through oral and venous methods in animal models [94, 95]. Extracellular and intracellular metabolic reactions involving these labelled compounds result in the synthesis of downstream metabolites and lipids with specific labelling patterns, from which metabolic flux can be deduced [96]. The extent of metabolite labelling, or the fractional contribution of each isotope, measured from tracer-based metabolomics, reflects metabolic pathway activity. Combining this metabolic information, with genomic, transcriptomic or proteomic data allows direct calculation of metabolic pathway rates occurring within the cell [97]. The accuracy of fluxomics however, is predicated on the assumption that metabolic flux is at a constant rate, and therefore deviations from this steady state can lead to misinterpretations of the cellular metabolic map [96].

Where fluxomics is limited by its inability to quantify metabolic flux in cells with fluctuating metabolic activity, extracellular flux assays prevail. Extracellular flux analysis provides real-time measurements of OXPHOS and glycolysis in live cells by measuring changes in dissolved oxygen and free protons within the cell culture medium, respectively [98]. Through the use of various compounds such as FCCP, oligomycin and rotenone/antimycin A, different electron transport chain complexes are inhibited, or the mitochondrial membrane is uncoupled, resulting in measurable parameters of mitochondrial function and ATP production [48, 99]. Similarly, mitochondrial ATP synthase inhibitors and glucose starvation are used to test the boundaries of glycolysis. This technique is ideal for understanding how cellular interventions such as genetic deletion, enzyme inhibition or compound addition affects the basic metabolic functions of cells and thus identify the modulating properties of immunometabolites.

Validating immunometabolism: lessons from existing therapies

Whilst the topic of immunometabolism has only been coined in the last decade, there are existing therapies available to treat inflammatory diseases that are directed against components of cellular metabolism. Through modulation of key metabolic pathways, these therapies ameliorate aberrant immune responses in inflammatory diseases, thereby alleviating the progression of the disease. These treatments emphasize the therapeutic potential of developing novel drugs that target immunometabolites and their associated enzymes or transporters to combat inflammatory diseases.

Metformin improves glucose uptake and suppresses gluconeogenesis

Diabetes mellitus is a metabolic disease that diminishes glucose homeostasis due to a lowered, or absent, production and release of insulin by pancreatic β-cells as well as tissue desensitization to insulin [100]. The biguanide metformin is the first treatment prescribed to type 2 diabetic patients. Metformin is transported into liver cells via solute carrier family 22 (SLC22) transporters and reduces the availability of gluconeogenic substrates as well as increasing the translocation of glucose membrane transporters, facilitating increased rates of glucose transport and glycolysis [101, 102]. Additionally, metformin inhibits complex I of the mitochondrial electron transport chain, which suppresses ATP synthesizing pathways whilst increasing AMP [103]. Through amplified AMP:ATP ratios, the intracellular energy sensor 5' AMP-activated protein kinase (AMPK) is activated, leading to a cascade of anti-inflammatory signals that result in lower IL-6, TNFα and IL-1β cytokine synthesis. Moreover, lower mitochondrial complex I activity decreases the production of mitochondrial ROS, a highly reactive oxidant that attributes to oxidative stress and inflammatory responses. The anti-inflammatory nature of metformin led to its application in treating other inflammatory diseases. Interestingly, diabetic patients who receive metformin treatment are at a lower risk of developing cancer than patients on other anti-diabetics, as it modifies the immune status of the tumour microenvironment as well as promoting tumour immunogenicity [104]. In fact, the use of metformin as an anti-inflammatory treatment has been studied in other inflammatory diseases such as neurodegenerative diseases and cardiovascular diseases, however with contrasting results, requiring deeper mechanistic insight. Metformin is therefore a leading example of the broad therapeutic potential of metabolic targeted treatments that alter the immune response.

DMF is a TCA cycle derivative that induces anti-inflammatory signalling

The drug dimethyl fumarate (DMF), originally prescribed for the treatment of the autoimmune disorder psoriasis and now used to treat relapsing-remitting multiple sclerosis (RRMS), is a structurally modified, cell-permeable derivative of fumarate [105].

DMF can be intracellularly converted to fumarate and subsequently fuel the TCA cycle [106]. DMF, and its metabolised derivative monomethyl fumarate (MMF), activate the anti-inflammatory mediator and redox sensor NRF2. By means of post-translational succination of cysteine residue 151 on the NRF2 inhibitor KEAP1, NRF2 becomes available to translocate into the nucleus for subsequent translation of antioxidant genes [107]. DMF similarly modifies cysteine residues on NF-κB pathway proteins, such as A20 and IKKβ. As such, translocation of NF-κB subunits p65 and p52 to the nucleus and formation of the NF-κB complex is blocked, suppressing synthesis of pro-inflammatory cytokine IL-6 in macrophages [108-110]. An additional mechanism that has been observed is DMF's capability to bind glutathione (GSH), a thiol that acts as an antioxidant, also via cysteine residues, and subsequently upregulates the anti-inflammatory enzyme heme oxygenase 1 (HO-1) [111]. These studies together show how an immunometabolite such as DMF, whilst once thought to replenish intracellular fumarate levels to restore TCA cycle activity, can also possess other immunomodulatory mechanisms by interacting with and modifying proteins that are essential to elicit an immune response.

Immunometabolism as a potential target to control atherosclerosis progression

Despite the clinical success of plasma cholesterol lowering statins to reduce CVD-related events, there is still a portion of patients who suffer from residual inflammatory risk and thus still experience life threatening CVD events [112]. The CANTOS trial enrolled patients within this residual inflammatory risk group and were treated with canakinumab, an anti-IL-1β antibody, which displayed marked decrease in CVD events when compared to placebo-treated patients [5]. Whilst this provides a clear indication that anti-inflammatory treatment will benefit this group of patients, immunodeficiency in these patients caused an increase in sepsis and fatal infection [5]. An alternative method for controlling innate immune responses is therefore required. As such, harnessing macrophage polarisation through immunometabolic interventions may be the key to gaining back control of the plaque microenvironment. Currently, there are still very limited studies that elucidate the immunometabolic interactions of innate immune cells in the context of atherosclerosis, however the few that exist support the need to recognise immunometabolism as a relevant target.

Evidence from both mouse and human studies has shown that monocytes are already primed by an array of stimuli that exist in the systemic environment of atherosclerotic individuals before migrating to the plaque [113, 114]. In humans, this leads to TLR4 stimulated monocytes secreting increased levels of IL-6 and IL-1β, upregulating glycolysis and OXPHOS activity and subsequently generating more mitochondrial ROS when compared to monocytes from healthy individuals. Once migrated into the atheroma, these monocytes differentiate into a heterogeneous population of macrophages, which together create a highly glycolytic environment when compared to healthy vessels,

resulting in large accumulations of downstream glycolysis and TCA cycle intermediates [115]. In fact, human carotid atherosclerotic plaques can be distinguished between stable and high-risk plaques solely based on their metabolic profile, expressing increased glycolysis and amino acid metabolism, as well as decreased fatty acid oxidation [116]. Suppression of glucose uptake by GLUT1 inhibitors prevents this high metabolic activity and expansion of macrophage progenitors as well as atherosclerosis progression [113]. This provides evidence that modulating cellular metabolism in myeloid cells can indeed slow atherogenesis. Furthermore, the fluctuating abundance of central metabolism intermediates in inflammatory macrophages and atherosclerotic plaques offers a group of potential immunomodulating metabolic candidates worth exploring. Altogether, the recent advances in immunometabolism and atherosclerosis paint a positive outlook on implementation of immunometabolic targeted therapy for improved atherosclerosis outcome [117-119].

Aim and outline of the thesis

This thesis explores how shifts in immunometabolite profiles during macrophage inflammation shape their inflammatory response and investigates their potential to be implemented in inflammatory diseases, with a focus on atherosclerosis. Knowledge on the immunomodulating properties of metabolites has recently grown, but there has been a failure to translate this into a cardiovascular setting. Consequently, this thesis aims to place both established and novel immunometabolites in the context of macrophage inflammation and atherosclerosis.

The study of metabolism and its position in driving inflammatory diseases has been growing exponentially for the last decade. Investigation into the metabolism of malignant and healthy cells in the tumour microenvironment defined these immunomodulating metabolites as oncometabolites. The field has, however, expanded into the immunomodulating effects of metabolites in the context of non-cancer inflammatory diseases. **Chapter 2** presents the definition of what constitutes as an immunometabolite and offers a background in some of the most studied immunometabolites and their influence on the immune system. By providing a clear explanation as to what an immunometabolite is and how continued research in immunometabolism could yield novel therapeutic value, we put the term immunometabolite on the map and aim to increase interest into this developing field.

Combining multiple omics techniques provides a more complete picture of the current metabolic state of inflammatory macrophages, which is highlighted in **chapters 3 and 4.** Differentiation of monocytes into macrophages can occur through binding of ubiquitous M-CSF or inflammation secreted GM-CSF. Whilst both cytokines can contribute to the production of inflammatory macrophages, GM-CSF has been implicated in the

generation and development of numerous inflammatory diseases. In **chapter 3** we use a metabolomics approach to characterize immunometabolites that are differentially regulated in M-CSF or GM-CSF-differentiated human macrophages. We identify adenine as an immunometabolite that accumulates in M-CSF-differentiated macrophages and delve into its immunomodulatory properties. Moreover, we investigate how adenine affects inflammation-induced macrophage rewiring and energetics through an extracellular flux approach. In **chapter 4** we similarly use metabolomics to identify D-2HG as an immunometabolite regulated in both mouse and human inflammatory macrophages. From this, we outlined changes in metabolic enzyme expression, on a transcriptomic level, that could lead to the accumulation of D-2HG, followed by functional testing to explore D-2HG's immunomodulatory properties. Finally, we implemented D-2HG into a mouse model of systemic inflammation to validate these observations.

Succinate is one of the most well described immunometabolites. Nonetheless, extensive research on succinate-based regulation of macrophage responses led to a discrepancy in how binding its extracellular receptor SUCNR1 affects the inflammatory response. A handful of papers claimed a pro-inflammatory role of succinate through binding of SUCNR1 by increased activity of HIF-1α followed by a secretion of IL-1β, whilst other research groups showed SUCNR1 deficiency also led to a pro-inflammatory phenotype. In **chapter 5** we focus on clarifying the role of succinate in macrophage inflammation. We use multiple tools that affect regulation of the succinate-SUCNR1 axis, gaining insight into how this axis controls inflammatory responses in macrophages. In this chapter we use a combination of *SUCNR1*$^{-/-}$ and *SUCNR1*$^{+/+}$ macrophages, structurally modified diethyl succinate for passive cellular transport, dimethyl malonate (DMM) as a SDH inhibitor and disodium succinate, which releases the non-permeable and natural form of succinate when dissolved.

Currently there are very few research articles that focus on the potential of immunometabolism-based therapies in treating atherosclerosis. Altering the metabolic status of macrophages within the plaque environment may not only alter their inflammatory status but could also ameliorate macrophages' lipid handling and metabolizing capabilities. In **chapter 6** we investigate the role of the anti-inflammatory immunometabolite itaconate, and its synthesizing enzyme ACOD1, in the development of atherosclerosis. Plaque physiology and blood immune cell populations were reported in atherosclerotic mice transplanted with *Acod1* deficient bone marrow. From this, we use a multi-omics approach to reveal how macrophages deficient in *Acod1* have modified lipid flux and content, as well as changes in apoptotic and necrotic induction. In this chapter we highlight immunometabolic pathways that control the development of atherosclerosis.

Finally, in **chapter 7** we discuss how the results of this thesis impact the field of immunometabolism by placing our findings in the context of current literature. We also

provide insight into the future applications of immunometabolism, particularly in the context of macrophage inflammation and how targeting macrophage immunometabolic pathways may be a promising avenue in the treatment of atherosclerosis.

References

1. Organisation, W.H., Global Health Estimates 2020: Deaths by Cause, Age, Sex, by Country and by Region, 2000-2019. 2020.
2. Pahwa, R., A. Goyal, and I. Jialal, Chronic Inflammation. In: StatPearls [Internet]. Treasure Island (FL): StatPearls Publishing, 2023.
3. Chen, L., et al., Inflammatory responses and inflammation-associated diseases in organs. Oncotarget, 2017. 9(6).
4. Waldman, A.D., J.M. Fritz, and M.J. Lenardo, A guide to cancer immunotherapy: from T cell basic science to clinical practice. Nat Rev Immunol, 2020. 20(11): p. 651-668.
5. Ridker, P.M., et al., Antiinflammatory Therapy with Canakinumab for Atherosclerotic Disease. N Engl J Med, 2017. 377(12): p. 1119-1131.
6. Song, C., et al., Immunotherapy for Alzheimer's disease: targeting beta-amyloid and beyond. Transl Neurodegener, 2022. 11(1): p. 18.
7. Palsson-McDermott, E.M. and L.A.J. O'Neill, Targeting immunometabolism as an anti-inflammatory strategy. Cell Res, 2020. 30(4): p. 300-314.
8. Jung, J., H. Zeng, and T. Horng, Metabolism as a guiding force for immunity. Nat Cell Biol, 2019. 21(1): p. 85-93.
9. Ganeshan, K. and A. Chawla, Metabolic regulation of immune responses. Annu Rev Immunol, 2014. 32: p. 609-34.
10. Marshall, J.S., et al., An introduction to immunology and immunopathology. Allergy Asthma Clin Immunol, 2018. 14(Suppl 2): p. 49.
11. Gasteiger, G., et al., Cellular Innate Immunity: An Old Game with New Players. J Innate Immun, 2017. 9(2): p. 111-125.
12. Janeway, C.A., Jr. and R. Medzhitov, Innate immune recognition. Annu Rev Immunol, 2002. 20: p. 197-216.
13. Stuart, L.M. and R.A. Ezekowitz, Phagocytosis: elegant complexity. Immunity, 2005. 22(5): p. 539-50.
14. Uribe-Querol, E. and C. Rosales, Phagocytosis: Our Current Understanding of a Universal Biological Process. Front Immunol, 2020. 11: p. 1066.
15. Rock, K.L., E. Reits, and J. Neefjes, Present Yourself! By MHC Class I and MHC Class II Molecules. Trends Immunol, 2016. 37(11): p. 724-737.
16. Pishesha, N., T.J. Harmand, and H.L. Ploegh, A guide to antigen processing and presentation. Nat Rev Immunol, 2022. 22(12): p. 751-764.
17. Daniels, M.A. and E. Teixeiro, TCR Signaling in T Cell Memory. Front Immunol, 2015. 6: p. 617.
18. Kwak, K., M. Akkaya, and S.K. Pierce, B cell signaling in context. Nat Immunol, 2019. 20(8): p. 963-969.
19. Newton, K. and V.M. Dixit, Signaling in innate immunity and inflammation. Cold Spring Harb Perspect Biol, 2012. 4(3).

20. Libby, P., et al., Atherosclerosis. Nature Reviews Disease Primers, 2019. 5(56).
21. Insull, W., The Pathology of Atherosclerosis: Plaque Development and Plaque Responses to Medical Treatment. The American Journal of Medicine, 2009. 122.
22. Hansson, G.K. and A. Hermansson, The immune system in atherosclerosis. Nat Immunol, 2011. 12(3): p. 204-12.
23. Frostegård, J., Immunity, atherosclerosis and cardiovascular disease. BMC Medicine, 2013. 11(117).
24. Hilgendorf, I., F.K. Swirski, and C.S. Robbins, Monocyte fate in atherosclerosis. Arterioscler Thromb Vasc Biol, 2015. 35(2): p. 272-9.
25. Jebari-Benslaiman, S., et al., Pathophysiology of Atherosclerosis. Int J Mol Sci, 2022. 23(6).
26. Tabas, I. and K.E. Bornfeldt, Macrophage Phenotype and Function in Different Stages of Atherosclerosis. Circ Res, 2016. 118(4): p. 653-67.
27. Poznyak, A.V., et al., Overview of OxLDL and Its Impact on Cardiovascular Health: Focus on Atherosclerosis. Front Pharmacol, 2020. 11: p. 613780.
28. Pirillo, A., G.D. Norata, and A.L. Catapano, LOX-1, OxLDL, and atherosclerosis. Mediators Inflamm, 2013. 2013: p. 152786.
29. Guerrini, V. and M.L. Gennaro, Foam Cells: One Size Doesn't Fit All. Trends Immunol, 2019. 40(12): p. 1163-1179.
30. Yu, X.H., et al., Foam cells in atherosclerosis. Clin Chim Acta, 2013. 424: p. 245-52.
31. Kim, K., et al., Transcriptome Analysis Reveals Nonfoamy Rather Than Foamy Plaque Macrophages Are Proinflammatory in Atherosclerotic Murine Models. Circ Res, 2018. 123(10): p. 1127-1142.
32. Ijaz, A., B. Yarlagadda, and M. Orecchioni, Foamy macrophages in atherosclerosis: unraveling the balance between pro- and anti-inflammatory roles in disease progression. Front Cardiovasc Med, 2025. 12: p. 1589629.
33. Dib, L., et al., Lipid-associated macrophages transition to an inflammatory state in human atherosclerosis increasing the risk of cerebrovascular complications. Nat Cardiovasc Res, 2023. 2(7): p. 656-672.
34. Mehu, M., C.A. Narasimhulu, and D.K. Singla, Inflammatory Cells in Atherosclerosis. Antioxidants (Basel), 2022. 11(2).
35. da Silva, R.F., et al., Conversion of human M-CSF macrophages into foam cells reduces their proinflammatory responses to classical M1-polarizing activation. Atherosclerosis, 2016. 248: p. 170-8.
36. Gui, Y., H. Zheng, and R.Y. Cao, Foam Cells in Atherosclerosis: Novel Insights Into Its Origins, Consequences, and Molecular Mechanisms. Front Cardiovasc Med, 2022. 9: p. 845942.
37. Li, M., et al., Programmed cell death in atherosclerosis and vascular calcification. Cell Death Dis, 2022. 13(5): p. 467.
38. Rock, K.L. and H. Kono, The inflammatory response to cell death. Annu Rev Pathol, 2008. 3: p. 99-126.
39. Moore, K.J. and I. Tabas, Macrophages in the pathogenesis of atherosclerosis. Cell, 2011. 145(3): p. 341-55.
40. Alonso-Herranz, L., J. Albarran-Juarez, and J.F. Bentzon, Mechanisms of fibrous cap formation in atherosclerosis. Front Cardiovasc Med, 2023. 10: p. 1254114.
41. Johnson, J.L., Metalloproteinases in atherosclerosis. Eur J Pharmacol, 2017.

816: p. 93-106.

42. Shalhoub, J., et al., Innate immunity and monocyte-macrophage activation in atherosclerosis. Journal of Inflammation, 2011. 8(9).
43. Bobryshev, Y.V., et al., Macrophages and Their Role in Atherosclerosis: Pathophysiology and Transcriptome Analysis. Biomed Res Int, 2016. 2016: p. 9582430.
44. Feig, J.E., et al., HDL promotes rapid atherosclerosis regression in mice and alters inflammatory properties of plaque monocyte-derived cells. Proc Natl Acad Sci U S A, 2011. 108(17): p. 7166-71.
45. Rayner, K.J., et al., Antagonism of miR-33 in mice promotes reverse cholesterol transport and regression of atherosclerosis. J Clin Invest, 2011. 121(7): p. 2921-31.
46. Barrett, T.J., Macrophages in Atherosclerosis Regression. Arterioscler Thromb Vasc Biol, 2020. 40(1): p. 20-33.
47. Mantovani, A., C. Garlanda, and M. Locati, Macrophage diversity and polarization in atherosclerosis: a question of balance. Arterioscler Thromb Vasc Biol, 2009. 29(10): p. 1419-23.
48. Van den Bossche, J., et al., Mitochondrial Dysfunction Prevents Repolarization of Inflammatory Macrophages. Cell Rep, 2016. 17(3): p. 684-696.
49. Travis, J., On the Origin of The Immune System. Science, 2009. 324: p. 580-582.
50. Hotamisligil, G.S., Foundations of Immunometabolism and Implications for Metabolic Health and Disease. Immunity, 2017. 47(3): p. 406-420.
51. Wang, A., H.H. Luan, and R. Medzhitov, An evolutionary perspective on immunometabolism. Science, 2019. 363(6423).
52. Warburg, O., F. Wind, and E. Negelein, The metabolism of tumors in the body. J Gen Physiol, 1927. 8(6): p. 519-30.
53. De Leon-Oliva, D., et al., Revisiting the biological role of the Warburg effect: Evolving perspectives on cancer metabolism. Pathol Res Pract, 2025. 273: p. 156151.
54. Liberti, M.V. and J.W. Locasale, The Warburg Effect: How Does it Benefit Cancer Cells? Trends Biochem Sci, 2016. 41(3): p. 211-218.
55. 55. Yang, M., T. Soga, and P.J. Pollard, Oncometabolites: linking altered metabolism with cancer. J Clin Invest, 2013. 123(9): p. 3652-8.
56. Dang, L., et al., Cancer-associated IDH1 mutations produce 2-hydroxyglutarate. Nature, 2009. 462(7274): p. 739-44.
57. Ward, P.S., et al., The common feature of leukemia-associated IDH1 and IDH2 mutations is a neomorphic enzyme activity converting alpha-ketoglutarate to 2-hydroxyglutarate. Cancer Cell, 2010. 17(3): p. 225-34.
58. Xu, W., et al., Oncometabolite 2-hydroxyglutarate is a competitive inhibitor of alpha-ketoglutarate-dependent dioxygenases. Cancer Cell, 2011. 19(1): p. 17-30.
59. Du, X. and H. Hu, The Roles of 2-Hydroxyglutarate. Front Cell Dev Biol, 2021. 9: p. 651317.
60. Intlekofer, A.M., et al., Hypoxia Induces Production of L-2-Hydroxyglutarate. Cell Metab, 2015. 22(2): p. 304-11.
61. Tyrakis, P.A., et al., S-2-hydroxyglutarate regulates CD8(+) T-lymphocyte fate. Nature, 2016. 540(7632): p. 236-241.
62. Jha, A.K., et al., Network integration of parallel metabolic and transcriptional data reveals metabolic modules that regulate macrophage polarization. Immunity, 2015. 42(3): p. 419-30.

63. Mills, E.L. and L.A. O'Neill, Reprogramming mitochondrial metabolism in macrophages as an anti-inflammatory signal. Eur J Immunol, 2016. 46(1): p. 13-21.

64. O'Neill, L.A., R.J. Kishton, and J. Rathmell, A guide to immunometabolism for immunologists. Nat Rev Immunol, 2016. 16(9): p. 553-65.

65. Van den Bossche, J., L.A. O'Neill, and D. Menon, Macrophage Immunometabolism: Where Are We (Going)? Trends Immunol, 2017. 38(6): p. 395-406.

66. Artyomov, M.N. and J. Van den Bossche, Immunometabolism in the Single-Cell Era. Cell Metab, 2020. 32(5): p. 710-725.

67. Artyomov, M.N., A. Sergushichev, and J.D. Schilling, Integrating immunometabolism and macrophage diversity. Semin Immunol, 2016. 28(5): p. 417-424.

68. Mills, E.L., et al., Succinate Dehydrogenase Supports Metabolic Repurposing of Mitochondria to Drive Inflammatory Macrophages. Cell, 2016. 167(2): p. 457-470 e13.

69. Littlewood-Evans, A., et al., GPR91 senses extracellular succinate released from inflammatory macrophages and exacerbates rheumatoid arthritis. J Exp Med, 2016. 213(9): p. 1655-62.

70. Tannahill, G.M., et al., Succinate is an inflammatory signal that induces IL-1beta through HIF-1alpha. Nature, 2013. 496(7444): p. 238-42.

71. Wu, J.Y., et al., Cancer-Derived Succinate Promotes Macrophage Polarization and Cancer Metastasis via Succinate Receptor. Mol Cell, 2020. 77(2): p. 213-227 e5.

72. Lampropoulou, V., et al., Itaconate Links Inhibition of Succinate Dehydrogenase with Macrophage Metabolic Remodeling and Regulation of Inflammation. Cell Metab, 2016. 24(1): p. 158-66.

73. Cordes, T., et al., Immunoresponsive Gene 1 and Itaconate Inhibit Succinate Dehydrogenase to Modulate Intracellular Succinate Levels. J Biol Chem, 2016. 291(27): p. 14274-14284.

74. He, W., et al., Citric acid cycle intermediates as ligands for orphan G-protein-coupled receptors. Nature, 2004. 429(6988).

75. Keiran, N., et al., SUCNR1 controls an anti-inflammatory program in macrophages to regulate the metabolic response to obesity. Nat Immunol, 2019. 20(5): p. 581-592.

76. Peruzzotti-Jametti, L., et al., Macrophage-Derived Extracellular Succinate Licenses Neural Stem Cells to Suppress Chronic Neuroinflammation. Cell Stem Cell, 2018. 22(3): p. 355-368 e13.

77. Michelucci, A., et al., Immune-responsive gene 1 protein links metabolism to immunity by catalyzing itaconic acid production. Proc Natl Acad Sci U S A, 2013. 110(19): p. 7820-5.

78. Murphy, M.P. and L.A.J. O'Neill, Krebs Cycle Reimagined: The Emerging Roles of Succinate and Itaconate as Signal Transducers. Cell, 2018. 174(4): p. 780-784.

79. Hooftman, A. and L.A.J. O'Neill, The Immunomodulatory Potential of the Metabolite Itaconate. Trends Immunol, 2019. 40(8): p. 687-698.

80. Bambouskova, M., et al., Electrophilic properties of itaconate and derivatives regulate the IkappaBzeta-ATF3 inflammatory axis. Nature, 2018. 556(7702): p. 501-504.

81. Mills, E.L., et al., Itaconate is an anti-inflammatory metabolite that activates

Nrf2 via alkylation of KEAP1. Nature, 2018. 556(7699): p. 113-117.

82. Qin, W., et al., Chemoproteomic Profiling of Itaconation by Bioorthogonal Probes in Inflammatory Macrophages. J Am Chem Soc, 2020. 142(25): p. 10894-10898.

83. Swain, A., et al., Comparative evaluation of itaconate and its derivatives reveals divergent inflammasome and type I interferon regulation in macrophages. Nat Metab, 2020. 2(7): p. 594-602.

84. Khodadadian, A., et al., Genomics and Transcriptomics: The Powerful Technologies in Precision Medicine. Int J Gen Med, 2020. 13: p. 627-640.

85. Pattan, V., et al., Genomics in medicine: A new era in medicine. World J Methodol, 2021. 11(5): p. 231-242.

86. Purohit, V., et al., Systems-based approaches to study immunometabolism. Cell Mol Immunol, 2022. 19(3): p. 409-420.

87. Stark, R., M. Grzelak, and J. Hadfield, RNA sequencing: the teenage years. Nat Rev Genet, 2019. 20(11): p. 631-656.

88. Shuken, S.R., An Introduction to Mass Spectrometry-Based Proteomics. J Proteome Res, 2023. 22(7): p. 2151-2171.

89. Han, X., A. Aslanian, and J.R. Yates, 3rd, Mass spectrometry for proteomics. Curr Opin Chem Biol, 2008. 12(5): p. 483-90.

90. Zhao, Y. and O.N. Jensen, Modification-specific proteomics: strategies for characterization of post-translational modifications using enrichment techniques. Proteomics, 2009. 9(20): p. 4632-41.

91. Hermann, J., L. Schurgers, and V. Jankowski, Identification and characterization of post-translational modifications: Clinical implications. Mol Aspects Med, 2022. 86: p. 101066.

92. Tamara, S., M.A. den Boer, and A.J.R. Heck, High-Resolution Native Mass Spectrometry. Chem Rev, 2022. 122(8): p. 7269-7326.

93. Nieman, D.C., M.A. Lila, and N.D. Gillitt, Immunometabolism: A Multi-Omics Approach to Interpreting the Influence of Exercise and Diet on the Immune System. Annu Rev Food Sci Technol, 2019. 10: p. 341-363.

94. Babele, P.K. and J.D. Young, Applications of stable isotope-based metabolomics and fluxomics toward synthetic biology of cyanobacteria. Wiley Interdiscip Rev Syst Biol Med, 2020. 12(3): p. e1472.

95. Fernandez-Garcia, J., et al., Stable Isotopes for Tracing Mammalian-Cell Metabolism In Vivo. Trends Biochem Sci, 2020. 45(3): p. 185-201.

96. Antoniewicz, M.R., A guide to (13)C metabolic flux analysis for the cancer biologist. Exp Mol Med, 2018. 50(4): p. 1-13.

97. Emwas, A.H., et al., Fluxomics - New Metabolomics Approaches to Monitor Metabolic Pathways. Front Pharmacol, 2022. 13: p. 805782.

98. Schmidt, C.A., K.H. Fisher-Wellman, and P.D. Neufer, From OCR and ECAR to energy: Perspectives on the design and interpretation of bioenergetics studies. J Biol Chem, 2021. 297(4): p. 101140.

99. Verberk, S.G.S., et al., An integrated toolbox to profile macrophage immunometabolism. Cell Rep Methods, 2022. 2(4): p. 100192.

100. Banday, M.Z., A.S. Sameer, and S. Nissar, Pathophysiology of diabetes: An overview. Avicenna J Med, 2020. 10(4): p. 174-188.

101. Pernicova, I. and M. Korbonits, Metformin--mode of action and clinical implications for diabetes and cancer. Nat Rev Endocrinol, 2014. 10(3): p. 143-

56.

102. Foretz, M., B. Guigas, and B. Viollet, Metformin: update on mechanisms of action and repurposing potential. Nat Rev Endocrinol, 2023. 19(8): p. 460-476.

103. Rena, G., D.G. Hardie, and E.R. Pearson, The mechanisms of action of metformin. Diabetologia, 2017. 60(9): p. 1577-1585.

104. Decensi, A., et al., Metformin and cancer risk in diabetic patients: a systematic review and meta-analysis. Cancer Prev Res (Phila), 2010. 3(11): p. 1451-61.

105. Moharregh-Khiabani, D., et al., Fumaric Acid and its esters: an emerging treatment for multiple sclerosis. . Curr Neuropharmacol. , 2009. 7(1).

106. Ocana, M.C., et al., New insights in the targets of action of dimethyl fumarate in endothelial cells: effects on energetic metabolism and serine synthesis in vitro and in vivo. Commun Biol, 2023. 6(1): p. 1084.

107. Chen, H., et al., Hydroxycarboxylic acid receptor 2 mediates dimethyl fumarate's protective effect in EAE. J Clin Invest, 2014. 124(5): p. 2188-92.

108. Kastrati, I., et al., Dimethyl Fumarate Inhibits the Nuclear Factor kappaB Pathway in Breast Cancer Cells by Covalent Modification of p65 Protein. J Biol Chem, 2016. 291(7): p. 3639-47.

109. Gillard, G.O., et al., DMF, but not other fumarates, inhibits NF-kappaB activity in vitro in an Nrf2-independent manner. J Neuroimmunol, 2015. 283: p. 74-85.

110. Blewett, M.M., et al., Chemical proteomic map of dimethyl fumarate-sensitive cysteines in primary human T cells. Sci Signal, 2016. 9(445).

111. Montes Diaz, G., et al., Dimethyl fumarate treatment in multiple sclerosis: Recent advances in clinical and immunological studies. Autoimmun Rev, 2018. 17(12): p. 1240-1250.

112. Ridker, P.M., Residual inflammatory risk: addressing the obverse side of the atherosclerosis prevention coin. Eur Heart J, 2016. 37(22): p. 1720-2.

113. Sarrazy, V., et al., Disruption of Glut1 in Hematopoietic Stem Cells Prevents Myelopoiesis and Enhanced Glucose Flux in Atheromatous Plaques of ApoE(-/-) Mice. Circ Res, 2016. 118(7): p. 1062-77.

114. Shirai, T., et al., The glycolytic enzyme PKM2 bridges metabolic and inflammatory dysfunction in coronary artery disease. J Exp Med, 2016. 213(3): p. 337-54.

115. Yamashita, A., et al., Increased metabolite levels of glycolysis and pentose phosphate pathway in rabbit atherosclerotic arteries and hypoxic macrophage. PLoS One, 2014. 9(1): p. e86426.

116. Tomas, L., et al., Altered metabolism distinguishes high-risk from stable carotid atherosclerotic plaques. Eur Heart J, 2018. 39(24): p. 2301-2310.

117. Groh, L., et al., Monocyte and macrophage immunometabolism in atherosclerosis. Semin Immunopathol, 2018. 40(2): p. 203-214.

118. Koelwyn, G.J., et al., Regulation of macrophage immunometabolism in atherosclerosis. Nat Immunol, 2018. 19(6): p. 526-537.

119. Ketelhuth, D.F.J., et al., Immunometabolism and atherosclerosis: perspectives and clinical significance: a position paper from the Working Group on Atherosclerosis and Vascular Biology of the European Society of Cardiology. Cardiovasc Res, 2019. 115(9): p. 1385-1392.Organisation, W.H., Global Health Estimates 2020: Deaths by Cause, Age, Sex, by Country and by Region, 2000-2019. 2020.

2



Let's Enter the Wonderful World of Immunometabolites

Kyra E. de Goede,[1*] Karl J. Harber,[1*] and Jan Van den Bossche[1]

Trends in Endocrinology & Metabolism, 30 (6), 329–331 (2019)

[1]Amsterdam UMC, Vrije Universiteit Amsterdam, Department of Molecular Cell Biology and Immunology, Amsterdam Cardiovascular Sciences, Cancer Center Amsterdam, Amsterdam, The Netherlands
*Shared authorship

Abstract

Over the past decade, cancer metabolism research taught us that metabolites are much more than intermediate or end products of metabolism. As such, the name 'oncometabolite' emerged. Immunometabolism research has developed tremendously over the past few years and, in analogy to the cancer metabolism field, the term 'immunometabolite' has been used for different metabolites and purposes. Here, we propose a definition for the term 'immunometabolite' and provide some historical background and future perspectives on this matter. By doing so, we aim to increase interest in this fast-expanding field and to encourage further research.

The term 'oncometabolite' was first used in the scientific literature by Ward *et al*. in reference to R-2-hydroxyglutarate (R-2HG) in 2010 and now also refers to the metabolically adjacent and structurally similar intermediates succinate, fumarate, and the S-2-hydroxyglutarate enantiomer [1] (Figure 1, bottom). The term also refers to intermediates of metabolism that aberrantly accumulate in cancer cells downstream or upstream of mutated genes that encode metabolic enzymes. The increased abundance of oncometabolites can promote tumorigenesis via distinct routes, including immunosuppression [2]. Within cancer cells, these metabolites can drive epigenetic remodeling and trigger oncogenic signaling cascades that contribute to tumorigenesis. Moreover, metabolic rewiring in malignant cells can also affect other cells in the tumor microenvironment (TME) through nutrient competition and the action of oncometabolites as signaling molecules. As such, tumor cell-derived metabolites can negatively influence immune cells to shape a TME that hijacks antitumor immune responses. As an example, R-2-hydroxyglutarate (R-2HG) derived from isocitrate dehydrogenase 1 (*IDH1*)-mutant glioma cells can be actively taken up by T cells, where it results in the suppression of antitumor T cell activities via the perturbation of various signaling cascades [3]. Similarly, lactate produced by tumor cells can induce arginase-1 activity and vascular endothelial growth factor (VEGF) production in tumorassociated macrophages (TAMs), which support tumor growth [4].

Importantly, immune cells also undergo extensive metabolic rewiring upon activation. As in cancer cells, these metabolites serve many roles beyond energy production and directly drive immune cell phenotype and function. Within immune cells, metabolic intermediates can serve as cofactors for (metabolic) enzymes and can mediate post-translational modifications of histones, transcription factors, enzymes, and other key proteins. Moreover, immune cell-derived 'immunometabolites' can leave the cell and signal endogenously to neighboring cells in a cytokine-like manner to affect the local microenvironment and possibly also the systemic environment. In analogy with oncometabolites, immunometabolites can be defined as metabolic intermediates that accumulate in immune cells upon activation. Their overabundance then regulates intracellular pathways that drive the phenotype and specific functions of the cell. The term 'immunometabolite' was first applied to S-2-hydroxyglutarate (S-2HG) by Tyrakis *et al*. when they observed that it accumulates in CD8+ T cells upon T cell receptor triggering [5]. S-2HG production in these cells is regulated by hypoxia-inducible factor (HIF)1α and alters T cell differentiation and proliferation through the modulation of histone and DNA methylation (Figure 1, top left).

Again in the T cell field, Xu *et al*. later discovered that 2HG also regulates the balance between proinflammatory T helper 17 (Th17) cells and anti-inflammatory induced regulatory T (iTreg) cells, in favor of the former [6]. In their search for compounds that reprogram Th17 differentiation towards iTreg cells, they found that 2HG increases in

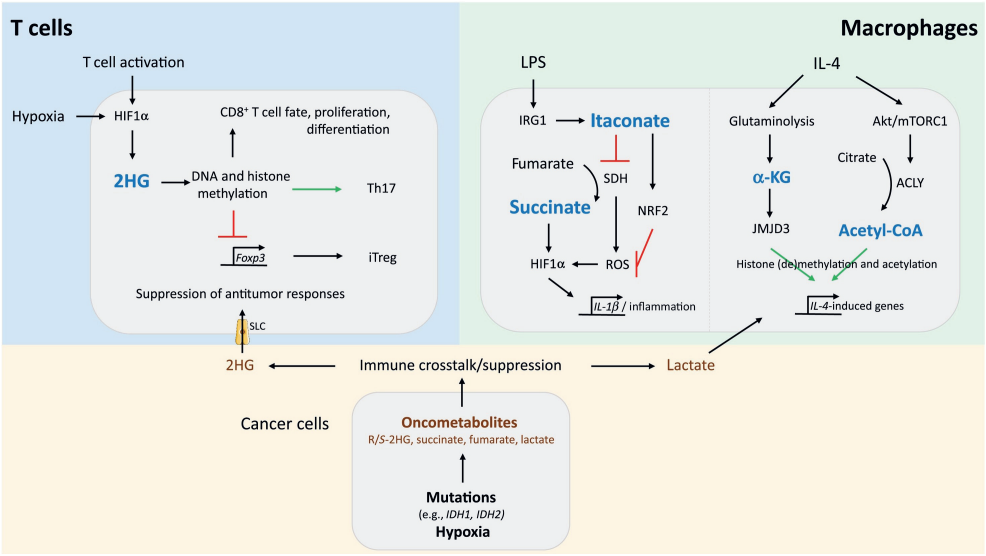

Figure 1. Immunometabolites accumulate in immune cells upon activation and regulate cell fate and function. 2-hydroxyglutarate (2HG) emerged as a key immunometabolite that regulates T cell fate. Succinate promotes lipopolysaccharide (LPS)-induced inflammatory responses, whereas itaconate acts as an anti-inflammatory metabolite. α-ketoglutarate and acetyl-CoA were demonstrated to support interleukin (IL)-4-induced macrophage responses via metabolic and/or epigenetic crosstalk. Metabolites (both oncometabolites and immunometabolites) can be released and signal to neighboring cells in the microenvironment. Abbreviations: ACLY, ATP citrate lyase; iTreg, induced regulatory T cell; R-2HG, R-2-hydroxyglutarate; ROS, reactive oxygen species; S-2HG, S-2-hydroxyglutarate; SDH, succinate dehydrogenase; SLC, solute carriers; Th17, T helper 17 cell.

Th17 cells, resulting in the inhibition of demethylases, hypermethylation, and associated inhibition of *Foxp3* gene expression, which is crucial for differentiation towards Th17 cells. Accordingly, inhibition of 2HG production with the small molecule (aminooxy)acetic acid (AOA) blocked Th17 and promoted iTreg differentiation to improve experimental autoimmune encephalomyelitis as a model for multiple sclerosis (MS).

The term 'immunometabolite' was also used by Ma *et al.* for serine when they discovered that this amino acid is an essential metabolite for effector T cell proliferation [7]. However, we would like to encourage the use of the term 'immunometabolite' solely for intermediates that are produced by immune cells upon activation, rather than for exogenous metabolites that affect immune cell function. Otherwise, almost every cellular metabolite could be categorized as an immunometabolite. According to this strict definition, L-2HG, succinate, and itaconate are probably the most recognized and studied immunometabolites currently. While 2HG shapes T cell responses, as discussed earlier, the latter two are crucial controllers of macrophage activation.

Similar to T cells, macrophages come in different 'flavors'. Macrophages stimulated with the bacterial outer membrane molecule lipopolysaccharide (LPS) in the presence

and/or absence of the cytokine interferon (IFN)-γ are prototypical proinflammatory macrophages [$M_{(LPS+/-IFN\gamma)}$], whereas interleukin (IL)-4-treated cells are the most commonly studied model for anti-inflammatory macrophages [$M_{(IL-4)}$]. Akin to cancer cells, inflammatory macrophages show a Warburg-like metabolism characterized by a switch from mitochondrial oxidative phosphorylation towards aerobic glycolysis [8]. Along with this shift, a rewired tricarboxylic acid cycle (TCA) cycle in LPS-treated macrophages causes the accumulation of the Krebs cycle intermediates succinate and itaconate [9]. These metabolites directly control the inflammatory status and function of macrophages, with succinate acting as an inflammatory signal and itaconate having anti-inflammatory effects (Figure 1, top right). Succinate can drive the production of the inflammatory cytokine IL-1β by promoting HIF1α stability and by repurposing the electron transport chain from ATP production to reactive oxygen species (ROS) generation. Moreover, succinate can be released into the extracellular milieu to propagate inflammatory signaling in adjacent cells within the microenvironment via the succinate receptor GPR91/SUCNR1 (for more details on the proinflammatory role, we direct readers to recent reviews on this subject [8,9]).

While 2-HG and succinate are also produced by nonimmune cells, itaconate production appears specific for immune cells, particularly macrophages. As such, it could be considered the prototypical immunometabolite. Inflammatory macrophages make itaconate via the decarboxylation of the TCA cycle metabolite cisaconitate. In 2013, it was revealed that itaconate production in inflammatory macrophages is mediated by the LPS-induced gene *Irg1*. This 'immune-responsive gene 1' was discovered in 1995, but its function had remained unknown (we refer to a recent extensive review on this interesting immunometabolite for further insight [10]). Irg1-derived itaconate can serve as an endogenous inhibitor of succinate dehydrogenase to counteract one of the proinflammatory effects of succinate [11,12]. In parallel, itaconate can mediate its antiinflammatory effects via the activation of the antioxidant/anti-inflammatory Nrf2 pathway [13].

Whereas succinate supports inflammatory responses, as discussed earlier, IL-4-induced anti-inflammatory macrophages were shown to require the production of α-ketoglutarate (α-KG) via glutaminolysis [14]. This TCA cycle intermediate serves as a cofactor of the epigenetic enzyme Jmjd3 and promotes IL-4 responses in macrophages, while repressing proinflammatory cues. As such, the succinate/α-KG ratio within a macrophage appears to be a key controller of its functional fate. In addition to α-KG, ATP citrate lyase (ACLY)-mediated accumulation of the Krebs cycle metabolite acetyl-CoA was shown to support anti-inflammatory macrophage responses by promoting histone acetylation and subsequent transcription of IL-4-induced genes [15]. However, care is needed when interpreting these experiments since they used pharmacological compounds that are now known to show important off-target effects. Therefore, new genetic tools will be

key to univocally address the role of the ACLY-derived immunometabolite acetyl-CoA in regulating macrophage responses.

Other future directions for follow-up research concern the ins and outs of immunometabolite transport and localization. How are these distinct immunometabolites transported out of the cell? Furthermore, once outside the cell, what is their actual fate? Which receptors, on which cells, do they target? Although distinct solute carriers (SLCs) were proposed as transporters for succinate and 2-hydroxyglutarate, no such transporter has yet been shown for itaconate. Single-cell metabolomics and other new high-end techniques that enable one to map the metabolic configuration of cells within complex microenvironments will be key to address these questions. Another important point to further investigate is the subcellular location of metabolites and their dynamics. Such spatiotemporal insight should help us to understand how immunometabolites translate metabolic rewiring into functional changes and disease progression. So far, most of our knowledge is derived from mouse models, but how could these data be translated to humans? Moreover, most studies have assessed the immunometabolism of immune cells in bulk; thus, how might this manifest at the single cell level? Finally, the milliondollar question is whether these immunometabolites or their derivatives could provide new therapeutic opportunities. For example, the effects of itaconate and other immunometabolites on macrophage function are mostly assessed by applying derivatives such as dimethylitaconate and 4-octyl-itaconate. While these compounds can have strong effects on macrophage function and potential therapeutic value, they do not fully recapitulate the endogenous effects of the 'real' immunometabolites that they mimic. Understanding their specific mode of action will be a key area of research and should clarify their applicability for future therapy. While waiting elucidation of these questions, we have also emphasized the importance of immunometabolites in regulating immune cell fate and disease outcome. Moreover, we stress the necessity of carefully defining them as metabolites that are generated within immune cells after activation, rather than as external metabolites that affect immune cell function.

References

1. Ward, P.S. et al. (2010) The common feature of leukemia-associated IDH1 and IDH2 mutations is a neomorphic enzyme activity converting alpha-ketoglutarate to 2-hydroxyglutarate. Cancer Cell 17, 225–234
2. Corrado, M. et al. (2016) Changing perspective on oncometabolites: from metabolic signature of cancer to tumorigenic and immunosuppressive agents. Oncotarget 7, 46692–46706
3. Bunse, L. et al. (2018) Suppression of antitumor T cell immunity by the oncometabolite (R)-2-hydroxyglutarate. Nat. Med. 24, 1192–1203
4. Colegio, O.R. et al. (2014) Functional polarization of tumour-associated macrophages by tumour-derived lactic acid. Nature 513, 559–563
5. Tyrakis, P.A. et al. (2016) S-2-hydroxyglutarate regulates CD8(+) T-lymphocyte fate. Nature 540, 236–241
6. Xu, T. et al. (2017) Metabolic control of TH17 and induced Treg cell balance by an epigenetic mechanism. Nature 548, 228–233
7. Ma, E.H. et al. (2017) Serine is an essential metabolite for effector T cell expansion. Cell Metab. 25, 345–357
8. Van den Bossche, J. et al. (2017) Macrophage immunometabolism: where are we (going)? Trends Immunol. 38, 395–406
9. Murphy, M.P. and O'Neill, L.A.J. (2018) Krebs cycle reimagined: the emerging roles of succinate and itaconate as signal transducers. Cell 174, 780–784
10. O'Neill, L.A.J. and Artyomov, M.N. (2019) Itaconate: the poster child of metabolic reprogramming in macrophage function. Nat. Rev. Immunol. Published online January 31, 2019. https://doi.org/10.1038/s41577-019-0128-5
11. Cordes, T. et al. (2016) Immunoresponsive gene 1 and itaconate inhibit succinate dehydrogenase to modulate intracellular succinate levels. J. Biol. Chem. 291, 14274–14284
12. Lampropoulou, V. et al. (2016) Itaconate links inhibition of succinate dehydrogenase with macrophage metabolic re-modeling and regulation of inflammation. Cell Metab. 24, 158–166
13. Mills, E.L. et al. (2018) Itaconate is an anti-inflammatory metabolite that activates Nrf2 via alkylation of KEAP1. Nature 556, 113–117
14. Liu, P.S. et al. (2017) alpha-ketoglutarate orchestrates macrophage activation through metabolic and epigenetic reprogramming. Nat. Immunol. 18, 985–994
15. Covarrubias, A.J. et al. (2016) Akt-mTORC1 signaling regulates Acly to integrate metabolic input to control of macrophage activation. eLife 5, e1161

3



Adenine is an Anti-Inflammatory Metabolite Found to be More Abundant in M-CSF Over GM-CSF-Differentiated Human Macrophages

Karl J. Harber,[1,2,3,4] Thuc-Anh Nguyen,[1] Bauke V. Schomakers,[5,6] Daan A. F. Heister,[4] Helga E. de Vries,[4,7] Michel van Weeghel,[5,6] Jan Van den Bossche,[2,3,4,8] and Menno P. J. de Winther[1,2,3]

Immunology Letters, 265, 23–30 (2024)

[1] Department of Medical Biochemistry, Amsterdam UMC, University of Amsterdam, 1105 AZ, Amsterdam, Netherlands

[2] Amsterdam Cardiovascular Sciences (ACS), Atherosclerosis & ischemic syndromes, Amsterdam, UMC, Netherlands

[3] Amsterdam institute for Infection and Immunity (AII), Inflammatory diseases, Amsterdam, UMC, Netherlands

[4] Department of Molecular Cell Biology and Immunology, Amsterdam UMC, Vrije Universiteit Amsterdam, 1081 HV, Amsterdam, Netherlands

[5] Department of Genetic Metabolic Diseases, Amsterdam UMC, University of Amsterdam, 1105 AZ, Amsterdam, Netherlands

[6] Core Facility Metabolomics, Amsterdam UMC, University of Amsterdam, 1105 AZ, Amsterdam, Netherlands

[7] Amsterdam Neuroscience, Amsterdam, Netherlands

[8] Amsterdam Gastroenterology Endocrinology Metabolism (AGEM), Amsterdam, UMC, Netherlands

Abstract

Immunometabolism has been unveiled in the last decade to play a major role in controlling macrophage metabolism and inflammation. There has been a constant effort to understand the immunomodulating properties of regulated metabolites during inflammation with the aim of controlling and re-wiring aberrant macrophages in inflammatory diseases. M-CSF and GM-CSF-differentiated macrophages play a key role in mounting successful innate immune responses. When a resolution phase is not achieved however, GM-CSF macrophages contribute substantially more towards an adverse inflammatory milieu than M-CSF macrophages, consequently driving disease progression. Whether there are specific immunometabolites that determine the homoeostatic or inflammatory nature of M-CSF and GM-CSF-differentiated macrophages is still unknown. As such, we performed metabolomics analysis on LPS and IL-4-stimulated M-CSF and GM-CSF-differentiated human macrophages to identify differentially accumulating metabolites. Adenine was distinguished as a metabolite significantly higher in M-CSF-differentiated macrophages after both LPS or IL-4 stimulation. Human macrophages treated with adenine before LPS stimulation showed a reduction in inflammatory gene expression, cytokine secretion and surface marker expression. Adenine caused macrophages to become more quiescent by lowering glycolysis and OXPHOS which resulted in reduced ATP production. Moreover, typical metabolite changes seen during LPS-induced macrophage metabolic reprogramming were absent in the presence of adenine. Phosphorylation of metabolic signalling proteins AMPK, p38 MAPK and AKT were not responsible for the suppressed metabolic activity of adenine-treated macrophages. Altogether, in this study we highlight the immunomodulating capacity of adenine in human macrophages and its function in driving cellular quiescence.

Introduction

Macrophages are key players in driving innate immune responses for fighting off infection and disease as well as repairing and restoring the local tissue environment [1,2]. With the opportunity to induce or limit inflammation, having the right balance of both pro- and anti-inflammatory macrophages is essential in preventing the generation of large populations of aberrant macrophages [3,4]. Diseases such as atherosclerosis develop once pro-inflammatory macrophages are stimulated and recruited to sites of excess lipids within vessel walls. Once migrated through the endothelium, macrophages engulf oxidised LDL, secrete further pro-inflammatory cytokines and subsequently dominate the emergence of protective anti-inflammatory macrophages [5]. As such, the exponential expansion of plaque macrophages and their inability to revert back to their homoeostatic state advances plaques into rupture-prone lesions [5]. On the other hand, in diseases such as cancer, the tumour microenvironment is overwhelmed by anti-inflammatory macrophages that dampen the anti-tumour capability of pro-inflammatory macrophages [6,7]. This allows the tumour to develop in an unhostile environment ultimately leading to a more severe stage of the disease that is more challenging to treat. Consequently, finding a method to phenotypically switch these macrophages from a detrimental to a more protective state would provide a better prognostic outcome for inflammatory diseases [8,9].

Monocytes are the circulating innate immune cells that scour the environment for foreign or dead material to clear. Once at the site of an inflammatory stimulus, monocytes develop into more specialised macrophages. Differentiation into macrophages can occur in response to two cytokines: the ubiquitously available macrophage colony-stimulating factor (M-CSF) or the inflammation-induced granulocyte-macrophage colony-stimulating factor (GM-CSF) [10,11]. These growth factors are responsible for differentiating monocytes into an array of macrophage states with varying inflammatory signatures [12,13,14]. In the context of pro-inflammatory diseases, GM-CSF-differentiated macrophages are considered to drive aberrant immune responses and lack the ability to elicit a successful resolution phase [11]. Whilst necessary for mounting a successful immune response, GM-CSF-differentiated macrophages' persistence is detrimental in inflammatory diseases [10,15]. However, an imbalance in favour of M-CSF-differentiated macrophages can allow for diseases such as cancer to thrive with limited threat and as such, restoring the balance of M-CSF and GM-CSF-differentiated macrophages could be an effective mechanism for treating inflammatory diseases [12,16].

Macrophage TLR4 activation has recently been tied to major metabolic rewiring, shifting cells into a highly glycolytic state and dysregulated TCA cycle [17,18,19]. Metabolites involved in these metabolic shifts are referred to as immunometabolites

and possess potent immunomodulatory effects [19]. Extensive research shows that the metabolic signatures of GM-CSF and M-CSF-differentiated macrophages are distinct on a proteomic, lipidomic and metabolomic level [13,14,20,21]. These distinct signatures become exaggerated in conditions of inflammation. Considering this, we anticipated that the metabolite signature in GM-CSF-differentiated macrophages may play a role in not only their differentiation process but also in their inflammatory response. Additionally, persistence of such metabolite profiles may also prevent macrophage phenotype switching, and subsequent failure to resolve the inflammatory response, as previously shown with nitric oxide in inflammatory macrophage re-programming [22].

In this paper, we therefore intended to identify immunometabolites that are differentially expressed between M-CSF or GM-CSF-differentiated human macrophages, followed by functional assessment of their impact on the inflammatory response. By interfering with the balance of these specific immunometabolites, we aim to phenotypically switch macrophages from an inflammatory state to a more homoeostatic profile.

Materials and methods

Monocyte isolation, differentiation and stimulation

PBMCs were isolated from buffy coats (50 mL) ordered from Sanquin blood bank using the Ficoll/Lymphoprep gradient technique. After layering, cells were centrifuged to generate a PBMC interface which was extracted and used for monocyte isolation. PBMC's were applied to magnetic columns following specific monocyte selection with Miltenyi magnetic CD14+ beads. After washing to remove the negative fraction, monocytes were eluted using a plunger. Monocytes were then seeded at 0.1×10^6, 0.5×10^6 or 2×10^6 per well in 96-, 24- or 6-well plates, respectively, in IMDM medium containing HEPES (Gibco) supplemented with 2 mM l-glutamine, 100 U/ml penicillin, 100 µg/ml streptomycin (full IMDM medium), and containing 1% FCS. After attaching for one hour, medium was replaced with full IMDM medium with 10% FCS and 50 ng/ml M-CSF or 10 ng/mL GM-CSF (Miltenyi), using previous publications as a guideline, for 6-day differentiation, replacing with fresh supplemented medium after 3 days [23]. Fully differentiated macrophages (day 6) were subsequently pre-treated with adenine (1 mM) dissolved in dimethyl sulfoxide (DMSO) followed by stimulation with 10 ng/mL of LPS serotype O55:B5 or 20 ng/mL of IL-4, respectively [24].

Mass spectrometry metabolomics

Metabolomics was performed as previously described, with minor adjustments [25]. Briefly, macrophages seeded at a density of 0.8×10^6 cells/well in 24-well plate, were

cultured in either M-CSF or GM-CSF. Before harvest on day 6, they were stimulated with 10 ng/mL LPS serotype O55:B5 (Sigma-Aldrich) for 24 h. For adenine metabolomics, M-CSF macrophages were stimulated with 1 mM of adenine for 1 hour prior to 10 ng/mL LPS serotype O55:B5 (Sigma-Aldrich) for 24 h. A 75 µL mixture of the following internal standards in water was added to each sample: adenosine-$^{15}N_5$-monophosphate (5 nmol), adenosine-$^{15}N_5$-triphosphate (5 nmol), D_4-alanine (0.5 nmol), D_7-arginine (0.5 nmol), D_3-aspartic acid (0.5 nmol), D_3-carnitine (0.5 nmol), D_4-citric acid (0.5 nmol), $^{13}C_1$-citrulline (0.5 nmol), $^{13}C_6$-fructose-1,6-diphosphate (1 nmol), $^{13}C_2$-glycine (5 nmol), guanosine-$^{15}N_5$-monophosphate (5 nmol), guanosine-$^{15}N_5$-triphosphate (5 nmol), $^{13}C_6$-glucose (10 nmol), $^{13}C_6$-glucose-6-phosphate (1 nmol), D_3-glutamic acid (0.5 nmol), D_5-glutamine (0.5 nmol), D_5-glutathione (1 nmol), $^{13}C_6$-isoleucine (0.5 nmol), D_3-lactic acid (1 nmol), D_3-leucine (0.5 nmol), D_4-lysine (0.5 nmol), D_3-methionine (0.5 nmol), D_6-ornithine (0.5 nmol), D_5-phenylalanine (0.5 nmol), D_7-proline (0.5 nmol), $^{13}C_3$-pyruvate (0.5 nmol), D_3-serine (0.5 nmol), D_6-succinic acid (0.5 nmol), D_4-thymine (1 nmol), D_5-tryptophan (0.5 nmol), D_4-tyrosine (0.5 nmol), D_8-valine (0.5 nmol). Subsequently, 425 µL water, 500 µL methanol and 1 mL chloroform were added to the same 2 mL tube before thorough mixing and centrifugation for 10 min at 14.000 rpm. The top layer of the liquid-liquid extraction was transferred to a clean 1.5 mL tube and dried using a vacuum concentrator at 60 °C. Dried samples were reconstituted in 100 µL 6:4 (v/v) methanol:water. Metabolites were analysed using a Waters Acquity ultra-high performance liquid chromatography system coupled to a Bruker Impact II™ Ultra-High Resolution Qq-Time-Of-Flight mass spectrometer. Samples were kept at 12 °C during analysis and 5 µL of each sample was injected. Chromatographic separation was achieved using a Merck Millipore SeQuant ZIC-cHILIC column (PEEK 100 × 2.1 mm, 3 µm particle size). Column temperature was held at 30 °C. Mobile phase consisted of (A) 1:9 (v/v) acetonitrile:water and (B) 9:1 (v/v) acetonitrile:water, both containing 5 mmol/L ammonium acetate. Using a flow rate of 0.25 mL/min, the LC gradient consisted of: Dwell at 100 % Solvent B, 0–2 min; Ramp to 54 % Solvent B at 13.5 min; Ramp to 0 % Solvent B at 13.51 min; Dwell at 0 % Solvent B, 13.51–19 min; Ramp to 100% B at 19.01 min; Dwell at 100 % Solvent B, 19.01–19.5 min. Column was equilibrated by increasing flow rate to 0.4 mL/min at 100 % B for 19.5–21 min. MS data were acquired using negative and positive ionisation in full scan mode over the range of *m/z* 50–1200. Data were analysed using Bruker TASQ software version 2.1.22.3. Metabolite identification has been based on a combination of accurate mass, (relative) retention times, ion mobility data and fragmentation spectra, compared to the analysis of a library of standards. All reported metabolite intensities were normalised to the total protein content, determined by Thermo Scientific™ Pierce™ BCA Protein Assay, as well as to internal standards with comparable retention times and response in the MS.

ELISA

Cytokines were measured in supernatants of macrophages treated with adenine for 1 hour followed by LPS stimulation for 24 h. Tumour necrosis factor (TNF), interleukin 10 (IL-10), and IL-12p40 were quantified using sandwich enzyme-linked immunosorbent assay (ELISA) kits, following supplier's protocols (Life Technologies).

Flow Cytometry

Cells were incubated with Fc-block in addition to labelling antibodies and dyes listed in Supplemental Table 1 for 1 hour. Cell viability was assessed by fixable viability staining according to the manufacturer's protocol (eBioscience). Data were acquired with an LSR Fortessa X20 (Becton Dickinson) and analysed using FlowJo v10 (Becton Dickinson). Surface expression was calculated as ΔMFI = $(\text{Median fluorescence intensity})_{\text{positive staining}}$ – $(\text{Median fluorescence intensity})_{\text{negative staining}}$.

Gene expression analysis

RNA was isolated with GeneJET RNA Purification kits (ThermoFisher), cDNA was synthesised with High-Capacity cDNA Reverse Transcription Kit (Applied Biosystems) and quantified using an Implen nanodrop N60. qPCR was performed using Sybr Green Fast mix (Applied Biosytems) on a ViiA7 (Applied Biosystems). Housekeeping genes *HRPT1* and *GNB2L1* were used for normalisation. Primer sequences are available upon request.

Extracellular flux analysis

XF analysis was performed using the Seahorse XFe-96 Flux Analyser (Agilent) to examine oxygen consumption (OCR) and extracellular acidification rates (ECAR) as described previously [26]. In short, macrophages were seeded at a density of 75,000 cells per well in XF-96-cell culture plates (Agilent) and treated with 1 mM of adenine for 3 h prior to 24 h of LPS stimulation or left untreated. After LPS, supernatant was removed, macrophages were washed and Seahorse base medium (Agilent) without glucose, phenol red, and sodium bicarbonate, supplemented with 5 mM HEPES and 2 mM l-glutamine was added for 1 hour. During the Seahorse run, the plate underwent 3 cycles of mixing for 3 min followed by measurement for 3 min before the first injection, between all injections and after the final injection. The run consisted of 4 total injections; Glucose (GLU, final concentration in well 25 mM), Oligomycin (OM, final concentration 1.5 µM), FCCP (final concentration 1.5 µM), and Rotenone and antimycin A (ROT/AA, final concentration 1.25 µM and 2.5 µM, respectively, all Sigma Aldrich). Directly after the run, light microscope images were taken using Cytation 5 Cell Imaging multi-mode reader (BioTek) with a 4X magnification and cell counts were analysed using Gen 5™ software. Subsequently, flux rate data was normalised to cell counts with the following equation:

Normalised OCR or ECAR = OCR or ECAR / (well cell count / average cell count in unstimulated wells)

Data were analysed using Wave software version 2.6.0.31 as described previously [26]. In order to evaluate mitochondrial and glycolytic ATP production we used calculations as previously described [27].

Western blot

Macrophages seeded at 2×10^6 per well in a 6 well plate were treated with 1 mM of adenine for 3.5 h with or without a subsequent stimulation of LPS for 30 min. Cells were then washed and lysed with Nonidet p-40 (NP40) lysis buffer containing 0.2 mM phenylmethylsulfonyl fluoride (PMSF) and 2.5uL of dissolved phosphoSTOP tablet (Sigma-Aldrich) for 15 min on ice. Lysates were quantified using the DC assay (Bio-Rad). 25 µg of lysate were separated on a 10 % Tris Gel and transferred onto nitrocellulose membranes (Bio-Rad). Membranes were blocked in 5 % BSA in Tris-buffered saline containing 0.05 % Tween 20 (TBS–T) for 1 h at room temperature. After blocking, membranes were incubated with primary antibodies (Supplementary Table 1) at 4°C overnight. After primary antibody incubation, membranes were incubated with the corresponding fluorescent-conjugated secondary antibodies (Azure) and imaged with the Sapphire Biomolecular Imager (Azure). Finally, ImageJ software was used for analysis.

Statistics

Statistics were performed using GraphPad Prism 9 by means of a paired *t*-test or a two-way ANOVA which is stated in the figure legends. Data are displayed as mean ± SEM. Statistical significance is displayed as * = $p < 0.05$, ** = $p < 0.01$ and *** = $p < 0.001$ whilst a statistical trend of $p < 0.1$ and > 0.05 is displayed as a number.

Results

Adenine is more abundant in M-CSF-differentiated macrophages and suppresses inflammation

With the aim of identifying differentially abundant metabolites in M-CSF- and GM-CSF-differentiated macrophages, we performed a metabolomics analysis on human macrophages in either naïve, LPS- or interleukin 4-activated (IL-4) conditions (Figure 1A-C). We observed that adenine was the only metabolite that was more abundant in M-CSF macrophages stimulated with either LPS or IL-4 (Figure 1D). Since M-CSF macrophages have a more homoeostatic phenotype in comparison to GM-CSF macrophages, we wanted to investigate whether adenine contributed to this homoeostatic feature. Therefore,

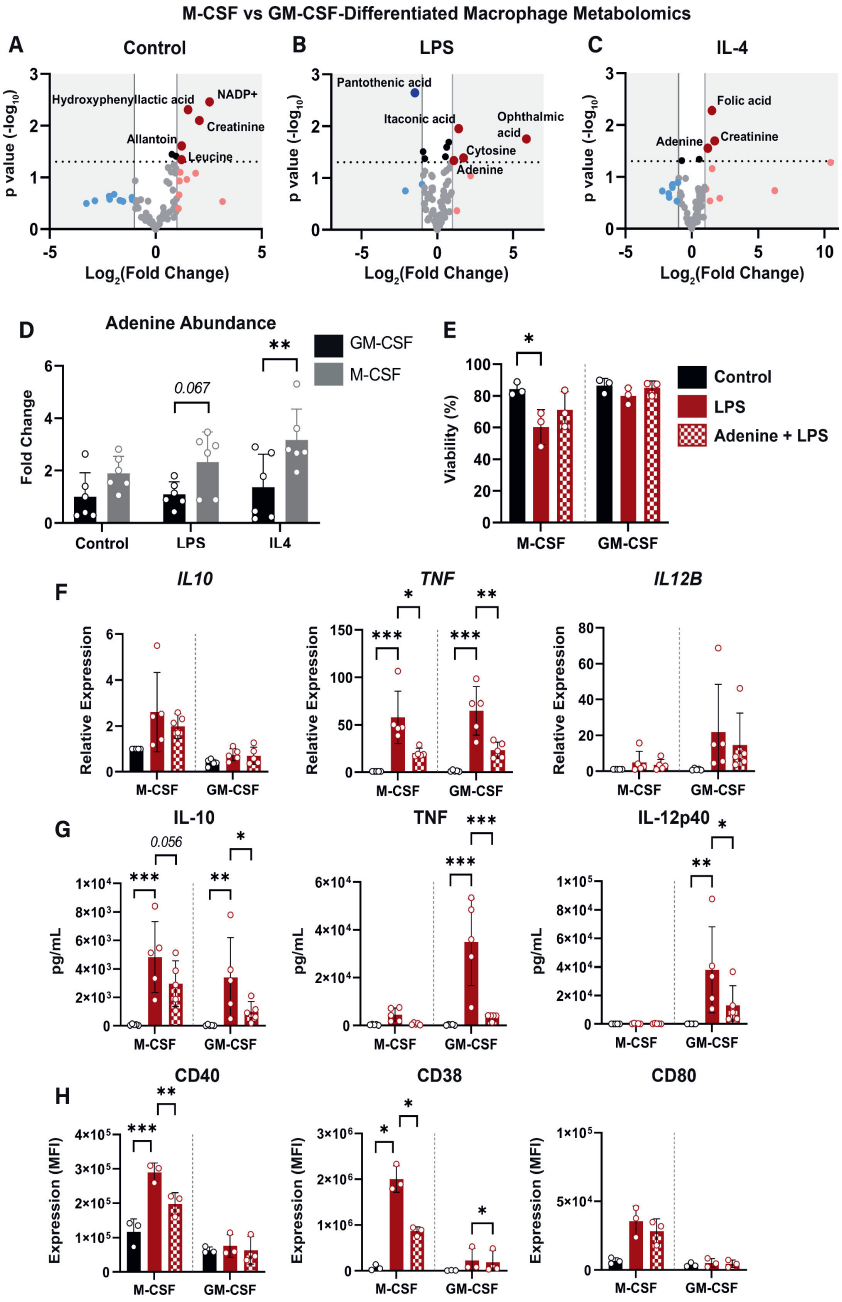

Figure 1. Adenine is significantly more abundant in M-CSF-differentiated human macrophages which dampens inflammation. A) Metabolomics volcano plots of GM-CSF vs M-CSF-differentiated human macrophages in unstimulated control, B) LPS (10 ng/mL) stimulated or C) IL-4 (20 ng/mL) stimulated conditions for 24 h. Metabolites are shown to either be reduced (blue), increased (red) or unchanged (black) in comparisons. Vertical grey lines indicate +1/-1 Log2(Fold Change) and horizontal dotted line indicates significance by ANOVA. D) Fold change of adenine in M-CSF and GM-CSF human macrophage

metabolomics stimulated with either LPS, IL-4 or unstimulated control. Baseline set to GM-CSF control (n = 6, two-way ANOVA). E) Cell viability in unstimulated (black), LPS stimulated (red) or adenine (1 mM) and LPS stimulated (red checkered) M-CSF and GM-CSF human macrophages after 24 h, measured via flow cytometry analysis of fixable viability dye (n = 3, two-way ANOVA). F) Secretion of IL-10 (left), TNF (middle) and IL-12p40 (right) from M-CSF and GM-CSF human macrophages after treatment with (stripes) or without (filled) adenine for 1 hour before stimulation with (red) or without (black) LPS for 24 h (n = 5, two-way ANOVA). G) Inflammatory cytokine gene expression after 1 hour of adenine and 3 h of LPS (n = 5, two-way ANOVA). H) Flow cytometry quantification of human macrophages after 1 hour of adenine and 24 h of LPS (n = 3, two-way ANOVA). Data points in bar graphs display individual human donors and error bars show SD whilst data points of volcano plots represent the mean of 3 donors.

macrophages were pre-treated with adenine for 1 hour prior to 24 h with or without LPS to induce inflammatory cytokine secretion. Addition of adenine to human macrophages did not affect cell viability of inflammatory macrophages (Figure 1E). Gene expression of TNF was suppressed by adenine in both M-CSF and GM-CSF macrophages, however expression of *IL10* and *IL12B* were not significantly affected (Figure 1F). When looking at secretion of cytokines however, inflammatory cytokines TNF and IL-12p40 and the anti-inflammatory cytokine IL-10 were significantly suppressed in adenine-treated GM-CSF macrophages (Figure 1G). We also observed a significant decrease in cell surface markers CD40 and CD38 in M-CSF, but not GM-CSF- differentiated macrophages (Figure 1H). CD40 is a co-stimulatory molecule in antigen presentation for T-cell stimulation and CD38 is an adenine salvage pathway marker, involved in generating new adenosine nucleotides [28]. CD80, a co-stimulatory molecule for the activation of T cells was unaffected by adenine. Combined, we show that adenine is more abundant in M-CSF macrophages and has a immunosuppressive action on both M-CSF and GM-CSF macrophages.

Adenine prevents inflammatory metabolite signatures and drives macrophages into quiescence

Due to the immunosuppressive nature of adenine in inflammatory and homoeostatic macrophages, and the fact that it is a metabolite itself, we considered that adenine may also influence human macrophage metabolism directly. A change in the metabolic profile of macrophages can determine their inflammatory potential. To ensure sufficient time for adenine to enter the cell, we pre-treated macrophages with adenine for 3 h before stimulation with or without LPS for 24 h. Metabolites that are known to be regulated in LPS conditions (such as itaconate, succinate, fumarate and 2-hydroxyglutarate) and appeared to be regulated in our setting were attenuated when macrophages were pre-treated with adenine (Figure 2A; Supplemental Table 2) [17,29]. Moreover, ADP-ribose was reduced after adenine treatment, the product of marker CD38, as well as adenosine, both of which are also involved in the adenine salvage pathway (Supplementary Figure 1) [28,30]. From this data we can also observe that adenine is readily taken up by the cell, since intracellular abundance increased upon adenine treatment in both naïve and LPS macrophages (Figure 2B). Subsequently, we preformed Seahorse extracellular flux analysis

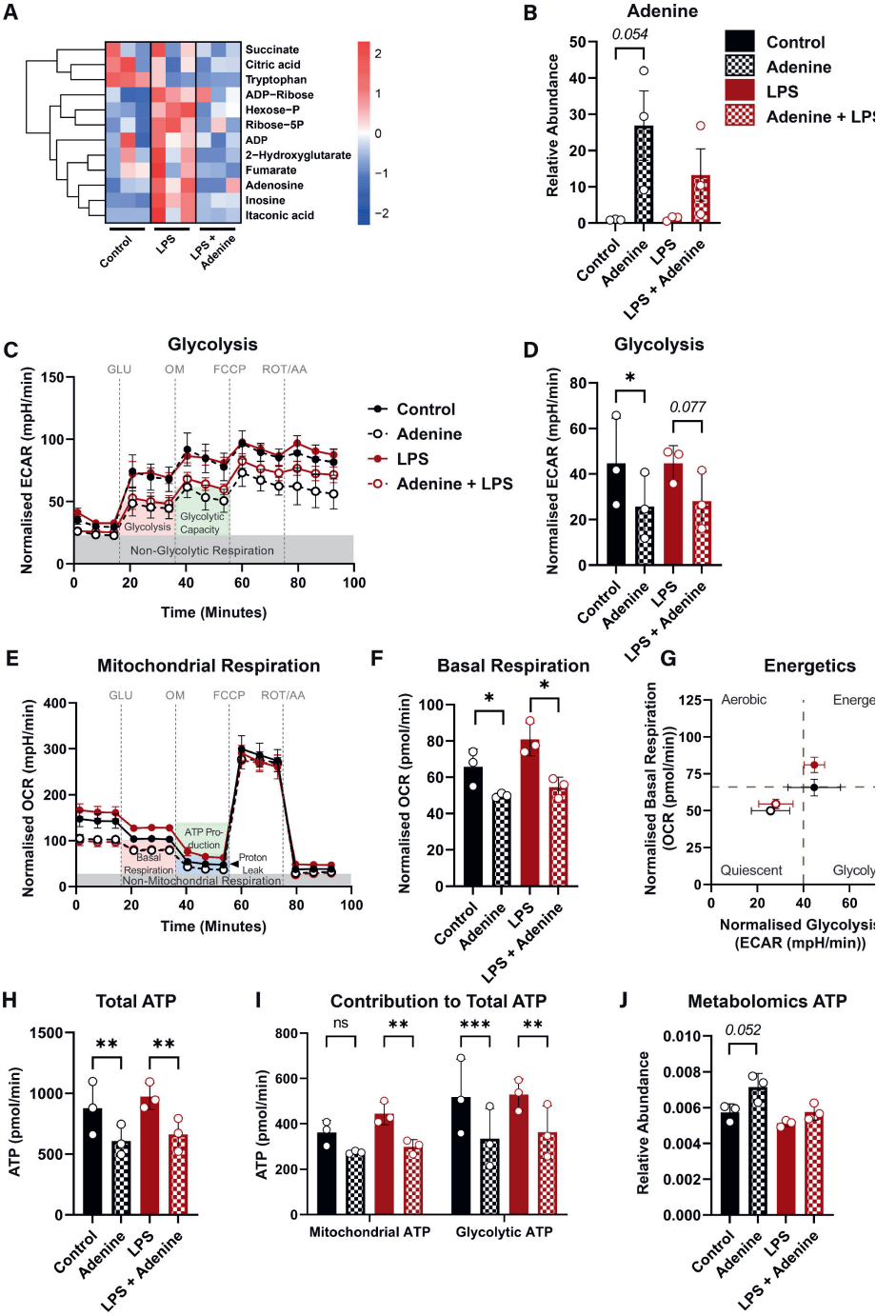

Figure 2. Adenine drives LPS stimulated macrophages towards metabolic quiescence. A) Metabolomics heatmap of human M-CSF macrophages pre-treated with adenine for 3 h (1 mM) followed by 24 h of LPS (10 ng/mL) stimulation. B) Relative abundance of adenine in M-CSF human macrophage metabolomics

stimulated with adenine and LPS (n = 3, paired t-test). C) Seahorse extracellular flux on M-CSF macrophages stimulated with adenine and LPS showing glycolytic flux with D) quantified glycolysis and E) mitochondrial respiratory flux with F) quantified basal respiration (n = 3). G) Cellular energetics profile from Seahorse extracellular flux analysis of M-CSF macrophages (n = 3). H) Total cellular production of ATP from Seahorse extracellular flux analysis with I) mitochondrial and glycolytic contribution (n = 3, paired *t*-test). J) Relative abundance of ATP in M-CSF human macrophage metabolomics stimulated with adenine and LPS (n = 3, paired *t*-test). Data points in bar graphs display individual human donors and error bars show SD whilst data points of Seahorse extracellular flux and energetics represent the mean of 3 donors and error bars show SEM.

on macrophages treated with adenine and LPS (Figure 2C-F). We observed adenine had a suppressive effect on both glycolysis and mitochondrial respiration, pushing macrophages towards a more quiescent metabolic phenotype (Figure 2G). As such, adenine slowed ATP production significantly in both glycolysis and OXPHOS, (Figure 2H & 2I). Reverting back to the metabolomics, we observed an increase in total intracellular ATP content for adenine-treated naïve macrophages, although not significant. This suggests a reduced utilisation of intracellular ATP molecules in combination with the reduced ATP production, regardless of the fact that adenine is a precursor of ATP synthesis (Figure 2J). As such, adenine prevents accumulation of typical inflammatory metabolite signatures and steers human macrophages into a metabolically quiescent state, highlighting it as an attractive immunometabolite to study in inflammatory disease models.

The anti-inflammatory effects of adenine are not facilitated through metabolic signalling pathways NF-κB, AKT, AMPK and p38 MAPK

In order to further understand the mechanisms behind these observations, we measured the expression of NF-κB and TNF inhibitors *NFKBIA* and *TNFAIP3* as we saw significant reduction of TNF. At a transcriptional level however, these markers were unaffected by adenine (Figure 3A). Adenine is also incorporated into the adenine salvage pathway which can be utilised to generate ATP for use as either nucleic acid bases or providing energy. Enzymes APRT and PNP are the first enzymes responsible for synthesising AMP and adenosine from adenine in the adenine salvage pathway, respectively (Figure 3B & Supplementary Figure 1) [30,31]. Therefore we investigated gene expression of *APRT* and *PNP* but these genes were also stable in adenine-treated macrophages. Due to adenines' ability to steer macrophage metabolic activity towards a quiescent phenotype, we explored whether this was mediated through changes in phosphorylation levels of metabolic regulators p38 MAPK, AKT and AMPK. Nevertheless, phosphorylation of all three of these metabolic regulators were unaffected by treatment with adenine (Figure 3C & D). Together this demonstrates that adenines' immunoregulatory properties are mediated through alternative pathways to NF-κB, p38 MAPK, AKT and AMPK, whilst also not having an effect on the adenine salvage pathway on the gene expression level.

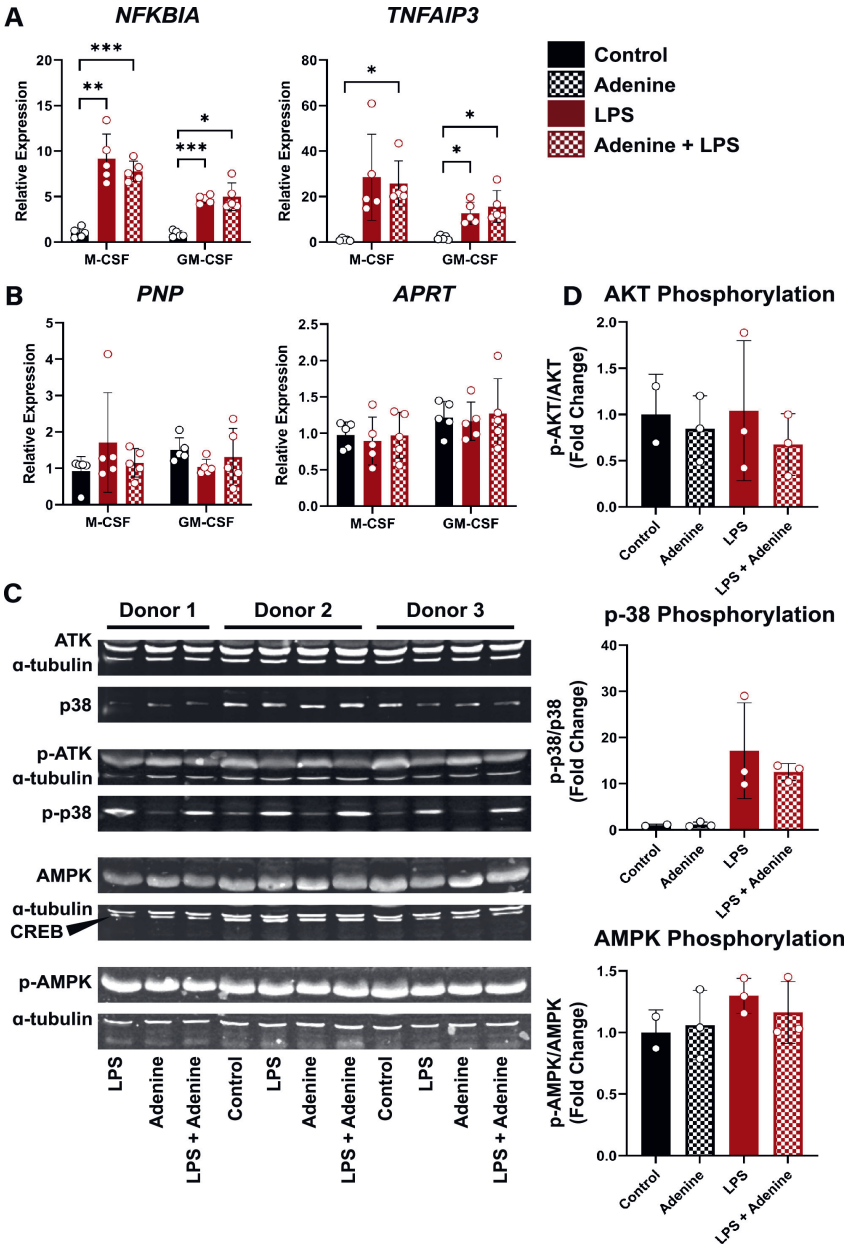

Figure 3. Adenine does not signal through inflammatory regulator NF-κB, adenine salvage pathway or metabolic signalling pathways AMPK, AKT and p38 MAPK. A) qPCR derived gene expression of NF-κB or B) adenine salvage pathway related genes in human macrophages after 1 hour of adenine (1 mM) and 3 h of LPS (10 ng/mL) (n = 5, two-way ANOVA). C) Western blot plots of M-CSF human macrophages treated with 3.5 h of adenine and 30 min of LPS with D) calculated fold changes of stained markers AMPK, AKT and p38 MAPK and respective phosphorylation (n = 3, paired *t*-test). Data points display individual human donors and error bars show SD.

Discussion

In this study, we examined the immunomodulatory effects of metabolites specifically regulated in either M-CSF or GM-CSF-differentiated human macrophages with the aim of shifting macrophage inflammatory states. In the context of inflammatory diseases, it is widely accepted that restoring the balance of macrophage populations would lead to better disease outcomes in patients [3,4]. Accordingly, we identified the metabolite adenine to specifically accumulate in M-CSF-differentiated macrophages and therefore hypothesised that this metabolite may contribute to the generation of more homoeostatic macrophages. We show that adenine dampens immune responses in human macrophages, as illustrated by the suppression of inflammatory cytokine gene expression and subsequent cytokine secretion. Expression of inflammatory surface markers were also reduced. This observation supports previous data that showed the anti-inflammatory properties of adenine on RAW264.7 and THP-1 macrophage cell lines as well as within the peritoneal cavity of mice [24,32]. Increased conversion of adenine to AMP by means of enzyme APRT was measured in these cell lines. This conversion was a potential mechanism to explain how AMPK was phosphorylated and thus contributed to the anti-inflammatory potential of exogenous adenine. In our setting however, neither AMP nor p-AMPK were altered, whilst the anti-inflammatory effects of adenine were retained, consequently indicating that adenine signals independently of AMPK in human macrophages. We also observed a suppressive effect of adenine on both glycolysis and OXPHOS, resulting in lower ATP production. Whilst we do not show a clear mechanism on how this effect is achieved, we do believe that adenine is an interesting metabolite to study further in the context of inflammatory diseases.

Additionally, there have been numerous studies observing different lung carcinoma metabolomes which identify adenine as a significantly accumulated metabolite [33,34,35]. Whilst this is likely a result of increased nucleotide metabolism in order to meet the demands of sustained cancer cell proliferation, this could lead to the release of adenine into the tumour microenvironment. On the basis of the anti-inflammatory activity of adenine, demonstrated in this study as well as others, we consider that adenine released in this manor may drive macrophages into a quiescent state. As such, this would generate an environment that supports tumour growth and progressively decelerates sequential anti-tumour responses. Moreover, nucleotide metabolism, which requires a substantial supply of adenine amongst other purines and pyrimidines, is considered a vital aspect of cancer development and evidence shows that interfering with these pathways could dampen disease progression as reviewed extensively recently [36,37,38]. Thus, targeting purine metabolism and lowering adenine levels in tumours could potentially increase macrophage anti-tumour activity, whilst decreasing cancer cell proliferation. Aside from the immunomodulatory aspect of adenine, targeting purine metabolism in cancer has

already been suggested as a way to improve immunogenicity in patients. It is thought that this occurs by lowering purine production so that pyrimidines are in excess and lead to pyrimidine transversion mutations, increasing the immunogenicity of tumours [30]. Consequently, targeting adenine metabolism to control the functional activity of cells may be worth investigating in the context of cancer and other inflammatory diseases. However, understanding the mechanism by which adenine induces these anti-inflammatory signals is essential before considering the development of adenine-based therapies.

Overall, the data presented in this research article show adenine's immunomodulatory role on human macrophages by dampening inflammatory cytokine secretion and surface marker expression. This suppression occurs in parallel with dampened OXPHOS and glycolysis resulting in a deficiency in ATP synthesis. As such, this work sheds light on how the accumulation of adenine within inflammatory disease environments may support or hinder macrophage facilitated disease resolution.

Acknowledgements

Funding

This research received financial support from the Amsterdam Cardiovascular Sciences (ACS) research institute. J.V.d.B. was funded by a consortia grant from European Research Area Network on Cardiovascular Diseases (ERA-CVD 2019T108), the Netherlands Heart Foundation senior fellowship (2017T048) and an ENW-Klein-1 grant from NWO (OCENW. KLEIN.268).

CRediT authorship contribution statement

Karl J Harber: Conceptualization, Methodology, Formal analysis, Investigation, Visualization, Writing – original draft, Writing – review & editing. Thuc-Anh Nguyen: Methodology, Formal analysis, Investigation, Writing – review & editing. Bauke V Schomakers: Methodology, Investigation, Writing – review & editing. Daan A F Heister: Investigation. Helga E. de Vries: Writing – review & editing. Michel van Weeghel: Conceptualization, Writing – review & editing, Funding acquisition. Jan Van den Bossche: Conceptualization, Writing – review & editing, Funding acquisition. Menno P J de Winther: Conceptualization, Writing – review & editing, Funding acquisition.

Declaration of competing interest

The authors declare the following financial interests/personal relationships which may be considered as potential competing interests: Jan Van den Bossche reports financial support was provided by European Research Area Network on Cardiovascular Diseases.

Jan Van den Bossche reports financial support was provided by Amsterdam Cardiovascular Sciences.

References

1. T.A. Wynn, A. Chawla, J.W. Pollard, Macrophage biology in development, homeostasis and disease, Nature 496 (7446) (2013) 445–455.
2. T.A. Wynn, K.M. Vannella, Macrophages in Tissue Repair, Regeneration, and Fibrosis. Immunity 44 (3) (2016) 450–462.
3. E.A. Ross, A. Devitt, J.R. Johnson, Macrophages: the Good, the Bad, and the Gluttony, Front Immunol 12 (2021) 708186.
4. N. Wang, H. Liang, K. Zen, Molecular mechanisms that influence the macrophage m1-m2 polarization balance, Front Immunol 5 (2014) 614.
5. K.J. Moore, F.J. Sheedy, E.A. Fisher, Macrophages in atherosclerosis: a dynamic balance, Nat Rev Immunol 13 (10) (2013) 709–721.
6. D.G. DeNardo, B. Ruffell, Macrophages as regulators of tumour immunity and immunotherapy, Nat Rev Immunol 19 (6) (2019) 369–382.
7. A. Mantovani, et al., Tumour-associated macrophages as treatment targets in oncology, Nat Rev Clin Oncol 14 (7) (2017) 399–416.
8. T. Gauthier, W. Chen, Modulation of Macrophage Immunometabolism: a New Approach to Fight Infections, Front Immunol 13 (2022) 780839.
9. E.M. Palsson-McDermott, L.A.J. O'Neill, Targeting immunometabolism as an antiinflammatory strategy, Cell Res 30 (4) (2020) 300–314.
10. B. Becher, S. Tugues, M. Greter, GM-CSF: from Growth Factor to Central Mediator of Tissue Inflammation, Immunity 45 (5) (2016) 963–973.
11. J.A. Hamilton, Colony-stimulating factors in inflammation and autoimmunity, Nat Rev Immunol 8 (7) (2008) 533–544.
12. I. Brocheriou, et al., Antagonistic regulation of macrophage phenotype by M-CSF and GM-CSF: implication in atherosclerosis, Atherosclerosis 214 (2) (2011) 316–324.
13. A. Lukic, et al., GM-CSF- and M-CSF-primed macrophages present similar resolving but distinct inflammatory lipid mediator signatures, FASEB J 31 (10) (2017) 4370–4381.
14. Y.R. Na, et al., GM-CSF Induces Inflammatory Macrophages by Regulating Glycolysis and Lipid Metabolism, J. Immunol 197 (10) (2016) 4101–4109.
15. S.N. Zhu, M. Chen, J. Jongstra-Bilen, M.I. Cybulsky, GM-CSF regulates intimal cell proliferation in nascent atherosclerotic lesions, J. Exp. Med 206 (10) (2009) 2141–2149.
16. S. Yadav, A. Priya, D.R. Borade, R. Agrawal-Rajput, Macrophage subsets and their role: co-relation with colony-stimulating factor-1 receptor and clinical relevance, Immunol Res 71 (2) (2023) 130–152.
17. D.G. Ryan, et al., Coupling Krebs cycle metabolites to signalling in immunity and cancer, Nat. Metab 1 (2019) 16–33.
18. J. Van den Bossche, L.A. O'Neill, D. Menon,

Macrophage Immunometabolism: where are we (going)? Trends Immunol 38 (6) (2017) 395–406.

19. L.A. O'Neill, R.J. Kishton, J. Rathmell, A guide to immunometabolism for immunologists, Nat. Rev. Immunol 16 (9) (2016) 553–565.
20. Y.R. Na, et al., Proteomic analysis reveals distinct metabolic differences between granulocyte-macrophage colony stimulating factor (gm-csf) and macrophage colony stimulating factor (m-csf) grown macrophages derived from murine bone marrow cells, Mol. Cell Proteomics 14 (10) (2015) 2722–2732.
21. M. Wessendarp, et al., Role of GM-CSF in regulating metabolism and mitochondrial functions critical to macrophage proliferation, Mitochondrion 62 (2022) 85–101.
22. J. Van den Bossche, et al., Mitochondrial dysfunction prevents repolarization of inflammatory macrophages, Cell Rep 17 (3) (2016) 684–696.
23. R. Luque-Martin, et al., IFN-gamma drives human monocyte differentiation into highly proinflammatory macrophages that resemble a phenotype relevant to psoriasis, J. Immunol 207 (2) (2021) 555–568.
24. P. Silwal, et al., Adenine attenuates lipopolysaccharide-induced inflammatory reactions, Korean J Physiol Pharmacol 22 (4) (2018) 379–389.
25. B.V. Schomakers, et al., Polar metabolomics in human muscle biopsies using a liquid-liquid extraction and full-scan LC-MS, STAR Protoc 3 (2) (2022) 101302.
26. J. Van den Bossche, J. Baardman, M.P. de Winther, Metabolic Characterization of Polarized M1 and M2 Bone Marrow-derived Macrophages Using Real-time Extracellular Flux Analysis, J. Vis Exp (105) (2015).
27. S.G.S. Verberk, et al., An integrated toolbox to profile macrophage immunometabolism, Cell Rep Methods 2 (4) (2022) 100192.
28. K.A. Hogan, C.C.S. Chini, E.N. Chini, The Multi-faceted Ecto-enzyme CD38: roles in Immunomodulation, Cancer, Aging, and Metabolic Diseases, Front Immunol 10 (2019) 1187.
29. K.E. de Goede, et al., D-2-Hydroxyglutarate is an anti-inflammatory immunometabolite that accumulates in macrophages after TLR4 activation, Biochim Biophys Acta Mol Basis Dis 1868 (9) (2022) 166427.
30. H.L. Wu, et al., Targeting nucleotide metabolism: a promising approach to enhance cancer immunotherapy, J Hematol Oncol 15 (1) (2022) 45.
31. J. Huyet, et al., Structural Insights into the Forward and Reverse Enzymatic Reactions in Human Adenine Phosphoribosyltransferase, Cell Chem Biol 25 (6) (2018) 666-676 e4.
32. T.T. Wu, et al., The anti-inflammatory function of adenine occurs through AMPK activation and its downstream transcriptional regulation in THP-1 cells, Biosci. Biotechnol. Biochem. 83 (12) (2019) 2220–2229.
33. P. Moreno, et al., Metabolomic profiling of human lung tumor tissues - nucleotide metabolism as a candidate for therapeutic interventions and biomarkers, Mol Oncol. 12 (10) (2018) 1778–1796.
34. W.R. Wikoff, et al., Metabolomic markers of altered nucleotide metabolism in early stage adenocarcinoma, Cancer Prev Res (Phila) 8 (5) (2015) 410–418.
35. B. Callejon-Leblic, et al., Metabolic profiling of potential lung cancer

biomarkers using bronchoalveolar lavage fluid and the integrated direct infusion/gas chromatography mass spectrometry platform, J. Proteomics 145 (2016) 197–206.

36. D.D. Shi, M.R. Savani, K.G. Abdullah, S.K. McBrayer, Emerging roles of nucleotide metabolism in cancer, Trends Cancer 9 (8) (2023) 624–635.

37. N.J. Mullen, P.K. Singh, Nucleotide metabolism: a pan-cancer metabolic dependency, Nat. Rev. Cancer 23 (5) (2023) 275–294.

38. Y. Ariav, et al., Targeting nucleotide metabolism as the nexus of viral infections, cancer, and the immune response, Sci. Adv 7 (21) (2021).

Supplementary materials

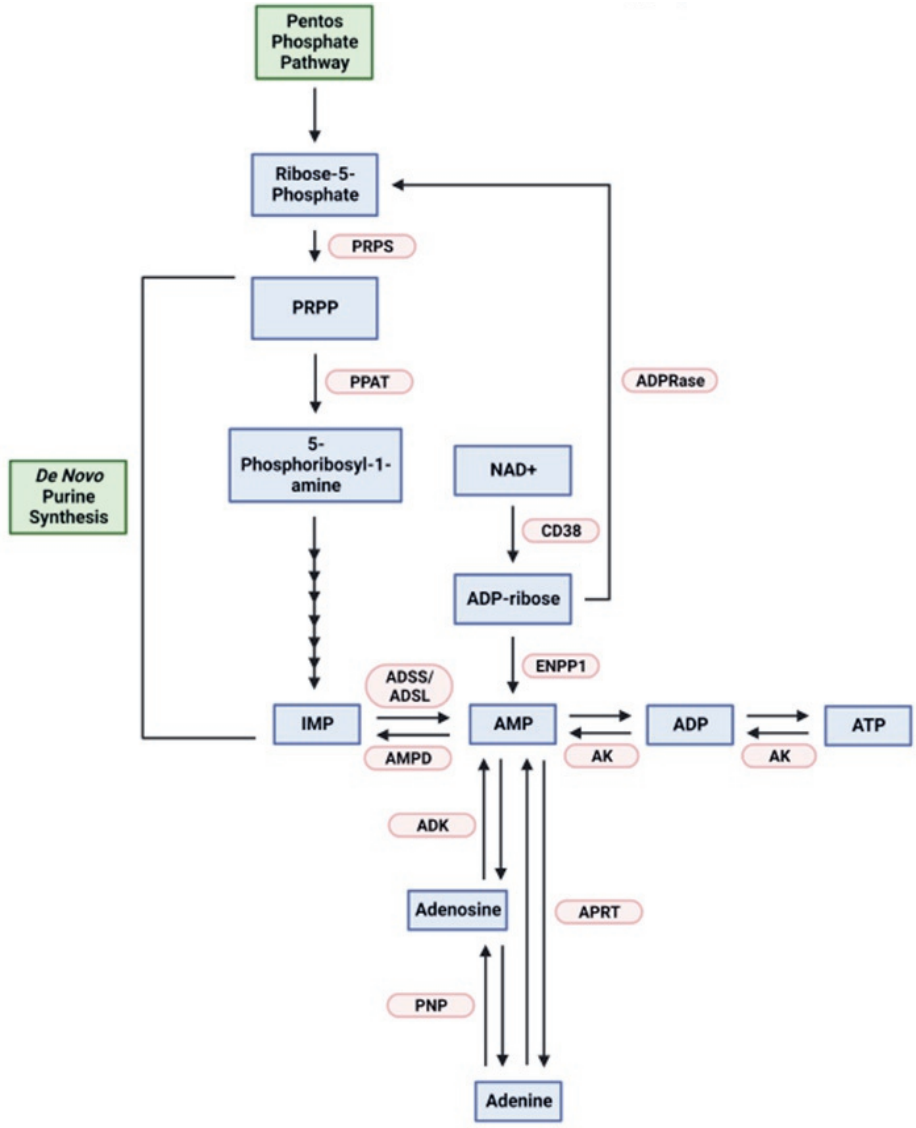

Supplemental Figure 1. Adenine salvage pathway and purine metabolism. A schematic displaying the incorporation of adenine into the purine salvage pathway and de novo purine synthesis. Blue rectangles are metabolites, brown oblongs are enzymes, green rectangles are metabolic pathways. Created with BioRender.com.

Supplemental Table 1. Reagent list

Antibodies		
Antibody	**Source**	**Identifier**
Fixable Viability Dye eFluor™ 780	eBioscience	65-0865-14
PE anti-human CD40 Antibody	Biolegend	334307
PE/Cyanine7 anti-human CD38 Antibody	Biolegend	356607
Alexa Fluor® 700 Mouse Anti-Human CD80	BD bioscience	561133
CD16/CD32 Monoclonal Antibody	eBioscience	14-0161
p38 MAPK	Cell Signaling	9212
Phospho-p38 MAPK	Cell Signaling	9211
AMPKα	Cell Signaling	2532
Phospho-AMPKα (Thr172)	Cell Signaling	2535
Akt	Cell Signaling	9272
Phospho-Akt (Ser473)	Cell Signaling	9271
α-tubulin	Cedarlane	CLT9002
ELISA MAX™ Standard Set Human IL-10	Biolegend	430601
ELISA MAX™ Standard Set Human TNF-α	Biolegend	430201
ELISA MAX™ Standard Set Human IL-12/IL-23 (p40)	Biolegend	430701
Reagents		
Reagent	**Source**	**Identifier**
D-(+)-Glucose solution (45%)	Sigma Aldrich	G8769
Oligomycin	Sigma Aldrich	O4876
FCCP	Sigma Aldrich	C2920
Rotenone	Sigma Aldrich	R8875
Antimycin A	Sigma Aldrich	A8674
Adenine	Sigma Aldrich	A2786
Itaconic Acid	Sigma Aldrich	I29204
D-Pantothenic acid hemicalcium salt	Sigma Aldrich	P5155
β-Alanine	Sigma Aldrich	A9920
Primers		
Target	**Source**	**Sequence**
TNF-FW	Invitrogen	GGCGTGGAGCTGAGAGAT
TNF-RV	Invitrogen	TGGTAGGAGACGGCGATG
IL10-FW	Invitrogen	AAGAGGAAAGTAAGGGACCTCCT
IL10-RV	Invitrogen	GGAAGAAGTTGAAATAACAAGGAAA
IL12B-FW	Invitrogen	CACCGTAAGTGTCTGGAAGG
IL12B-RV	Invitrogen	TGTGTATCAGGTTCATTCATGC
CD86-FW	Invitrogen	CACTATGGGACTGAGTAACATTC
CD86-RV	Invitrogen	CAGGTCTGCAGTCTCATTGAA

Supplemental Table 1. Continued

CD163-FW	Invitrogen	GATGTGGATCTGCACTCAAA
CD163-RV	Invitrogen	TCCAGAGAGAAGTCCGAATC
IL23A-FW	Invitrogen	TGTTCCCCATATCCAGTGTG
IL23A-RV	Invitrogen	TCCTTTGCAAGCAGAACTGA
NFKBIA-FW	Invitrogen	GCTACCAACTACAATGGCCACAC
NFKBIA-RV	Invitrogen	GGACACCAAAAGCTCCACGA
TNFAIP3-FW	Invitrogen	CCCTTGGAAGCACCATGTTTG
TNFAIP3-RV	Invitrogen	CTGGCTCGATCTCAGTTGCT
PNP-FW	Invitrogen	GGCCCAATGATGAAAGGTTTGG
PNP-RV	Invitrogen	TAGTCCGGTCGTAGGCATCA
APRT-FW	Invitrogen	GCGTGGTATTCAGGGACATCT
APRT-RV	Invitrogen	GTCTAGGCCTGCGATGTAGT

Supplemental Table 2. Metabolomics data of adenine treated macrophages

Metabolite	Control_01	Control_02	Control_03	LPS_01	LPS_02	LPS_03	AdenineLPS_01	AdenineLPS_02	AdenineLPS_03
2-Hydroxyglutarate	8.806	21.764	10.590	33.982	12.901	21.362	6.802	6.687	10.521
Adenosine	0.307	0.475	0.493	0.953	0.622	0.958	0.334	0.335	0.738
ADP-Ribose	1.611	0.742	0.791	3.066	2.409	2.072	2.607	1.290	1.788
Citric acid	37.820	47.281	18.638	30.825	15.306	28.966	17.591	24.684	24.355
Hexose-P	2.642	2.307	1.169	5.529	7.267	8.766	1.830	3.819	4.217
Inosine	3.302	3.190	1.537	40.356	20.489	27.239	7.906	11.863	11.374
Ribose-5P	1.057	1.850	0.675	3.500	4.194	2.658	1.110	2.524	1.218
Succinate	49.045	22.065	15.607	55.353	15.451	32.372	23.515	14.050	22.412
Itaconic acid	0.001	0.001	0.001	344.586	41.508	190.795	8.840	0.844	21.383
ADP	85.547	168.390	57.977	145.674	108.206	119.279	99.143	68.262	94.802
Tryptophan	8.769	7.998	6.232	4.829	0.341	0.941	0.788	1.017	1.095
Fumarate	8.886	13.923	13.197	24.609	9.086	15.433	9.488	9.207	7.527


4

D-2-Hydroxyglutarate is an Anti-Inflammatory Immunometabolite that Accumulates in Macrophages After TLR4 Activation

Kyra E. de Goede,[1] Karl J. Harber,[1,2,3] Friederike S. Gorki,[1,4] Sanne G.S. Verberk,[1] Laszlo A. Groh,[1] Eelco D. Keuning,[1] Eduard A. Struys,[5] Michel van Weeghel,[3] Arvand Haschemi,[6] Menno P.J. de Winther,[2] Xanthe A.M.H. van Dierendonck,[1] and Jan Van den Bossche[1]

Biochimica et Biophysica Acta - Molecular Basis of Disease, 1868 (9), 166427 (2022)

[1] Department of Molecular Cell Biology and Immunology, Amsterdam Cardiovascular Sciences, Amsterdam Gastroenterology Endocrinology Metabolism, Amsterdam Institute for Infection and Immunity, Cancer Centre Amsterdam, Amsterdam UMC, Vrije Universiteit Amsterdam, Amsterdam, the Netherlands

[2] Amsterdam UMC, University of Amsterdam, Department of Medical Biochemistry, Experimental Vascular Biology, Amsterdam Cardiovascular Sciences, 1105, AZ, Amsterdam, the Netherlands

[3] Amsterdam UMC, University of Amsterdam, Laboratory Genetic Metabolic Diseases, Amsterdam Cardiovascular Sciences, 1105, AZ, Amsterdam, the Netherlands

[4] Institute of Innate Immunity, University Hospital Bonn, University of Bonn, Bonn 53127, Germany

[5] Metabolic Unit, Department of Clinical Chemistry, Amsterdam UMC, Amsterdam, the Netherlands

[6] Department of Laboratory Medicine, Medical University of Vienna, 1090 Vienna, Austria

Abstract

Macrophages undergo extensive metabolic rewiring upon activation which assist the cell in roles beyond energy production and synthesis of anabolic building blocks. So-called immunometabolites that accumulate upon immune activation can serve as co-factors for enzymes and can act as signaling molecules to modulate cellular processes. As such, the Krebs-cycle-associated metabolites succinate, itaconate and alpha-ketoglutarate (αKG) have emerged as key regulators of macrophage function.

Here, we describe that 2-hydroxyglutarate (2HG), which is structurally similar to αKG and exists as two enantiomers, accumulates during later stages of LPS-induced inflammatory responses in mouse and human macrophages. D-2HG was the most abundant enantiomer in macrophages and its LPS-induced accumulation followed the induction of Hydroxyacid-Oxoacid Transhydrogenase (HOT). HOT interconverts αKG and gamma-hydroxybutyrate into D-2HG and succinic semialdehyde, and we here identified this enzyme as being immune-responsive and regulated during the course of macrophage activation. The buildup of D-2HG may be further explained by reduced expression of D-2HG Dehydrogenase (D2HGDH), which converts D-2HG back into αKG, and showed inverse kinetics with HOT and D-2HG levels.

We tested the immunomodulatory effects of D-2HG during LPS-induced inflammatory responses by transcriptomic analyses and functional profiling of D-2HG-pre-treated macrophages *in vitro* and mice *in vivo*. Together, these data suggest a role for D-2HG in the negative feedback regulation of inflammatory signaling during late-stage LPS-responses *in vitro* and as a regulator of local and systemic inflammatory responses *in vivo*. Finally, we show that D-2HG likely exerts distinct anti-inflammatory effects, which are in part independent of αKG-dependent dioxygenase inhibition.

Together, this study reveals an immunometabolic circuit resulting in the accumulation of the immunomodulatory metabolite D-2HG that can inhibit inflammatory macrophage responses.

Introduction

Macrophages are innate immune cells that mount a first line defence against a broad range of pathogens. However, unbalanced macrophage responses play a perpetuating role in diseases that impact society. Pro-inflammatory (M1-like) macrophages drive chronic inflammation and the progression of diseases like atherosclerosis, obesity, and diabetes [1,2]. On the other hand, the immunosuppressive and reparative functions of anti-inflammatory (M2-like) macrophages can be hijacked by cancer cells to support tumor growth [3]. Despite recent successes of immunomodulatory treatments in the clinic, some current therapies are only moderately effective in dampening disease progression. Hence, there is an unmet need for new therapeutic strategies. Since macrophages play a central role in inflammatory responses, a better understanding of how these cells are regulated will pave the way for the development of new therapeutic strategies aimed at reprogramming aberrant macrophage activation with the goal of treating a wide spectrum of diseases. Depending on the setting, the goal is to inhibit macrophage effector functions to dampen (chronic) inflammation, or to activate macrophages to combat cancer progression.

Recent advances in the immunometabolism field have highlighted how metabolic processes are central to regulating macrophage function and are further shown to have a causal relation in disease progression. To meet their increased energy and biosynthetic demands in a timely manner, macrophages rapidly ramp up glycolysis upon activation, ultimately leading to increased abundance of specific metabolites. In this context, metabolites are more than intermediates of biochemical reactions having much broader roles in modulating cellular processes. They do so by acting as co-factors for enzymes and by mediating posttranslational modifications of histones, transcription factors, enzymes and other key proteins regulate cellular phenotypes. As such, so-called immunometabolites like succinate, itaconate and αKG are now being recognized as important signaling molecules that regulate immunity and disease [4,5,6,7].

Understanding the kinetics of such immunometabolites during the course of an immune challenge and studying the subsequent functional consequences are essential to define the exact role of metabolites in regulating inflammation [8,9]. To progress the immunometabolism field towards clinical application, immunometabolites should be identified that are regulated in both mice and humans, and for which the kinetics of induction fits their function. This is important since some earlier observations in mouse macrophages (e.g. iNOS/arginase-1-balance in "M1/M2") do not always occur in human cells [10]. Moreover, the temporal aspect of immunometabolism has been largely overlooked so far [11].

Here, we describe D-2-hydroxyglutarate (D-2HG) as a regulatory immunometabolite that is induced by LPS in a time frame relevant for the resolution of inflammation in macrophages. 2HG exists in two stereoisomers: D-2HG (also known as R-2HG) and L-2HG (or S-2HG) that are produced from α-ketoglutarate (αKG) by distinct enzymes [12]. L-2HG is promiscuously formed by Malate Dehydrogenase (MDH1/2) and Lactate Dehydrogenase A (LDHA) in hypoxic and acidic conditions [12,13,14]. While mutant Isocitrate Dehydrogenase 1 or 2 (IDH1/2) are the most studied producers of D-2HG in certain cancers, Phosphoglycerate Dehydrogenase (PHGDH), Hydroxyacid-Oxoacid Transhydrogenase (HOT) and to some extent also wild-type IDH1/2, can generate D-2HG [15,16]. PHGDH is the first enzyme in serine biosynthesis and along with the oxidation of 3-phosphoglycerate, PHGDH catalyzes the NADH-dependent reduction of αKG into D-2HG. Similarly, HOT catalyzes the conversion of gamma-hydroxybutarate to succinic semialdehyde, coupled to the reduction of αKG to D-2HG as a byproduct. In normal conditions, D- and L-2HG levels are kept low by their respective dehydrogenases (D2HGDH and L2HGDH) which oxidize D- and L-2HG back into αKG. Defects in these enzymes cause 2-hydroxyglutaric aciduria, a rare inherited metabolic disorder mainly affecting the brain [17]. As mentioned above, D-2HG is best known as a so-called oncometabolite that aberrantly accumulates in cancer cells with *IDH1/2* mutations and plays a key role in the initiation and progression of glioma and acute myeloid leukemia [18]. D-2HG not only exerts its regulatory effects within cancer cells, but can also be released into the tumor microenvironment to suppress anti-tumor effector functions of T cells and macrophages [19,20]. Opposed to D-2HG being generated by cancer cells, L-2HG was found to be generated within activated T cells and hence was named an "immunometabolite" [14]. L-2HG affects the differentiation, proliferation and function of T cells and was recently also described to promote the LPS-induced expression of the pro-inflammatory cytokine IL-1β in macrophages [14,21]. While D-2HG has been well-documented as an oncometabolite in transformed cancer cells and L-2HG has been studied to some extent as an immunometabolite in T cells and macrophages, endogenous D-2HG production and its functional consequences has to be further investigated in macrophages [14,18,21].

Here, we detected 2HG among the most highly induced metabolites in LPS-induced human and mouse macrophages. D-2HG was the most abundant 2HG enantiomer and accumulated at time points when the initial inflammatory response begins to resolve. The kinetics of D-2HG accumulation aligns with our functional and transcriptomics data indicating that D-2HG suppresses inflammatory responses in macrophages. Our data suggest that the accumulation of D-2HG in response to LPS-stimulation is mediated by HOT and D2HGDH and that the immunomodulatory effects of D-2HG are in part independent of its function as a competitive inhibitor of αKG-dependent dioxygenases.

Materials and methods

Animal studies and cell cultures

All described animal experiments were approved by the animal welfare committee of Amsterdam UMC (0750-MCB19-01A4). Mice were acclimatized and housed in humidity- and temperature-controlled specific pathogen-free conditions under normal light-dark cycles. For the isolation of primary *in vitro* cell cultures, both male and female mice were used. For *in vivo* and *ex vivo* experiments, male C57Bl/6 mice aged 9 weeks were randomized according to body weight and allocated to the different treatments. Mice were weighed prior to each injection. At day 1, mice received an intraperitoneal injection of 900 µl 3% thioglycollate broth (#70157, Sigma-Aldrich, MO, USA). For the *in vivo* experiment, at day 5, mice received an intraperitoneal injection of 50 µg/g body weight (2R)-Octyl-α-hydroxyglutarate (D-2HG; #16366, Cayman Chemicals, MI, USA) or vehicle (5% DMSO in sterile phosphate-buffered saline (PBS), ~200 µl total volume). After 30 min, mice were either injected with PBS or 5 µg/g body weight lipopolysaccharide (LPS, from *E. coli* O55:B5, #L2637, Sigma-Aldrich) dissolved in PBS. After 2 h, mice were sacrificed by CO_2 and blood was collected via heart puncture. Peritoneal lavage and spleen were harvested.

Peritoneal immune cells were harvested by flushing the peritoneal cavity with ice-cold PBS supplemented with 2 mM EDTA. Peritoneal macrophages were directly used for flow cytometry or cultured in RPMI-1640 medium (Gibco, Waltham, MA, USA) supplemented with 10% fetal calf serum (FCS, Biowest, Nuaillé, France), 2 mM l-glutamine (Lonza, Basel, Switzerland), 100 U/ml penicillin (Lonza), 100 µg/ml streptomycin (Lonza) at 37 °C and 5% CO_2. To enrich the peritoneal macrophage fraction, non-adherent cells were washed away with PBS after 3 h and cells were stimulated for 24 h. Supernatants were stored at −80 °C, cells were harvested for flow cytometry or stained in the plate with Hoechst 33342 (#H3570, ThermoFisher) for determination of relative cell count by use of a Cytation 5 multi-mode imager (Agilent Technologies, Santa Clara, CA, USA).

To differentiate BMDMs for *in vitro* experiments, 8–12-week old C57Bl/6, *Phgdh*$^{fl/fl}$ or *Phgdh*$^{Cx3cr1\text{-}Cre}$ mice were sacrificed by CO_2 and hind legs were isolated at the hip joint. Bone marrow was flushed from femur and tibia and differentiated in RPMI-1640 supplemented with 10% FCS, 2 mM l-glutamine, 100 U/ml penicillin, 100 µg/ml streptomycin and 15% L929 cell line-conditioned medium at 37 °C and 5% CO_2. After differentiation for six days, cells were harvested and plated as appropriate.

For the differentiation of human monocyte-derived macrophages (HMDMs), buffy coats were obtained from Sanquin blood Bank (Amsterdam, Netherlands). PBMCs were isolated with a Ficoll/Lymphoprep gradient (Greiner Biosciences) and monocytes were isolated by

applying a 46% Percoll™ (Cytiva) gradient. Monocytes were counted and plated in IMDM medium with HEPES (Gibco) supplemented with 2 mM l-glutamine, 100 U/ml penicillin, 100 µg/ml streptomycin (full IMDM medium) and 1% FCS. After settling for 1 h, medium was replaced with full IMDM medium with 10% FCS and 50 ng/ml M-CSF (Miltenyi). On day 3, medium was replaced with fresh medium supplemented with M-CSF (Miltenyi) and on day 6, the cells (>95% macrophages) were used for *in vitro* experiments.

Primary cells were pre-treated with 0.5 mM (2R)-Octyl-α-hydroxyglutarate (D-2HG; #16366, Cayman Chemicals), 0.1–5 mM dimethyl-2-oxoglutarate (#349631, Sigma-Aldrich), for 1 h and subsequently treated with LPS from *E. coli* (O55:B5, #L2637, Sigma-Aldrich) in a concentration of 100 ng/ml for time points ranging from 15 min to 24 h.

Metabolomics and measurement of L- and D-2HG enantiomers

Metabolomics was performed as detailed previously [22]. Briefly, a 75 µl mixture of the following internal standards in water was added to each sample: adenosine-$^{15}N_5$-monophosphate (100 µM), adenosine-$^{15}N_5$-triphosphate (1 mM), D_4-alanine (100 µM), D_7-arginine (100 µM), D_3-aspartic acid (100 µM), D_3-carnitine (100 µM), D_4-citric acid (100 µM), $^{13}C_1$-citrulline (100 µM), $^{13}C_6$-fructose-1,6-diphosphate (100 µM), guanosine-$^{15}N_5$-monophosphate (100 µM), guanosine-$^{15}N_5$-triphosphate (1 mM), $^{13}C_6$-glucose (1 mM), $^{13}C_6$-glucose-6-phosphate (100 µM), D_3-glutamic acid (100 µM), D_5-glutamine (100 µM), $^{13}C_6$-isoleucine (100 µM), D_3-leucine (100 µM), D_4-lysine (100 µM), D_3-methionine (100 µM), D_6-ornithine (100 µM), D_5-phenylalanine (100 µM), D_7-proline (100 µM), $^{13}C_3$-pyruvate (100 µM), D_3-serine (100 µM), D_5-tryptophan (100 µM), D_4-tyrosine (100 µM), D_8-valine (100 µM). Subsequently, 425 µl water, 500 µl methanol and 1 ml chloroform were added to the same 2 ml tube before thorough mixing and centrifugation (10 min; 14.000 rpm). The upper layer, containing the polar phase, was transferred to a new 1.5 ml tube and dried using a vacuum concentrator at 60 °C. Dried samples were reconstituted in 100 µl methanol/water (6/4; v/v). Metabolites were analyzed using a Waters Acquity ultra-high performance liquid chromatography system coupled to a Bruker Impact II™ Ultra-High Resolution Qq-Time-Of-Flight mass spectrometer. Samples were kept at 12 °C during analysis and 5 µl of each sample was injected. Chromatographic separation was achieved using a Merck Millipore SeQuant ZIC-cHILIC column (PEEK 100 × 2.1 mm, 3 µm particle size). Column temperature was held at 30 °C. Mobile phase consisted of (A) 1:9 acetonitrile:water and (B) 9:1 acetonitrile:water, both containing 5 mM ammonium acetate. Using a flow rate of 0.25 ml/min, the LC gradient consisted of: 100% B for 0–2 min, ramp to 0% B at 28 min, 0% B for 28–30 min, ramp to 100% B at 31 min, 100% B for 31–35 min. MS data were acquired using negative and positive ionization in full scan mode over the range of *m/z* 50–1200. Data were analyzed using Bruker TASQ software version 2.1.22.3. All reported metabolite intensities were normalized to the sum of AMP/ADP/ATP (TAN) relative intensities, as well as to internal standards with comparable retention times and response in the MS.

Metabolite identification has been based on a combination of accurate mass, (relative) retention times and fragmentation spectra, compared to the analysis of a library of standards.

D- and L-2HG were individually quantified using LC-MS/MS based upon published methodology [23]. In brief, to each well with 1 million cells, 200 µl of methanol containing 180 pmol of D/L-$^{2}H_{4}$-2HG serving as internal standards, was added. Subsequently, the mixture was vigorously mixed, and transferred to a glass vial. After drying, diastereomers of D- and L-2HG were formed by the diacetyl-L-tartaric anhydride derivatization procedure, and finally the analytes were redissolved in demineralized water and injected onto the LC-MS/MS system (AB Sciex 4000 Q-Trap). The intracellular concentrations of D- and L-2HG were calculated relative to known calibrators included in each individual series.

Gene expression analysis

For qPCR, total RNA was isolated with the GeneJET RNA Purification Kit (#K0732, ThermoFisher Scientific), and cDNA was synthesized with the High-Capacity cDNA Reverse Transcription Kit (#4368814, Applied Biosystems, ThermoFisher Scientific) according to manufacturer's instructions. The QuantStudio™ 5 Real-Time PCR System (Applied Biosystems, ThermoFisher Scientific) was used to assess amplification using primers listed in Supplementary Table 1 with SYBR green fast mix (Applied Biosystems). *36b4* and *Cypa* expression was used to normalize gene expression.

RNA-sequencing and analysis were performed as previously described [24]. BMDMs (n = 3 biological replicates) were pre-treated for 1 h with D-2HG or vehicle and subsequently stimulated for 5 h with LPS or vehicle. In short, the RNeasy Micro Kit (QIAGEN, Hilden, Germany) was used to isolate total RNA from BMDMs. RNA was used to construct strand-specific libraries with the KAPA mRNA Hyper-Prep kit (KAPA Biosystems, Wilmington, MA, USA). Samples were sequenced on an Illumina HiSeq 4000 instrument (Illumina, San Diego, CA, USA) and reads were aligned to the mouse genome mm10 by STAR 2.5.2b with default settings. Analyses and visualization for the RNAseq data were performed with the R language (CRAN, RRID: SCR_003005, https://www.r-project.org) using the package DESeq2 for differential expression, and the packages ggplot2, ggrepel and pheatmap for volcano plots and heatmaps. Pathway analysis was performed using the Metascape analysis platform (https://metascape.org/) [25] using differentially regulated genes between D-2HG + LPS treated versus LPS-treated BMDMs. Data are deposited at the NCBI GEO database (GSE196315) and accessible for reviewers using the following access token: ylwpuqymvhubpad. The dataset will be made publicly available at publication.

Cytokine and nitric oxide (NO) measurements

IL-6, TNFα, IL-10 and IL-1β concentrations were measured in plasma, peritoneal lavage

or cell supernatants with uncoated ELISA kits (#88-7064-77/#88-7324-77/#88-7105-88/#88-7013-22, Invitrogen, ThermoFisher) according to manufacturer's instructions. Data measured in peritoneal macrophage supernatants was normalized for the relative cell count determined in the Cytation 5 imaging multi-mode reader (BioTek, Agilent Technologies) after staining nuclei with Hoechst. NO production was measured by adding 50 µl Griess reagent (2.5% H_3PO_4 (Merck), 1% sulfanilamide (Sigma Aldrich), and 0.1% naphtylene diamide dihydrochloride (Sigma Aldrich) in H_2O) to 50 µl cell supernatants and absorbance was measured at 540 nm.

Flow cytometry

Flow cytometry samples were acquired at the MCBI O2Flow Facility at Amsterdam UMC (the Netherlands) on an X20 Fortessa flow cytometer (BD Biosciences, Franklin Lakes, NJ, USA) which was daily calibrated with CS&T beads (BD Biosciences). Primary cells were stained with antibodies listed in Supplementary Table 2 and results were analyzed using FlowJo™ analysis software (TreeStar, Ashland, OR, USA, v10).

Immunoblotting

Cells were lysed in RIPA lysis buffer supplemented with phosphatase (Halt™ Phosphatase Inhibitor Cocktail, #78420, ThermoFisher Scientific) and protease inhibitors (cOmplete, #11836153001, Roche, Basel, Switzerland). Protein lysates were separated by electrophoresis on 10% polyacrylamide gels and proteins were transferred onto nitrocellulose membranes using the Trans-Blot® Turbo™ Semi-Dry transfer cell with Trans-Blot® Turbo™ nitrocellulose Transfer Packs (Bio-Rad Laboratories). After blocking, membranes were incubated overnight at 4 °C with primary antibody against total-NF-κB-p65 (#8242, Cell Signaling Technology, MA, USA), phosphorylated-NF-κB-p65 (ser536, #3033, Cell Signaling) or β-Actin (#A5441, Sigma-Aldrich). Membranes were subsequently incubated with secondary antibody (IRDye 680RD Goat anti-Mouse or IRDye 800CW Goat anti-Rabbit; LI-COR Biosciences, USA) for 1 h and imaged with the Azure Sapphire Biomolecular Imager (Azure Biosystems, CA, USA). Bands were quantified with ImageJ (Rasband, W.S., U. S. National Institutes of Health, MD, USA, https://imagej.nih.gov/ij/).

Metabolic extracellular flux (XF) analysis

XF analysis was performed using the Seahorse XFe-96 Flux Analyzer (Agilent) to examine oxygen consumption (OCR) and extracellular acidification rates (ECAR) as described previously [26]. Briefly, BMDMs were plated at a density of $7.5*10^4$ cells per well in XF-96-cell culture plates (Agilent) and stimulated for 24 h with 100 ng/ml LPS or vehicle. 1 h prior to the assay, cells were washed and medium was replaced by Seahorse base medium (Sigma-Aldrich) without glucose, phenol red, and sodium bicarbonate, and supplemented with 5 mM HEPES and 2 mM l-glutamine. 15 min before the first measurement, BMDMs

were treated with D-2HG or vehicle and the subsequent protocol included 2 min mixing, 3 min measuring and 4 subsequent injections; Glucose (final concentration in well 25 mM), Oligomycin (O, final concentration 1.5 µM), FCCP (final concentration 1.5 µM), and antimycin A (AA, final concentration 2.5 µM) with rotenone (rot, final concentration 1.25 µM) and Hoechst 33342 (Thermo Fisher) (final concentration 5 µg/ml). Directly after the run, Hoechst signal was measured on the Cytation 5 Cell Imaging multi-mode reader (BioTek) with a 4× magnification using a 365 nm LED in combination with an EX377/50 EM 447/60 filter cube and cell counts were analyzed using Gen 5™ software. Subsequently, flux rate data was normalized to cell counts with the following equation: normalized OCR or ECAR = recorded OCR or ECAR / (cell count in center of well)/(average of plate). Data were analyzed using Wave software version 2.6.0.31 as described previously [26].

Statistical analysis

N represents either the number of animals used or the number of *in vitro* replications performed. Data are represented as means ± SD or as indicated. Statistical analyses were performed using one-way ANOVA or two-way ANOVA followed by Tukey's or Dunnett's post-hoc multiple comparisons test. Details on statistical analyses can be found in figure legends. A value of $p < 0.05$ was considered statistically significant. All data were analyzed and visualized using GraphPad Prism version 9.0 (GraphPad Software, La Jolla, California, USA) or R Studio (PBC, Boston, MA http://www.rstudio.com/).

Results

D-2HG accumulates at late stages of LPS-induced activation of mouse and human macrophages

To identify potential new immunometabolites that regulate inflammatory responses in both mouse and human macrophages, we analyzed differential abundance of metabolites upon LPS stimulation in both species. We performed metabolomics to profile changes in metabolite levels in response to 24 h LPS stimulation in mouse bone marrow-derived macrophages (BMDMs) and human monocyte-derived macrophages (HMDMs). In alignment with previous reports, the top LPS-induced metabolites in BMDMs included lactate, succinate, itaconate and various metabolites related to the pentose phosphate pathway. Notably, we detected 2-hydroxyglutarate (2HG) among the top-10 most elevated intracellular metabolites in LPS-stimulated BMDMs and this was the second most significant LPS-induced metabolite in human macrophages (Figure 1A, B). We were further able to validate the strong induction of 2HG in LPS-stimulated BMDMs by analyzing previously published metabolomics datasets [27,28], indicating that this observation was not dependent on specific experimental conditions (Figure 1C, D). When plotting

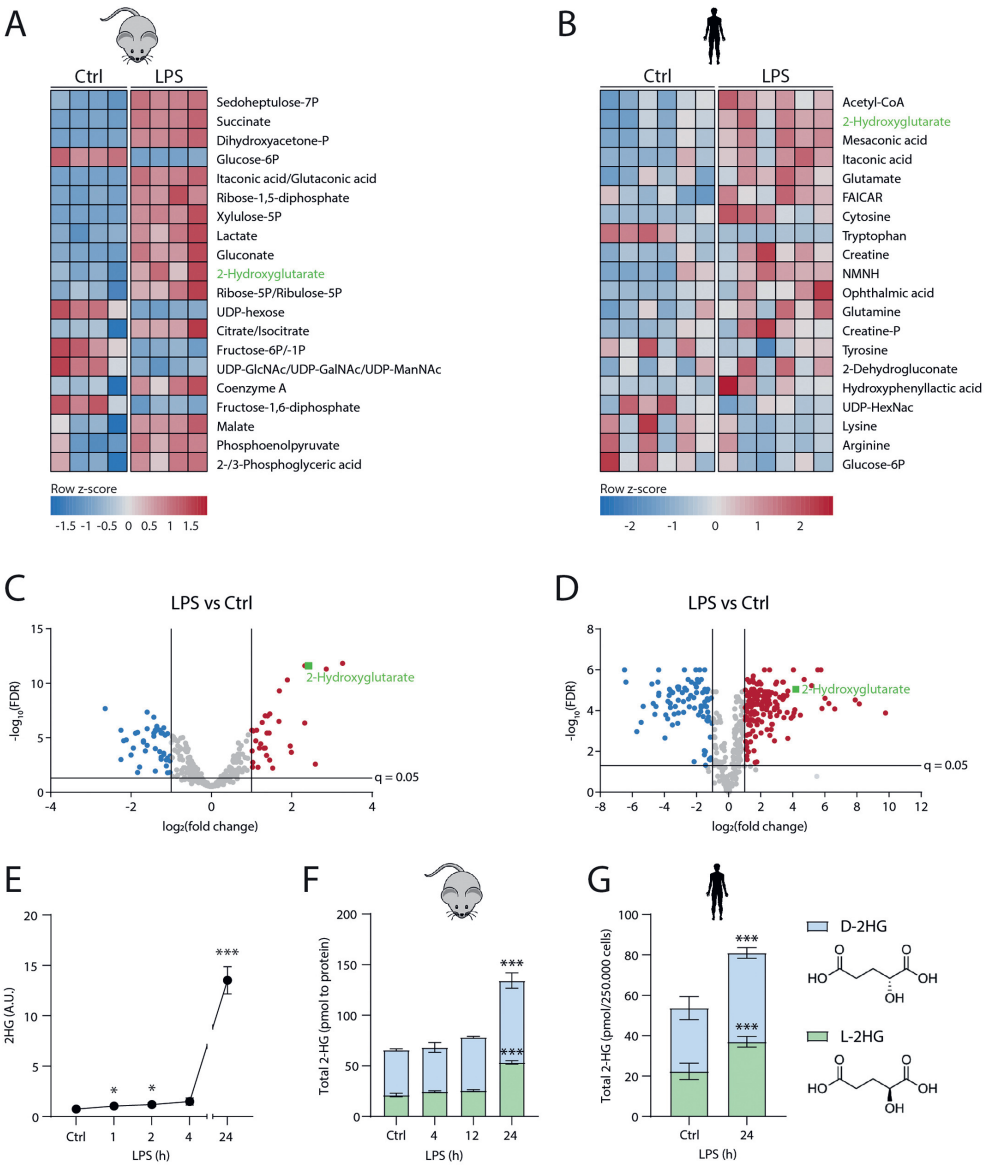

Figure 1. D-2HG is the most abundant 2HG enantiomer in mouse and human macrophages, and accumulates at later stages of LPS-induced inflammatory responses. Relative abundance of top-20 most regulated metabolites sorted on *P*-value in naïve (ctrl) and LPS-stimulated mouse BMDMs (A) and HMDMs (B) (n = 4 or 6 individual mice or donors, 24 h). Red and blue dots represent metabolites significantly up- (red) and downregulated (blue) after 24 h LPS treatment of BMDMs in two independently published datasets; (C) Mills et al., 2018, n = 5, 24 h [28] and (D) Lauterbach et al., 2019, n = 4, 24 h [27]. (E) Kinetics of total 2HG abundance derived from the metabolomics analysis of BMDMs stimulated with 10 ng/ml LPS for indicated time points by Lauterbach et al. [27] (analyzed by Brown-Forsythe and Welch ANOVA). Intracellular concentration of D-2HG and L-2HG enantiomers in BMDMs (F, n = 3) and HMDMs (G, technical triplicate of 1 out of 2 donors) treated with LPS for indicated times (both analyzed by two-way ANOVA with Tukey post-hoc test). *P*-values are indicated as <0.05*, <0.01**, <0.001***. FDR, false discovery rate; A.U., arbitrary units.

the kinetics of LPS-induced 2HG accumulation, we noted a biphasic response with very modest increase at early stages (1.5–2-fold at 1–4 h) and pronounced accumulation at later stages after LPS stimulation (15–20-fold increase at 24 h) (Figure 1E). Since 2HG exists as two enantiomers which cannot be distinguished by conventional metabolomics, we next performed chiral derivatization followed by LC-MS that enables enantiomer-specific analysis. Whereas D-2HG has mostly been studied as an oncometabolite and L-2HG as an immunometabolite [4], we found D-2HG to be the most abundant enantiomer in naïve and LPS-treated macrophages with levels peaking 24 h after stimulation of both mouse and human macrophages (Figure 1F, G). This observation led us to further explore the induction and function of D-2HG in LPS-stimulated macrophages.

HOT and D2HGDH possibly contribute to D-2HG elevation in LPS-stimulated macrophages

2HG levels can be regulated by various enzymes that specifically synthesize and degrade both enantiomers as detailed in the schematic overview in Figure 2A for D-2HG. To get a first idea about the most likely candidate enzymes contributing to the observed LPS-induced D-2HG accumulation, we assessed D-2HG-associated genes in RNA-seq data (GSE196315) of LPS-versus vehicle-stimulated BMDMs. Especially *Adhfe1* (HOT), and to a lesser extent *Phgdh*, were induced by LPS, whereas *D2hgdh* expression was downregulated (Figure 2B). As such, *Adhfe1*, *Phgdh* and *D2hgdh* could potentially mediate the LPS-induced accumulation of D-2HG.

To further dissect D-2HG induction in response to LPS, we assessed the kinetics of LPS-induced gene expression of 2HG-regulating enzymes. Interestingly, the expression of *Adhfe1* was strongly induced by LPS and reached maximal levels just before D-2HG levels itself started rising (Figure 2C). Conversely, gene expression of the D-2HG-degrading enzyme *D2hgdh* dropped prior to the moment at which D-2HG peaked. Based on the kinetics of D-2HG, *Adhfe1* and *D2hgdh*, it is likely that at least one of these two enzymes contribute to the observed increase in D-2HG levels at late stages after LPS stimulation.

Idh1 and *Idh2* expression levels were mostly unaltered or suppressed after LPS stimulation, we could exclude them as potential contributors to LPS-induced D-2HG accumulation. Also, *Phgdh* gene expression was not significantly regulated by LPS over time (Figure 2C) and accordingly, PHGDH did not contribute to LPS-induced D-2HG formation as evidenced by normal D-2HG levels in *Phgdh*-deficient BMDMs (Figure 2D).

Interestingly, the kinetics of metabolite and enzyme levels suggest that D-2HG is not required for the initial LPS-induced inflammatory response. Moreover, comparing the kinetics of D-2HG and its regulating enzymes to pro-inflammatory gene expression clearly indicated that this metabolic branch was only actively regulated after genes like *Il6*, *Tnf*,

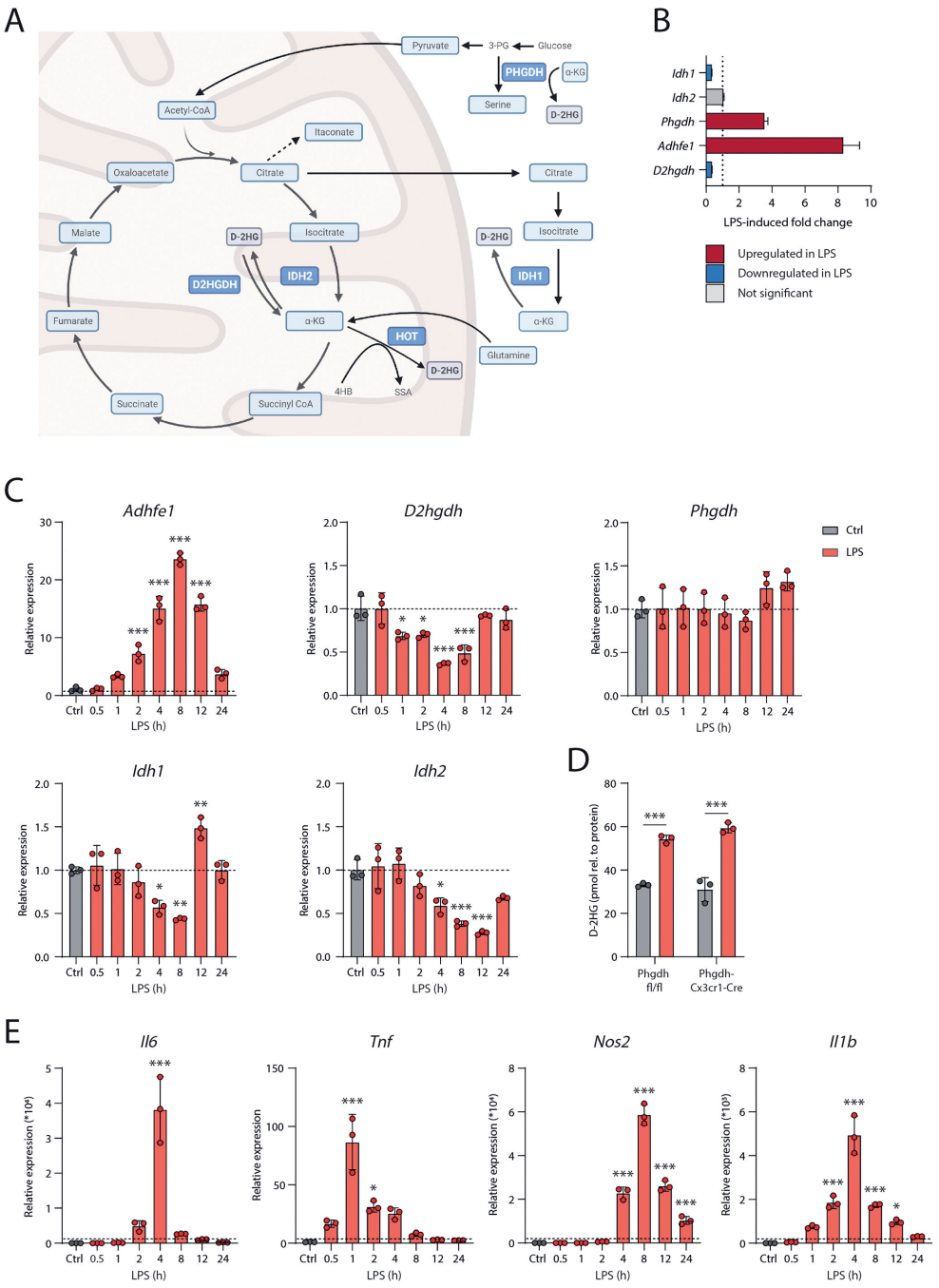

Figure 2. LPS rewires D-2HG metabolism in a time frame relevant for resolution of inflammation. (A) Schematic overview of the enzymes involved in D-2HG metabolism (created with Biorender). (B) LPS-induced fold change of genes associated with D-2HG metabolism in RNA-seq data from BMDMs stimulated with LPS or vehicle. Relative mRNA fold change of (C) D-2HG-associated genes *Adhfe1* (HOT), *D2hghd*, *Phgdh*, *Idh1* and

Idh2 (analyzed by one-way ANOVA with Tukey post-hoc test). (D) Concentration of D-2HG in control (*Phgdh*$^{fl/fl}$) and *Phgdh*-deficient (*Phgdh*$^{fl/fl * Cx3cr1\text{-}Cre}$) BMDMs in control conditions and after 24 h of LPS treatment (n = 3 mice, analyzed by two-way ANOVA with Tukey post-hoc test). (E) inflammatory genes *Il6*, *Tnf*, *Il1b* and *Nos2* in BMDMs treated with LPS for indicated times (n = 3 mice, analyzed by one-way ANOVA with Tukey post-hoc test). *P*-values are indicated as <0.05*, <0.01**, <0.001***, only comparisons to naïve untreated controls (Ctrl) are shown.

Nos2 and *Il1b* peaked and started to decline again (30 min to 12 h post LPS stimulation, Figure 2E). Together, these data suggest that HOT and/or D2HGDH likely contribute to the LPS-induced increase of D-2HG and that the accumulated metabolite itself might play a role in the resolution of inflammatory responses.

D-2HG dampens inflammatory responses in mouse and human macrophages

To further dissect the potential role of D-2HG during inflammatory responses, we pre-treated BMDMs with cell-permeable octyl-D-2HG followed by LPS stimulation. D-2HG did not impair cell viability as demonstrated via viability staining during flow cytometry (Supplementary Figure 1A). To obtain an unbiased view on the effect of D-2HG on LPS responses, we first performed RNA-sequencing and plotted the differentially regulated genes in a volcano plot (Figure 3A). Pathway analysis revealed that genes related to myeloid cell activation, signaling, cytokine production, and innate immune response were affected by D-2HG administration (Figure 3B) and the majority of those were reduced by D-2HG (Table S3). When selecting the top LPS-induced genes ($\log_2$FC > 5 and adjusted $p < 0.05$, 107 genes), we observed that 19 of those genes were suppressed and only 2 genes were increased by D-2HG (Figure 3C, Supplementary Figure 1B). Together, this RNA-seq analysis suggested that D-2HG dampens LPS-induced inflammatory macrophage activation.

To validate RNA-seq data functionally, we analyzed the effect of D-2HG on LPS-induced inflammatory cytokine secretion and marker expression in mouse and human macrophages. D-2HG pre-treatment suppressed the LPS-induced secretion of the key inflammatory mediators IL-6, TNFα and NO by BMDMs, and this was paralleled by reduced expression of CD40 and iNOS as demonstrated by flow cytometry (Figure 3D, E). Also in human macrophages, D-2HG suppressed LPS-induced secretion of IL-6 and TNFα, and reduced the surface expression of CD80, CD197 (CCR7), and CD274 (PD-L1) (Figure 3F, G). Interestingly, we observed a more potent reduction of TNFα and CD80 levels by D-2HG in HMDMs compared to BMDMs. Importantly, the inhibitory effects of D-2HG on LPS-induced inflammatory macrophage responses did not depend on the cell source and were also observed in mouse thioglycollate-elicited peritoneal macrophages when stimulated *ex vivo* (Supplementary Figure 1C, D). Together, these data indicate that D-2HG suppresses LPS-induced inflammatory activation of distinct mouse and human macrophages.

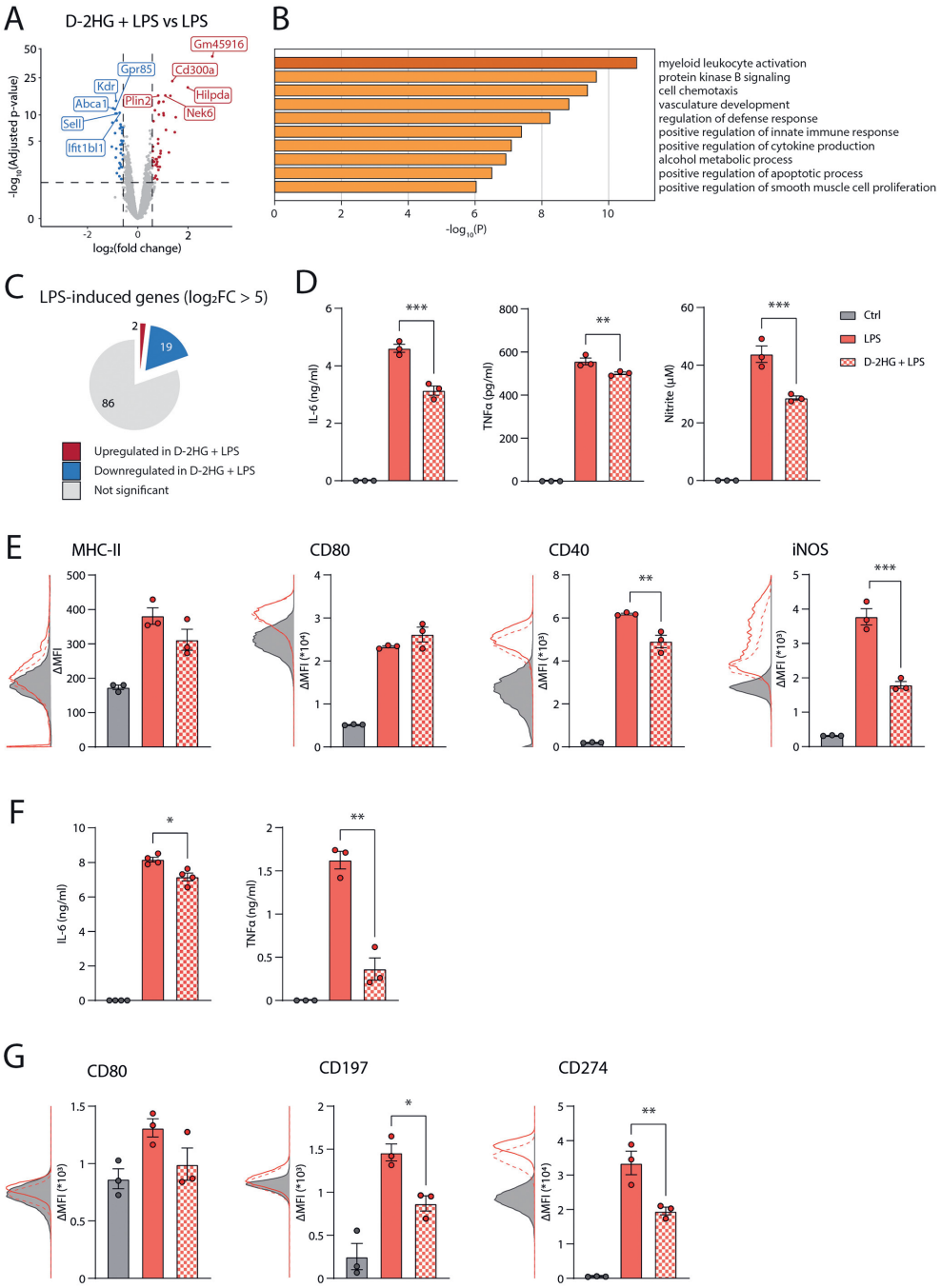

Figure 3. D-2HG dampens LPS-induced inflammatory responses in mouse and human macrophages. BMDMs were pre-treated with 0.5 mM octyl D-2HG or vehicle control for 1 h, followed by 100 ng/ml LPS stimulation (or naïve control) for 5 h before RNA-sequencing. (A) Volcano plot shows genes upregulated (red) and downregulated (blue) in D-2HG-pre-treated LPS-stimulated macrophages in comparison to

vehicle-pre-treated plus LPS (5 h). (B) Top regulated pathways in D-2HG + LPS vs LPS-treated BMDMs. (C) Pie chart quantifying up-, down-, and not significantly regulated genes in D-2HG + LPS vs LPS-treated BMDMs within top LPS-induced genes (p adjusted <0.05, log2FC >5). Cytokine and NO (nitrite) concentration in (D) BMDM (analyzed by one-way ANOVA with Dunnett post-hoc test) and (F) HMDM (analyzed by Brown-Forsythe and Welch ANOVA with Dunnett post-hoc test) supernatants as measured by ELISA and Griess reaction, respectively. Expression of indicated LPS-induced marker proteins as measured by flow cytometry and shown as ΔMFI (median fluorescence intensity = MFI(sample)-MFI(FMO)) in (E) BMDMs and (G) HMDMs (both analyzed by one-way ANOVA with Dunnett post-hoc test). *P*-values are indicated as <0.05*, <0.01**, <0.001***.

D-2HG regulates local and systemic inflammatory responses *in vivo*

Next, we aimed to test whether, similar to the observed effects in activated BMDMs and HMDMs *in vitro*, D-2HG was involved in regulating macrophages in inflammatory conditions *in vivo*. Hereto, mice were injected with thioglycollate intraperitoneally (i.p.) to elicit macrophage influx and priming, followed by pre-treatment with D-2HG and subsequent LPS challenge (Figure 4A, modified Schwartzman reaction [29]). This protocol yielded a systemic and local inflammatory reaction as evidenced by increased inflammatory cytokine concentrations in blood plasma and peritoneal lavage fluid (Figure 4B, C). Consistent with the anti-inflammatory effects of D-2HG *in vitro*, LPS-induced circulating and peritoneal TNFα levels were reduced in the presence of D-2HG, whereas the concentration of the anti-inflammatory cytokine IL-10 was increased by D-2HG treatment in both locations. Plasma IL-6 and IL-1β were not affected by D-2HG, but peritoneal IL-6 levels were increased in the D-2HG + LPS group.

Pre-treatment with D-2HG resulted in an overall decrease in the amount of peritoneal exudate cells recovered from LPS-injected mice (Supplementary Figure 2A). To assess the effect of D-2HG on the abundance of macrophages and other immune cell subsets in the peritoneal lavage, we performed flow cytometry analysis. After selecting live single cells, $CD11b^{hi}Ly6G^{hi}$ neutrophils and $CD11b^{hi}Ly6G^{-}$ other myeloid cells were gated (Figure 4D i–iv). The latter were further subdivided in $Ly6C^{hi}$ monocytes and $F4/80^{+}$ macrophages (Figure 4D v). D-2HG decreased overall cell counts and the percentage of $CD11b^{hi}Ly6G^{-}$ $F4/80^{+}$ macrophages, increased the abundance of $Ly6G^{hi}$ neutrophils and did not alter $Ly6C^{hi}$ inflammatory monocyte abundance in the peritoneal cavity of both LPS- and vehicle-treated mice (Supplementary Figure 2B). Focusing on $F4/80^{+}$ macrophages, we noted that D-2HG suppressed the LPS-induced expression of CD40, CD80 and iNOS, while CD86 and MHC-II expression was not significantly altered (Figure 4E). Since $F4/80^{+}$ macrophages showed heterogeneous CD80 and MHC-II expression as shown in the histograms (Figure 4E), we also plotted both markers against each other (Figure 4D vi). D-2HG particularly reduced the abundance of $CD80^{hi}$ $MHC\text{-}II^{lo}$ macrophages and concomitantly, the proportion of $CD80^{lo}$ $MHC\text{-}II^{lo}$ cells was increased in D-2HG-injected mice. The manual gating-based cytometry analysis was verified by visualizing the data on t-SNE plots (Supplementary Figure 2C). This unsupervised analysis validated that D-2HG

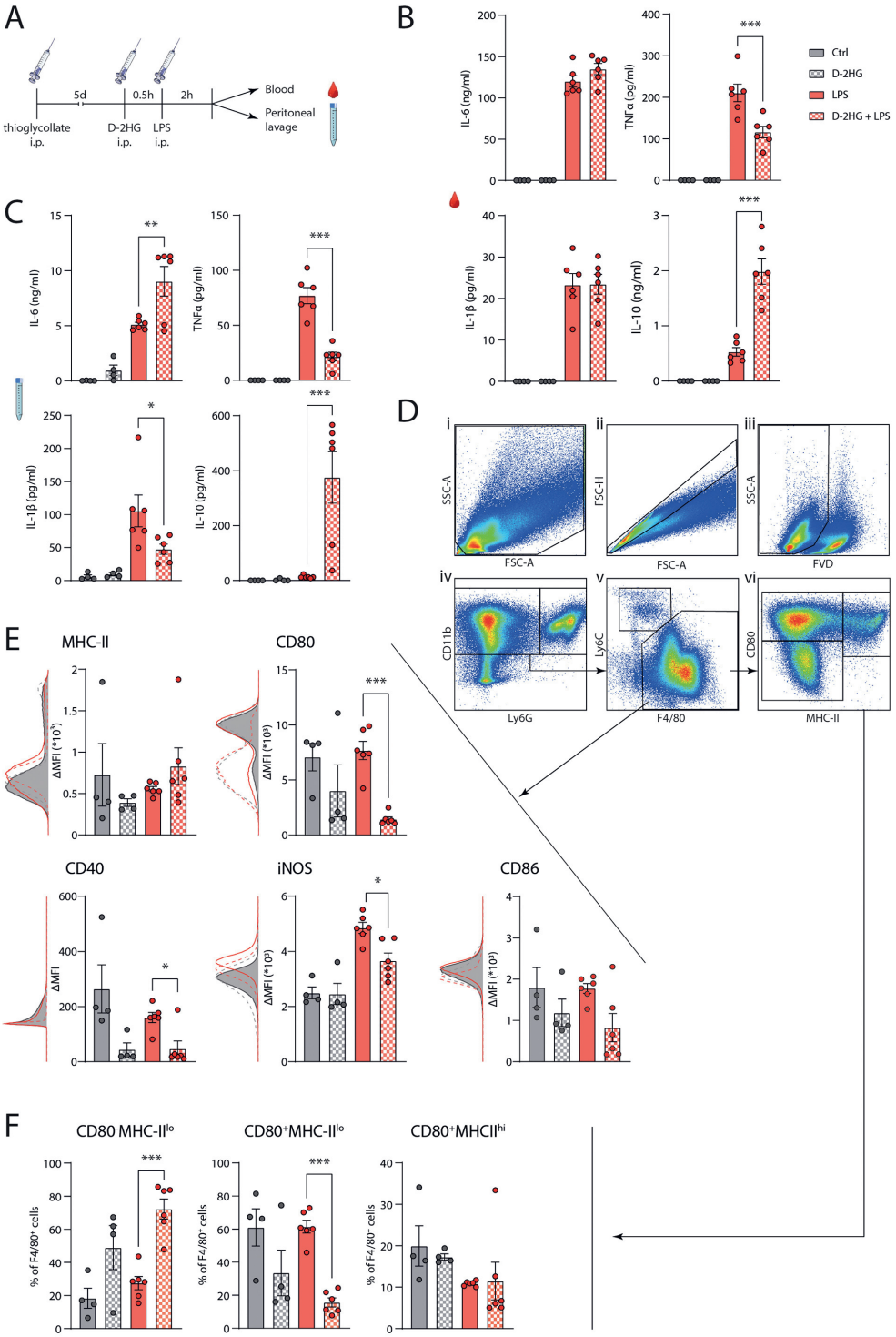
A
5d
0.5h
2h
Blood
Peritoneal lavage
thioglycollate i.p.
D-2HG i.p.
LPS i.p.
B
IL-6 (ng/ml)
TNFα (pg/ml)
IL-1β (pg/ml)
IL-10 (ng/ml)
Ctrl
D-2HG
LPS
D-2HG + LPS
C
D
SSC-A
FSC-A
FSC-H
FVD
CD11b
Ly6G
Ly6C
F4/80
CD80
MHC-II
E
MHC-II
CD80
CD40
iNOS
CD86
ΔMFI (*10³)
ΔMFI
F
CD80⁻MHC-II^lo
CD80⁺MHC-II^lo
CD80⁺MHCII^hi
% of F4/80⁺ cells

Figure 4. D-2HG injection affects LPS-induced systemic and local inflammatory responses *in vivo*. (A) Thioglycollate-primed mice were i.p. injected with octyl-D-2HG or vehicle, followed by i.p. injection of LPS or vehicle control after 30 min. After 2 h, blood and peritoneal fluid were collected (n = 4 or 6 for control or LPS-challenged groups, respectively). (B) Plasma and (C) peritoneal cytokine levels in mice (analyzed by one-way ANOVA with Dunnett post-hoc test. Flow cytometry gating strategy (D), surface marker expression on F4/80^{+} macrophages (E, shown as MFI, analyzed by Brown-Forsythe and Welch ANOVA with Dunnett post-hoc test), and relative abundance of specific peritoneal exudate macrophage subsets (F, shown as percentage, analyzed by Brown-Forsythe and Welch ANOVA with Dunnett post-hoc test). *P*-values are indicated as <0.05*, <0.01**, <0.001***. Manual gating was validated by visualizing the data on t-SNE plots as shown in Supplementary Figure 2C.

mainly suppressed the proportion of CD80^{hi} MHC-II^{lo} macrophages (upper left cluster in t-SNE) and slightly increased the abundance of Ly6G^{hi} neutrophils (lower right cluster) in LPS-injected mice (Supplementary Figure 2C). Together, these data demonstrate that i.p. D-2HG injection regulates LPS-induced local and systemic inflammatory responses *in vivo*.

D-2HG affects IL-6 and NO production independently of effects on αKG-dependent dioxygenases

Having established D-2HG as an immunometabolite that accumulates during late stages of LPS-responses, we further aimed to unravel the mechanisms by which this metabolite regulates inflammatory signaling. To further elaborate on transcription factors and pathways involved in mediating the effects of D-2HG, we employed the Metascape TRRUST analysis tool [30] using genes differentially regulated between D-2HG- and vehicle-pre-treated LPS-stimulated macrophages. Especially genes regulated by the key inflammatory transcription factor NF-κB were affected in the D-2HG-pre-treated group (Figure 5A). To study whether direct D-2HG-mediated inhibition of NF-κB was responsible for the observed suppression of NF-κB target genes, we measured phosphorylated (P) versus total (T) levels of the NF-κB subunit p65. D-2HG pre-treatment did not affect LPS-induced activation of NF-κB as evidenced by equal P-p65/T-p65 ratios after 15 and 30 min of LPS stimulation (Figure 5B).

Since both D-2HG and L-2HG can act as competitive inhibitors of multiple αKG-dependent dioxygenases that also affect macrophage activation, we reasoned that D-2HG might exert its inhibitory effects on LPS-induced NF-κB target genes by competing with αKG. According to this hypothesis, the inhibitory effects of D-2HG on inflammatory markers should be rescued by a surplus of αKG. To test this, we pre-treated macrophages with a combination of D-2HG and increasing concentrations of αKG followed by LPS stimulation. Even at the highest concentration, αKG could not reverse the D-2HG-mediated inhibition of IL-6 and NO secretion in LPS-stimulated macrophages and even increased the effects of D-2HG (Figure 5C). However, the effect of D-2HG on TNFα was rescued by adding ten times more αKG. This indicates that D-2HG exerted diverse effects, which are at least partially independent of its known function as a competitive inhibitor of αKG-dependent dioxygenases, including JmjC-domain containing histone lysine demethylase 6B (KDM6B/

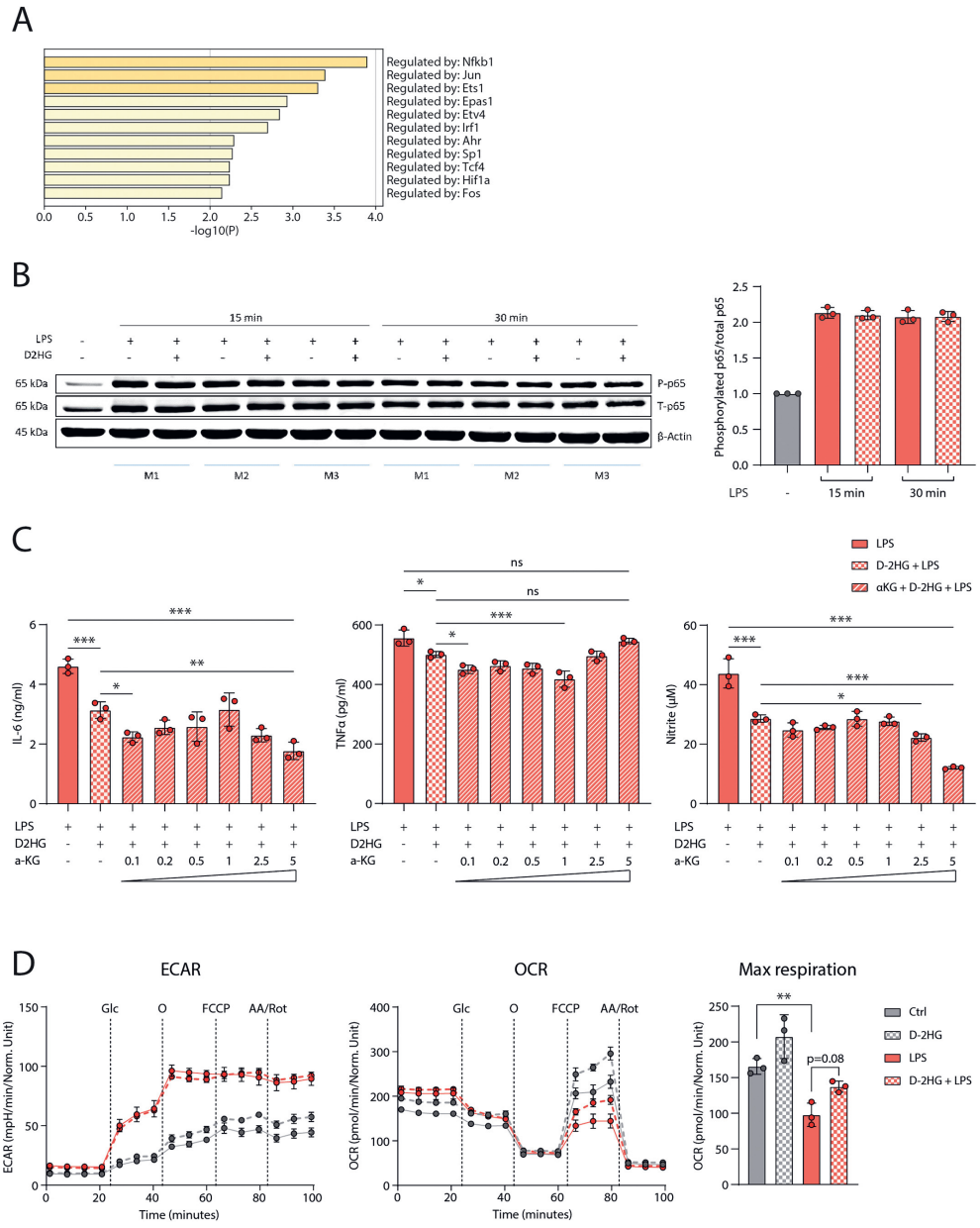

Figure 5. D-2HG affects NF-κB target genes independently of effects on αKG-dependent dioxygenases. (A) Metascape TRRUST RNA-seq analysis using genes differentially regulated between D-2HG- and vehicle-pre-treated LPS-stimulated macrophages reveals NF-κB target genes as most regulated by D-2HG. (B) Phosphorylation of p65 after 15 or 30 min LPS stimulation after 1 h D-2HG (+) or vehicle pre-treatment (–) treatment of BMDMs (n = 3 mice). Both phosphorylated (P) p65 and total (T) p65 were measured and phosphorylation was quantified relative to the total p65 and β-actin served as a loading control. Quantification was done with ImageJ. (C) TNFα, IL-6 and nitrite levels released by BMDMs pre-treated with (different concentrations of) αKG, D-2HG and/or vehicle and stimulated with LPS (n = 3 mice, one-way

ANOVA with Tukey post-hoc test). To assess effects of αKG, only relevant statistic comparisons to D-2HG + LPS-treated BMDMs are shown. (D) Extracellular flux analysis of extracellular acidification rates (ECAR), oxygen consumption rates (OCR) and maximal respiration (calculated as OCR(after FCCP) – OCR(after AA/Rot), analyzed by one-way ANOVA with Tukey post-hoc test) during an adapted mitochondrial stress test in BMDMs treated with vehicle, D-2HG, LPS or LPS + D-2HG for 24 h (n = 3 mice). *P*-values are indicated as <0.05*, <0.01**, <0.001***.

JMJD3) and HIF prolyl hydroxylases (PHDs) that were previously reported to regulate macrophages [21,31]. What is noteworthy, is that αKG supplementation did rescue TNFα production, suggesting that D-2HG may dampen TNFα expression by competing with αKG, thereby affecting the activity of αKG-dependent dioxygenases.

Based on the fact that glycolysis and inflammatory signaling are often strongly connected, together with the recent observation that L-2HG affects glycolysis in macrophages [9,21], we explored the effect of D-2HG on the metabolism of BMDMs via extracellular (Seahorse) flux analysis. While D-2HG did not alter extracellular acidification rates (ECAR, a measurement of glycolysis), D-2HG appeared to reduce the drop in oxygen consumption rates (OCR, a measurement of mitochondrial respiration) that is induced by 24 h LPS stimulation (Figure 5D). Yet, the changes in OCR-derived mitochondrial parameters did not reach statistical significant. Altogether, these data indicate that D-2HG can dampen LPS-induced expression of inflammatory genes independently of competition with αKG and NF-κB activation.

Discussion

Studies into cancer metabolism, and more recently also immunometabolism, have revealed that metabolites are much more than simple intermediates or end products of metabolism. Our work uncovers the induction of D-2HG in macrophages after long-term LPS-stimulation, where our kinetic, transcriptomic and functional data suggest that D-2HG serves as an anti-inflammatory immunometabolite that aids the transition from inflammation towards resolution. This was unexpected since D-2HG has mainly been studied as an oncometabolite that is produced by mutant IDH1 and IDH2 in transformed cancer cells [18]. Of the 2HG enantiomers, L-2HG was appointed as an immunometabolite when it was discovered that it accumulates upon T-cell receptor engagement to regulate $CD8^+$ T-cell differentiation and proliferation [14]. In macrophages, the immunometabolites succinate and itaconate have received much attention but a recent study also identified a role for L-2HG in HIF-1α activation and the induction of downstream pro-inflammatory signaling [21]. Yet, the induction and role of D-2HG in macrophages remained to be explored.

We show that D-2HG levels peak at later stages after LPS stimulation at the moment when

gene expression of prototypical inflammatory genes start to decay. The fact that this increase in D-2HG is preceded by the regulation of the genes encoding HOT and D2HGDH suggests that D-2HG accumulation is not solely an indirect side product of LPS-induced metabolic rewiring. HOT converts gamma-hydroxybutyrate into succinic semialdehyde and this reaction is coupled to the reduction of αKG to D-2HG. Normally, D-2HG levels are controlled by D2HGDH which oxidizes D-2HG back into αKG. Yet, the combined suppression of D2HGDH and induction of HOT, as observed after LPS-stimulation of macrophages, may result in the observed increased intracellular D-2HG concentrations. While the D2HGDH and HOT kinetics hint towards a role for both 2HG-regulating enzymes, further research with new genetic tools is needed to define precisely which enzyme(s) are responsible for the D-2HG induction in response to LPS stimulation. D-2HG synthesis appears more regulated than L-2HG, since the latter is particularly produced by non-specific promiscuous enzyme activities of lactate dehydrogenase A (LDHA) and malate dehydrogenase (MDH1 and MDH2) in acidic and hypoxic environments. As such, targeting D2HGDH or HOT in macrophages might provide a therapeutic opportunity to modulate endogenous D-2HG production and inflammatory signaling. Indeed, we observed that administration of cell-permeable D-2HG dampens inflammatory responses in macrophages *in vitro* and also regulates local and systemic inflammation *in vivo*. This anti-inflammatory effect of D-2HG aligns with the earlier notions that cancer cell-derived D-2HG inhibits anti-tumor immune responses of glioma-associated macrophages and T cells [19,20].

The immunosuppressive effects of D-2HG are in sharp contrast with the observations that L-2HG can promote inflammatory signaling in macrophages and enhances the proliferation of $CD8^+$ T cells [14]. This important functional difference between both 2HG enantiomers might be explained by the minor structural differences that make L-2HG a much more potent competitive inhibitor of certain αKG-dependent dioxygenases. Indeed, L-2HG has been shown to inhibit prolyl hydroxylases (PHDs), resulting in the stabilization of HIF-1α and the activation of genes related to inflammation and glycolysis, while D-2HG did not induce HIF1α and even suppressed it in specific conditions [21]. Conversely, both 2HG enantiomers are expected to be equally effective in inhibiting αKG-dependent JMJD histone demethylases. Yet, such inhibitory effects should be reversed by surplus αKG and therefore a lack of this reversal for IL-6 and NO suggests that D-2HG exerts at least part of its anti-inflammatory effects independently of αKG-dependent dioxygenases and epigenetic remodeling. As such, the mechanism by which D-2HG suppresses LPS-induced upregulation of inflammatory mediators remains open for future investigation. In this context, it would also be interesting to study how combining D- and L-2HG at different concentration affects inflammatory signaling in macrophages. Possibly, recent insight from the cancer metabolism field might help to explain the observed anti-inflammatory effects of D-2HG. Friedrich et al. recently reported that D-2HG may act as an allosteric activator of

tryptophan 2,3-dioxygenase (TDO2) that converts tryptophan into kynurenine. The latter is an endogenous ligand of the aryl hydrocarbon receptor (AHR) which has been shown to mediate the induction the anti-inflammatory cytokines IL-10 and TGF-β by cancer cell-derived D-2HG in macrophages [20]. Further dissecting the mechanisms by which endogenous D-2HG controls macrophage activation is important to better understand intracellular inflammatory signaling and may also aid in understanding how exogenous D-2HG suppresses macrophage effector functions. An aspect of 2HG biology that needs further study is its intercellular and intracellular trafficking between mitochondria and cytosol.

An important open question that was not addressed here is what the actual role of D-2HG induction in macrophages is and whether its anti-inflammatory effects are the main purpose, or rather consequential side effects. In this respect, L-2HG has been proposed as an electron sink and carrier under conditions of reductive stress induced by hypoxia [32]. Similarly, D-2HG production in inflammatory macrophages might help to regenerate NAD^+ from NADH to maintain the flux of glucose through glycolysis when mitochondrial function is impaired. As a consequence of restoring the NAD^+/NADH balance, D-2HG accumulation could serve as a feedback loop to resolve inflammation and induce homeostasis. While it is clear that supplementation with D-2HG dampens inflammatory macrophage responses, it remains to be demonstrated whether changes in endogenous D-2HG levels are sufficient to modulate inflammatory signaling. D-2HG possibly acts in concert with other metabolic and signaling events to tune down and resolve inflammation. While many LPS-induced inflammatory genes were suppressed by D-2HG, NO production downstream of iNOS appeared to be one of the most affected inflammatory mediators by D-2HG. This D-2HG-mediated suppression of NO production probably explains the slight increase in maximal mitochondrial respiration in LPS-treated macrophages. A direct stimulatory effect of D-2HG on mitochondrial function is less likely since 2HG was previously shown to bind and inhibit mitochondrial ATP synthase and mTOR signaling [33]. Accordingly, D-2HG did not affect mTOR signaling as evidenced by equal Psingle bondS6 levels in our setting (data not shown).

In conclusion, our work identifies D-2HG as an immunomodulatory metabolite that is induced at later stages of inflammatory responses, possibly by the regulation of a metabolic circuit including HOT and D2HGDH. Together, our data suggest that D-2HG can dampen inflammatory signaling by several means, including αKG-independent mechanisms that remain to be explored. In contrast to L-2HG which has been shown to stimulate T cell and macrophage activation, our data support the idea that D-2HG can act as an immunosuppressive signaling metabolite that might be employed to modulate inflammation.

Acknowledgements

Funding

We thank dr. Thomas Weichhart and dr. Jayne Louise Wilson for the kind gift of the bone marrow from *Phgdh*$^{fl/fl}$ and *Phgdh*$^{Cx3cr1\text{-}Cre}$ mice. AH was funded by grants of the Austrian Science Fund (SFB F83 and I 4646). JVdB and AH were both funded by a consortia grant from European Research Area Network on Cardiovascular Diseases (ERA-CVD 2019T108). JVdB received a Netherlands Heart Foundation senior fellowship (2017T048) and an Enw-Klein-1 grant from NWO (OCENW.KLEIN.268). Lastly, we acknowledge support from Cancer Center Amsterdam.

Declaration of competing interest

The authors declare that they have no known competing financial interests or personal relationships that could have appeared to influence the work reported in this paper.

References

1. H.L. Caslin, M. Bhanot, W.R. Bolus, A.H. Hasty, Adipose tissue macrophages: unique polarization and bioenergetics in obesity, Immunol. Rev. 295 (2020) 101–113.
2. K.J. Moore, F.J. Sheedy, E.A. Fisher, Macrophages in atherosclerosis: a dynamic balance, Nat. Rev. Immunol. 13 (2013) 709–721.
3. L. Cassetta, J.W. Pollard, Targeting macrophages: therapeutic approaches in cancer, Nat. Rev. Drug Discov. 17 (2018) 887–904.
4. K.E. de Goede, K.J. Harber, J. Van den Bossche, Let's enter the wonderful world of immunometabolites, Trends Endocrinol. Metab. 30 (2019) 329–331.
5. L.A.J. O'Neill, M.N. Artyomov, Itaconate: the poster child of metabolic reprogramming in macrophage function, Nat. Rev. Immunol. (2019) 273–281.
6. D.G. Ryan, et al., Coupling Krebs cycle metabolites to signalling in immunity and cancer, Nat. Metab. 1 (2019) 16–33.
7. P.S. Liu, et al., Alpha-ketoglutarate orchestrates macrophage activation through metabolic and epigenetic reprogramming, Nat. Immunol. 18 (2017) 985–994.
8. L.A. O'Neill, R.J. Kishton, J. Rathmell, A guide to immunometabolism for immunologists, Nat. Rev. Immunol. 16 (2016) 553–565.
9. J. Van den Bossche, L.A. O'Neill, D. Menon, Macrophage immunometabolism: where are we (going)? Trends Immunol. (2017) 395–406.
10. T.J. Gross, et al., Epigenetic silencing of the human NOS2 gene: rethinking the role of nitric oxide in human macrophage inflammatory responses, J. Immunol. 192 (2014) 2326–2338.
11. C. Nagy, A. Haschemi, Time and demand are two critical dimensions of immunometabolism: the process of

macrophage activation and the pentose phosphate pathway, Front. Immunol. 6 (2015) 164.

12. D. Ye, K.L. Guan, Y. Xiong, Metabolism, activity, and targeting of D- and L-2-hydroxyglutarates, Trends Cancer 4 (2018) 151–165.
13. A.M. Intlekofer, et al., Hypoxia induces production of L-2-hydroxyglutarate, Cell Metab. 22 (2015) 304–311.
14. P.A. Tyrakis, et al., S-2-hydroxyglutarate regulates CD8(+) T-lymphocyte fate, Nature 540 (2016) 236–241.
15. J. Fan, et al., Human phosphoglycerate dehydrogenase produces the oncometabolite D-2-hydroxyglutarate, ACS Chem. Biol. 10 (2015) 510–516.
16. E.A. Struys, et al., Kinetic characterization of human hydroxyacid-oxoacid transhydrogenase: relevance to D-2-hydroxyglutaric and gamma-hydroxybutyricacidurias, J. Inherit. Metab. Dis. 28 (2005) 921–930.
17. M. Kranendijk, et al., Progress in understanding 2-hydroxyglutaric acidurias, J. Inherit. Metab. Dis. 35 (2012) 571–587.
18. P.S. Ward, et al., The common feature of leukemiaassociated IDH1 and IDH2 mutations is a neomorphic enzyme activity converting alpha-ketoglutarate to 2-hydroxyglutarate, Cancer Cell 17 (2010) 225–234.
19. L. Bunse, et al., Suppression of antitumor T cell immunity by the oncometabolite (R)-2-hydroxyglutarate, Nat. Med. 24 (2018) 1192–1203.
20. M. Friedrich, et al., Tryptophan metabolism drives dynamic immunosuppressive myeloid states in IDH-mutant gliomas, Nat. Can. 2 (2021) 723–740.
21. N.C. Williams, et al., Signaling metabolite L-2-hydroxyglutarate activates the transcription factor HIF-1alpha in lipopolysaccharide-activated macrophages, J. Biol. Chem. 298 (2021), 101501.
22. M. Molenaars, et al., A conserved mito-cytosolic translational balance links two longevity pathways, Cell Metab. 31 (2020) 549–563 e547.
23. E.A. Struys, et al., Measurement of urinary Dand L-2-hydroxyglutarate enantiomers by stable-isotope-dilution liquid chromatography-tandem mass spectrometry after derivatization with diacetyl-Ltartaric anhydride, Clin. Chem. 50 (2004) 1391–1395.
24. J. Baardman, et al., A defective pentose phosphate pathway reduces inflammatory macrophage responses during hypercholesterolemia, Cell Rep. 25 (2018) 2044–2052 e2045.
25. Y. Zhou, et al., Metascape provides a biologist-oriented resource for the analysis of systems-level datasets, Nat. Commun. 10 (2019) 1523.
26. J. Van den Bossche, J. Baardman, M.P. de Winther, Metabolic characterization of polarized M1 and M2 bone marrow-derived macrophages using real-time extracellular flux analysis, JoVE (Journal of Visualized Experiments) (2015) e53424.
27. M.A. Lauterbach, et al., Toll-like receptor signaling rewires macrophage metabolism and promotes histone acetylation via ATP-citrate lyase, Immunity 51 (2019) 997–1011 e1017.
28. E.L. Mills, et al., Itaconate is an anti-inflammatory metabolite that activates Nrf2 via alkylation of KEAP1, Nature 556 (2018) 113–117.
29. E.M. Palmieri, et al., Nitric oxide orchestrates metabolic rewiring in M1 macrophages by targeting aconitase 2 and pyruvate dehydrogenase, Nat.

Commun. 11 (2020) 698.

30. H. Han, et al., TRRUST v2: an expanded reference database of human and mouse transcriptional regulatory interactions, Nucleic Acids Res. 46 (2018) D380–D386.

31. F. De Santa, et al., The histone H3 lysine-27 demethylase Jmjd3 links inflammation to inhibition of polycomb-mediated gene silencing, Cell 130 (2007) 1083–1094.

32. W.M. Oldham, et al., Hypoxia-mediated increases in L-2-hydroxyglutarate coordinate the metabolic response to reductive stress, Cell Metab. 22 (2015) 291–303.

33. X. Fu, et al., 2-Hydroxyglutarate inhibits ATP synthase and mTOR signaling, Cell Metab. 22 (2015) 508–515.

Supplementary materials

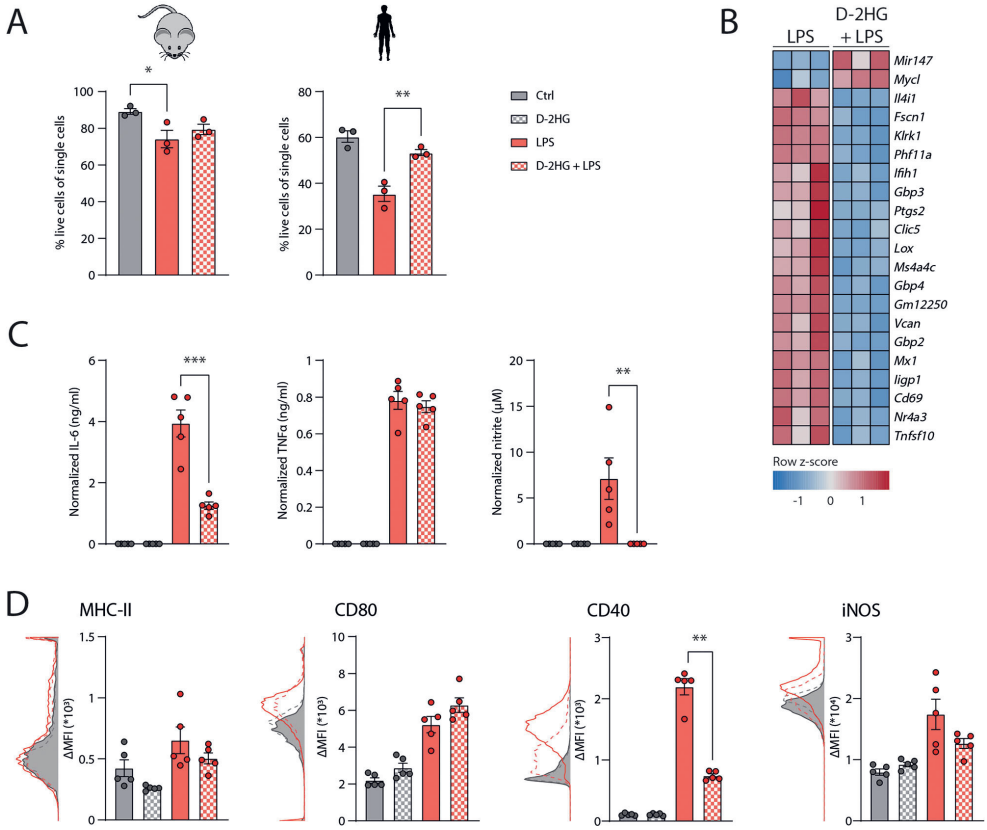

Supplemental Figure 1. D-2HG pre-treatment does not impair cell viability in mouse and human macrophages and dampens LPS-induced inflammatory responses in mouse peritoneal exudate macrophages *ex vivo*. Related to Figure 3. (A) Percentage of viable cells for mouse and human macrophages treated with D-2HG and/or vehicle and stimulated with LPS, measured by flow cytometry (n = 3 mice and donors, both analyzed by one-way ANOVA with Dunnett post-hoc test). (B) Heatmap of LPS-induced genes significantly affected by D-2HG pre-treatment. Cytokine levels in peritoneal fluid (analyzed by one-way ANOVA with Tukey post-hoc test) (C) and surface markers on peritoneal macrophages (analyzed by Brown-Forsythe and Welch ANOVA with Dunnett post-hoc test) (D) of thioglycollate-elicited macrophages, treated *ex vivo* with D-2HG and/or vehicle and stimulated with LPS (n = 4 mice for naïve groups and n = 6 for LPS-stimulated groups). *P*-values are indicated as <0.05*, <0.01**, <0.001***.

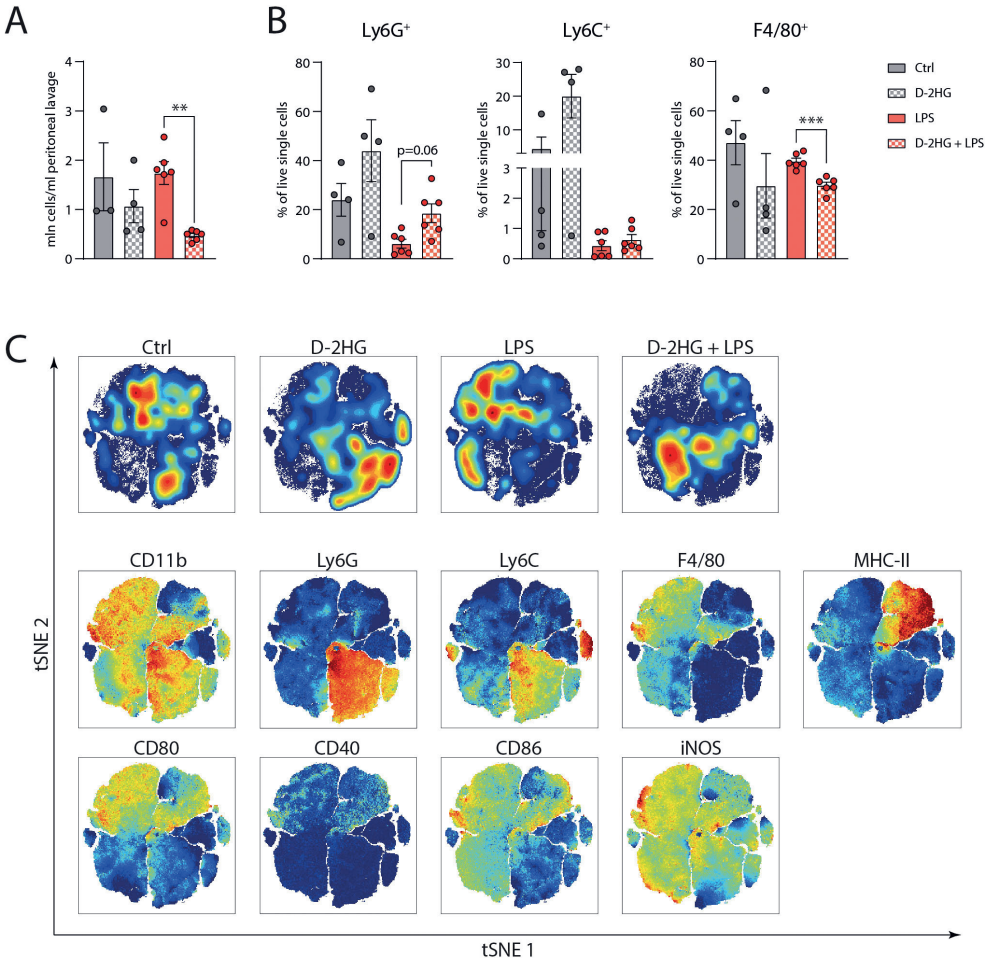

Supplemental Figure 2. Major cell subset abundance and validation of gating strategy in peritoneal exudates *in vivo*. Related to Figure 4. (A) Number peritoneal cells in peritoneal lavage (PL) for D-2HG- or vehicle- pre-treated and LPS-injected mice (n = 6 per group, analyzed by one-way ANOVA with Dunnett post-hoc test). (B) Major cell subset abundance in peritoneal exudates shown as percentage (analyzed by Brown-Forsythe and Welch ANOVA with Dunnett post-hoc test). (C) Validation of gating strategy by unsupervised tSNE dimensionality reduction and density plots per condition. *P*-values are indicated as <0.01**, <0.001***.

Supplemental Table 1. List of primers

Primers
Adhfe1 (FW: TTCACGAGCCATCAAACCCA; RV: TCCAGAGCATGGCAAAGGAC)
36b4 (FW: ATGGGTACAAGCGCGTCCTG; RV: GCCTTGACCTTTTCAGTAAG)
Cypa (FW: CAGACGCCACTGTCGCTTT; RV: TGTCTTTGGAACTTTGTCTGCAA)
D2hgdh (FW: CCAACCCAGTACAAGAGAGTCC; RV: CAGGACGTTCGTCAGCTTCT)
Idh1 (FW: ACTCAGTCGCCCAAGGTTATG; RV: CCCTTTCTGGTACATGCGGT)
Idh2 (FW: GGACAGTCACCCGCCATTAC; RV: GCGTCTGTGCAAACCTGATA)
Il6 (FW: GCTACCAAACTGGATATAATCAGGAAA; RV: CTTGTTATCTTTTAAGTTGTTCTTCATGTACTC)
L2hgdh (FW: GAGGTGGAATTGTGGGCCTT; RV: GTCCAGTCTGGTGAAGAGCTAA)
Ldha (FW: TCCAAGATGGCAACCCTCAA; RV: CATCCGCCAAGTCCTTCATT)
Mdh1 (FW: GGGAGAGTTCATCACGACTGT; RV: CTCCCTCTGGGGTTCCAAAC)
Mdh2 (FW: TGTGGCAGAGCTAAAGGGTTT; RV: TGGGGAAAGTCAACCTTCGG),
Il1b (FW: AAAGAATCTATACCTGTCCTGTGTAATGAAA; RV: GGTATTGCTTGGGATCCACACT)
Nos2 (FW: GCAAACCCAAGGTCTACGTTCA; RV: CCTCATTGGCCAGCTGCTT)
Phgdh (FW: GGACCGGAAGAAGTTCATGGG; RV: CGGCGACTTCAGGAGAGATG)
Tnf (FW: CATCTTCTCAAAATTCGAGTGACAA; RV: TGGGAGTAGACAAGGTACAACCC),

Supplemental Table 2. List of used antibodies and dyes

Target	Species	Clone	Fluorochrome	Article number	Company
CD40	M	3/23	APC	124612	BioLegend
CD11b	M	M1/70	PE-Cy7	101216	BioLegend
CD80	M	16-10A1	BV650	104732	BioLegend
F4/80	M	BM8	BV711	123147	BioLegend
iNOS	M	CXNFT	PE	12-5920-80	eBioScience
Ly6C	M	HK1.4	BV605	128035	BioLegend
Ly6G	M	1A8	FITC	127605	BioLegend
MHC-II	M	M5/114.15.2	PerCP/Cy5.5	107626	BioLegend
Fc block	M	93	n/a	14-0161-86	eBioScience
CD197 (CCR7)	H	G043H7	BV421	353207	BioLegend
CD274 (PD-L1)	H	MIH3	APC	374513	BioLegend
CD80	H	2D10	PE-Cy7	305218	BioLegend
Fc block	H	Fc1.3216	n/a	564220	BD Biosciences
Phopho-NF_KB-p65	M	93H1	n/a	3033	Cell Signaling
Total-NF_KB-p65	M	D14E12	n/a	8242	Cell Signaling
β-actin	M	AC-15	n/a	A5441	Sigma-Aldrich
Fixable Viability Dye	n/a	n/a	eFluor780	65-0865-14	eBioScience


5

Succinate is an Inflammation-Induced Immunoregulatory Metabolite in Macrophages

Karl J. Harber,[1,2,3] Kyra E. de Goede,[1] Sanne G.S. Verberk,[1] Elisa Meinster,[1] Helga E. de Vries,[1] Michel van Weeghel,[3] Menno P.J. de Winther,[2] and Jan Van den Bossche[1]

Metabolites, 10 (9), 372 (2020)

[1] Department of Molecular Cell Biology and Immunology, Amsterdam UMC, Vrije Universiteit Amsterdam, 1081 HV Amsterdam, The Netherlands

[2] Department of Medical Biochemistry, Amsterdam UMC, University of Amsterdam, Experimental Vascular Biology, 1105 AZ Amsterdam, The Netherlands

[3] Laboratory Genetic Metabolic Diseases, Amsterdam UMC, University of Amsterdam, 1105 AZ Amsterdam, The Netherlands

Abstract

Immunometabolism revealed the crucial role of cellular metabolism in controlling immune cell phenotype and functions. Macrophages, key immune cells that support progression of numerous inflammatory diseases, have been well described as undergoing vast metabolic rewiring upon activation. The immunometabolite succinate particularly gained a lot of attention and emerged as a crucial regulator of macrophage responses and inflammation. Succinate was originally described as a metabolite that supports inflammation via distinct routes. Recently, studies have indicated that succinate and its receptor SUCNR1 can suppress immune responses as well. These apparent contradictory effects might be due to specific experimental settings and particularly the use of distinct succinate forms. We therefore compared the phenotypic and functional effects of distinct succinate forms and receptor mouse models that were previously used for studying succinate immunomodulation. Here, we show that succinate can suppress secretion of inflammatory mediators IL-6, tumor necrosis factor (TNF) and nitric oxide (NO), as well as inhibit *Il1b* mRNA expression of inflammatory macrophages in a SUCNR1-independent manner. We also observed that macrophage SUCNR1 deficiency led to an enhanced inflammatory response without addition of exogenous succinate. While our study does not reveal new mechanistic insights into how succinate elicits different inflammatory responses, it does indicate that the inflammatory effects of succinate and its receptor SUCNR1 in macrophages are clearly context dependent.

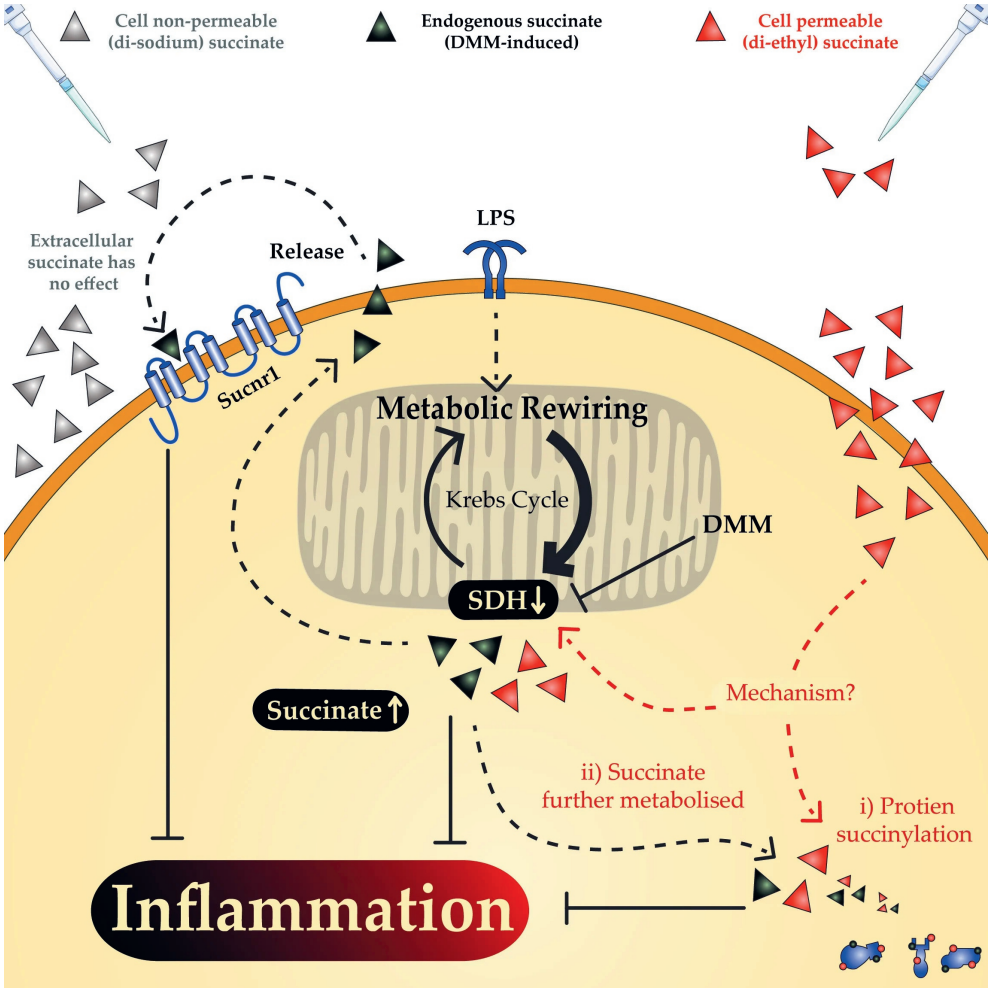
Cell non-permeable
(di-sodium) succinate
Endogenous succinate
(DMM-induced)
Cell permeable
(di-ethyl) succinate
Extracellular
succinate has
no effect
Release
LPS
Sucnr1
Metabolic Rewiring
Krebs Cycle
DMM
SDH↓
Succinate↑
Mechanism?
ii) Succinate
further metabolised
i) Protien
succinylation
Inflammation

Introduction

Macrophages play a significant role in innate immunity, driving inflammatory responses in health and disease. Upon stimulation of pattern recognition receptors by ligands such as lipopolysaccharide (LPS), macrophages undergo vast metabolic rewiring in order to compensate for changes in energy requirements [1,2,3,4,5]. Such a mechanism, comparable to the Warburg Effect observed in tumor cells, results in a major shift from high oxidative phosphorylation (OXPHOS) to a more glycolytic phenotype, termed aerobic glycolysis [6,7,8]. Krebs cycle intermediates such as succinate, itaconate, fumarate and citrate have all been described to accumulate in inflammatory macrophages [9,10,11]. Interleukin-4 (IL-4)-induced alternatively activated macrophages have been shown to accumulate the metabolite α-ketoglutarate. These accumulated metabolites have the potential to regulate immune responses and could play a role in disease progression. With the new concept of immunometabolism, we now believe there is potential to harness this switch in macrophage metabolic profiles to revert them to a more protective state as a treatment for disease, particularly in inflammatory diseases [12,13,14].

The Krebs cycle metabolite succinate is one of the most well-described immunometabolites in macrophages. Succinate is synthesized within the mitochondrial matrix and is the ligand for electron transport chain (ETC) complex II, supplying ATP synthase electrons to drive ETC through oxidation to fumarate. In spite of this, upon Toll-like receptor 4 (TLR4) activation of macrophages, the canonical Krebs cycle becomes truncated, causing lower SDH activity at the site of ETC complex II. Consequently, succinate oxidation is limited and subsequent accumulation of succinate occurs [11,15]. As a result, mitochondrial ROS production is increased and subsequent stabilization of hypoxic inducible factor 1-alpha (HIF-1α) occurs, the driver of further pro-inflammatory responses in macrophages [16]. Traditionally, HIF-1α is regulated by prolyl hydroxylases (PHDs), where hydroxylation induces targeting of HIF-1α for proteosomal degradation [17]. However, when succinate levels rise, PHDs are inhibited by succinate through product inhibition, activating the HIF-1 transcriptional pathway, which has been described to induce interleukin-1β (IL-1β) secretion in inflammatory macrophages and potentially lead to the development of inflammatory diseases [16]. Although reducing PHD inhibition could alleviate disease progression, there is an alternative pathway by which succinate is able to induce inflammatory responses.

The succinate receptor SUCNR1 is present on the cell surface of many tissue cell types, including kidney, spleen and small intestine cells, while also being expressed in myeloid cells such as dendritic cells (DCs) and macrophages [18]. The SUCNR1 receptor is a G protein-coupled receptor (GPR91) which consists of both a tightly bound βγ dimer and an α subunit [19]. Once succinate binds SUCNR1, the α and βγ subunits dissociate and

induce signaling down the mitogen-activated protein kinase (MAPK) pathway, resulting in transcription of a set of genes, differing based on cell type [20]. In myeloid cells, the succinate–SUCNR1 axis is thought to play a role in the inflammatory response. Rubic et al. showed that succinate accumulation activated SUCNR1, increasing inflammatory cytokine production in both human and mouse DCs [18]. Furthermore, Littlewood-Evans et al. observed that inflammatory macrophages of antigen-induced arthritic mice accumulated extracellular succinate, sequentially binding SUCNR1 [21]. Activation of the succinate–SUCNR1 axis resulted in increased IL-1β secretion and, as such, inflammation was reduced in mice deficient for SUCRN1. Although there is strong evidence to suggest the succinate–SUCNR1 axis induces a pro-inflammatory state in macrophages, anti-inflammatory effects of succinate and SUCNR1 have also been elucidated for numerous diseases. Wu et al. observed that cancer cell-derived succinate in the tumor microenvironment can polarize tumor-associated macrophages (TAMs) to a suppressive phenotype through SUCNR1 binding. This was confirmed when silencing of *Sucnr1* led to a lack of anti-inflammatory genes *Retnla*, *Arg1*, and *Clec10a* being expressed [22]. In a study focused on succinate's role in obesity, Keiran et al. showed a similar effect when myeloid-specific SUCNR1 deficiency resulted in upregulation of pro-inflammatory genes *Il1b*, *Il6* and *Il12b* [23]. The anti-inflammatory effect of the succinate–SUCNR1 axis in attribution to obesity and cancer convincingly suggests a role of succinate and SUCNR1 in driving anti-inflammatory responses.

Although in recent years researchers have demonstrated both the pro- and anti-inflammatory effects of the succinate–SUCNR1 axis in macrophages, conclusions are drawn from the use of two types of succinate forms—diethyl succinate, a synthetically generated cell-permeable form; and di-sodium succinate, a cell non-permeable form whose sodium ions dissipate upon dissolving in water, leaving the naturally abundant form present. Additionally, other articles investigate the succinate–SUCNR1 axis with the use of *Sucnr1*-deficient mice. Therefore, in this paper, we aimed to clarify the immunomodulatory effects of succinate by incorporating all three models into an experimental comparison. Here, we show that succinate can inhibit inflammatory response in macrophages via a SUCNR1-independent manner, while SUCNR1 likely also plays a role in dampening the inflammatory response.

Materials and methods

Mice

Wild-type C57BL/6J(c) 8- to 16-week-old mice were obtained from Charles River Laboratories, and bone marrow of 40-week-old *Sucnr1*$^{-/-}$ mice and WT controls, generated

as previously described [34], was generously gifted from Peter Deen (Radboud University Nijmegen). All experiments were approved by the Committee for Animal Welfare (Vrije Universiteit Amsterdam, Amsterdam, The Netherlands).

Macrophage cultures

Mouse bone marrow cells were isolated and cultured in RPMI-1640 with 2 mM L-glutamine, 10% fetal calf serum (FCS), penicillin (100 U/mL), streptomycin (100 µg/mL) (Gibco), and 15% L929-conditioned medium. On day 6, cells were harvested, seeded at 10^6 cells/mL and treated for 1 h with succinate or DMM at a concentration of 5 or 10 mM, respectively, unless otherwise stated. Following succinate or DMM treatment, BMDMs were stimulated for 4 or 24 h with 100 ng/mL LPS serotype O55:B5 (Sigma-Aldrich), 10 U/mL IFN-γ (PeproTech) + 10 ng/mL LPS or 20 U/mL IL-4 (Peprotech) to generate pro-inflammatory (LPS and LPS + IFN-γ) or anti-inflammatory (IL-4) macrophages, respectively. After stimulation, the supernatant was harvested for use in functional assays and macrophages were washed with PBA and harvested for phenotyping by flow cytometry and gene expression analysis.

Macrophage function

IL-6 and TNF were quantified by ELISA in accordance with the supplier's protocols (Life Technologies). NO production was measured by NO_2^- quantification in a Griess reaction (Sigma-Aldrich). Arginase activity (1 U = amount of enzyme that catalyzes the formation of 1 µmol urea/min/10^6 cells) was assessed as described previously [35].

Gene expression analysis

RNA was isolated with GeneJET RNA Purification kits (ThermoFisher), cDNA was synthesized with a High-Capacity cDNA Reverse Transcription Kit (Applied Biosystems) and quantified using an Implen nanodrop N60. qPCR was performed using a Sybr Green Fast mix (Applied Biosytems) on a ViiA7 (Applied Biosystems). Housekeeping genes *Rplp0* (*Arbp*) and *Cycloa* were used for normalization. Primer sequences are available upon request.

Flow cytometry

Cells were incubated with Fc block in addition to labeling antibodies and dyes listed in Supplementary Table 1 for 1 h. Cell viability was assessed by fixable viability staining according to the manufacturer's protocol (eBioscience). Data were acquired with an LSRFortessa X20 (Becton Dickinson) and analyzed using FlowJo v10 (Becton Dickinson) or FCSExpress v7 (De Novo Software). Surface expression was calculated as ΔMFI = (median fluorescence intensity) positive staining—(median fluorescence intensity) negative staining/background fluorescence.

A full list of antibodies, dyes and chemicals used in this article can be found listed in supplementary Figures; Supplementary Table 1.

Statistical analysis

Data are presented as the mean ± standard deviation (SD) and were tested using either one- or two-way ANOVA with a Bonferroni post hoc test in GraphPad Prism version 8.2.1 software. p values < 0.05 were considered significant, with levels of significance being indicated as follows: * $p < 0.05$; ** $p < 0.01$; *** $p < 0.001$; **** $p \leq 0.0001$.

Results

Cell-permeable diethyl succinate reduces secretion and expression of inflammatory mediators in macrophages

In a previous paper from our lab, we detected a significant induction of succinate in bone marrow-derived macrophages (BMDMs) upon LPS stimulation [24]. Since this confirmed previous observations, we set out to re-evaluate its effect on inflammatory responses in macrophages [16]. Hereto, BMDMs were pre-treated for 1 h with different concentrations of diethyl succinate, followed by 24 h activation with lipopolysaccharide (LPS) or LPS + interferon-gamma (IFN-γ). Diethyl succinate suppressed the LPS (+/-IFN-γ)-induced secretion of the inflammatory mediators interleukin-6 (IL-6), tumor necrosis factor (TNF) and nitric oxide (NO) in a dose-dependent manner (Figure 1A–C). These effects were not due to toxicity since diethyl succinate-treated macrophages were more viable than those left untreated, as evidenced by fixable viability staining in these cells (Supplementary Figure 1). Since *Il1b* expression was previously shown to be regulated by LPS-induced succinate accumulation [16], we also assessed *Il1b* expression (Figure 1D). In our setting, diethyl succinate did not increase LPS-induced *Il1b* expression as expected and instead decreased it.

While succinate has been well described for its induction of transcription factor HIF-1α protein expression and inflammatory cytokine production, how succinate affects classical macrophage surface biomarker expression has not been defined [16,21,25]. Therefore, using the same culturing conditions as previously stated, we investigated the effect of diethyl succinate on the expression of proteins associated with classical macrophage activation (Figure 1E; gating strategy and representative cytometry data in Supplementary Figures 2 and 3). In line with our above-mentioned observations, we observed that diethyl succinate pre-treatment downregulated CD40 and CD86 surface expression and intracellular iNOS levels in LPS (+/-IFN-γ)-stimulated BMDMs. These findings suggest that in contrast to some previous articles [16,21], diethyl succinate has the ability to inhibit

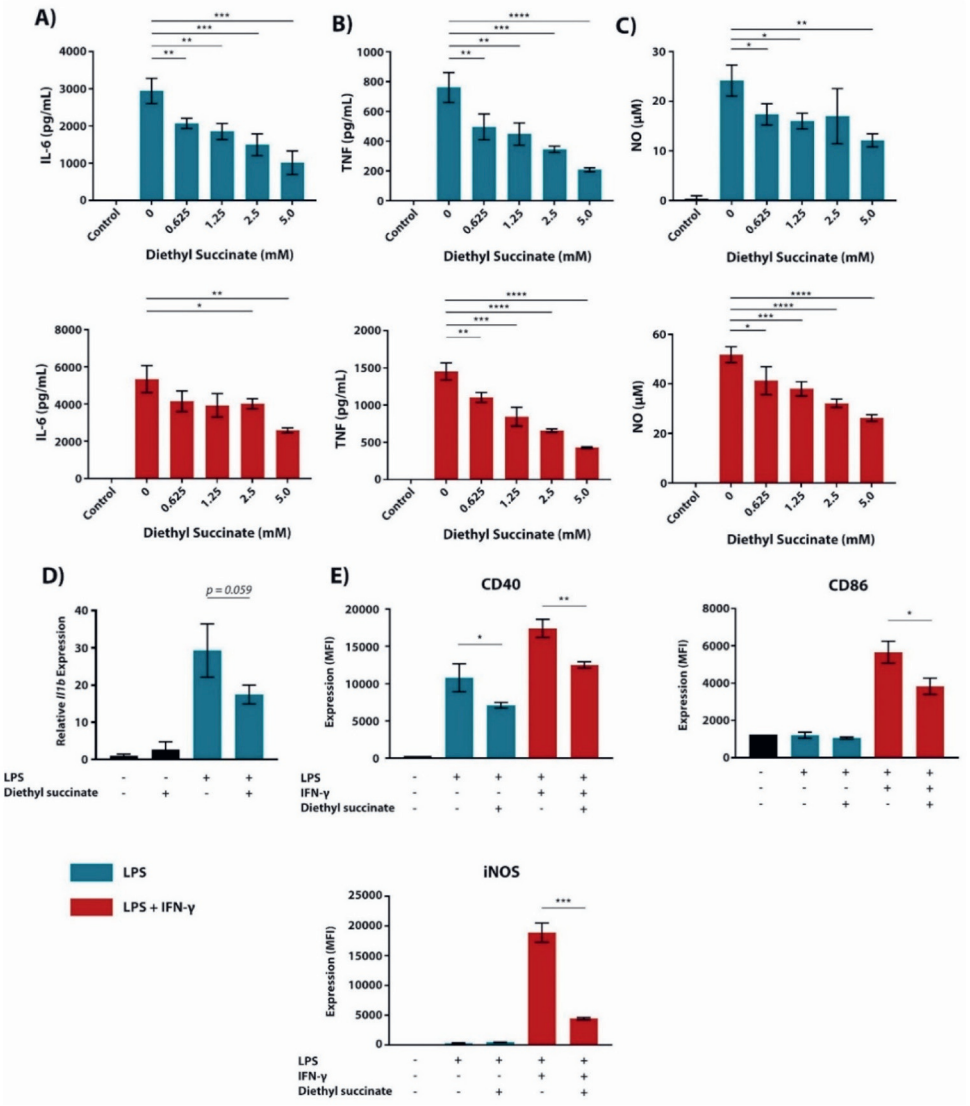

Figure 1. Succinate reduces pro-inflammatory cytokine secretion, gene and marker expression in BMDMs. (A) BMDMs were pre-treated with diethyl succinate (0.625–5.0 mM; A–C or 5 mM; D,E) 1 h prior to LPS (100 ng/mL; blue bars) or LPS + IFN-γ (10 ng/mL + 10 U/mL, respectively; red bars) stimulation for 24 h (A–C,E) or 4 h (D). The supernatant was then analyzed for IL-6 (A) and TNF (B) cytokine secretion by ELISA. Additionally, NO secretion (C) was measured by use of Griess Reagent. Subsequently, cells were either lysed and mRNA extracted from cell lysate to measure gene expression of *Il1b* by qPCR (D) or stained with fluorescently labelled antibodies against CD40, CD86 and iNOS (E). Stained cells were then read by a BD LSRFortessa X-20 and cell biomarker surface expression was analyzed in FCSExpress 7. All data are in triplicate (A–D) or quadruplicates (E) represented as the mean ± SD and are representative of three independent experiments. Controls are unstimulated BMDMs. * $p \leq 0.05$, ** $p \leq 0.01$, *** $p \leq 0.001$, and **** $p \leq 0.0001$.

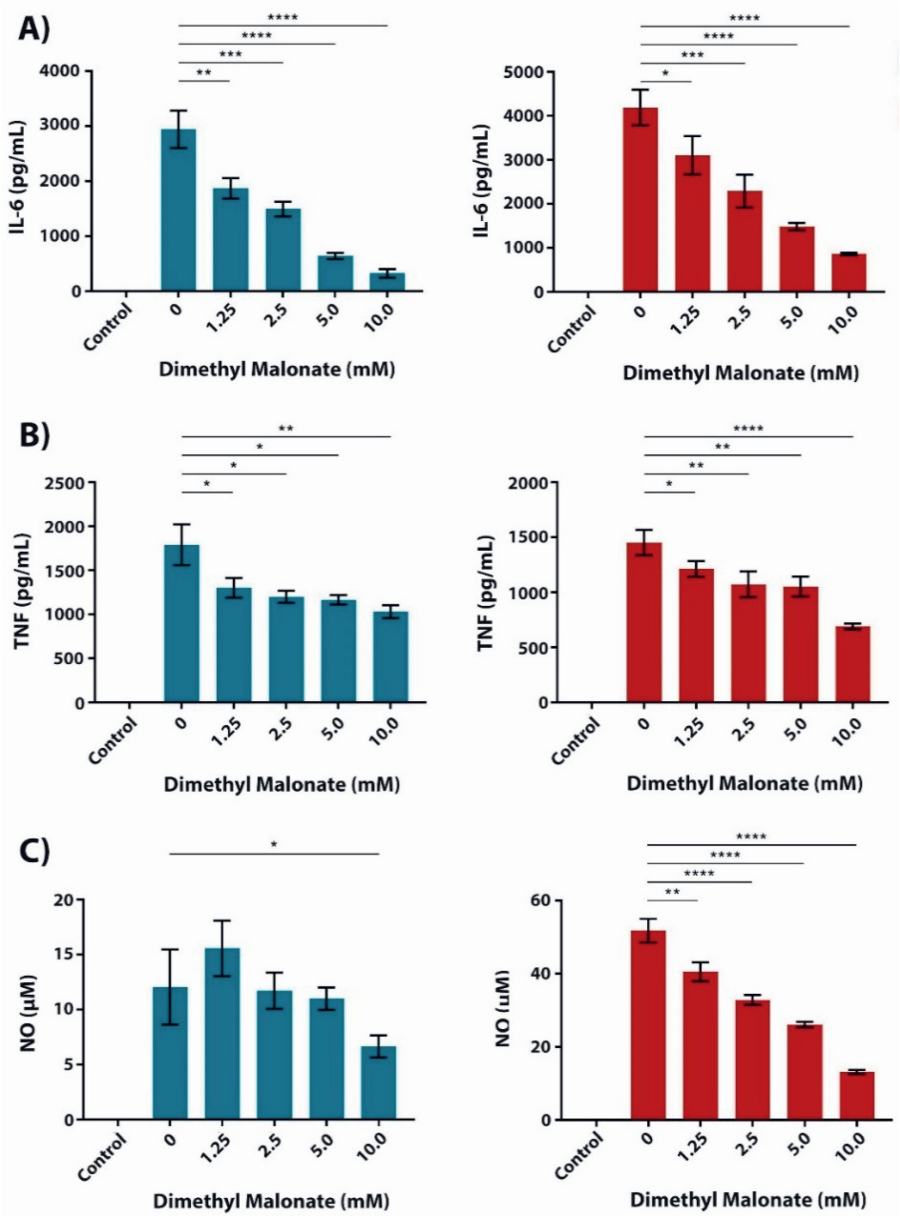

Figure 2. Cell-permeable malonate, an inhibitor of SDH, elicits similar functional responses in pro-inflammatory BMDMs as cell-permeable succinate. (A) BMDMs were pre-treated with dimethyl malonate (DMM) 1 h prior to LPS (100 ng/mL; blue bars) or LPS + IFN-γ (10 ng/mL + 10 U/mL, respectively; red bars) stimulation for 24 h. The supernatant was then analyzed for IL-6 (A) and TNF (B) cytokine secretion by ELISA. Additionally, NO secretion (C) was measured by use of Griess Reagent. All data are in quadruplicates represented as the mean ± SD and are representative of three independent experiments. * $p \leq 0.05$, ** $p \leq 0.01$, *** $p \leq 0.001$, and **** $p \leq 0.0001$.

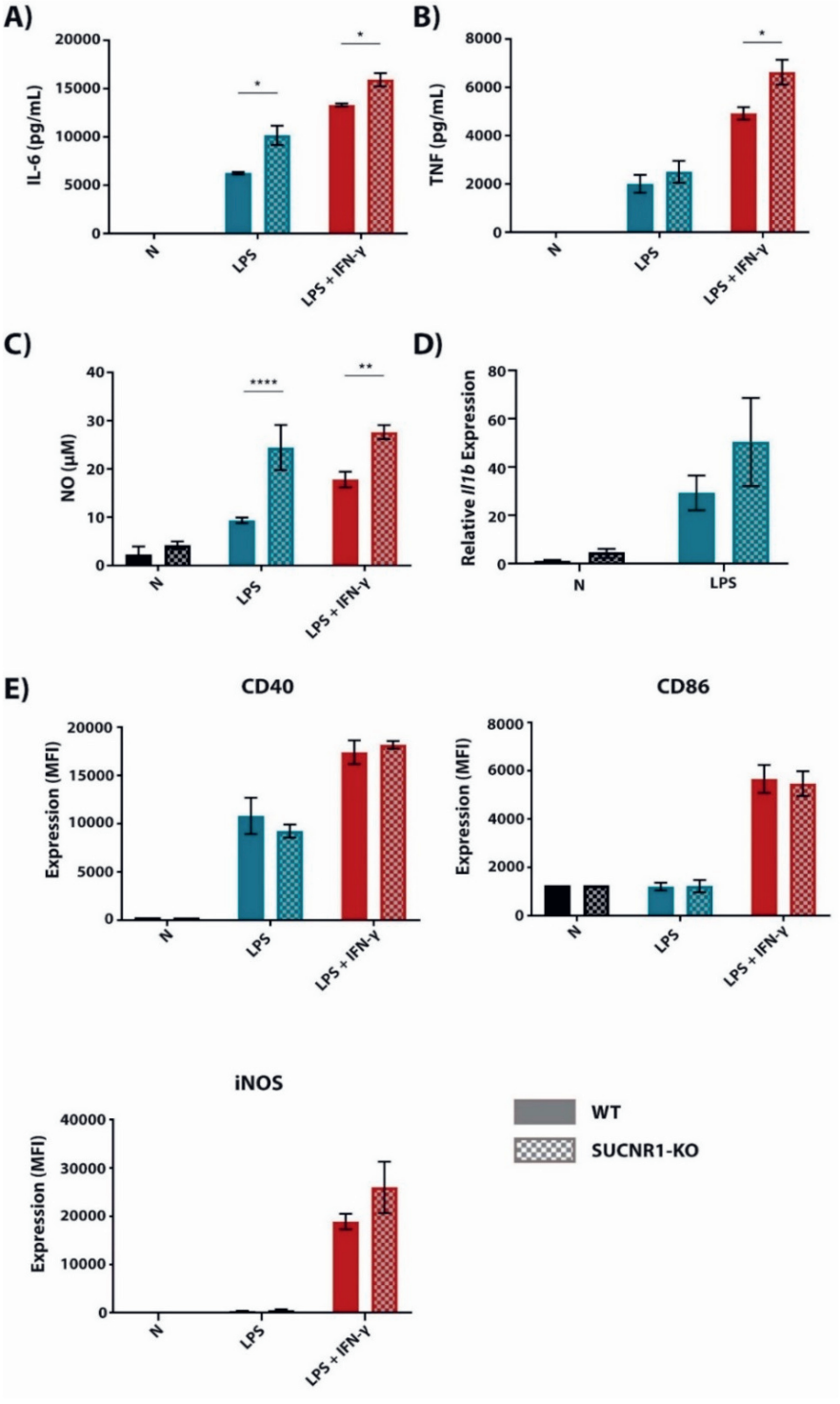
A)
IL-6 (pg/mL)
20000
15000
10000
5000
0
*
*
N
LPS
LPS + IFN-γ
B)
TNF (pg/mL)
8000
6000
4000
2000
0
*
N
LPS
LPS + IFN-γ
C)
NO (μM)
40
30
20
10
0
****
**
N
LPS
LPS + IFN-γ
D)
Relative Il1b Expression
80
60
40
20
0
N
LPS
E)
CD40
Expression (MFI)
20000
15000
10000
5000
0
N
LPS
LPS + IFN-γ
CD86
Expression (MFI)
8000
6000
4000
2000
0
N
LPS
LPS + IFN-γ
iNOS
Expression (MFI)
40000
30000
20000
10000
0
N
LPS
LPS + IFN-γ
WT
SUCNR1-KO

Figure 3. BMDMs deficient in succinate receptor SUCNR1 have an increased pro-inflammatory phenotype. BMDMs derived from SUCNR1-KO and WT littermate controls were stimulated with LPS (100 ng/mL) or LPS + IFN-γ (10 ng/mL + 10 U/mL, respectively) for 24 h (A–C,E) or 4 h (D). The supernatant was then analyzed for IL-6 (A) and TNF (B) cytokine secretion by ELISA. Additionally, NO secretion (C) was measured by use of Griess Reagent. Subsequently, cells were lysed and mRNA was extracted from cell lysate to measure gene expression of *Il1b* by qPCR (D). Cells were also stained with fluorescently labelled antibodies against CD40, iNOS and CD86 (E). Stained cells were then read by a BD LSRFortessa X-20 and cell biomarker surface expression was analyzed in FCSExpress 7. All data are in quadruplicates represented as the mean ± SD and are representative of three independent experiments. * $p \leq 0.05$, ** $p \leq 0.01$ and **** $p \leq 0.0001$.

macrophage activation in LPS (+/-IFN-γ)-stimulated cells by suppressing inflammatory cytokine, gene and cell marker expression.

Given that succinate is known to accumulate in LPS- and LPS + IFN-γ-stimulated cells at least partially due to succinate dehydrogenase (SDH) inhibition [15], we simulated this effect by pre-treating BMDMs with dimethyl malonate (DMM) as a competitive inhibitor of SDH [16,25,26]. DMM-mediated inhibition of SDH caused a similar dose-dependent reduction in IL-6, TNF and NO secretion as observed in diethyl succinate-treated macrophages (Figure 2). Together, these data show that increased succinate levels, elicited by exogenous pre-treatment with diethyl succinate or through SDH inhibition with DMM, reduce the expression of pro-inflammatory mediators in macrophages.

The succinate receptor SUCNR1 suppresses classically activated macrophages

Extracellular succinate is reported to induce p38 MAPK signaling through the G protein-coupled receptor 91 (GPR91; i.e., succinate receptor SUCNR1), thereby increasing transcription of at least some pro-inflammatory genes [18,21]. Therefore, we used BMDMs from *Sucnr1*-KO and control mice in order to investigate the role of SUCNR1 on LPS (+/-IFN-γ)-induced expression of pro-inflammatory mediators. We detected that *Sucnr1*-deficient macrophages had an increased inflammatory state, identified by increased secretion of IL-6, TNF and NO (Figure 3A–C) upon LPS (+/-IFN-γ) activation, and a trend towards increased *Il1b* expression (Figure 3D) in comparison to their control counterparts. When measuring the expression of membrane-bound markers, CD40 and CD86 were unaffected in LPS (+/-IFN-γ)-stimulated *Sucnr1*-KO macrophages (Figure 3E). Intracellular levels of iNOS were slightly higher in *Sucnr1*-KO BMDMs, however, not significantly. Together, these results show that SUCNR1 regulates inflammatory macrophage activation in a negative manner, lowering *Il1b* expression at the mRNA level and IL-6 and TNF secretion at the protein level.

The anti-inflammatory effect of succinate is mediated through SUCNR1-independent mechanisms

Since we used diethyl succinate in the experiments listed above, the observed effects of this cell-permeable succinate form could be mediated through both intracellular or surface

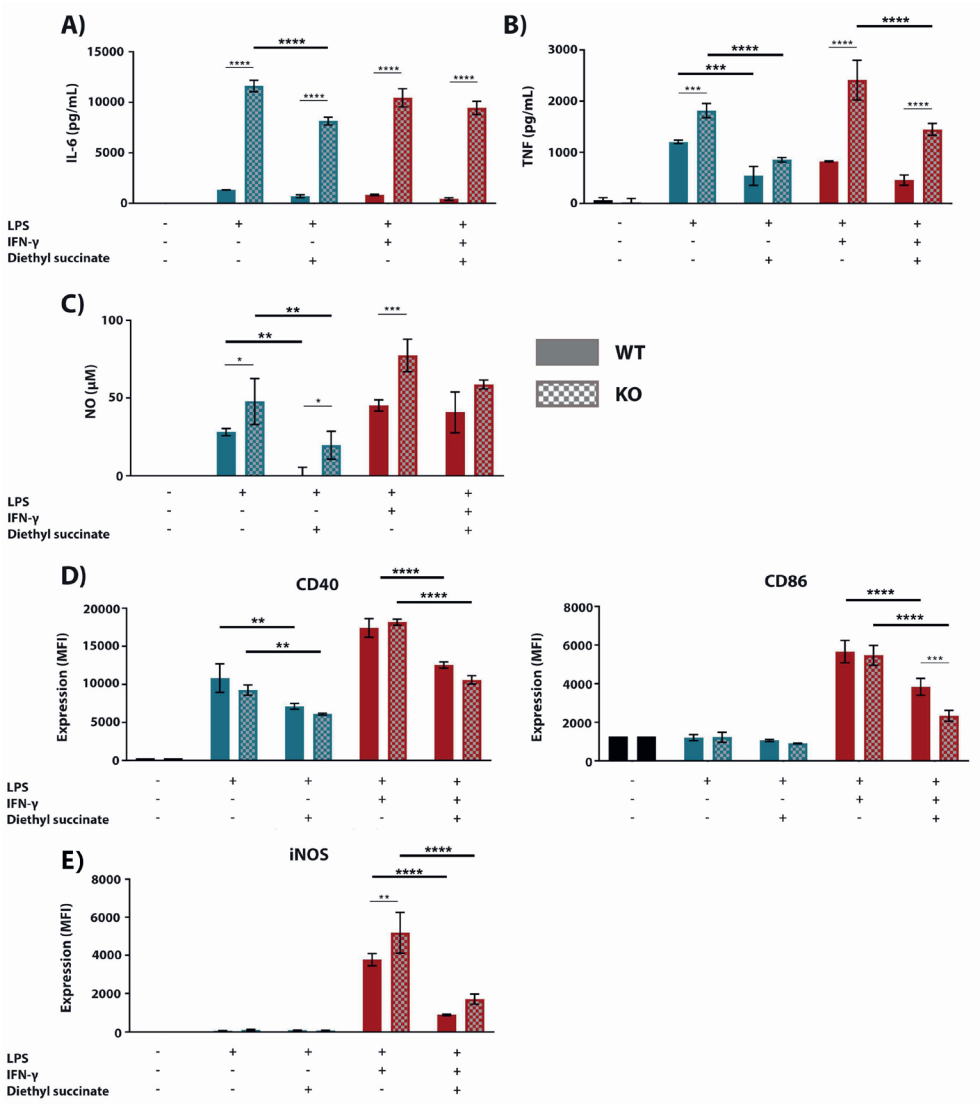

Figure 4. BMDMs deficient in succinate receptor SUCNR1 express a dampened pro-inflammatory phenotype in response to succinate. BMDMs derived from SUCNR1-KO and WT littermate controls were pre-treated with succinate (5 mM) 1 h prior to stimulation with LPS (100 ng/mL) or LPS + IFN-γ (10 ng/mL + 10 U/mL, respectively) for 24 h (A–C,E) or 4 h (D). The supernatant was then analyzed for IL-6 (A) and TNF (B) cytokine secretion by ELISA. Additionally, NO secretion (C) was measured by use of Griess Reagent. Cells were subsequently stained with fluorescently labelled antibodies against CD40, iNOS and CD86 (D). Stained cells were then read by a BD LSRFortessa X-20 and cell biomarker surface expression was analyzed in FCSExpress 7. All data are in quadruplicates represented as the mean ± SD and are representative of three independent experiments. Statistical significance indicated in bold and larger asterisks are used to highlight essential comparisons of this figure, whereas smaller asterisks show significant comparisons which have already been made apparent in previous figures. * $p \leq 0.05$, ** $p \leq 0.01$, *** $p \leq 0.001$, and **** $p \leq 0.0001$.

receptor-dependent pathways [9,27]. Therefore, we tested the effect of cell-permeable diethyl succinate on the inflammatory response in WT versus *Sucnr1*-KO macrophages. Succinate inhibited the LPS (+/-IFN-γ)-induced expression of pro-inflammatory mediators and cell surface markers to a similar extent in WT and *Sucnr1*-deficient macrophages (Figure 4A–D). To confirm that the effect of succinate acts via a SUCNR1-independent intracellular mechanism, we pre-treated BMDMs with non-cell-permeable disodium succinate, followed by LPS (+/-IFN-γ) stimulation. Succinate did not affect inflammatory responses in macrophages as measured by the secretion of inflammatory mediators and the expression of surface markers (Figure 5A–D). Although succinate has been described to mediate an anti-inflammatory response through SUCNR1 [22,23], our data show that the anti-inflammatory effects are mediated through a SUCNR1-independent mechanism.

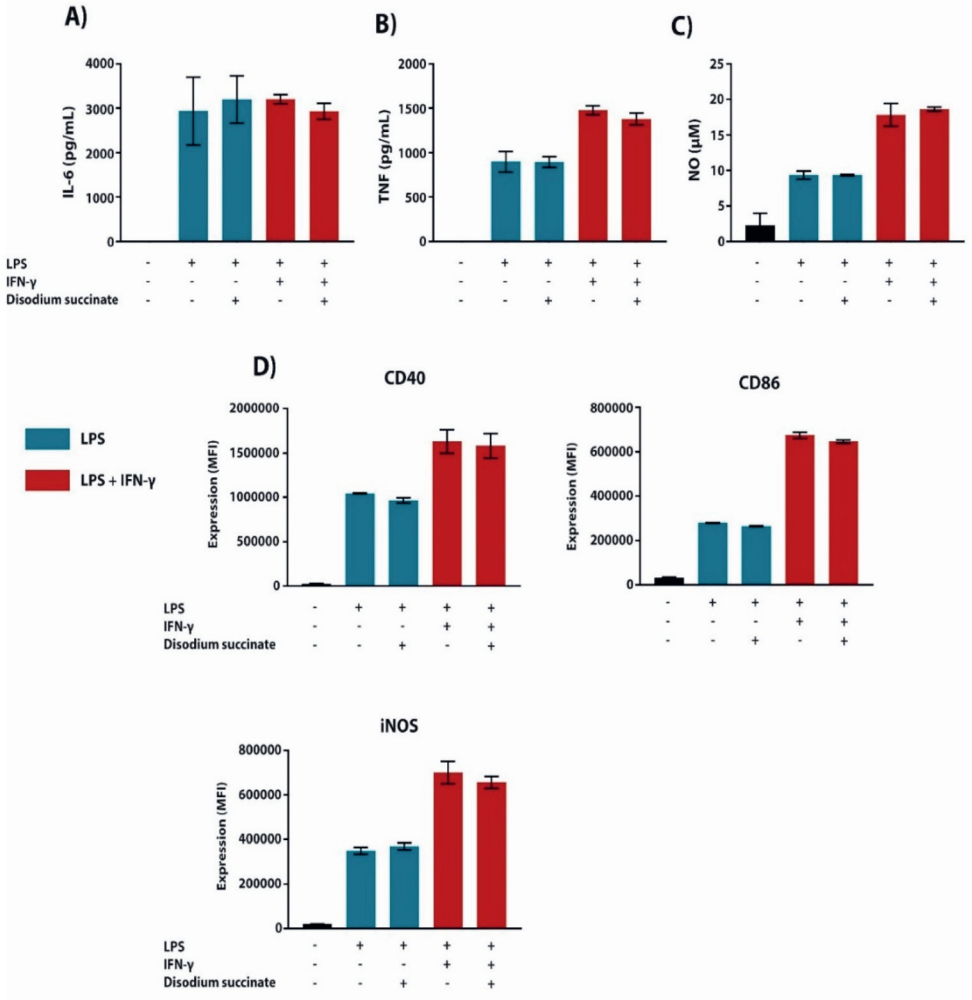

Figure 5. Cell non-permeable succinate has no effect on cytokine secretion or cell surface biomarker expression in pro-inflammatory BMDMs. (A–D) BMDMs were pre-treated with disodium succinate (5 mM) 1 h prior to LPS (100 ng/mL) or LPS + IFN-γ (10 ng/mL + 10 U/mL, respectively) stimulation for 24 h. The supernatant was then analyzed for IL-6 (A) and TNF (B) cytokine secretion by ELISA. Additionally, NO secretion (C) was measured by use of Griess Reagent. Cells were subsequently stained with fluorescently labelled antibodies against CD40, iNOS and CD86 (D). Stained cells were then read by a BD LSRFortessa X-20 and cell biomarker surface expression was analyzed in FCSExpress 7. All data are in quadruplicates represented as the mean ± SD and are representative of three independent experiments.

Discussion

In this work, we aimed to clarify how different succinate formulations modulate the inflammatory response of macrophages and how its receptor SUCNR1 partially mediates this. Here, we have shown that cell-permeable diethyl succinate elicits anti-inflammatory responses independently of the succinate receptor SUCNR1. Moreover, despite the fact that exogenous non-permeable succinate did not induce a response through SUCNR1, we observed an anti-inflammatory role for SUCNR1 since KO macrophages had an increased pro-inflammatory profile. Consequently, we have highlighted that succinate, although originally thought to be a pro-inflammatory metabolite, has the potential to induce anti-inflammatory responses in macrophages. What determines whether succinate is utilized in a pro- or anti-inflammatory manner still requires investigation.

Inflammatory macrophages are known to undergo vast metabolic rewiring in order to meet biosynthetic demands, resulting in accumulation of various metabolites [2,4,6,9,15]. Succinate, one of the most well described metabolites to accumulate in these macrophages, has been investigated for its role as an immunomodulatory mediator for inflammation. Initial articles describe succinate as a pro-inflammatory immunometabolite that elicits responses through HIF-1α and subsequent IL-1β secretion in addition to driving production of mitochondrial ROS [16,25]. Moreover, the cell surface receptor SUCNR1 has been shown to also induce IL-1β secretion upon succinate binding [21]. More recent studies demonstrate how succinate and SUCNR1 can also promote anti-inflammatory responses in macrophages and other cell types [22,23,27]. Since these articles use two different forms of succinate, namely a cell-permeable form (diethyl succinate) or the naturally occurring non-permeable form (disodium succinate), in addition to a *Sucnr1*-deficient mouse model, this asked for a comparison of these three different models in an identical experimental setting.

Succinate dehydrogenase activity is described to be altered in inflammatory macrophages and therefore can cause succinate accumulation [11,16]. Nevertheless, this enzyme still plays a role in succinate oxidation and generation of ROS in these macrophages, which has been shown to drive inflammatory responses [25]. Our data show that treating macrophages with cell-permeable succinate lowers secretion of pro-inflammatory cytokines IL-6, TNF and NO and dampens classical macrophage cell surface marker and

Il1β mRNA expression. While inhibition of iNOS, and thus NO production, shows how succinate can facilitate reduced macrophage activation, we also observe the capability for succinate to reduce expression of co-stimulatory factors CD40 and CD86 which are expected to stimulate the adaptive immune system. This observation is in apparent contrast to the previously described pro-inflammatory effects of intracellular succinate and therefore we wanted to explore succinate accumulation in an alternative model [16]. Mills et al. observed that the use of DMM to inhibit SDH, an effect which is seen in pro-inflammatory macrophages, additionally caused accumulation of endogenous succinate [25]. Using this model, we aimed to further support the notion that succinate may have the potential to induce anti-inflammatory responses through an intracellular mechanism. Here, we observed that DMM resulted in a dose-dependent inhibition of inflammatory mediators IL-6, TNF and NO, complementing our data on succinate-treated macrophages. This suggests a role for intracellular succinate to inhibit inflammatory responses rather than extracellular succinate. However, whether the intracellular succinate generated due to DMM is transported extracellularly and elicits membrane-mediated responses, or whether further inhibition of SDH and subsequent ROS synthesis is responsible for these observations, requires further studying.

Here, we demonstrate that BMDMs deficient in *Sucnr1* secrete higher concentrations of IL-6, TNF and NO as well as having slightly higher levels of classical macrophage activation marker iNOS after stimulation with LPS + IFN-γ. By completely removing the signal using a KO model, macrophages have a reduced ability to suppress pro-inflammatory responses. However, when permeable succinate is added to these *Sucnr1*-deficient macrophages, succinates' anti-inflammatory effect is still retained. These observations suggest that while permeable succinate has the capacity to regulate the immune response independent of SUCNR1, signaling through SUCNR1 augments this anti-inflammatory response further. This supports the earlier findings that succinate binding to SUCNR1 induces an anti-inflammatory feedback mechanism in BMDMs [22,23]. Moreover, Kieran et al. described that SUCNR1 is significantly higher expressed in BMDMs stimulated with IL-4 in comparison to LPS, sustaining the idea that the succinate–SUCNR1 axis plays a more important role in mediating a protective phenotype [23]. Indeed, the succinate–SUCNR1 axis was previously described to increase the expression of genes associated with alternative macrophage activation including *Arg1*, *Mrc1*, *Il10* and *Retnla* [23], which is supported by our own observations that arginase activity is increased in succinate as well as DMM-treated macrophages (Supplementary Figure 3).

In order to better understand the mechanism by which succinate lowers the pro-inflammatory profile of BMDMs, we compared cell-permeable succinate with the non-permeable, naturally occurring form of succinate. As mentioned above, permeable succinate lowered both pro-inflammatory cytokine production and cell surface marker

expression; however, the non-permeable form of succinate was unable to elicit these responses. This could be due to the fact that LPS (+/-IFN-γ)-stimulated BMDMs produce high concentrations of succinate and release succinate into the extracellular milieu [11,27,28]. This secretion of succinate may saturate the SUCNR1 signal, therefore masking the binding effect of additional succinate. Alternatively, SUCNR1 could be either desensitized or internalized as has previously been described in other cell types, rendering the succinate–SUCNR1 axis unavailable for further signaling [29,30]. Nonetheless, our data suggest that the anti-inflammatory effect observed by permeable succinate is through an unknown intracellular process. Potentially, succinate could be metabolized to fuel the production of other metabolites with potential anti-inflammatory effects in macrophages. Another intracellular mechanism could be through protein succinylation as this has been shown to adapt protein function, inducing distinct inflammatory roles, such as succinylation of lysine on PKM2 which induced IL-1β secretion [31,32]. However, whether succinylation of proteins that cause repurposing towards driving anti-inflammatory responses in classically activated macrophages occurs, remains to be addressed.

While our observations are indicative of an anti-inflammatory role for both succinate and SUCNR1, we are still striving to explain the discrepancy between our data and other articles that show succinate or SUCNR1 inducing pro-inflammatory responses [16,21,25]. Considering that we used LPS from the same *Escherichia. coli* serotype (O55:B5), followed by identical LPS concentrations and stimulation times as Tannahill et al. or Mills et al., we can only assume that minor differences in culture methods, such as medium (RPMI-1640 vs. DMEM) or fetal calf serum (FCS), results in these differences in response to succinate [16,25]. To further understand what could cause this, we pre-treated macrophages with succinate for 3 h instead of 1 h, as performed in both Tannahil et al. and Mills et al. (data not shown) [16,25]. This resulted in succinate inducing anti-inflammatory responses in macrophages to a similar extent to the 1 h treated macrophages. Although the inhibition of cytokine production and cell marker expression was not as strong as those treated for 1 h, we still observed significance. Nevertheless, we observed a much clearer and significant suppression of *Il1b* mRNA in 3 h of succinate-treated cells compared with the previous 1 h treatment. Therefore, our data demonstrate that the effect of succinate on inflammatory signaling in macrophages is anti-inflammatory, even after attempting to exactly replicate previous articles' experimental conditions. This leads us to believe that the inflammatory effects of succinate are highly context dependent and should be considered as a dynamic immunometabolite that can induce various inflammatory responses [16,22]. Immunometabolism is a quickly expanding field that could give us further insight into the pathophysiology of many diseases by studying how metabolism can affect inflammation [10,33]. More specifically, this study highlights the role of succinate in regulating inflammatory responses which can later be applied to diseases that display altered local or systemic succinate levels. In particular, the synovium fluid of patients with

the chronic autoimmune disease rheumatoid arthritis has been shown to have increased succinate levels [21]. By observing the immunomodulatory properties of succinate as well as its derivatives, as done so in this study, we can better consider how to develop appropriate treatments for such diseases. Since it has also been shown that succinate is one of the most highly induced metabolites in pro-inflammatory macrophages, applying the knowledge gained from studying succinate should stretch to inflammatory diseases beyond that of rheumatoid arthritis [24].

Together, these data show that succinate can induce anti-inflammatory responses in BMDMs, most likely intracellularly, in addition to SUCNR1 further augmenting this effect. However, since this is in contradiction to many initial articles describing the immunomodulatory effects of succinate, this generates a lot of unanswered questions on how succinate is truly regulating inflammation in macrophages and requires an appropriate human setting to explore this. These data, in combination with those of other research institutes, highlight the complexity of immunometabolism and that succinate and SUCNR1 may play a more diverse role than originally anticipated.

Acknowledgements

The authors thank Peter Deen and his student Elja Louer from the Radboud University Medical Centre in Nijmegen for donating *Sucnr1*$^{-/-}$ mice and WT control bone marrow used in this article.

Author contributions

Conceptualization, J.V.d.B. and M.P.J.d.W.; Formal Analysis, K.J.H.; Investigation, K.J.H., K.E.d.G., S.G.S.V., and E.M.; Data Curation, K.J.H.; Writing—Original Draft Preparation, K.J.H.; Writing—Review and Editing, K.J.H., J.V.d.B., M.P.J.d.W., M.v.W., and H.E.d.V.; Visualization, K.J.H.; Supervision, J.V.d.B., M.P.J.d.W., M.v.W., and H.E.d.V.; Project Administration, J.V.d.B. and M.P.J.d.W.; Funding Acquisition, J.V.d.B., M.P.J.d.W., and M.v.W. All authors have read and agreed to the published version of the manuscript.

Funding

This research received financial support from the Amsterdam Cardiovascular Sciences (ACS) research institute.

Declaration of competing interest

The authors declare no conflict of interest.

References

1. O'Neill, L.A. A critical role for citrate metabolism in LPS signalling. Biochem. J. 2011, 438, e5–e6.
2. Benit, P.; Letouze, E.; Rak, M.; Aubry, L.; Burnichon, N.; Favier, J.; Gimenez-Roqueplo, A.P.; Rustin, P. Unsuspected task for an old team: Succinate, fumarate and other krebs cycle acids in metabolic remodeling. Biochim. Biophys. Acta 2014, 1837, 1330–1337.
3. Galvan-Pena, S.; O'Neill, L.A. Metabolic reprograming in macrophage polarization. Front. Immunol. 2014, 5, 420.
4. Artyomov, M.N.; Sergushichev, A.; Schilling, J.D. Integrating immunometabolism and macrophage diversity. Semin. Immunol. 2016, 28, 417–424.
5. O'Neill, L.A.; Pearce, E.J. Immunometabolism governs dendritic cell and macrophage function. J. Exp. Med. 2016, 213, 15–23.
6. O'Neill, L.A. A broken krebs cycle in macrophages. Immunity 2015, 42, 393–394.
7. Krawczyk, C.M.; Holowka, T.; Sun, J.; Blagih, J.; Amiel, E.; DeBerardinis, R.J.; Cross, J.R.; Jung, E.; Thompson, C.B.; Jones, R.G.; et al. Toll-like receptor-induced changes in glycolytic metabolism regulate dendritic cell activation. Blood 2010, 115, 4742–4749.
8. DeBerardinis, R.J.; Chandel, N.S. We need to talk about the Warburg effect. Nat. Metab. 2020, 2, 127–129.
9. Ryan, D.G.; O'Neill, L.A.J. Krebs cycle rewired for macrophage and dendritic cell effector functions. FEBS Lett. 2017, 591, 2992–3006.
10. Ryan, D.G.; Murphy, M.P.; Frezza, C.; Prag, H.A.; Chouchani, E.T.; O'Neill, L.A.; Mills, E.L. Coupling Krebs cycle metabolites to signalling in immunity and cancer. Nat. Metab. 2018, 1, 16–33.
11. Murphy, M.P.; O'Neill, L.A.J. Krebs cycle reimagined: The emerging roles of succinate and itaconate as signal transducers. Cell 2018, 174, 780–784.
12. Lyssiotis, C.A.; Kimmelman, A.C. Metabolic interactions in the tumor microenvironment. Trends Cell Biol. 2017, 27, 863–875.
13. Mills, E.L.; O'Neill, L.A. Reprogramming mitochondrial metabolism in macrophages as an anti-inflammatory signal. Eur. J. Immunol. 2016, 46, 13–21.
14. Haas, R.; Cucchi, D.; Smith, J.; Pucino, V.; Macdougall, C.E.; Mauro, C. Intermediates of metabolism: From bystanders to signalling molecules. Trends Biochem. Sci. 2016, 41, 460–471.
15. Jha, A.K.; Huang, S.C.; Sergushichev, A.; Lampropoulou, V.; Ivanova, Y.; Loginicheva, E.; Chmielewski, K.; Stewart, K.M.; Ashall, J.; Everts, B.; et al. Network integration of parallel metabolic and transcriptional data reveals metabolic modules that regulate macrophage polarization. Immunity 2015, 42, 419–430.
16. Tannahill, G.M.; Curtis, A.M.; Adamik, J.; Palsson-McDermott, E.M.; McGettrick, A.F.; Goel, G.; Frezza, C.; Bernard, N.J.; Kelly, B.; Foley, N.H.; et al. Succinate is an inflammatory signal that induces IL-1beta through HIF-1alpha. Nature 2013, 496, 238–242.
17. Majmundar, A.J.; Wong, W.J.; Simon, M.C. Hypoxia-inducible factors and the response to hypoxic stress. Mol. Cell 2010, 40, 294–309.
18. Rubic, T.; Lametschwandtner, G.; Jost, S.; Hinteregger, S.; Kund, J.; Carballido-

Perrig, N.; Schwarzler, C.; Junt, T.; Voshol, H.; Meingassner, J.G.; et al. Triggering the succinate receptor GPR91 on dendritic cells enhances immunity. Nat. Immunol. 2008, 9, 1261–1269.

19. Gilissen, J.; Jouret, F.; Pirotte, B.; Hanson, J. Insight into SUCNR1 (GPR91) structure and function. Pharmacol. Ther. 2016, 159, 56–65.
20. de Castro Fonseca, M.; Aguiar, C.J.; da Rocha Franco, J.A.; Gingold, R.N.; Leite, M.F. GPR91: Expanding the frontiers of Krebs cycle intermediates. Cell Commun. Signal 2016, 14, 3.
21. Littlewood-Evans, A.; Sarret, S.; Apfel, V.; Loesle, P.; Dawson, J.; Zhang, J.; Muller, A.; Tigani, B.; Kneuer, R.; Patel, S.; et al. GPR91 senses extracellular succinate released from inflammatory macrophages and exacerbates rheumatoid arthritis. J. Exp. Med. 2016, 213, 1655–1662.
22. Wu, J.Y.; Huang, T.W.; Hsieh, Y.T.; Wang, Y.F.; Yen, C.C.; Lee, G.L.; Yeh, C.C.; Peng, Y.J.; Kuo, Y.Y.; Wen, H.T.; et al. Cancer-derived succinate promotes macrophage polarization and cancer metastasis via succinate receptor. Mol. Cell 2020, 77, 213–227.e5.
23. Keiran, N.; Ceperuelo-Mallafre, V.; Calvo, E.; Hernandez-Alvarez, M.I.; Ejarque, M.; Nunez-Roa, C.; Horrillo, D.; Maymo-Masip, E.; Rodriguez, M.M.; Fradera, R.; et al. SUCNR1 controls an anti-inflammatory program in macrophages to regulate the metabolic response to obesity. Nat. Immunol. 2019, 20, 581–592.
24. Baardman, J.; Verberk, S.G.S.; Prange, K.J.H.M.; van Weeghel, M.; van der Velden, S.; Ryan, D.G.; Wust, R.C.I.; Neele, A.E.; Speijer, D.; Denis, S.W.; et al. A defective pentose phosphate pathway reduces inflammatory macrophage responses during hypercholesterolemia. Cell Rep. 2018, 25, 2044–2052.e2045.
25. Mills, E.L.; Kelly, B.; Logan, A.; Costa, A.S.H.; Varma, M.; Bryant, C.E.; Tourlomousis, P.; Dabritz, J.H.M.; Gottlieb, E.; Latorre, I.; et al. Succinate dehydrogenase supports metabolic repurposing of mitochondria to drive inflammatory macrophages. Cell 2016, 167, 457–470.e413.
26. Lampropoulou, V.; Sergushichev, A.; Bambouskova, M.; Nair, S.; Vincent, E.E.; Loginicheva, E.; Cervantes-Barragan, L.; Ma, X.; Huang, S.C.; Griss, T.; et al. Itaconate links inhibition of succinate dehydrogenase with macrophage metabolic remodeling and regulation of inflammation. Cell Metab. 2016, 24, 158–166.
27. Peruzzotti-Jametti, L.; Bernstock, J.D.; Vicario, N.; Costa, A.S.H.; Kwok, C.K.; Leonardi, T.; Booty, L.M.; Bicci, I.; Balzarotti, B.; Volpe, G.; et al. Macrophage-derived extracellular succinate licenses neural stem cells to suppress chronic neuroinflammation. Cell Stem. Cell 2018, 22, 355–368.e313.
28. Infantino, V.; Iacobazzi, V.; Menga, A.; Avantaggiati, M.L.; Palmieri, F. A key role of the mitochondrial citrate carrier (SLC25A1) in TNFalpha- and IFNgamma-triggered inflammation. Biochim. Biophys. Acta 2014, 1839, 1217–1225.
29. He, W.H.; Miao, F.J.P.; Lin, D.C.H.; Schwandner, R.T.; Wang, Z.L.; Gao, J.H.; Chen, J.L.; Tian, H.; Ling, L. Citric acid cycle intermediates as ligands for orphan G-protein-coupled receptors. Nature 2004, 429, 188–193.
30. Robben, J.H.; Fenton, R.A.; Vargas, S.L.; Schweer, H.; Peti-Peterdi, J.; Deen, P.M.; Milligan, G. Localization of the succinate receptor in the distal nephron and its signaling in polarized MDCK cells. Kidney Int. 2009, 76, 1258–1267.

31. Park, J.; Chen, Y.; Tishkoff, D.X.; Peng, C.; Tan, M.; Dai, L.; Xie, Z.; Zhang, Y.; Zwaans, B.M.; Skinner, M.E.; et al. SIRT5-mediated lysine desuccinylation impacts diverse metabolic pathways. Mol. Cell 2013, 50, 919–930.

32. Wang, F.; Wang, K.; Xu, W.; Zhao, S.; Ye, D.; Wang, Y.; Xu, Y.; Zhou, L.; Chu, Y.; Zhang, C.; et al. SIRT5 desuccinylates and activates pyruvate kinase M2 to block macrophage IL-1beta production and to prevent DSS-induced colitis in mice. Cell Rep. 2017, 19, 2331–2344.

33. O'Neill, L.A.; Kishton, R.J.; Rathmell, J. A guide to immunometabolism for immunologists. Nat. Rev. Immunol. 2016, 16, 553–565.

34. van Diepen, J.A.; Robben, J.H.; Hooiveld, G.J.; Carmone, C.; Alsady, M.; Boutens, L.; Bekkenkamp-Grovenstein, M.; Hijmans, A.; Engelke, U.F.H.; Wevers, R.A.; et al. SUCNR1-mediated chemotaxis of macrophages aggravates obesity-induced inflammation and diabetes. Diabetologia 2017, 60, 1304–1313.

35. Van den Bossche, J.; Lamers, W.H.; Koehler, E.S.; Geuns, J.M.; Alhonen, L.; Uimari, A.; Pirnes-Karhu, S.; Van Overmeire, E.; Morias, Y.; Brys, L.; et al. Pivotal advance: Arginase-1-independent polyamine production stimulates the expression of IL-4-induced alternatively activated macrophage markers while inhibiting LPS-induced expression of inflammatory genes. J. Leukoc. Biol. 2012, 91, 685–699.

Supplementary materials

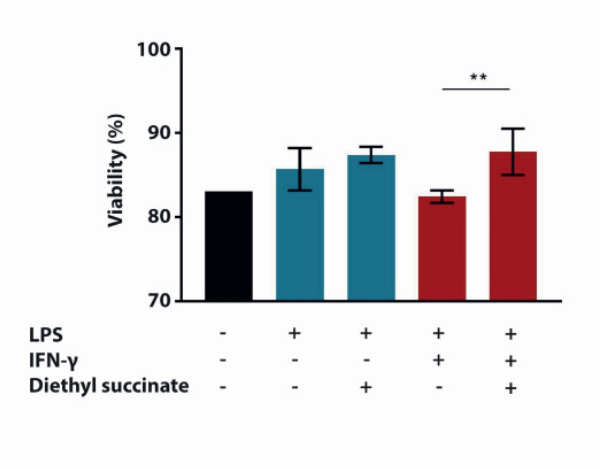

Supplementary Figure 1. Cell-permeable succinate increases viability of inflammatory BMDMs. BMDMs were pretreated with diethyl succinate (5 mM) 1 hour prior to LPS (100 ng/mL) or LPS + IFN-γ (10 ng/mL + 10 U/mL, respectively) stimulation for 24 hours. Cells were subsequently stained with fixable viability dye. Stained cells were then read by a BD LSRFortessa X-20 and cell biomarker surface expression was analysed in FCSExpress 7. All data are in quadruplicates represented by mean ± SD and are representative of three independent experiments. *$p \leq 0.05$, **$p \leq 0.01$, ***$p \leq 0.001$, ****$p \leq 0.0001$.

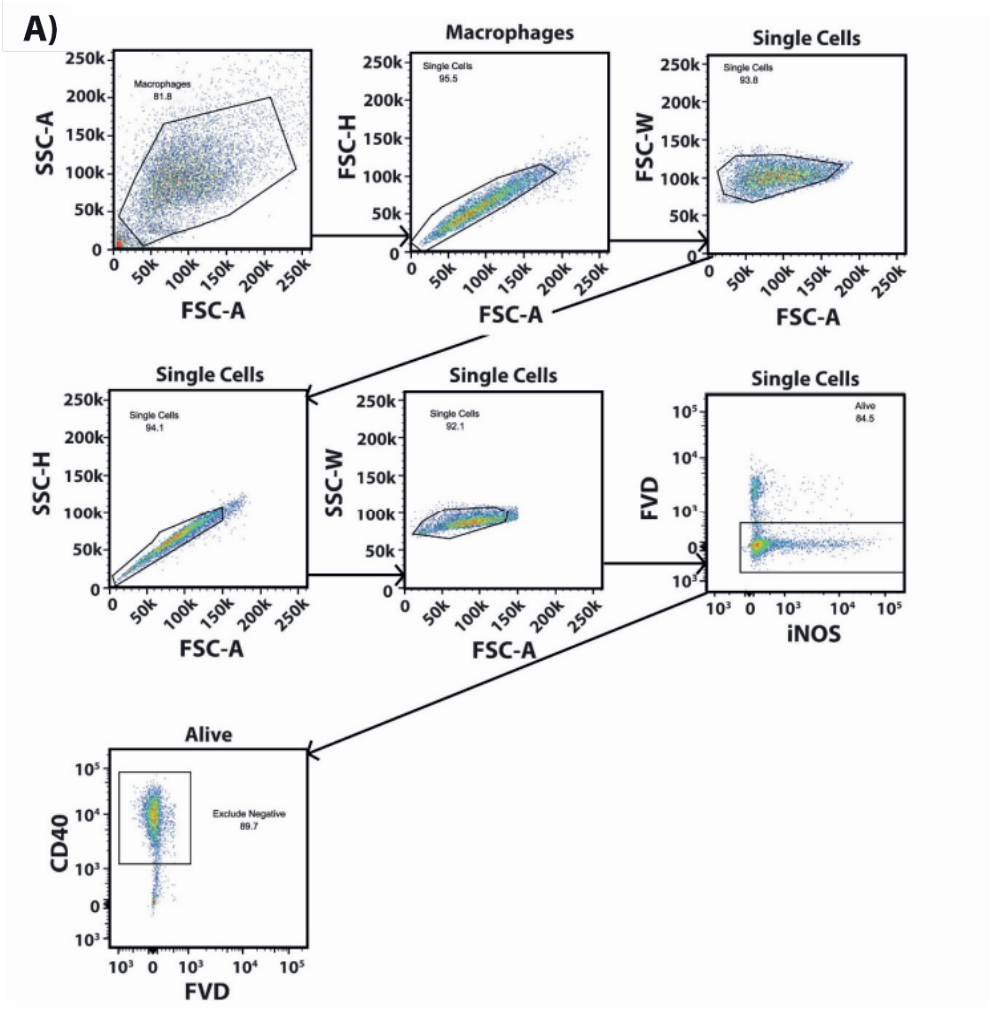
A)
Macrophages
Single Cells
SSC-A
FSC-A
FSC-H
FSC-W
SSC-H
SSC-W
FVD
iNOS
CD40
Alive
Exclude Negative
B)
LPS
LPS + IFN-γ
Figure 1
Figure 3
Figure 4
Non-treated
Succinate
WT
KO
KO non-treated
KO succinate
CD86
CD40
iNOS

Supplementary Figure 2. Gating strategy and overlay plots of macrophage marker expression. (A) Here we supply the gating strategy used to analyse cell marker expression for all figures in the manuscript. The gate of "exclude negative" was drawn to remove cells negative for all markers used and subsequently used for generating expression results. (B) representative overlay plots of triplicate samples stained for CD86, CD40 and iNOS are displayed with annotations of which figures from the manuscript they correspond to. All overlays are normalised to the mode on the y-axis in order to improve peak comparisons. Sample conditions for each figure are shown in blue (control) or red (experimental sample). The left half of the panel are LPS and the right are LPS + IFN-γ treated macrophages. Significance are shown in each overlay where *p ≤ 0.05, **p ≤ 0.01, ***p ≤ 0.001, ****p ≤ 0.0001.

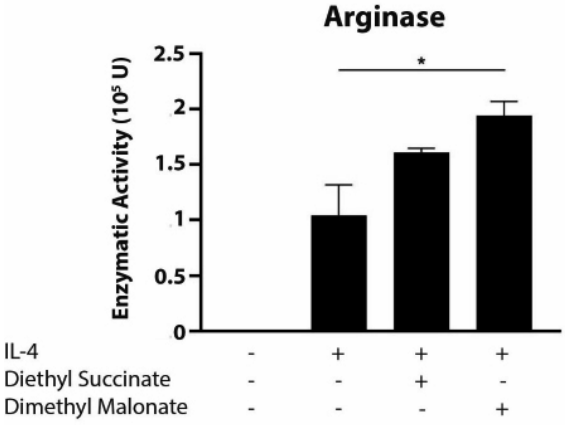

Supplementary Figure 3. Arginase activity in IL-4-stimulated macrophages is enhanced by cell-permeable succinate and malonate. BMDMs were pre-treated with either diethyl succinate (5 mM) or dimethyl malonate (10 mM) 1 hour prior to IL-4 (20 ng/mL) stimulation for 24 hours. Cells were subsequently assessed for arginase activity. All data are in duplicate represented by mean ± SD. *p ≤ 0.05, **p ≤ 0.01, ***p ≤ 0.001, ****p ≤ 0.0001.

Supplemental Table 1. List of used antibodies, dyes and chemicals

Antibodies		
Marker/Substrate	Clone	Supplier
Mouse iNOS-PE	CXNFT	eBioscience
Mouse CD40-APC	3/23	BD BioSciences
Mouse CD86-BV510	GL-1	BioLegend
Mouse CD301-PerCP/Cy5.5	LOM-14	BioLegend
Mouse CD301b-PE/Cy7	URA-1	BioLegend
Mouse CD16/CD32 (Fc-block)	93	eBioscience
Dyes		
Fixable Viability Dye-eFluor™ 780		eBioscience
Chemicals		
Diethyl succinate		Sigma Aldrich
Disodium succinate		Sigma Aldrich
Dimethyl malonate		Sigma Aldrich


6

Targeting the ACOD1-Itaconate Axis Stabilizes Atherosclerotic Plaques

Karl J. Harber,[1,2,3,4] Annette E. Neele,[1,2,3] Cindy P. A. A. van Roomen,[1] Marion J. J. Gijbels,[1,5] Linda Beckers,[1] Myrthe den Toom,[1] Bauke V.Schomakers,[6] Daan A. F. Heister,[4] Lisa Willemsen,[1,2,3] Guillermo R. Griffith,[1] Kyra E. de Goede,[3,4,7] Xanthe A. M. H. van Dierendonck,[4,5,7] Myrthe E. Reiche,[1,2,8] Aurélie Poli,[9] Frida L-H Mogensen,[9] Alessandro Michelucci,[9] Sanne G. S. Verberk,[2,3,4] Helga E. de Vries,[4,10] Michel van Weeghel,[6,11] Jan Van den Bossche,[2,3,4,7] and Menno P. J. de Winther,[1,2,3]

Redox Biology, 265, 23–30 (2024)

[1] Department of Medical Biochemistry, Amsterdam UMC, University of Amsterdam, 1105 AZ, Amsterdam, the Netherlands

[2] Amsterdam Cardiovascular Sciences (ACS), Atherosclerosis & Ischemic Syndromes, Amsterdam UMC, the Netherlands

[3] Amsterdam Institute for Infection and Immunity (AII), Inflammatory Diseases, Amsterdam UMC, the Netherlands

[4] Department of Molecular Cell Biology and Immunology, Amsterdam UMC, Vrije Universiteit Amsterdam, 1081 HV, Amsterdam, the Netherlands

[5] Department of Pathology, CARIM, Cardiovascular Research Institute Maastricht, GROW-School for Oncology and Developmental Biology, Maastricht UMC, University of Maastricht, 6229 HX, Maastricht, the Netherlands

[6] Department of Genetic Metabolic Diseases, Amsterdam UMC, University of Amsterdam, 1105 AZ, Amsterdam, the Netherlands

[7] Amsterdam Gastroenterology Endocrinology Metabolism (AGEM), Amsterdam UMC, the Netherlands

[8] Department of Medical Cell Biology, Uppsala University, 75236, Uppsala, Sweden

[9] Neuro-Immunology Group, Department of Cancer Research, Luxembourg Institute of Health, 6A Rue Nicolas-Ernest Barblé, L-1210, Luxembourg, Luxembourg

[10] Amsterdam Neuroscience, Amsterdam, the Netherlands

[11] Core Facility Metabolomics, Amsterdam UMC, University of Amsterdam, 1105 AZ Amsterdam, the Netherlands

Abstract

Inflammatory macrophages are key drivers of atherosclerosis that can induce rupture-prone vulnerable plaques. Skewing the plaque macrophage population towards a more protective phenotype and reducing the occurrence of clinical events is thought to be a promising method of treating atherosclerotic patients. In the current study, we investigate the immunomodulatory properties of itaconate, an immunometabolite derived from the TCA cycle intermediate *cis*-aconitate and synthesised by the enzyme Aconitate Decarboxylase 1 (ACOD1, also known as IRG1), in the context of atherosclerosis. *Ldlr*$^{-/-}$ atherogenic mice transplanted with *Acod1*$^{-/-}$ bone marrow displayed a more stable plaque phenotype with smaller necrotic cores and showed increased recruitment of monocytes to the vessel intima. Macrophages from *Acod1*$^{-/-}$ mice contained more lipids whilst also displaying reduced induction of apoptosis. Using multi-omics approaches, we identify a metabolic shift towards purine metabolism, in addition to an altered glycolytic flux towards production of glycerol for triglyceride synthesis. Overall, our data highlight the potential of therapeutically blocking ACOD1 with the aim of stabilizing atherosclerotic plaques.

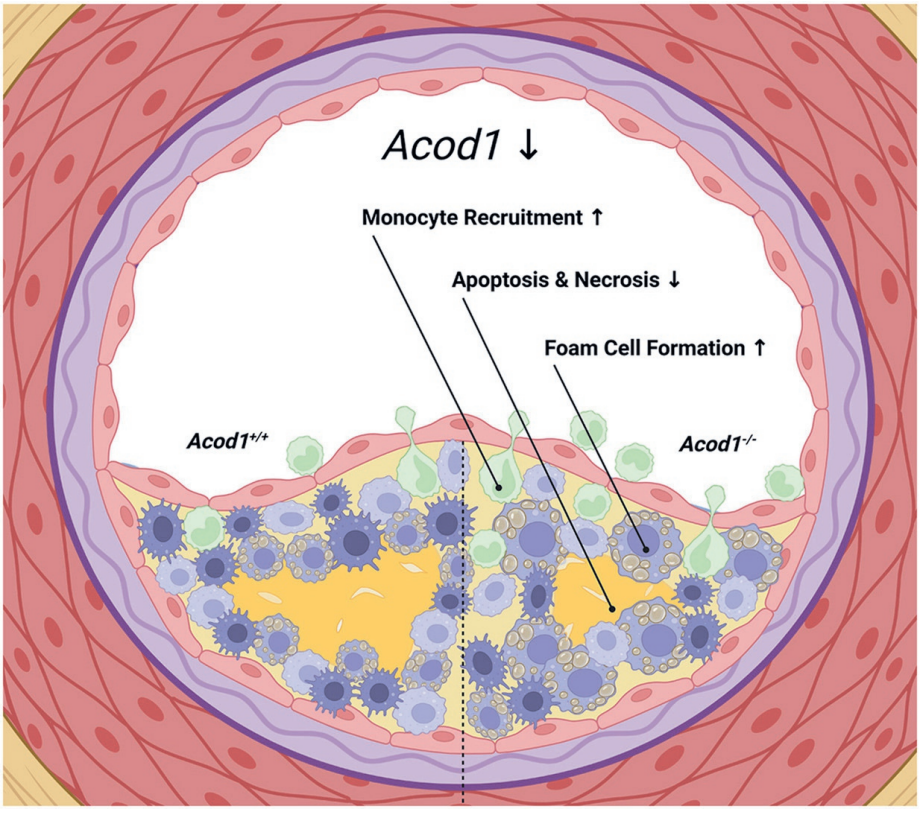

Introduction

Atherosclerosis is the leading cause of cardiovascular disease (CVD) and consequently a global health concern, where CVD is responsible for over 30 % of deaths worldwide. Use of cholesterol-lowering interventions such as statins and PCSK9 inhibitors, although effective in lowering low-density lipoprotein (LDL) cholesterol, comes with numerous side effects and does not address the residual inflammatory risk of CVD patients [1,2,3,4]. In atherosclerosis patients, lipid deposition and subsequent oxidation in vessel sub-endothelium initiates recruitment of monocytes to the lesion area, developing into mature macrophages [5,6]. As such, macrophages attempt to clear modified lipids by scavenger receptor-mediated endocytosis and therefore become lipid-laden foam cells (FCs), a characteristic cell type of atherosclerosis. Dysregulated lipid handling of FCs ultimately leads to cell necrosis and subsequent plaque growth [7]. Development of the necrotic core drives further recruitment of monocytes and release of pro-inflammatory mediators, generating unstable plaques that may rupture, leading to thrombus formation and subsequent infarction [8]. Contrary to this, anti-inflammatory macrophages are critical in stabilizing plaques through necrotic core maintenance and fibrous cap thickening [9]. Promoting an increased ratio of anti-inflammatory to pro-inflammatory macrophage subsets thus may improve plaque stability whilst also tackling residual inflammation in atherosclerosis patients. As such, monoclonal antibodies targeting interleukin-1 beta (IL-1β) in the CANTOS trial resulted in lower cardiovascular events, however total mortality was unaffected due to severe leukopenia and subsequent sepsis [10]. Therefore, new combined methods of specifically reducing plaque inflammation and LDL content are needed for successful reduction of CVD related deaths [11].

In the last 10 years it has been unveiled that metabolites have a broader function outside of their energetic roles [12]. Upon inflammatory activation, macrophages undergo vast re-wiring of their TCA cycle, resulting in accumulation or depletion of certain metabolites. Such alterations in metabolite levels can elicit functional changes through receptor binding, post-translational modifications or act as co-factors for enzymes [13,14,15]. Itaconate is a macrophage-specific, inflammation-induced derivative of the TCA cycle intermediate *cis*-aconitate, produced by the enzyme *cis*-aconitate-decarboxylase (encoded by *ACOD1*, also known as IRG1), formed from the metabolite *cis*-aconitate [16]. Upon LPS stimulation, *ACOD1* and itaconate are one of the most upregulated genes and metabolites in both human and mouse macrophages. Functional testing of itaconate and its derivatives on macrophages identified these molecules as potent regulators of inflammatory signaling and redox biology [16,17,18,19,20]. In parallel, *Acod1*$^{-/-}$ bone marrow-derived macrophages (BMDMs), depleted of endogenous itaconate, display significantly higher inflammatory responses than their *Acod1*$^{+/+}$ BMDMs counterparts [17]. Moreover, Acod1 has been

shown to modulate the generation of reactive oxygen species (ROS), a key player in the development of atherosclerotic plaques [21,22,23,24]. As such, understanding the effects of itaconate on the handling of excessive lipids, oxidative stress and inflammatory responses during atherogenesis could help harness control over immune cell-driven CVD and form the basis for novel therapeutic options [25,26].

In this paper, we explore *Acod1* as a modulator of atherosclerosis progression. We show that *Acod1*-deficiency increases plaque stability and reduces necrosis in the *Ldlr*$^{-/-}$ atherosclerosis mouse model, as well as increasing macrophage viability and lipid content.

Materials & methods

Mice

Bone marrow obtained from Wild-type C57BL/6J(c) 8- to 16-week-old mice originated from Charles River Laboratories and were housed in the Universitair Proefdiercentrum, Vrije Universiteit Amsterdam and terminated by CO2 asphyxiation. Bone marrow from female *Acod1*$^{+/+}$ and *Acod1*$^{-/-}$ mice on a C57BL/6 N background, aged between 8 and 13 weeks, housed at the SPF animal facility at the University of Luxembourg and terminated by cervical dislocation, were generously gifted from Dr. Alessandro Michelucci (Luxembourg Institute of Health). Using embryonic stem cells (ESC) from the Knockout Mouse Project Repository (KOMP, University of California, DAVIS), Dr. Haruhiko Koseki produced the Irg1$^{tm1a(KOMP)Wtsi}$ strain at the RIKEN Institute [55]. Briefly, recipient female C57BL/6 N blastocysts were injected with *Acod1*$^{-/-}$ C57BL/6 N ESCs and subsequently bred with wild-type C57BL/6 N mice. *Acod1*$^{-/-}$ mice and *Acod1*$^{-/-}$ C57BL/6 N littermate controls were then generated by crossing heterozygote mice. *Acod1*$^{+/+}$ and *Acod1*$^{-/-}$ were then phenotyped using qPCR. For atherosclerosis studies, low density lipoprotein receptor (*Ldlr*) KO mice with a C57BL/6 background (Jackson laboratories) were used. All mice were housed in 12 h light/dark cycle and had free access to sterile food and water. All experiments were approved by the Committee for Animal Welfare under license number AVD118002016750 (Amsterdam UMC, Amsterdam, The Netherlands).

Human donors

Human monocytes were harvested from anonymous donor buffy coats provided by Sanquin blood bank in Amsterdam, The Netherlands. All donors had granted permission to use material for medical research through written informed consent and all experiments using such material adhered to the Declaration of Helsinki.

Bone marrow isolation, differentiation and stimulation

Bone marrow of C57BL/6 or *Acod1*$^{+/+}$ and *Acod1*$^{-/-}$ mice was isolated by flushing femurs and tibias. BMDMs were then generated by culturing bone marrow for 6 days in RPMI-

1640 medium supplemented with 10 % FCS, 2 mM l-glutamine (Thermo Fisher Scientific), 100 U/mL penicillin-streptomycin (Thermo Fisher Scientific) and 15 % L929 conditioned medium. BMDMs were then plated at a density of 1 x 10^6/mL and pre-treated with 5 mM unmodified itaconate (Sigma-Aldrich) for 3 h in itaconate related functional experiments. To elicit an inflammatory response and to activate macrophages, BMDMs were subsequently treated with 100 ng/mL of lipopolysaccharide (LPS from Escherichia coli; O111:B4; Sigma) as indicated (3, 24 or 72 h). For fluxomics experiments, isotopic labelling was achieved by supplementing glucose-free medium with U13C-glucose, as well as previously mentioned supplementations, for 12 h prior to stimulations.

Human monocyte isolation, differentiation and activation

Human monocytes were harvested using Ficoll based density gradient separation of PBMC's followed by isolation of $CD14^+$ monocytes with the use of magnetic beads (Miltenyi). Monocytes were then seeded in plates at a density of 1 x 10^6/mL and cultured for 6 days in Iscove's Modified Dulbecco's Medium (IMDM) medium supplemented with 10 % FCS, 2 mM l-glutamine (Thermo Fisher Scientific), 100 U/mL penicillin-streptomycin (Thermo Fisher Scientific) and 50 ng/mL human M-CSF (Miltenyi). On day 3 and 6 of culturing, old medium was replaced with fresh medium with the same supplements. Differentiated macrophages were stimulated with either 5 mM itaconate or 10 ng/mL LPS as described above.

Atherosclerosis in vivo

Atherogenic *Ldlr*$^{-/-}$ female mice were irradiated with a lethal amount of 6 Gy on 2 consecutive days. Within each cage containing 5 mice, mice were randomly selected to be intravenously transplanted with 5 x 10^6 cells of either *Acod1*$^{+/+}$ or *Acod1*$^{-/-}$ bone marrow, with no cage containing less than 2 mice transplanted with the same bone marrow. This resulted in 22 *Acod1*$^{+/+}$ → *Ldlr*$^{-/-}$ and 23 *Acod1*$^{-/-}$ → *Ldlr*$^{-/-}$ mice. After 6 weeks of bone marrow reconstitution, regular chow diet was substituted for HFD (15 % fat and 0.15 % cholesterol, Ssniff Spezialdiäten) for the remaining 9 weeks of the experiment. Roughly 100uL of blood was isolated via tail incision on weeks 0, 5 and 8. 4 days prior to sacrifice, a subset of 5 vs 5 *Acod1*$^{+/+}$ → *Ldlr*$^{-/-}$ and *Acod1*$^{-/-}$ → *Ldlr*$^{-/-}$ mice were intraperitoneally injected with 3 % thioglycollate, to induce a sterile inflammation. On week 9, mice were terminated by CO_2 asphyxiation. Hearts were punctured immediately after sacrifice to drain mice of blood for storage of plasma and quantifying engraftment through measurement of *Ldlr* expression by qPCR. Mice injected with thioglycollate received a peritoneal lavage with ice cold PBS and isolated FCs were placed in RPMI-1640 culture medium supplemented with 10 % FCS, 2 mM l-glutamine, 100 U/mL penicillin-streptomycin. Hearts were then removed and stored in tissue-tek (DAKO) for histological staining whilst spleens were halved, to be immediately used for leukocyte quantification as well as storage in tissue-

tek. Bone marrow was isolated from a subgroup of 5 vs 5 *Acod1*$^{+/+}$ → *Ldlr*$^{-/-}$ and *Acod1*$^{-/-}$ → *Ldlr*$^{-/-}$ mice for precursor quantification.

Blood and spleen parameters

Spleens were weighed and crushed through a 45 µm filter and then stained for leukocyte markers as stated in Supplemental Table 2 and measured by flow cytometry. Leukocyte composition was normalized on spleen weight. Blood plasma was used to enzymatically determine cholesterol and triglyceride levels according to the manufacturer's protocol (Roche). Leukocyte quantification was performed on blood after 3 steps of erylysis treatment. 10 µL of blood was used to quantify CD45^{+} cell content per mL. Leukocyte subsets were assessed by flow cytometry using antibody stains as stated in Supplemental Table 2 and percentages were used to calculate subset per mL of blood from quantified CD45^{+} cells per mL.

Histology

Aortic root segments were cut from tissue-tek stored organs using the Leica CM3050S cryostat at –20 °C. Aortic roots sections were then either stained for Toluidine Blue (0.2 % in PBS, Sigma-Aldrich) to quantify plaque size and necrotic burden or with Sirius Red (30 min, 0.05 % Direct Red in saturated picric acid, Sigma) to measure plaque collagen levels using Adobe Photoshop software. Aortic root segments were also fixated using dry acetone and blocked with Avidin/Biotin Blocking Kit (Vector Laboratories) before staining for ER-MP58 and secondarily stained with biotin-labeled rabbit anti-rat antibody. ER-MP58 binding was amplified using ABC kit (Vector Laboratories) in combination with ImmPACT AMEC Red Peroxidase Substrate kit (Vector Laboratories). Plaque parameters were determined by our expert pathologist. Plaque size was calculated as a total area of all 3 aortic root valves from the average of 4 consecutive slides, whilst necrosis and collagen content was expressed as a percentage of this total area. Plaque cell size was calculated in Adobe Photoshop software by counting nuclei within a defined and measured area. ER-MP58 staining was quantified by counting luminal positively stained cells.

Flow cytometry

To quantify bone marrow precursor populations and BMDM/FC viability, cells were blocked with anti-CD16/CD32 Fc-block in a V-bottom plate. Subsequent stains against cell surface markers for identifying bone marrow precursors or FC viability are displayed in Supplemental Table 2. BMDM viability was measured by first staining for Annexin V-FITC diluted in Annexin V binding buffer before staining with 7AAD. Stained cells were measured on a Beckman Coulter CytoFLEX or BD LSR II Fortessa and analyzed using FlowJo (Tree Star).

Gene expression analysis

RNA was isolated from either BMDMs or FCs cultured at a density of 0.5 x 10^6 per well in 24 well plates using the GeneJET RNA Purification Kit (Thermo Fisher Scientific) or aortic arches using RNeasy Mini Kit (Qiagen). Aortic arches were homogenized in Trizol and RNA was extracted using chloroform to layer the RNA content. RNA from plaques were subsequently added to RNeasy columns and DNase I was added on top prior to further wash and spin steps. An Implen nanodrop N60 was used to quantify the RNA and then was reverse-transcribed into cDNA using the High-Capacity cDNA Reverse Transcription Kit (ThermoFisher). cDNA was used for gene expression analysis in a qPCR with SYBR Green Fast mix dye (Applied Biosystems) using the ViiA 7 system (Applied Biosystems). Cycloa and Rplp0 were used as housekeeping genes to normalize expression of measured genes. Primer sequences can be found in Supplemental Table 3.

Transcriptomics

Fastq files were extracted using experiment accession GSE145950 from Gene Expression Omnibus (GEO). Reads were trimmed using Trimmomatic and then aligned to the mouse genome mm10 using RNAStar. Mapped reads in the BAM format were assigned to genomic features with featureCounts, providing feature base lengths alongside to calculate reads per kilobase million (RPKM) values. Differential gene expression was subsequently derived by means of the DESeq2 package. The resulting data was then run through the GSEA program (University of California San Diego) against KEGG gene sets to identify differentially regulated pathways.

Fluxomics

Fluxomics was performed by combining a fluxomics method with a metabolomics and lipidomics method [56,57]. To a 2 mL tube, containing BMDMs, solvents were added to achieve a total volume of 2 mL containing 1 mL of chloroform, 500 µL of methanol and 425 µL of water. All samples were mixed thoroughly, before centrifugation for 10 min at 14.000 rpm.

For polar fluxomics, the visible polar phase on the top layer was pipetted into a 1.5 mL tube and dried at 60 °C with a vacuum concentrator. 100 µL 6:4 (v/v) methanol:water was added to dried samples for reconstitution. A Waters Acquity ultra-high performance liquid chromatography system in combination with a Bruker Impact II™ Ultra-High Resolution Qq-Time-Of-Flight mass spectrometer was used to analyze metabolites. Subsequent sample acquisition was performed as previously described [58]. Bruker TASQ software version 2.1.22.3 was used to analyze the data. Accurate mass, ion mobility data, (relative) retention times and fragmentation spectra was used to identify metabolites. For fluxomics, relative isotope contribution was calculated using IsoCorrectoR Release 3.13

[59,60].

For lipid fluxomics, the visible phase on the bottom layer of the liquid-liquid extraction was pipetted in to a clean 1.5 mL tube and dried at 60 °C with a nitrogen concentrator. 100 µL of 1:1 (v/v) methanol:chloroform was added to the dried sample to dissolve it. A Thermo Scientific Ultimate 3000 binary HPLC in combination with a Q Exactive Plus Orbitrap mass spectrometer was used to analyze lipids in the samples. Subsequent sample acquisition was performed as previously described [61]. Matlab was used to write an in-house pipeline and analyze data (https://www.mathworks.com) by annotating the monoisotopic lipid peaks and corresponding ^{13}C isotopes [62]. Accurate mass, (relative) retention times, analysis of samples with known metabolic defects, fragmentation spectra and relevant standards was used to identify lipids.

Metabolomics

Metabolomics was performed as previously described, with minor adjustments [58,63]. 75 µL of internal standard was combined with 1 mL of chloroform, 500 µL of methanol and 425 µL of water to add to each sample containing cells, which was then mixed and centrifuged for 10 min at 14.000 rpm. The visible polar phase on the top layer was pipetted into a 1.5 mL tube and dried at 60 °C with a vacuum concentrator. The subsequent sample preparation and mass spectrometry method are as described for polar fluxomics. Internal standards with comparable retention times and response in the MS was used to normalize all metabolite intensities, and subsequently to total metabolite content. Accurate mass, ion mobility data, (relative) retention times and fragmentation spectra was used to identify metabolites.

Lipidomics

Lipidomics sample preparation was performed as previously described [64,65]. Briefly: 1:1 (v/v) methanol:chloroform was used to dissolve internal standards and then added to a 2 mL tube containing BMDMs before centrifugation for 10 min at 14.000 rpm. Supernatant was pipetted in to a clean 1.5 mL tube and dried at 60 °C with a nitrogen concentrator. 100 µL of 1:1 (v/v) methanol:chloroform was added to the dried sample to dissolve it. A Thermo Scientific Ultimate 3000 binary HPLC in combination with a Q Exactive Plus Orbitrap mass spectrometer was used to analyze lipids in the samples. Subsequent sample acquisition was performed as previously described [61]. R programming language was used to write an in-house pipeline and analyze data (http://ww.r-project.org). Internal standards for each lipid class were used to normalize reported lipids. Accurate mass, (relative) retention times, analysis of samples with known metabolic defects, fragmentation spectra and relevant standards was used to identify lipids.

Oil red O cell culture

Peritoneal FCs were cultured at a semi-confluent density in Ibidi glass bottom 8-well culture slides and fixed in 4 % formalin. After fixation, cells were incubated with 60 % isopropanol followed by staining with Oil red O (0.3 % in a 3:2 isopropanol:water solution). FCs were then washed with more 60 % isopropanol and subsequently stained with hematoxylin. VectaMount was subsequently used to mount the cells for imaging. Neutral lipid content and nuclei count was analyzed using Image J to quantify lipid area per cell.

Cytokine and NO synthesis

IL6 and TNFα cytokine content in cell culture supernatant was measured using ELISA kits (Invitrogen) following the manufacturers protocol. Secreted NO was measured by $NO2^-$ quantification using a Griess reagent reaction (Sigma).

Statistics

Data were evaluated with GraphPad Prism 9 using either t-tests or two-way ANOVA. Values are displayed as mean ± SEM of one representative experiment unless otherwise stated. Statistical significance is displayed as * $p < 0.05$, ** $p < 0.01$ and *** $p < 0.001$ whilst a statistical trend of $p < 0.1$ and >0.05 is displayed as a number.

Results

Transplantation of *Acod1*$^{-/-}$ bone marrow cells increases circulating Ly6C^{low} monocytes in an atherosclerosis mouse model

Since targeting the Acod1-itaconate axis could be a promising modulator of atherosclerosis progression, we first reassessed itaconate's immunomodulatory properties. In this study, we used LPS to activate macrophages via TLR4 to elicit itaconate production for *in vitro* functional studies. We consider this an appropriate model to complement our *in vivo* atherosclerosis studies since (i) TLR4 and its' signalling pathways play a major role in atherosclerosis progression and (ii) atherosclerosis-relevant stimuli like oxLDL do not induce itaconate *in vitro* (data not shown) [27,28,29]. We confirmed accumulation of itaconate upon inflammatory activation in both mouse and human macrophages by metabolomics (Supplementary Figure 1A and B) as previously described [16,17,19]. Additionally, we confirmed the anti-inflammatory effects of the natural unmodified form of itaconate by measuring cytokine secretion (Supplementary Figure 1C). Next, we verified itaconate deficiency in *Acod1*$^{-/-}$ BMDMs (Supplementary Figure 1D), which increased pro-inflammatory responses compared to *Acod1*$^{+/+}$ BMDMs at the protein and genetic level (Supplementary Figure 1E and F). After confirmation that unmodified itaconate and *Acod1* deficiency modulate macrophage inflammation, we investigated the role of Acod1-derived itaconate in a mouse model for atherosclerosis. Here, we transplanted

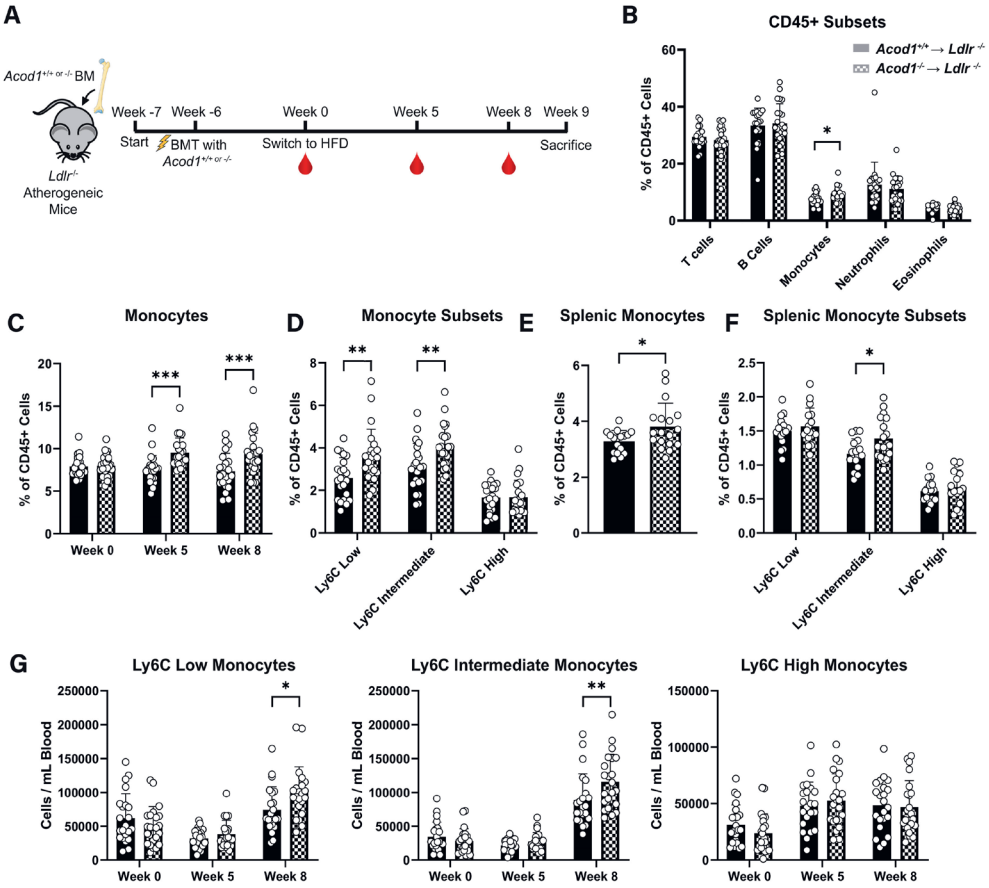

Figure 1. *Ldlr*$^{-/-}$ mice transplanted with *Acod1*$^{-/-}$ bone marrow contain more circulating and splenic Ly6c^{Low} patrolling monocytes. A) Irradiated atherosclerosis-susceptible *Ldlr*$^{-/-}$ mice were transplanted with either *Acod1*$^{+/+}$ or *Acod1*$^{-/-}$ bone marrow (BM) and were given 6 weeks for efficient engraftment prior to initiating a high-fat diet (HFD). Blood samples are taken on weeks 0, 5 and 8 of HFD and mice were sacrificed on week 9. B) leukocyte subsets in *Acod1*$^{+/+}$ → *Ldlr*$^{-/-}$ (filled) or *Acod1*$^{-/-}$ → *Ldlr*$^{-/-}$ (checkered) mice at week 8 expressed as a percentage of circulating CD45^{+} cells (n = 22/23 for *Acod1*$^{+/+}$ → *Ldlr*$^{-/-}$/*Acod1*$^{-/-}$ → *Ldlr*$^{-/-}$, unpaired t-test). C) Blood monocytes in *Acod1*$^{+/+}$ → *Ldlr*$^{-/-}$ (filled) or *Acod1*$^{-/-}$ → *Ldlr*$^{-/-}$ (checkered) mice at week 0, 5 and 8 expressed as a percentage of circulating CD45^{+} cells (n = 22/23 for *Acod1*$^{+/+}$ → *Ldlr*$^{-/-}$/*Acod1*$^{-/-}$ → *Ldlr*$^{-/-}$, two-way ANOVA). D) Blood Ly6C monocyte subsets in *Acod1*$^{+/+}$ → *Ldlr*$^{-/-}$ (filled) or *Acod1*$^{-/-}$ → *Ldlr*$^{-/-}$ (checkered) mice at week 8 expressed as a percentage of circulating CD45^{+} cells (n = 22/23, two-way ANOVA). E) Splenic monocytes in *Acod1*$^{+/+}$ → *Ldlr*$^{-/-}$ (filled) or *Acod1*$^{-/-}$ → *Ldlr*$^{-/-}$ (checkered) BM expressed as a percentage of splenic CD45^{+} cells (n = 17/18, unpaired t-test). F) Splenic Ly6C monocyte subsets in *Acod1*$^{+/+}$ → *Ldlr*$^{-/-}$ (filled) or *Acod1*$^{-/-}$ → *Ldlr*$^{-/-}$ (checkered) mice expressed as a percentage of splenic CD45^{+} cells (n = 17/18, two-way ANOVA). G) Ly6C low (left), intermediate (middle) and high (right) counts per mL of blood in *Acod1*$^{+/+}$ → *Ldlr*$^{-/-}$ (filled) or *Acod1*$^{-/-}$ → *Ldlr*$^{-/-}$ (checkered) mice at weeks 0, 5 and 8 of HFD (n = 22/23, two-way ANOVA). Gating strategies for flow cytometry is provided in Supplemental Figure 3. Data points display individual mice and error bars show SD.

bone marrow from either *Acod1*$^{+/+}$ or *Acod1*$^{-/-}$ mice into lethally irradiated atherosclerosis-susceptible *Ldlr*$^{-/-}$ mice (*Acod1*$^{+/+}$ → *Ldlr*$^{-/-}$ and *Acod1*$^{-/-}$ → *Ldlr*$^{-/-}$, respectively) (Figure 1A). Successful engraftment was confirmed prior to switching to a high fat diet with 0.125 % cholesterol (HFD) (Supplementary Figure 2A). All mice showed a similar increase in plasma cholesterol, triglyceride levels, and body weight (Supplementary Figs. 2B–D). In addition, both groups displayed similar blood leukocyte composition except monocyte percentage which was elevated in the blood of mice transplanted with *Acod1*$^{-/-}$ BM when compared to mice transplanted with *Acod1*$^{+/+}$ BM (Figure 1B and C & Supplementary Figure 2E, 3A & 3B). Ly6C^{low} and Ly6C^{int} subsets were responsible for the increase (Figure 1D). The raised monocyte content was further supported by increased percentage of splenic monocytes (Figure 1E & 1F & Supplementary Figure 3C) and monocytosis of Ly6C^{low} and Ly6C^{int} monocytes in *Acod1*$^{-/-}$ → *Ldlr*$^{-/-}$ mice 8 weeks after HFD. This suggests that the observed differences in monocyte abundance and composition between *Acod1*$^{+/+}$ → *Ldlr*$^{-/-}$ and *Acod1*$^{-/-}$ → *Ldlr*$^{-/-}$ mice were not due to differences in BM composition prior to transplantation, but rather occurred upon diet switching and atherosclerosis progression (Figure 1G). Consequently, transplantation of *Acod1*-deficient bone marrow leads to blood monocytosis skewed in the direction of patrolling Ly6C^{low} monocytes.

Acod1$^{-/-}$ monocytes show enhanced migration to atherosclerotic plaques

To assess the effect of *Acod1* deficiency on plaque phenotype, hearts were removed upon sacrifice to perform histological staining of the aortic root. Measurement of the total plaque size revealed no difference between *Acod1*$^{+/+}$ → *Ldlr*$^{-/-}$ and *Acod1*$^{-/-}$ → *Ldlr*$^{-/-}$ groups (Figure 2A & B). Examining the plaques of the aorta, we observed higher quantities of adherent cells attached to the endothelium in *Acod1*$^{-/-}$ → *Ldlr*$^{-/-}$ compared to *Acod1*$^{+/+}$ → *Ldlr*$^{-/-}$ mice, which was in line with the increase in circulating blood monocytes (Figure 2C). We next performed an IHC staining of monocyte-specific early recruitment marker ER-MP58 and quantified the number of positive monocytes, which showed significantly more ER-MP58^{+} monocytes in the *Acod1*$^{-/-}$ → *Ldlr*$^{-/-}$ group (Figure 2D & E), indicating enhanced monocyte recruitment [30]. In order to further understand why *Acod1*$^{-/-}$ → *Ldlr*$^{-/-}$ mice have increased circulating monocytes and recruitment, we measured the expression of inflammatory and transmigration genes within aortic arches (Figure 2F). As expected, *Acod1*$^{+/+}$ → *Ldlr*$^{-/-}$ control arches showed higher *Acod1* expression than *Acod1*$^{-/-}$ → *Ldlr*$^{-/-}$ arches, highlighting the presence of *Acod1*-positive bone marrow-derived cells in control atherosclerotic plaques and confirming effective transplantation of *Acod1* deficient bone marrow. Reduced *Acod1* expression in the *Acod1*$^{-/-}$ → *Ldlr*$^{-/-}$ arches resulted in increased expression of the pro-inflammatory marker *Tnf* and the anti-inflammatory marker *Il10* as well as endothelial transmigration gene *Icam1*. Expression of *Nos2*, which encodes the enzyme inducible nitric oxide synthase, was similar between the two groups. Subsequently, we measured the content of monocyte and dendritic progenitors (MDPs) and common

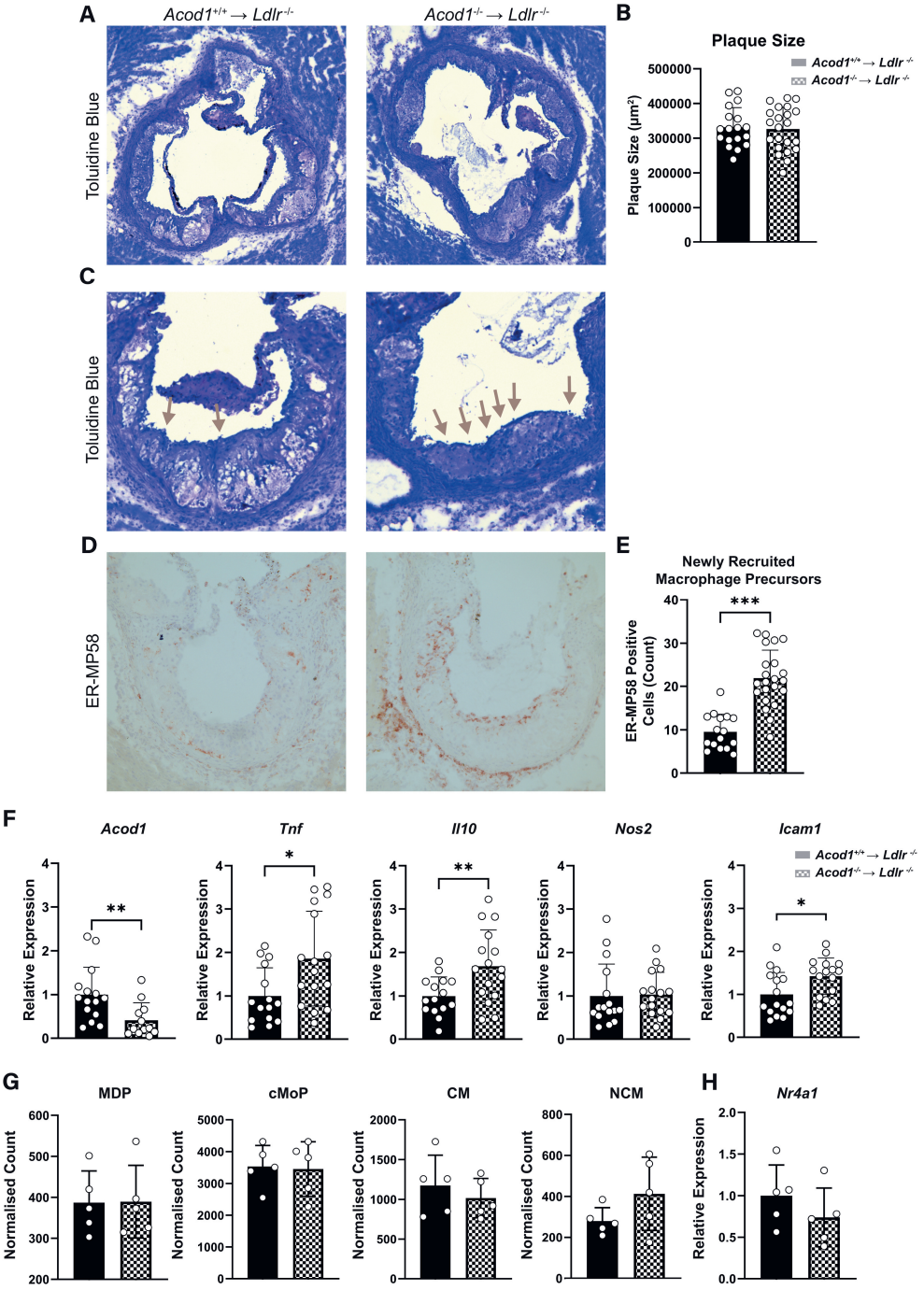

Figure 2. *Acod1*$^{-/-}$ transplanted *Ldlr*$^{-/-}$ mice have increased monocyte recruitment to the plaque. A) Aortic root segments were taken from *Acod1*$^{+/+}$ → *Ldlr*$^{-/-}$ (left) and *Acod1*$^{-/-}$ → *Ldlr*$^{-/-}$ (right) mice and stained with toluidine blue to B) quantify total plaque size of all 3 valve cusps (n = 18/22 for *Acod1*$^{+/+}$ → *Ldlr*$^{-/-}$/*Acod1*$^{-/-}$

→ *Ldlr*$^{-/-}$, unpaired t-test). C) One of the three valve cusps from the toluidine blue staining displaying luminal adhesion of monocytes (grey arrows). D) Immunohistochemical staining of monocyte antigen ER-MP58 (brown) which was then E) quantified by counting the number of positive cells on the luminal endothelium and within the plaque (n = 16/22, unpaired t-test). F) Gene expression of inflammatory and migration markers from mouse aortic arches (n = 15/16, unpaired t-test). G) Flow cytometry quantification of bone marrow myeloid precursors normalized to CD45^{+} count (n = 5, unpaired t-test). H) qPCR-derived gene expression of monocyte developmental marker *Nr4a1* in isolated peritoneal foam cells (FCs) (n = 5, unpaired t-test). Gating strategies for flow cytometry is provided in Supplemental Figure 4. Data points display individual mice and error bars show SD. MDP = Monocyte and Dendritic Progenitor; CMP = Common Monocyte Progenitor; CM = Classical Monocyte; NCM = Non-Classical Monocyte. (For interpretation of the references to colour in this figure legend, the reader is referred to the Web version of this article).

monocyte progenitors (CMPs) in the bone marrow of these mice. Bone marrow precursor populations, as well as bone marrow classical and non-classical monocytes, however, were unaffected between the groups (Figure 2G & Supplementary Figure 4A). Since bone marrow precursor proliferation could not explain the observed monocytosis, we analyzed the expression of pro-Ly6C^{low} transcription factor *Nr4a1* (*Nur77*). However, expression of *Nr4a1* was also unaffected in *Acod1*$^{-/-}$ → *Ldlr*$^{-/-}$ macrophages (Figure 2H). With this data, we show that blood monocytosis and increased monocyte recruitment to the plaque is not due to increased bone marrow proliferation, but could be pertained to the altered expression of inflammatory mediators such as *Tnf* and *Icam1*.

Acod1-deficient atherogenic mice show increased foam cell formation

As FCs are a specific subset of macrophages in atherosclerosis, we tested how *Acod1* deficiency affects these cells. Whilst there is a debate on the inflammatory potential of FCs, their ability to handle excessive lipids is known to be dysregulated which leads to cell death and necrotic core development [31]. Neutral lipid staining by Oil red O revealed a trend of increased lipid accumulation in peritoneal FCs from *Acod1*$^{-/-}$ → *Ldlr*$^{-/-}$ atherosclerotic mice compared to wild type littermates (Figure 3A & B). This increased FC lipid accumulation was confirmed by targeted mass spectrometry lipidomic assay (Figure 3C & D), where glycerol-containing lipids were the most elevated (Figure 3E). In order to identify the mechanism behind Acod1s' role in FC lipid homeostasis, we next examined gene expression of typical lipid transport markers. Since target genes of both *PPAR-γ* and *LXR* (*Nr1h3*) transcription factors encode proteins that are responsible for cellular lipid transport [32,33,34,35,36], we measured these in the FCs. Nevertheless, expression of lipid transport genes and their transcription factors was similar in the two groups (Figure 3F & G). Next, we quantified the size of macrophages within the plaque, as excessive lipid content can result in cellular hypertrophy. We found a significant increase in cell size in plaques from the *Acod1*$^{-/-}$ → *Ldlr*$^{-/-}$ group (Figure 3H & I). We thus show that *Acod1*$^{-/-}$ macrophages have a higher lipid content.

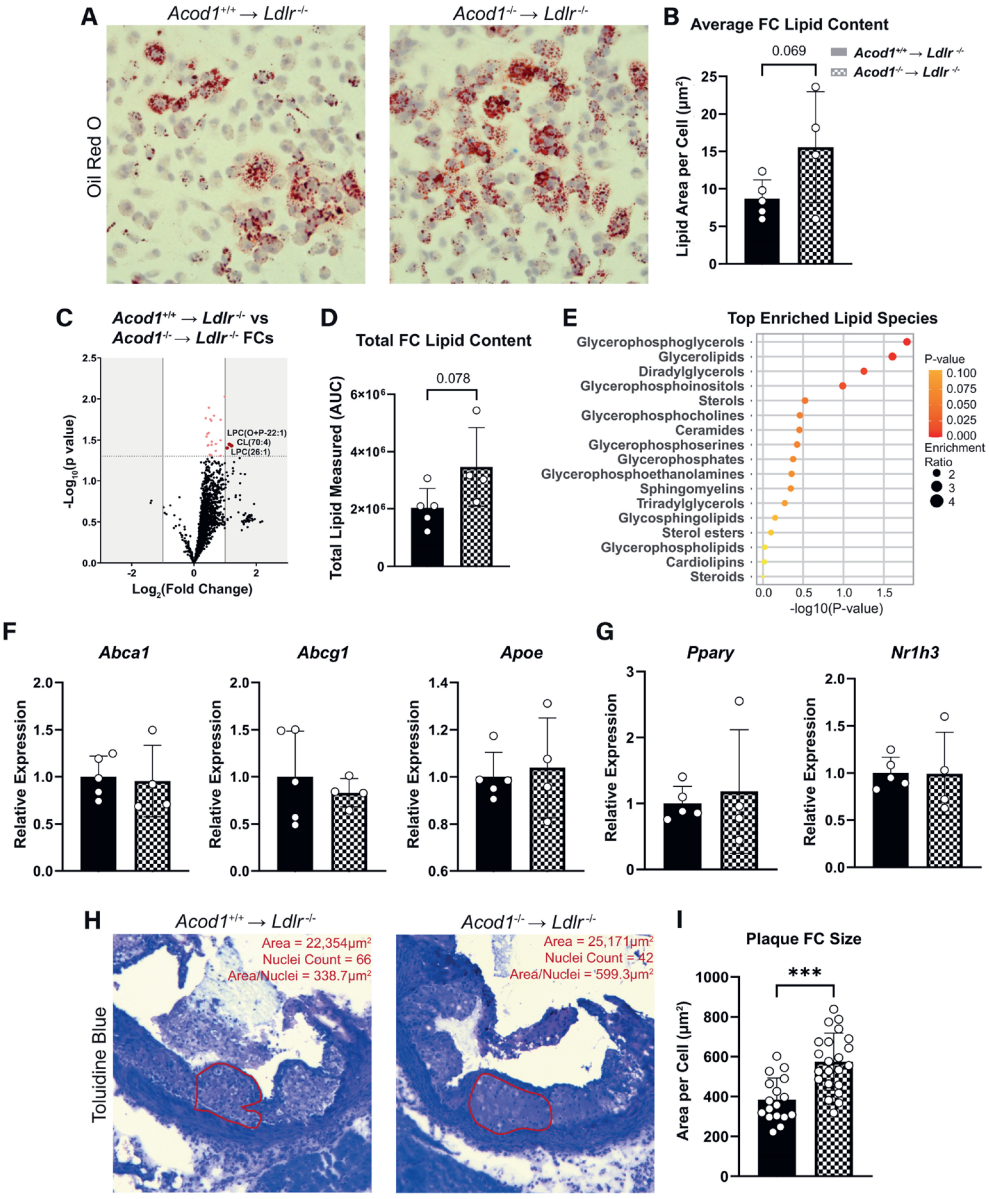

Figure 3. Itaconate deficiency leads to increased lipid content in foam cells. A) Oil red O staining of peritoneal foam cells (FCs) from *Acod1*$^{+/+}$ → *Ldlr*$^{-/-}$ (left) and *Acod1*$^{-/-}$ → *Ldlr*$^{-/-}$ (right) mice, B) quantified by calculating lipid area per nucleus stained with hematoxylin (n = 5/4 for *Acod1*$^{+/+}$ → *Ldlr*$^{-/-}$/*Acod1*$^{-/-}$ → *Ldlr*$^{-/-}$, unpaired t-test). C) Volcano plot of lipidomics from FCs (red = increased in *Acod1*$^{-/-}$ → *Ldlr*$^{-/-}$; blue = decreased in *Acod1*$^{-/-}$ → *Ldlr*$^{-/-}$; grey = not significant). Dotted line represents significance cut-off ($p < 0.05$). D) Total lipid content measured in all lipid species from lipidomics (n = 5/4, unpaired t-test). E) Lipid species enrichment analysis from the lipidomics dataset. F) qPCR-derived gene expression of proteins involved in lipid transport and G) their accompanying transcription factors from FCs (n = 5/4, unpaired t-test). H) One of the three aortic root valve cusps in *Acod1*$^{+/+}$ → *Ldlr*$^{-/-}$ (left) and *Acod1*$^{-/-}$ → *Ldlr*$^{-/-}$ (right) transplanted mice stained with toluidine blue where an area of foam cells (red) was measured and nuclei were counted

to I) calculate cell size (area/nuclei count; n = 17/22, unpaired t-test). Data points display individual mice and error bars show SD. FC = Foam Cell; AUC = Area Under the Curve; NES = Normalized Enrichment Score. (For interpretation of the references to colour in this figure legend, the reader is referred to the Web version of this article).

Plaque stability is improved by reduced apoptosis and necrotic core development in *Acod1*$^{-/-}$ mice

Considering that both FC formation and monocyte recruitment are two driving factors of plaque instability, we examined markers for plaque vulnerability. Plaques stained with Sirius Red showed no differences in fibrous cap collagen formation between the two groups (Figure 4A & B). Conversely, when we measured plaque necrotic burden using toluidine blue, we observed that plaques from *Acod1*$^{-/-}$ → *Ldlr*$^{-/-}$ mice had 50 % decreased necrotic plaque area (Figure 4C & D). A decrease in plaque necrosis raised the question as to whether *Acod1*$^{-/-}$ macrophages had an improved cell survival and were subjected to lower oxidative stress. Therefore, we explored the effect of Acod1 on cell death in inflammatory conditions, where we detected an increased viability in *Acod1*$^{-/-}$ → *Ldlr*$^{-/-}$ FCs (Figure 4E). Additionally, we performed gene set enrichment analysis (GSEA) on a dataset from Swain et al., 2020, which displayed that *Acod1*$^{-/-}$ BMDMs downregulate the P53 apoptosis pathway (Figure 4F). Hence, we performed an apoptosis/necrosis assay with 7AAD and Annexin V on BMDMs in inflammatory conditions. We observed that *Acod1*$^{-/-}$ BMDMs were protected from entering late apoptosis after 72 h of activation, resulting in higher percentages of viable cells (Figure 4G). Since generation of ROS and anti-oxidant responses are known to be regulated by Acod1 and itaconate, we analyzed the expression of ROS pathway genes in the dataset from Swain et al., 2020 (Figure 4H & I) [22,23,24]. This analysis indicated that inflammatory *Acod1*$^{+/+}$ BMDMs had higher expression of anti-oxidant genes than *Acod1*$^{-/-}$ BMDMs. Thus, we measured the expression of the most upregulated anti-oxidant genes from this dataset, as well as the key anti-oxidant marker *Hmox1*, in mouse aortic arches (Figure 4J). Expression of these suppressors of oxidative stress were however similar in both groups. We similarly measured expression of *Ifnb1* as this is described to be regulated by unmodified itaconate however this was unaffected (data not shown). Consequently, *Acod1* deficiency leads to increased plaque stability, which is likely facilitated by reduced macrophage and FC apoptosis, not occurring through differential regulation of anti-oxidant genes in vivo.

Shifted glycolytic flux towards glycerol synthesis in *Acod1*$^{-/-}$ macrophages enables increased de novo synthesis of triglycerides

Since the inflammatory state of FCs was similar between the two groups (Supplementary Figure 5A and 5B), we explored how *Acod1* deficiency affected the metabolic profile of macrophages to explain viability differences. Activated *Acod1*$^{+/+}$ and *Acod1*$^{-/-}$ BMDMs were metabolically distinct and displayed enriched purine metabolism, causing metabolites

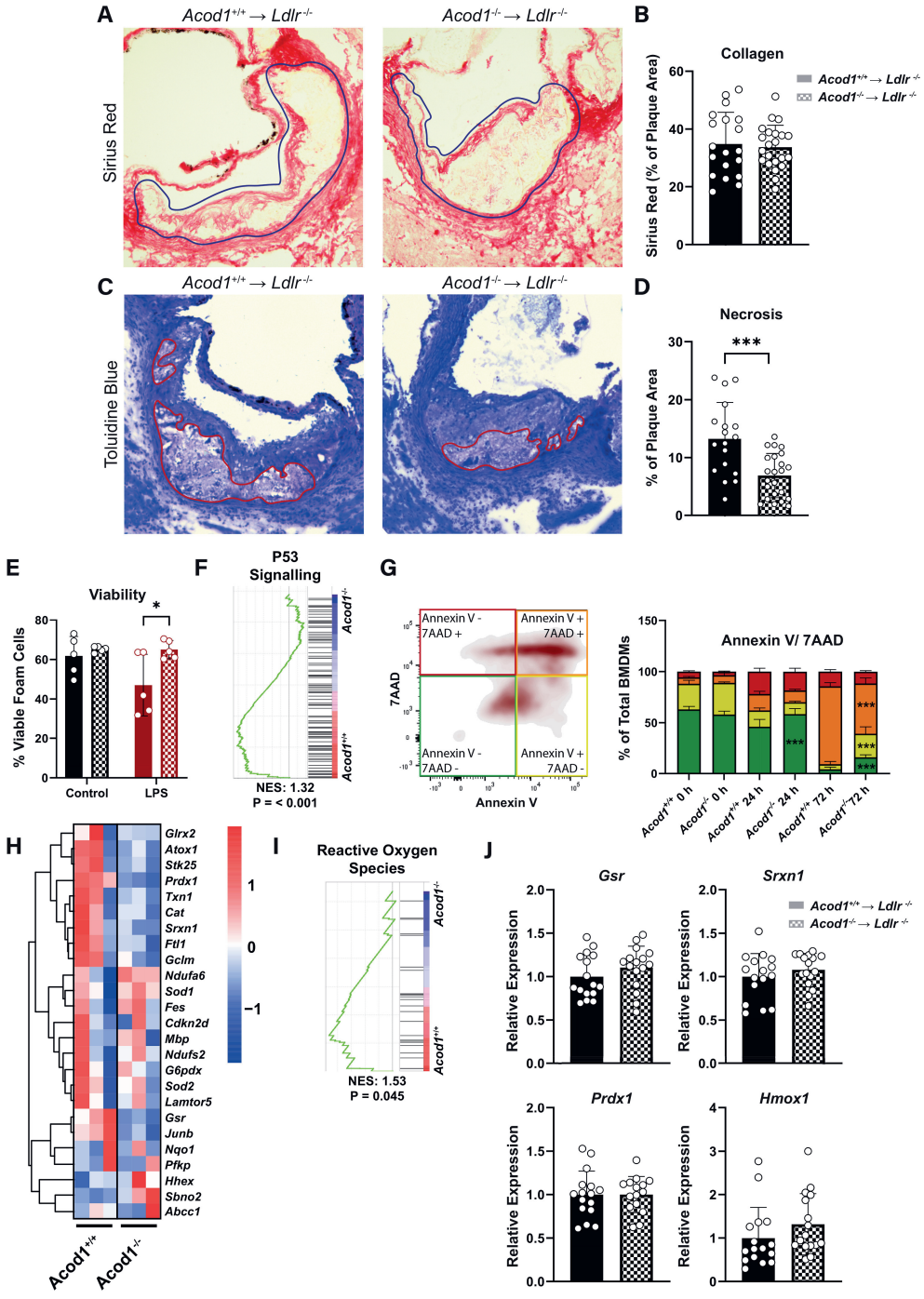
A
Acod1+/+ → Ldlr-/-
Acod1-/- → Ldlr-/-
Sirius Red
B
Collagen
Sirius Red (% of Plaque Area)
Acod1+/+ → Ldlr -/-
Acod1-/- → Ldlr -/-
C
Toluidine Blue
D
Necrosis
% of Plaque Area
***
E
Viability
% Viable Foam Cells
Control
LPS
F
P53 Signalling
NES: 1.32
P = < 0.001
G
Annexin V -
7AAD +
Annexin V +
7AAD +
Annexin V -
7AAD -
Annexin V +
7AAD -
7AAD
Annexin V
Annexin V/ 7AAD
% of Total BMDMs
H
Glrx2
Atox1
Stk25
Prdx1
Txn1
Cat
Srxn1
Ftl1
Gclm
Ndufa6
Sod1
Fes
Cdkn2d
Mbp
Ndufs2
G6pdx
Sod2
Lamtor5
Gsr
Junb
Nqo1
Pfkp
Hhex
Sbno2
Abcc1
I
Reactive Oxygen Species
NES: 1.53
P = 0.045
J
Gsr
Srxn1
Prdx1
Hmox1
Relative Expression

Figure 4. *Acod1* deficiency reduces apoptosis and necrosis. A) Aortic root segments were stained for Sirius Red to B) quantify red collagen staining area as a percentage of the plaque area (blue outline), expressed as an average of the three valve cusps in *Acod1*$^{+/+}$ → *Ldlr*$^{-/-}$ (left) and *Acod1*$^{-/-}$ → *Ldlr*$^{-/-}$ (right) mice (n = 19/22 for *Acod1*$^{+/+}$ → *Ldlr*$^{-/-}$/*Acod1*$^{-/-}$ → *Ldlr*$^{-/-}$, unpaired t-test). C) Necrotic core outlined (red) on one of the three aortic root valve cusps stained with toluidine blue which was then D) quantified as a percentage of the total plaque and expressed as an average of the three cusps (n = 18/22, unpaired t-test). E) Cell viability in unstimulated (black) or LPS (100 ng/mL) stimulated (red) FCs after 24 h, measured via flow cytometry analysis of fixable viability dye (FVD) eFluor™ 780 (n = 5, two-way ANOVA). F) P53 signaling pathway enrichment from a gene set enrichment analysis of dataset GSE145950 by Swain et al., 2020 comparing LPS-stimulated *Acod1*$^{+/+}$ and *Acod1*$^{-/-}$ BMDMs. G) Flow cytometry quantification of an Annexin V/7AAD apoptosis and necrosis assay on in vitro cultured *Acod1*$^{+/+}$ and *Acod1*$^{-/-}$ BMDMs stimulated with LPS (100 ng/mL) over 72 h (n = 3, two-way ANOVA). H) Gene expression heatmap of reactive oxygen species-related markers and I) subsequent gene set enrichment analysis comparing LPS stimulated *Acod1*$^{+/+}$ and *Acod1*$^{-/-}$ BMDMs from dataset GSE145950 by Swain et al., 2020. J) qPCR derived gene expression of redox markers from mouse aortic arches (n = 15/16, unpaired t-test). Gating strategies for flow cytometry is provided in Supplemental Figure 4. Data points display individual mice and error bars show SD. (For interpretation of the references to colour in this figure legend, the reader is referred to the Web version of this article).

inosine, inosinic acid and hypoxanthine to accumulate in *Acod1*$^{-/-}$ macrophages (Supplementary Figs. 6A–D, Supplementary Table 1). Next, given that biosynthesis of unsaturated fatty acids (FA) and FA metabolism pathways were enriched in *Acod1*$^{-/-}$ BMDMs, we tested whether the increased lipid content could be coming from de novo fatty acid synthesis (Figure 5A). Thus, we performed a stable isotope tracer-based experiment in BMDMs to study differences in glycolytic contribution towards lipid metabolism using U^{13}C-glucose. Fractional contribution of different triglyceride (TG) isotope species showed a trend of TG's with shorter long chain fatty acids (LCFA's) comprising of 40–49 total carbons (Figure 5B) contained more M+3 labelling in *Acod1*$^{-/-}$ BMDMs which was not observed for TG's with longer LCFA's containing 50–62 total carbons (Figure 5C & Supplementary Figure 7). This suggested de novo lipogenesis of TG species, particularly of TG's containing shorter LCFA's, supporting the previous observation that *Acod1*$^{-/-}$ → *Ldlr*$^{-/-}$ FCs contained more total glycerol-containing lipids (Figure 3E). When looking at glycolytic flux, phosphoenolpyruvate (PEP), the immediate step in glycolysis after synthesis of glycerate derivatives, had lower M+3 fractional contribution (Figure 5D). Additionally, we detected lower M+3 fractional contribution of glycerol-3-phosphate (G3P) (Figure 5E). Lower PEP labelling indicates a shift in glycolytic flux, whilst decreased G3P labelling points towards this shift being directed towards glycerol derivative synthesis. Due to the increased M+3 labelling of TG's, we suspect that the glycolytic flux in *Acod1*$^{-/-}$ BMDMs is redirected towards TG synthesis. Additionally, we observed that LPS induced an accumulation of acetylcarnitine in *Acod1*$^{+/+}$ BMDMs, which remained at a basal level in *Acod1*$^{-/-}$ BMDMs (Figure 5F). This accumulation was mediated by glucose-derived acetyl-CoA synthesis exhibited by a significant increase in M+2 labelling of acetylcarnitine in activated *Acod1*$^{+/+}$ BMDMs (Figure 5G). This significant accumulation of acetylcarnitine in *Acod1*$^{+/+}$ macrophages reduces the availability of carnitine to transport lipids for beta-oxidation. Together these data suggest that the observed increased lipid content

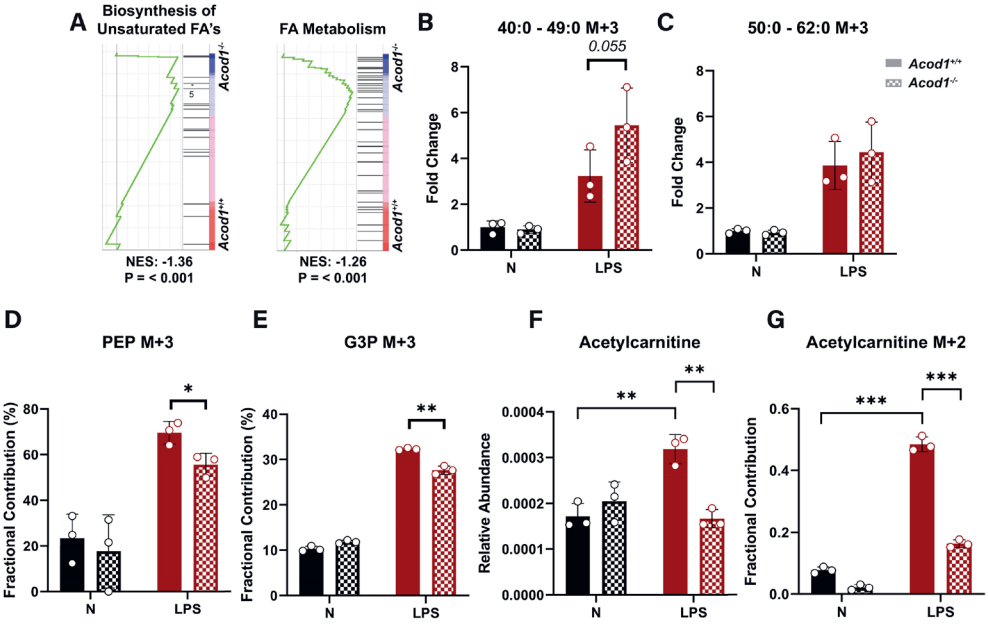

Figure 5. Broken glycolysis towards triglyceride synthesis may explain increased macrophage lipid content. A) Gene set enrichment analysis of de novo fatty acid (FA) synthesis-related pathways of dataset GSE145950 by Swain et al., 2020. B) Total M+3 fraction fold change of triglycerides with carbon content of either 40–49 carbons or C) 50–62 carbons from a lipid based fluxomics using ^{13}C-glucose isotopic labeling in *Acod1*$^{+/+}$ and *Acod1*$^{-/-}$ BMDMs stimulated with or without LPS (100 ng/ml) for 24 h (n = 3, two-way ANOVA). D) Fractional contribution of M+3 phosphoenolpyruvate (PEP) and E) M+3 glycerol-3-phosphate (G3P) in fluxomics of *Acod1*$^{+/+}$ and *Acod1*$^{-/-}$ BMDMs stimulated with or without LPS (100 ng/ml) for 24 h and cultured with ^{13}C-glucose for isotope labelling (n = 3, two-way ANOVA). F) Relative abundance of metabolite acetylcarnitine from the metabolomics dataset and G) the fractional contribution of M+2 acetyl carnitine in the total pool of acetylcarnitine isotopes from the fluxomics dataset (n = 3, two-way ANOVA). Data points display individual mice and error bars show SD.

in *Acod1*$^{-/-}$ macrophages can be partially explained by a shift in glycolytic flux towards synthesis of glycerol derivatives and subsequent de novo lipogenesis of TG's.

Discussion

Since its discovery as an immunomodulatory metabolite, itaconate gained increasing interest as a potential target to manage disease related to chronic inflammation and oxidative stress [37,38]. In this study, we focus on itaconates' role in the development of atherosclerotic plaques, demonstrating that myeloid-*Acod1* deficiency elevates overall monocyte recruitment and viability, which leads to increased plaque stability by slowing necrotic core growth. Moreover, *Acod1*-deficiency increases lipid-handling capabilities, which may lower the occurrence of aberrantly activated macrophages due to a restored balance of lipid efflux, uptake, biosynthesis and lysis, thus promoting less vulnerable plaques [39]. Consequently, we suggest that ACOD1 should be explored as a potential

target in human inflammatory diseases.

Our work exposes the modulating properties of Acod1 on the migration of circulating monocytes. As such, the patrolling Ly6C^{low} monocyte subset is more abundant in the *Acod1* deficient group and in turn, we observe increased recruitment of monocytes to the lesion site in mice with more stable plaques. This reported increase in circulating Ly6C^{low} monocytes occurring at week 8 post HFD suggests that monocytosis is elicited in response to the high cholesterol diet. No differences in BM composition after sacrifice further supports this and implies that there were no variations in BM composition during transplantation. The role of Ly6C^{low} monocytes and their differentiation into macrophages has been widely shown to be of an anti-inflammatory nature and inversely correlate with plaque growth, whilst Ly6C^{high} monocytes and macrophages are considered pro-inflammatory and promote plaque development [11,40,41,42]. In another study, *Nur77*-deficient mice with reduced Ly6C^{low} monocyte numbers promoted the differentiation of Ly6C^{high} monocytes into pro-inflammatory macrophages and resulted in exacerbated atherosclerosis progression [40,41]. These two observations suggest an atheroprotective role for Ly6C^{low}-monocyte-derived macrophages within the plaque. Comparatively, the Ly6C^{low} monocytes within the current study are at a higher quantity and monocytes have an improved recruitment capacity, potentially explained by upregulation of *Icam1*, in mice with reduced necrotic core development. Therefore, based on this data and previous research performed on the role of Ly6C^{low} monocytes in plaques, increased circulating Ly6C^{low} monocytes when targeting *Acod1* in atherosclerosis is not detrimental to disease progression.

Based on our own and others' in vitro data showing increased inflammatory responses in the absence of Acod1 in macrophages, one might expect a worse atherosclerosis outcome in *Acod1*-deficient mice [17,38]. A recent paper indeed shows that atherosclerosis induction by PCSK9-AAV administration results in increased inflammation and lesion area in mice that lack ACOD1, and the authors propose an important role of NRF2 in mediating this phenotype. Interestingly, the new in vivo data we present here rather shows that *Acod1* deficiency is beneficial in atherosclerosis, as highlighted by the decreased necrotic core size. Since this observation was unexpected, we looked further into the phenotype of these macrophages in order to explain how macrophages with an increased inflammatory state could result in more stable plaques. As such, we found that *Acod1* deficient macrophages underwent apoptosis at a lower rate. Considering that apoptosis can contribute to necrotic core development, we believe that cell survival in *Acod1*$^{-/-}$ → *Ldlr*$^{-/-}$ mice is a viable explanation for the observed reduction in necrotic core [43,44]. Together, the publication by Song et al. and our own research uncover similarities (i.e. increased circulating monocyte levels in the absence of ACOD1), but also important differences (inflammatory status and phenotype of atherosclerotic plaques), and complementary

mechanisms (apoptosis and necrosis aspect in our study, and the importance of NRF2 in the work of Song et al.) that should all be taken into account when considering exploiting the ACOD1-itaconate axis for atherosclerosis therapy. Differences between both studies might be explained by differences in experimental settings including for example the use of different mouse sources, and the application of bone marrow transplantation towards *Ldlr*$^{-/-}$mice versus PCSK9-AAV injection to elicit atherosclerosis.

Given the important role of apoptosis and necrosis, we next wanted to understand the underlying mechanisms that provided *Acod1*$^{-/-}$ macrophages with a more resilient survival. Reactive oxygen species, which have been demonstrated to drive apoptosis and plaque progression, are shown in numerous studies to be controlled to some extent by Acod1, where *Acod1* deficiency reduces ROS production [21,22,23]. Anti-oxidant genes, which are typically upregulated in environments with high ROS content, were expressed lower in *Acod1*$^{-/-}$ macrophages [24]. This indicates that ROS generation in *Acod1*$^{-/-}$ → *Ldlr*$^{-/-}$ plaques may be low, however when measuring aortic arch gene expression of top anti-oxidant genes, we were unable to detect a difference between the two groups, regardless of the difference in *Acod1* expression. This could be due to the fact that foam cells within the *Acod1*$^{-/-}$ → *Ldlr*$^{-/-}$ plaques contain more lipids and thus more oxLDL, which could upregulate anti-oxidant gene expression to the degree that is similar to *Acod1*$^{+/+}$ → *Ldlr*$^{-/-}$ plaques. Additionally, we observed increased expression of anti-inflammatory marker *Il10* within the plaque which is known to lessen plaque development [45,46]. Indeed, the increased *Il10* in our setting could contribute to a more stable plaque however in conjunction with increased *Tnf* it is unclear how effective IL-10 cytokine signalling would be.

In our metabolomics studies, we showed that *Acod1*$^{+/+}$ and *Acod1*$^{-/-}$ BMDMs had distinct metabolic profiles, owed in part to metabolites inosine, inosinic acid and hypoxanthine. Previously, a link has been shown between arrested de novo synthesis of guanine-containing metabolites and cell apoptosis, since replenishment of guanine pools to fulfil transcription requirements are unmet [47,48]. The larger availability of nucleotide generating metabolites in *Acod1*$^{-/-}$ BMDMs may sustain their high demand during inflammatory activation in plaques, possibly explaining the reduced apoptosis in *Acod1*$^{-/-}$ myeloid cells. *Acod1*$^{+/+}$ and *Acod1*$^{-/-}$ BMDMs were also in part metabolically distinct given that lipid content of *Acod1*-deficient myeloid cells and plaque cells were enriched. Since myeloid cells display lower apoptosis, this could explain the observation of increased lipid loading in our in vivo study, as these cells may be partially protected from excess lipid-induced apoptosis [49,50]. On the lipid metabolism front, we observed an upregulation of glucose utilisation for glycerol synthesis, which can be used in TG synthesis, which was also increased in *Acod1*$^{-/-}$ macrophages. Interestingly, TG synthesis in FCs was shown to enhance their secretion of inflammatory mediators such as prostaglandin E2 (PGE2), which

also has been shown to improve macrophage recruitment [51]. It is also an essential part of the cell membrane and thus increased production in *Acod1*$^{-/-}$ macrophages may allow the cell to better handle the cellular hypotrophy induced by lipid uptake in the plaque.

Carnitine, an enzyme responsible for shuttling LCFA's across the mitochondrial membrane for beta-oxidation, was greatly used as an acetyl-CoA sink in inflammatory *Acod1*$^{+/+}$ macrophages, generating more acetylcarnitine [52,53]. This phenomenon occurs when glycolytic activity is greater than the TCA cycle, leading to an accumulation of acetyl-CoA. Carnitine in this situation reduces the acetyl-CoA pool [53]. The consequence however is inhibition of carnitine-mediated LCFA transport and subsequent beta oxidation. We observed this through high M+2 acetylcarnitine labelling in *Acod1*$^{+/+}$ macrophages. Moreover, itaconate is another source of acetyl-CoA as it is converted into itaconyl-CoA and subsequently metabolised into acetyl-CoA, only further adding to the pool in inflammatory macrophages [54]. In contrast, itaconate-deficient macrophages have an amplified OXPHOS and thus a larger demand for acetyl-CoA pools, likely explaining the vastly reduced M+2 labelling of acetylcarnitine in *Acod1*$^{-/-}$ macrophages [17]. Therefore, in this paper we hypothesise a new mechanism for the poor lipid handling capability of plaque inflammatory macrophages, mediated by acetyl-CoA blocking carnitine transport of lipids and subsequent beta-oxidation (Figure 6).

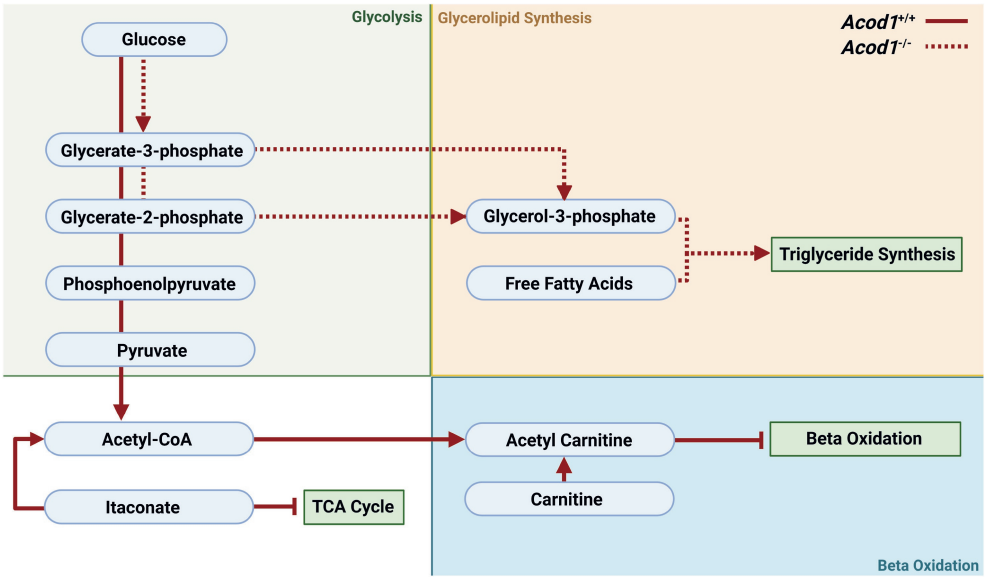

Figure 6. Glycolytic flux in *Acod1*$^{+/+}$ and *Acod1*$^{-/-}$ inflammatory BMDMs. Schematic of glucose flux in inflammatory (LPS) *Acod1*$^{+/+}$ (solid red) and *Acod1*$^{-/-}$ (dashed red) BMDMs. Arrows display where differences in glucose flux occur between the two groups but are not the only flux occurring. Blue curved boxes are metabolites and green straight boxes are pathways. Created with BioRender.com. (For interpretation of the references to colour in this figure legend, the reader is referred to the Web version of this article).

Based on the data provided in our study, we propose that silencing the Acod1-itaconate axis in atherosclerosis leads to a favourable plaque phenotype. Total circulating Ly6C^{low} monocytes and monocyte recruitment to the plaque are increased, whilst plaque FC viability is also increased, owed in part to re-wired glycolytic flux towards TG synthesis. As such, bone marrow *Acod1*-deficiency reduces necrotic core development in plaques. Yet, it should be noted that another recent publication that employs an alternate way of atherosclerosis induction rather shows that *Acod1* knockout elicits increased inflammation and larger plaques. Clearly our studies warrant future research into the potential use of the ACOD1-itaconate axis to manage atherosclerosis progression. The generation of ACOD1-targeting small molecules (both inhibitory and activating ones) will help to further uncover the potential benefit of modulating ACOD1/itaconate to improve disease outcome.

Acknowledgements

The authors would like to thank Dr. Djalil Coowar and staff of the Animal Facility at the University of Luxembourg for animal care and mouse breeding, Amandine Bernard at the Luxembourg Institute of Health for mouse genotyping.

CRediT authorship contribution statement

Karl J. Harber: Writing – review & editing, Writing – original draft, Visualization, Methodology, Investigation, Formal analysis, Conceptualization. Annette E. Neele: Writing – review & editing, Methodology, Investigation. Cindy PAA. van Roomen: Methodology, Investigation. Marion JJ. Gijbels: Writing – review & editing, Methodology, Investigation. Linda Beckers: Methodology, Investigation. Myrthe den Toom: Methodology, Investigation. Bauke V. Schomakers: Writing – review & editing, Methodology, Investigation. Daan AF. Heister: Investigation. Lisa Willemsen: Writing – review & editing, Investigation. Guillermo R. Griffith: Investigation. Kyra E. de Goede: Investigation. Xanthe AMH. van Dierendonck: Writing – review & editing, Investigation. Myrthe E. Reiche: Writing – review & editing, Methodology. Aurélie Poli: Investigation. Frida L-H Mogensen: Investigation. Alessandro Michelucci: Writing – review & editing. Sanne GS. Verberk: Writing – review & editing, Investigation. Helga de Vries: Writing – review & editing. Michel van Weeghel: Writing – review & editing, Funding acquisition, Conceptualization. Jan Van den Bossche: Writing – review & editing, Funding acquisition, Conceptualization. Menno PJ. de Winther: Writing – review & editing, Funding acquisition, Conceptualization.

Funding

MdW is supported by Amsterdam UMC, Amsterdam Cardiovascular Sciences, ZonMW

(ZonMW Open competition 09120011910025), NWO (Epi-Guide-Edit - KICH1.ST01.20.045) and the European Union (Doctoral Network MIRACLE).

This research received financial support from the Amsterdam Cardiovascular Sciences (ACS) research institute. J.V.d.B. was funded by a consortia grant from European Research Area Network on Cardiovascular Diseases (ERA-CVD 2019T108), the Netherlands Heart Foundation senior fellowship (2017T048) and an ENW-Klein-1 grant from NWO (OCENW. KLEIN.268).

AEN is supported by a Dutch Heart Foundation Dekker grant (03-006-2020-T029) and NWO Veni (VI.Veni.222.221).

Declaration of competing interest

The authors declare that they have no known competing financial interests or personal relationships that could have appeared to influence the work reported in this paper.

References

1. I. Dicembrini, et al., Effects of PCSK9 inhibitors on LDL cholesterol, cardiovascular morbidity and all-cause mortality: a systematic review and meta-analysis of randomized controlled trials, J. Endocrinol. Invest. 42 (9) (2019) 1029–1039. Epub 20190214.
2. H.F. Wang, et al., Effect of alirocumab and evolocumab on all-cause mortality and major cardiovascular events: a meta-analysis focusing on the number needed to treat, Front Cardiovasc Med 9 (2022) 1016802. Epub 20221202.
3. P.M. Ridker, Anticytokine Agents: targeting interleukin signaling pathways for the treatment of Atherothrombosis, Circ. Res. 124 (3) (2019) 437–450.
4. P.M. Ridker, How common is residual inflammatory risk? Circ. Res. 120 (4) (2017) 617–619.
5. G.K. Hansson, Inflammation, atherosclerosis, and coronary artery disease, N. Engl. J. Med. 21 (352) (2005) 1685–1695.
6. R. Ross, Atherosclerosis–an inflammatory disease, N. Engl. J. Med. 14 (340) (1999) 115–126.
7. I. Tabas, K.E. Bornfeldt, Macrophage phenotype and function in different Stages of atherosclerosis, Circ. Res. 118 (4) (2016) 653–667.
8. M. Back, et al., Inflammation and its resolution in atherosclerosis: mediators and therapeutic opportunities, Nat. Rev. Cardiol. 16 (7) (2019) 389–406.
9. G. Chinetti-Gbaguidi, S. Colin, B. Staels, Macrophage subsets in atherosclerosis, Nat. Rev. Cardiol. 12 (1) (2015) 10–17. Epub 20141104.
10. P.M. Ridker, et al., Antiinflammatory Therapy with Canakinumab for atherosclerotic disease, N. Engl. J. Med. 377 (12) (2017) 1119–1131. Epub 20170827.
11. T.J. Barrett, Macrophages in atherosclerosis Regression, Arterioscler.

Thromb. Vasc. Biol. 40 (1) (2020) 20–33. Epub 20191114.

12. L.A. O'Neill, R.J. Kishton, J. Rathmell, A guide to immunometabolism for immunologists, Nat. Rev. Immunol. 16 (9) (2016) 553–565. Epub 20160711.
13. J. Van den Bossche, L.A. O'Neill, D. Menon, Macrophage immunometabolism: where are We (going)? Trends Immunol. 38 (6) (2017) 395–406. Epub 20170407.
14. E.L. Mills, et al., Succinate dehydrogenase supports metabolic repurposing of mitochondria to drive inflammatory macrophages, Cell 167 (2) (2016) 457, 70 e13. Epub 20160922.
15. D.G. Ryan, L.A.J. O'Neill, Krebs cycle reborn in macrophage immunometabolism, Annu. Rev. Immunol. 38 (2020) 289–313. Epub 20200127.
16. A. Michelucci, et al., Immune-responsive gene 1 protein links metabolism to immunity by catalyzing itaconic acid production, Proc. Natl. Acad. Sci. U. S. A. 110 (19) (2013) 7820–7825. Epub 20130422.
17. V. Lampropoulou, et al., Itaconate links inhibition of succinate dehydrogenase with macrophage metabolic remodeling and regulation of inflammation, Cell Metabol. 24 (1) (2016) 158–166. Epub 20160630.
18. L.A.J. O'Neill, M.N. Artyomov, Itaconate: the poster child of metabolic reprogramming in macrophage function, Nat. Rev. Immunol. 19 (5) (2019) 273–281.
19. E.L. Mills, et al., Itaconate is an anti-inflammatory metabolite that activates Nrf2 via alkylation of KEAP1, Nature 556 (7699) (2018) 113–117. Epub 20180328.
20. T.S. Oh, et al., Itaconate and its derivatives repress early myogenesis in vitro and in vivo, Front. Immunol. 13 (2022) 748375. Epub 20220221.
21. A. Negre-Salvayre, et al., Role of reactive oxygen species in atherosclerosis: lessons from murine genetic models, Free Radic. Biol. Med. 149 (2020) 8–22. Epub 20191125.
22. C.J. Hall, et al., Immunoresponsive gene 1 augments bactericidal activity of macrophage-lineage cells by regulating beta-oxidation-dependent mitochondrial ROS production, Cell Metabol. 18 (2) (2013) 265–278.
23. X. Zhu, et al., Itaconic acid exerts anti-inflammatory and antibacterial effects via promoting pentose phosphate pathway to produce ROS, Sci. Rep. 11 (1) (2021) 18173. Epub 20210913.
24. X. Wang, et al., Metabolic Reprogramming via ACOD1 depletion enhances function of human induced pluripotent stem cell-derived CAR-macrophages in solid tumors, Nat. Commun. 14 (1) (2023) 5778. Epub 20230918.
25. G.J. Koelwyn, et al., Regulation of macrophage immunometabolism in atherosclerosis, Nat. Immunol. 19 (6) (2018) 526–537. Epub 20180518.
26. L. Groh, et al., Monocyte and macrophage immunometabolism in atherosclerosis, Semin. Immunopathol. 40 (2) (2018) 203–214. Epub 20171002.
27. K.S. Michelsen, et al., Lack of Toll-like receptor 4 or myeloid differentiation factor 88 reduces atherosclerosis and alters plaque phenotype in mice deficient in apolipoprotein E, Proc. Natl. Acad. Sci. U. S. A. 101 (29) (2004).
28. S. Kiechl, et al., Toll-like receptor 4 polymorphisms and atherogenesis, N. Engl. J. Med. 347 (3) (2002).
29. H. Bjorkbacka, et al., Reduced atherosclerosis in MyD88-null mice links elevated serum cholesterol levels to

activation of innate immunity signaling pathways, Nat. Med. 10 (4) (2004) 416–421. Epub 20040314.

30. P. Goossens, et al., Myeloid IkappaBalpha deficiency promotes atherogenesis by enhancing leukocyte recruitment to the plaques, PLoS One 6 (7) (2011) e22327. Epub 20110721.
31. Y. Gui, H. Zheng, R.Y. Cao, Foam cells in atherosclerosis: novel insights into its origins, consequences, and molecular mechanisms, Front Cardiovasc Med 9 (2022) 845942. Epub 20220413.
32. L. Nagy, et al., Oxidized LDL regulates macrophage gene expression through ligand activation of PPARgamma, Cell 17 (93) (1998) 229–240.
33. P. Tontonoz, et al., PPARgamma promotes monocyte/macrophage differentiation and uptake of oxidized LDL, Cell 17 (93) (1998) 241–252.
34. B.A. Laffitte, et al., LXRs control lipid-inducible expression of the apolipoprotein E gene in macrophages and adipocytes, Proc. Natl. Acad. Sci. U. S. A. 16 (98) (2001) 507–512.
35. X. Wang, et al., Macrophage ABCA1 and ABCG1, but not SR-BI, promote macrophage reverse cholesterol transport in vivo, J. Clin. Invest. 117 (8) (2007) 2216–2224.
36. N. Zelcer, et al., LXR regulates cholesterol uptake through Idol-dependent ubiquitination of the LDL receptor, Science 325 (5936) (2009) 100–104. Epub 20090611.
37. M. Diotallevi, et al., Itaconate as an inflammatory mediator and therapeutic target in cardiovascular medicine, Biochem. Soc. Trans. 49 (5) (2021) 2189–2198.
38. A. Swain, et al., Comparative evaluation of itaconate and its derivatives reveals divergent inflammasome and type I interferon regulation in macrophages, Nat. Metab. 2 (7) (2020) 594–602. Epub 20200525.
39. A. Vogel, et al., Lipid scavenging macrophages and inflammation, Biochim. Biophys. Acta Mol. Cell Biol. Lipids 1867 (1) (2022) 159066. Epub 20211006.
40. A.A. Hamers, et al., Bone marrow-specific deficiency of nuclear receptor Nur77 enhances atherosclerosis, Circ. Res. 110 (3) (2012) 428–438. Epub 20111222.
41. R.N. Hanna, et al., NR4A1 (Nur77) deletion polarizes macrophages toward an inflammatory phenotype and increases atherosclerosis, Circ. Res. 110 (3) (2012) 416–427. Epub 20111222.
42. Y.H. Li, et al., Occurrences and functions of Ly6C(hi) and Ly6C(lo) macrophages in health and disease, Front. Immunol. 13 (2022) 901672. Epub 20220530.
43. T. Seimon, I. Tabas, Mechanisms and consequences of macrophage apoptosis in atherosclerosis, J. Lipid Res. 50 (Suppl) (2009) S382–S387. Epub 20081025.
44. K.J. Moore, F.J. Sheedy, E.A. Fisher, Macrophages in atherosclerosis: a dynamic balance, Nat. Rev. Immunol. 13 (10) (2013) 709–721. Epub 20130902.
45. Z. Mallat, et al., Protective role of interleukin-10 in atherosclerosis, American Heart Association 85 (8) (1999) e17–e24.
46. M. Orecchioni, et al., Deleting interleukin-10 from myeloid cells exacerbates atherosclerosis in Apoe(-/-) mice, Cell. Mol. Life Sci. 80 (1) (2022) 10. Epub 20221210.
47. M. Camici, et al., Purine-metabolising enzymes and apoptosis in cancer, Cancers 11 (9) (2019). Epub 20190912.
48. A.J. Valvezan, et al., mTORC1 couples nucleotide synthesis to nucleotide

demand resulting in a targetable metabolic vulnerability, Cancer Cell 32 (5) (2017) 624–638, e5. Epub 20171019.

49. M.L. Brophy, et al., the dead to keep atherosclerosis at bay, Front Cardiovasc Med 4 (2017) 2. Epub 20170130.
50. A. Remmerie, C.L. Scott, Macrophages and lipid metabolism, Cell. Immunol. 330 (2018) 27–42. Epub 20180202.
51. A. Castoldi, et al., Triacylglycerol synthesis enhances macrophage inflammatory function, Nat. Commun. 11 (1) (2020) 4107. Epub 20200814.
52. M.A. Schroeder, et al., The cycling of acetyl-coenzyme A through acetylcarnitine buffers cardiac substrate supply: a hyperpolarized 13C magnetic resonance study, Circ Cardiovasc Imaging 5 (2) (2012) 201–209. Epub 20120111.
53. F.B. Stephens, D. Constantin-Teodosiu, P.L. Greenhaff, New insights concerning the role of carnitine in the regulation of fuel metabolism in skeletal muscle, J. Physiol. 581 (Pt 2) (2007) 431–444. Epub 20070301.
54. J. Lin, et al., The emerging application of itaconate: promising molecular targets and therapeutic opportunities, Front. Chem. 9 (2021) 669308. Epub 20210512.
55. T. Cordes, et al., Immunoresponsive gene 1 and itaconate inhibit succinate dehydrogenase to modulate intracellular succinate levels, J. Biol. Chem. 291 (27) (2016) 14274–14284. Epub 20160509.
56. M. Molenaars, et al., Metabolomics and lipidomics in Caenorhabditis elegans using a single-sample preparation, Dis Model Mech 14 (4) (2021). Epub 20210427.
57. I.A. Chatzispyrou, Set al., Barth syndrome cells display widespread remodeling of mitochondrial complexes without affecting metabolic flux distribution, Biochim. Biophys. Acta, Mol. Basis Dis. 1864 (11) (2018) 3650–3658. Epub 20180901.
58. A.R. Schuurman, et al., Inflammatory and glycolytic programs underpin a primed blood neutrophil state in patients with pneumonia, iScience 26 (7) (2023) 107181. Epub 20230619.
59. P. Heinrich, et al., Correcting for natural isotope abundance and tracer impurity in MS-, MS/MS- and high-resolution-multiple-tracer-data from stable isotope labeling experiments with IsoCorrectoR, Sci. Rep. 8 (1) (2018) 17910. Epub 20181217.
60. Bioconductor: IsoCorrectoR. c2003-2023. [Accessed 2022 Nov 21] https://bi oconductor.org/packages/release/bioc/html/IsoCorrectoR.html.
61. S.A.E. van Wouw, et al., Sterol-regulated transmembrane protein TMEM86a couples LXR signaling to regulation of lysoplasmalogens in macrophages, J. Lipid Res. 64 (2) (2023) 100325. Epub 20221231.
62. N.M. Held, et al., Pyruvate -dehydrogenase complex plays a central role in brown adipocyte energy expenditure and fuel utilization during short-term beta-adrenergic activation, Sci. Rep. 8 (1) (2018) 9562. Epub 20180622.
63. B.V. Schomakers, et al., Polar metabolomics in human muscle biopsies using a liquid-liquid extraction and full-scan LC-MS, STAR Protoc 3 (2) (2022) 101302. Epub 20220416.
64. K. Herzog, et al., Lipidomic analysis of fibroblasts from Zellweger spectrum disorder patients identifies disease-specific phospholipid ratios, J. Lipid Res. 57 (8) (2016) 1447–1454. Epub 20160609.
65. A.R. Schuurman, et al., The platelet

lipidome is altered in patients with COVID-19 and correlates with platelet reactivity, Thromb. Haemostasis 122 (10) (2022) 1683–1692. Epub 20220718.

Supplementary materials

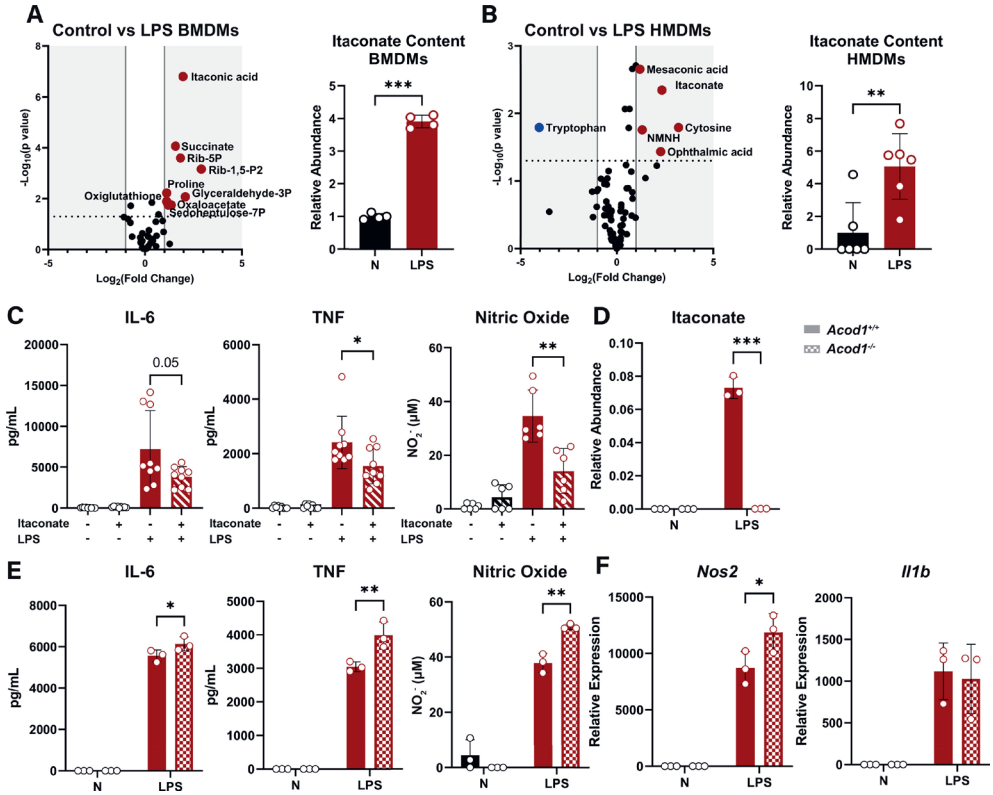

Supplemental Figure 1. Confirmation of previously published properties itaconate and itaconate deficiency have on BMDMs. A) Metabolomics data shown in a volcano plot with increased (red) or decreased (blue) metabolites and quantified itaconate content in a bar graph, of BMDMs (n = 4, unpaired t-test) or B) human macrophages s (n = 6, paired t-test) treated with LPS for 24 hours compared to unstimulated cells. Dotted line represents significance cut-off ($p < 0.05$). C) Secretion of IL6 (left), TNF (middle) and nitric oxide (right) after treatment with (stripes) or without (filled) itaconate (5mM) for 3 hours before stimulation with (red) or without (black) LPS for 24 hours (n = 9 for ELISA, n = 6 for NO assay, unpaired t-test). D) Itaconate content from metabolomics of *Acod1*$^{+/+}$ (filled) and *Acod1*$^{-/-}$ (checkered) BMDMs treated with LPS for 24 hours or control (n = 3, two-way ANOVA). E) Secretion of cytokines in control and LPS-treated *Acod1*$^{+/+}$ and *Acod1*$^{-/-}$ macrophages after 24 hours measured by either ELISA or NO assay and F) inflammatory gene expression after 3 hours of LPS (n = 3, two-way ANOVA). Data points display individual mice and error bars show SD.

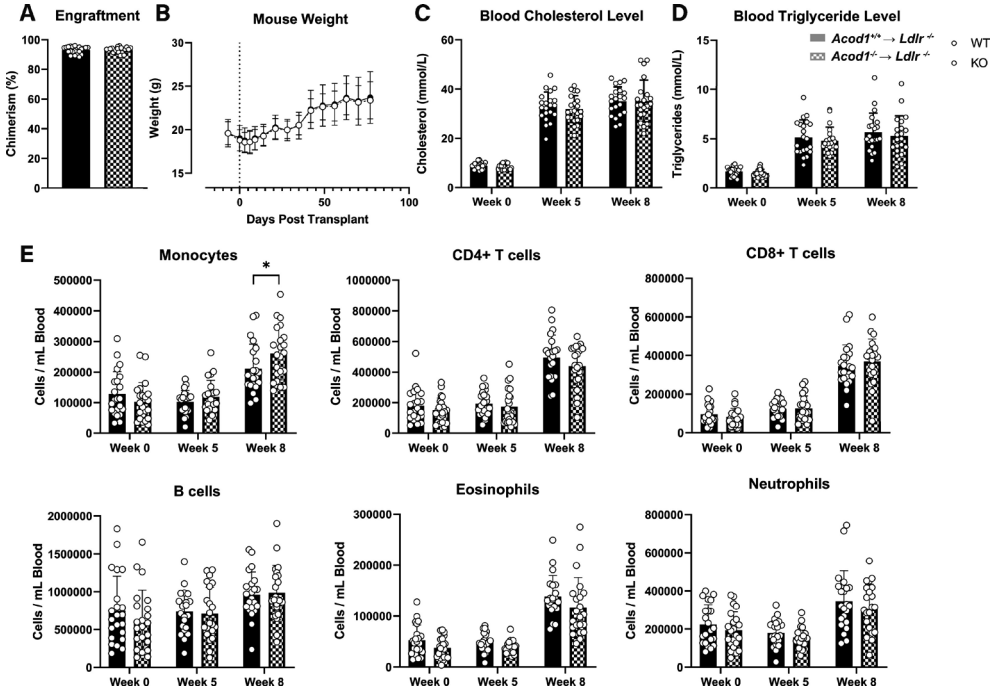

Supplemental Figure 2. In vivo mouse and blood measurements. A) Percentage chimerism of donor bone marrow measured by qPCR analysis of *Ldlr* expression in blood samples of *Acod1*$^{+/+}$ → *Ldlr*$^{-/-}$ (filled) and *Acod1*$^{-/-}$ → *Ldlr*$^{-/-}$ (checkered) mice (n = 22/23 for *Acod1*$^{+/+}$ → *Ldlr*$^{-/-}$ / *Acod1*$^{-/-}$ → *Ldlr*$^{-/-}$). B) Mouse weight over the entire in vivo experiment starting from 1 week before BMT in *Acod1*$^{+/+}$ → *Ldlr*$^{-/-}$ (black dots) and *Acod1*$^{-/-}$ → *Ldlr*$^{-/-}$ (white dots) mice (n = 22/23; dotted line is day of BMT). C) Cholesterol and D) triglyceride levels in blood plasma of mice at weeks 0, 5 and 8 of HFD (n = 22/23). E) In vivo blood cell subset composition per mL of blood at weeks 0, 5 and 8 of HFD (n = 22/23). Data points display individual mice and error bars show SD. BMT = Bone Marrow transplantation; HFD = High Fat Diet.

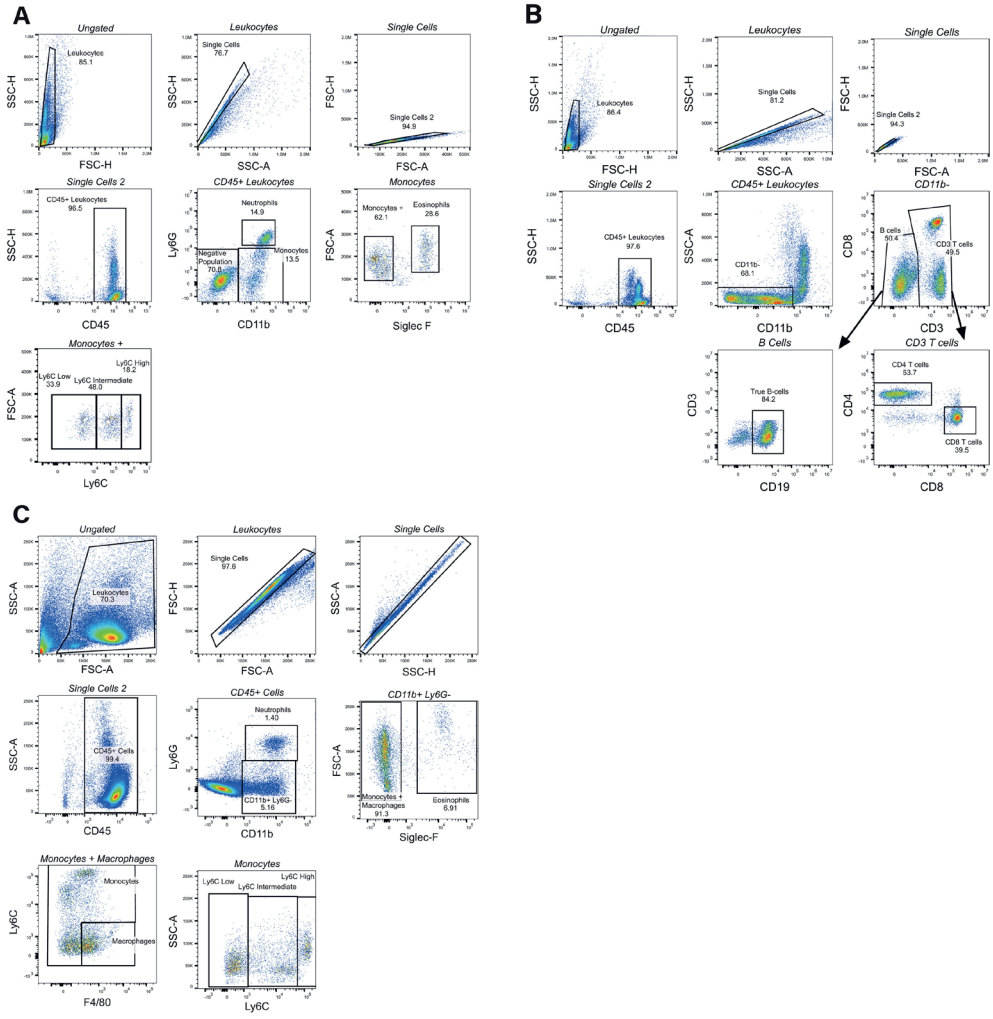

Supplemental Figure 3. Gating strategies for in vivo blood and spleen flow cytometry analysis. A) Example gating strategies for myeloid and B) lymphoid cell subsets during blood collections at week 0, 5 and 8 of HFD. C) Example flow cytometry gating for dissociated spleen samples on day of sacrifice. All plots are read from left to right and top to bottom unless highlighted by a black arrow. Italic plot titles highlight which gate is being displayed from the previous plot.

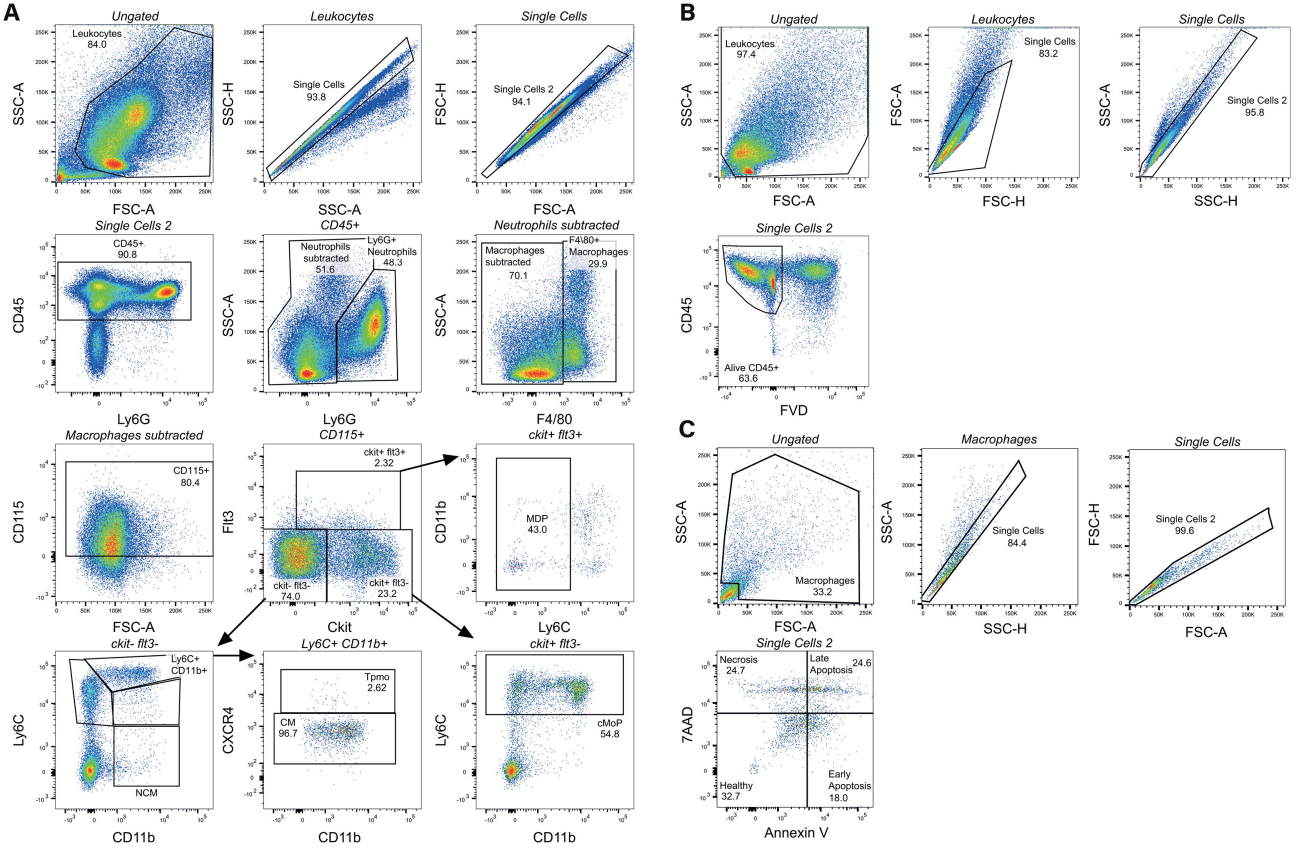

Supplemental Figure 4. Gating strategies for in vivo bone marrow and peritoneal lavage flow cytometry analysis. A) Example gating strategy of bone marrow, B) peritoneal lavage and C) BMDMs cells taken after sacrifice. All plots are read from left to right and top to bottom unless highlighted by a black arrow. Italic plot titles highlight which gate is being displayed from the previous plot. MDP = Monocyte and Dendritic Progenitor, CMP = Common Monocyte Progenitor, CM = Classical Monocyte, NCM = Non-Classical Monocyte.

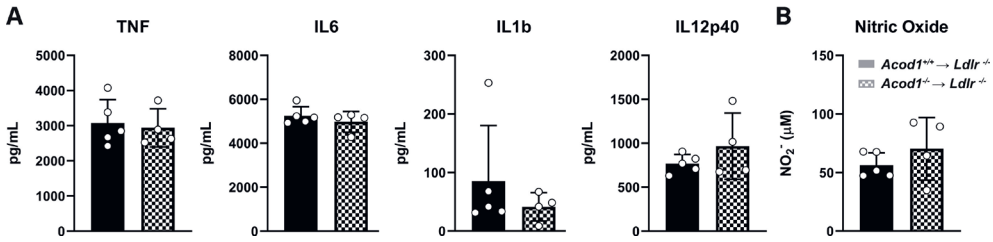

Supplemental Figure 5. Peritoneal foam cells from both *Acod1*$^{+/+}$ and *Acod1*$^{-/-}$ transplanted mice have the same cytokine secretion potential. A) Cytokine secretion from *Acod1*$^{+/+}$ → *Ldlr*$^{-/-}$ (filled) and *Acod1*$^{-/-}$→ *Ldlr*$^{-/-}$ (checkered) FCs stimulated with LPS for 24 hours measured by either ELISA or B) NO assay (n = 5/4 for *Acod1*$^{+/+}$/*Acod1*$^{-/-}$, unpaired t-test). Data points display individual mice and error bars show SD.

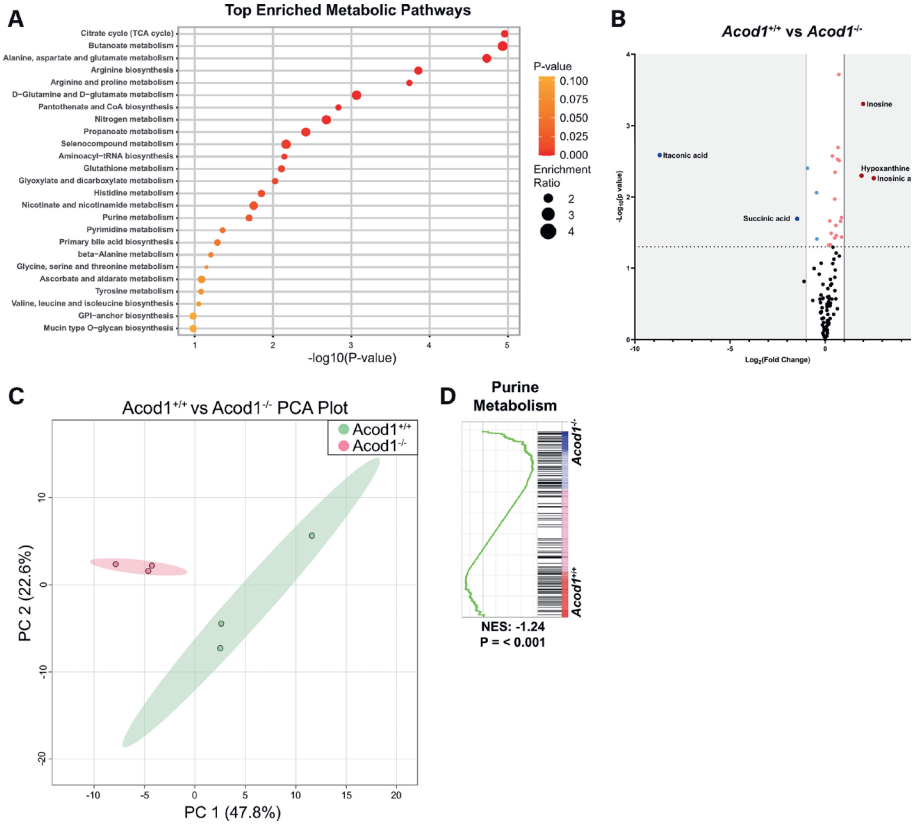

Supplemental Figure 6. Metabolome of *Acod1*$^{-/-}$ is distinct from *Acod1*$^{+/+}$ macrophages with upregulated purine metabolism. A) Metabolic pathway enrichment analysis from metabolomics of LPS (100 ng/mL) stimulated *Acod1*$^{+/+}$ and *Acod1*$^{-/-}$ BMDMs for 24 hours, along with B) a volcano plot displaying differentially accumulated metabolites (red = increased in *Acod1*$^{-/-}$; blue = decreased in *Acod1*$^{-/-}$; black = not significant). Dotted line represents significance cut-off ($p < 0.05$). C) Principal component analysis (PCA) plot of metabolomics data comparing *Acod1*$^{+/+}$ and *Acod1*$^{-/-}$ BMDMs stimulated with LPS for 24 hours (n = 3). D) Gene set enrichment analysis of the purine metabolism pathway from dataset GSE145950 by Swain et al., 2020.

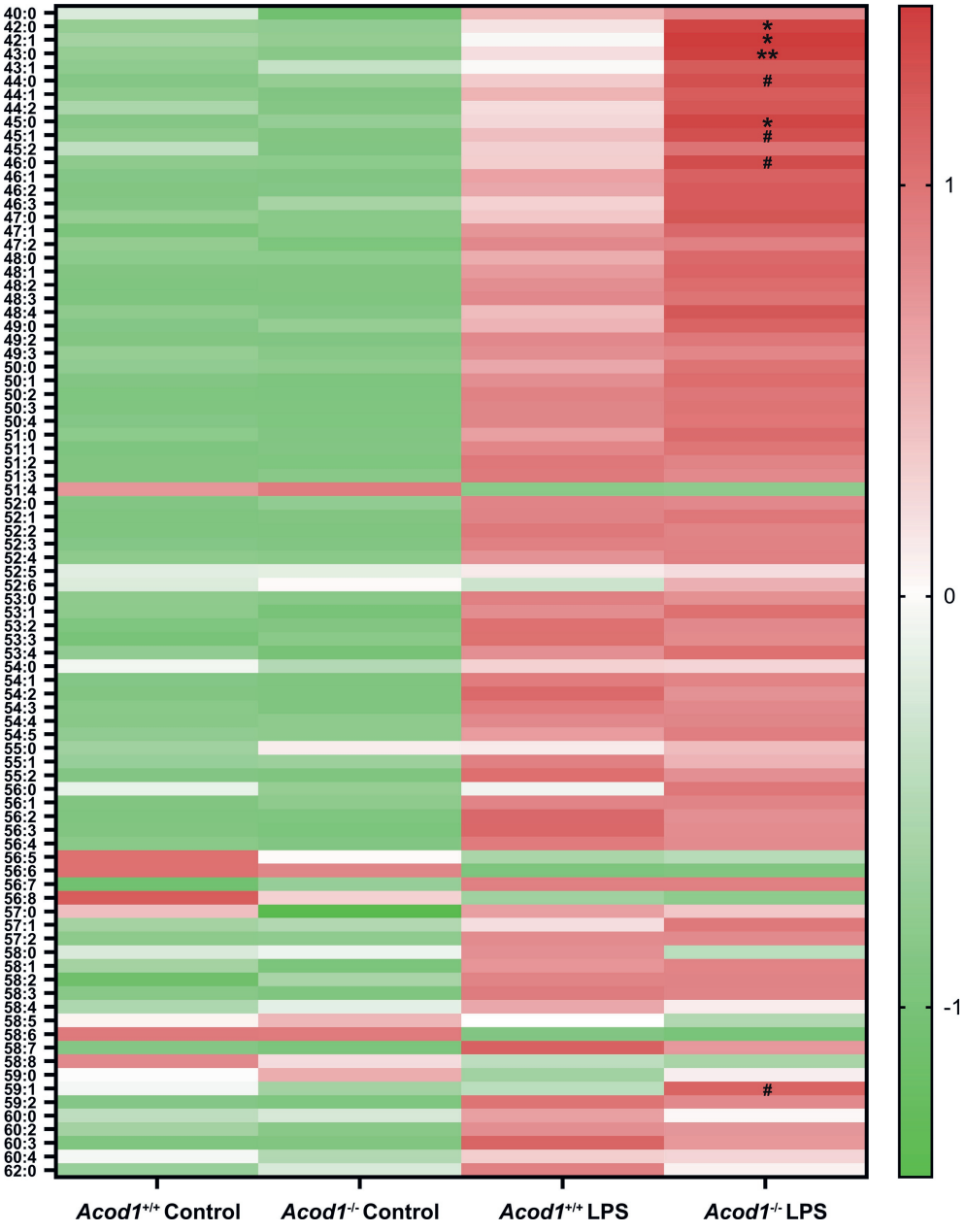

Supplemental Figure 7. Heatmap of triglyceride species in inflammatory *Acod1*$^{+/+}$ and *Acod1*$^{-/-}$ BMDMs. ^{13}C-glucose cultured *Acod1*$^{+/+}$ and *Acod1*$^{-/-}$ BMDMs stimulated with (red) or without (black) LPS (100 ng/ml) for 24 hours were measured in a fluxomics experiment for labeling of lipid species. Shown are Z-score averages of 3 samples from M+3 fraction fold changes of the displayed lipids (two-way ANOVA).

Supplemental Table 1. Metabolomics raw data from *Acod1*$^{+/+}$ and *Acod1*$^{-/-}$ BMDMs

Analyte.name	HMDB.name	Chemical.formula	Monoisotopic.weight	HMDB.id	KEGG.id	WTLPS_0 1	WTLPS_0 2	WTLPS_0 3	KOLPS_0 1	KOLPS_0 2	KOLPS_0 3	P_Value	Fold_change	Log2_fold_change
IMP	Inosinic acid	C10H13N4O8P	146.0	HMDB0000175	C00130	0.00006	0.00008	0.00007	0.00042	0.00043	0.00034	0.00545	5.86161	2.55130
Inosine	Inosine	C10H12N4O5	276.0	HMDB0000195	C00294	0.00023	0.00049	0.00036	0.00143	0.00153	0.00130	0.00050	3.97639	1.99146
Hypoxanthine	Hypoxanthine	C5H4N4O	664.1	HMDB0000157	C00262	0.00063	0.00085	0.00077	0.00299	0.00301	0.00241	0.00502	3.74777	1.90603
Threonine	L-Threonine	C4H9NO3	116.0	HMDB0000167	C00188	0.00470	0.00732	0.00990	0.01135	0.01437	0.01409	0.03656	1.81582	0.86062
Argininosuccinate	Argininosuccinic acid	C10H18N4O6	189.1	HMDB0000052	C03406	0.00052	0.00049	0.00067	0.00091	0.00094	0.00120	0.01950	1.81445	0.85953
Succinyl_AMP	Adenylsuccinic acid	C14H18N5O11P	665.1	HMDB0000536	C03794	0.00001	0.00002	0.00001	0.00003	0.00002	0.00002	0.02189	1.75864	0.81446
UDP	Uridine 5'-diphosphate	C9H14N2O12P2	607.1	HMDB0000295	C00015	0.00540	0.01174	0.01120	0.01806	0.01381	0.01558	0.06776	1.67377	0.74310
Xanthine	Xanthine	C5H4N4O2	607.1	HMDB0000292	C00385	0.00076	0.00093	0.00099	0.00150	0.00156	0.00140	0.00309	1.66172	0.73267
Glutamate	L-Glutamic acid	C5H9NO4	607.1	HMDB0000148	C00025	0.02779	0.03108	0.03060	0.05045	0.04791	0.04851	0.00019	1.64142	0.71494
Malate	L-Malic acid	C4H6O5	133.0	HMDB0000156	C00149	0.00562	0.00637	0.00550	0.00874	0.00998	0.00924	0.00203	1.59916	0.67731
Alpha-Ketoglutarate	Oxoglutaric acid	C5H6O5	612.2	HMDB0000208	C00026	0.00056	0.00067	0.00056	0.00098	0.00092	0.00093	0.00295	1.57767	0.65780
Gluconate-6P	6-Phosphogluconic acid	C6H13O10P	744.1	HMDB0001316	C00345	0.00032	0.00039	0.00045	0.00099	0.00040	0.00044	0.36899	1.56527	0.64641
NAD+	NAD	C21H28N7O14P2	148.0	HMDB0000902	C00003	0.00215	0.00319	0.00319	0.00467	0.00389	0.00415	0.03486	1.49273	0.57796
Fumarate	Fumaric acid	C4H4O4	148.0	HMDB0000134	C00122	0.00133	0.00157	0.00205	0.00244	0.00248	0.00245	0.06138	1.49163	0.57689
Acetylglutamic acid	N-Acetylglutamic acid	C7H11NO5	148.0	HMDB0001138	C00624	0.00027	0.00027	0.00021	0.00042	0.00033	0.00038	0.02516	1.47542	0.56113
NADH	NADH	C21H29N7O14P2	443.0	HMDB0001487	C00004	0.00078	0.00179	0.00160	0.00285	0.00164	0.00165	0.26899	1.47178	0.55756
UDP-HexNac	Uridine diphosphate-N-acetylglucosamine	C17H27N3O17P2	211.0	HMDB0000290	C00043	0.00736	0.01195	0.01097	0.01771	0.01229	0.01372	0.10619	1.44351	0.52958
UDP-HexNac	UDP-N-acetyl-D-mannosamine	C17H27N3O17P2	322.1	HMDB0013112	C01170	0.00736	0.01195	0.01097	0.01771	0.01229	0.01372	0.10619	1.44351	0.52958
UDP-HexNac	UDP-N-acetyl-alpha-D-galactosamine	C17H27N3O17P2	89.0	HMDB0060522	C00203	0.00736	0.01195	0.01097	0.01771	0.01229	0.01372	0.10619	1.44351	0.52958
Aspartate	L-Aspartic acid	C4H7NO4	566.1	HMDB0000191	C00049	0.01371	0.01505	0.01664	0.02033	0.02290	0.02205	0.00450	1.43765	0.52371
Oxiglutathione	Oxidized glutathione	C20H32N6O12S2	566.1	HMDB0003337	C00127	0.00707	0.01597	0.01647	0.01628	0.02261	0.01758	0.20570	1.42891	0.51492
NADP+	NADP	C21H29N7O17P3	324.0	HMDB0000217	C00006	0.00066	0.00114	0.00114	0.00170	0.00120	0.00128	0.13398	1.42431	0.51026
2-Hydroxyglutarate	D-2-Hydroxyglutaric acid	C5H8O5	767.1	HMDB0000606	C01087	0.00129	0.00136	0.00130	0.00182	0.00178	0.00202	0.01071	1.42318	0.50912
2-Hydroxyglutarate	L-2-Hydroxyglutaric acid	C5H8O5	75.0	HMDB0000694	C03196	0.00129	0.00136	0.00130	0.00182	0.00178	0.00202	0.01071	1.42318	0.50912
2-Hydroxyglutarate	2-Hydroxyglutarate	C5H8O5	89.0	HMDB0059655	C02630	0.00129	0.00136	0.00130	0.00182	0.00178	0.00202	0.01071	1.42318	0.50912
GDP	Guanosine diphosphate	C10H15N5O11P2	131.1	HMDB0001201	C00035	0.00725	0.01008	0.00869	0.01404	0.01164	0.01128	0.03754	1.42033	0.50623
Creatine-P	Phosphocreatine	C4H10N3O5P	403.0	HMDB0001511	C02305	0.00004	0.00006	0.00006	0.00007	0.00008	0.00007	0.07517	1.37943	0.46407
TMP	5-Thymidylic acid	C10H15N2O8P	179.1	HMDB0001227	C00364	0.00006	0.00005	0.00006	0.00005	0.00012	0.00007	0.44331	1.36113	0.44481
beta-Alanine	beta-Alanine	C3H7NO2	363.1	HMDB0000056	C00099	0.02300	0.02893	0.03162	0.03797	0.03979	0.03316	0.05074	1.32749	0.40870
UDP-hexose	Uridine diphosphate glucose	C15H24N2O17P2	88.0	HMDB0000286	C00029	0.00683	0.00998	0.00882	0.01248	0.01004	0.01116	0.08625	1.31422	0.39421
UDP-hexose	Uridine diphosphategalactose	C15H24N2O17P2	135.1	HMDB0000302	C00052	0.00683	0.00998	0.00882	0.01248	0.01004	0.01116	0.08625	1.31422	0.39421
UMP	Uridine 5'-monophosphate	C9H13N2O9P	323.1	HMDB0000288	C00105	0.00181	0.00179	0.00182	0.00242	0.00234	0.00231	0.00266	1.30260	0.38139
Coenzyme_A	Coenzyme A	C21H36N7O16P3S	196.1	HMDB0001423	C00010	0.00086	0.00113	0.00101	0.00164	0.00103	0.00116	0.27092	1.27776	0.35362
Glycine	Glycine	C2H5NO2	112.0	HMDB0000123	C00037	0.00041	0.00042	0.00044	0.00050	0.00064	0.00047	0.16562	1.26708	0.34151
Alanine	L-Alanine	C3H7NO2	174.1	HMDB0000161	C00041	0.02427	0.02374	0.02428	0.03228	0.02971	0.02833	0.03252	1.24933	0.32116
Creatine	Creatine	C4H9N3O2	307.1	HMDB0000064	C00300	0.02063	0.01738	0.01399	0.02114	0.01995	0.02242	0.17381	1.22122	0.28832
CDP	CDP	C9H15N3O11P2	90.0	HMDB0001546	C00112	0.00221	0.00348	0.00316	0.00430	0.00342	0.00301	0.30822	1.21294	0.27851
Hippuric acid	Hippuric acid	C9H9NO3	141.0	HMDB0000714	C01586	0.00399	0.00489	0.00557	0.00583	0.00628	0.00539	0.14351	1.21145	0.27673
GMP	Guanosine monophosphate	C10H14N5O8P	129.0	HMDB0001397	C00144	0.00031	0.00036	0.00037	0.00043	0.00040	0.00042	0.04666	1.20470	0.26867
Pyruvate	Pyruvic acid	C3H4O3	427.0	HMDB0000243	C00022	0.01072	0.00584	0.00667	0.00783	0.01215	0.00780	0.50828	1.19568	0.25783
Adenine	Adenine	C5H5N5	146.1	HMDB0000034	C00147	0.00004	0.00004	0.00007	0.00005	0.00007	0.00007	0.33556	1.19535	0.25743
CMP	Cytidine monophosphate	C9H14N3O8P	170.0	HMDB0000095	C00055	0.00035	0.00055	0.00056	0.00058	0.00058	0.00058	0.31074	1.18529	0.24525
Gluconate	Gluconic acid	C6H12O7	125.0	HMDB0000625	C00257	0.00373	0.00378	0.00389	0.00435	0.00437	0.00474	0.02173	1.18069	0.23963
Uracil	Uracil	C4H4N2O2	186.0	HMDB0000300	C00106	0.00010	0.00011	0.00010	0.00011	0.00010	0.00014	0.26421	1.14986	0.20146
Arginine	L-Arginine	C6H14N4O2	132.1	HMDB0000517	C00062	0.00790	0.00722	0.00934	0.00938	0.00824	0.01048	0.24866	1.14891	0.20027
dCMP	dCMP	C9H14N3O7P	161.1	HMDB0001202	C00239	0.00002	0.00005	0.00005	0.00005	0.00004	0.00005	0.58266	1.14370	0.19371
Lactate	L-Lactic acid	C3H6O3	321.1	HMDB0000190	C00256	0.03885	0.02707	0.02897	0.02655	0.04933	0.03228	0.60769	1.13986	0.18886
Phosphorylethanolamine	O-Phosphoethanolamine	C2H8NO4P	366.1	HMDB0000224	C00346	0.01659	0.01632	0.01398	0.01952	0.01479	0.01908	0.29376	1.13883	0.18755
Pyroglutamic acid	Pyroglutamic acid	C5H7NO3	276.1	HMDB0000267	C01879	0.00843	0.00785	0.00743	0.00901	0.00920	0.00865	0.04757	1.13306	0.18022
ADP	ADP	C10H15N5O10P2	117.1	HMDB0001341	C00008	0.02611	0.03618	0.03241	0.04483	0.03075	0.03022	0.55309	1.11708	0.15974
Lysine	L-Lysine	C6H14N2O2	168.0	HMDB0000182	C00047	0.00566	0.00444	0.00558	0.00485	0.00518	0.00735	0.56694	1.10817	0.14818
Dihydroxyacetone-P	Dihydroxyacetone phosphate	C3H7O6P	347.1	HMDB0001473	C00111	0.00501	0.00498	0.00526	0.00724	0.00443	0.00520	0.58477	1.10657	0.14609
Taurine	Taurine	C2H7NO3S	267.1	HMDB0000251	C00245	0.34679	0.31215	0.28544	0.33384	0.34502	0.36586	0.19340	1.10625	0.14567
2-phosphoglyceric acid	2-Phosphoglyceric acid	C3H7O7P	268.1	HMDB0000362		0.00005	0.00006	0.00007	0.00007	0.00007	0.00006	0.44463	1.10602	0.14537

Supplemental Table 1. Continued

2-phosphoglyceric acid	2-Phosphoglyceric acid	C3H7O7P	268.1	HMDB0000362		0.00005	0.00006	0.00007	0.00007	0.00007	0.00006	0.44463	1.10602	0.14537
3-Ureidopropionic acid	Ureidopropionic acid	C4H8N2O3	268.1	HMDB0000026	C02642	0.00118	0.00084	0.00079	0.00099	0.00113	0.00096	0.53658	1.10044	0.13808
Carnitine	L-Carnitine	C7H15NO3	208.1	HMDB0000062	C00318	0.00009	0.00011	0.00011	0.00011	0.00011	0.00012	0.25199	1.09699	0.13355
Homoglutathione	L-L-Homoglutathione	C11H19N3O6S	507.0	HMDB0029395		0.00012	0.00040	0.00045	0.00039	0.00032	0.00034	0.81155	1.08536	0.11817
FAICAR	Phosphoribosyl formamidocarboxamide	C10H15N4O9P	132.1	HMDB0001439	C04734	0.00009	0.00005	0.00005	0.00008	0.00007	0.00006	0.74212	1.08270	0.11464
Saccharopine	Saccharopine	C11H20N2O6	307.1	HMDB0000279	C00449	0.00227	0.00143	0.00126	0.00210	0.00145	0.00182	0.72999	1.08265	0.11456
Valine	L-Valine	C5H11NO2	244.1	HMDB0000883	C00183	0.00206	0.00211	0.00199	0.00196	0.00236	0.00229	0.34569	1.07244	0.10090
Uric acid	Uric acid	C5H4N4O3	113.1	HMDB0000289	C00366	0.00012	0.00011	0.00011	0.00010	0.00012	0.00014	0.57511	1.06953	0.09698
AMP	Adenosine monophosphate	C10H14N5O7P	149.1	HMDB0000045	C00020	0.00189	0.00231	0.00213	0.00239	0.00215	0.00221	0.38632	1.06588	0.09205
Adenosine	Adenosine	C10H13N5O4	340.0	HMDB0000050	C00212	0.00011	0.00012	0.00013	0.00013	0.00012	0.00012	0.31883	1.06576	0.09189
Homocystine	DL-Homocystine	C8H16N2O4S2	106.0	HMDB0000575	C01817	0.00150	0.00114	0.00110	0.00123	0.00149	0.00125	0.64932	1.05995	0.08399
Homocystine	L-Homocystine	C8H16N2O4S2	158.0	HMDB0000676	C01817	0.00150	0.00114	0.00110	0.00123	0.00149	0.00125	0.64932	1.05995	0.08399
Kynurenine	L-Kynurenine	C10H12N2O3	131.1	HMDB0000684	C00328	0.03197	0.01300	0.01186	0.02139	0.01263	0.02618	0.89171	1.05921	0.08299
ATP	Adenosine triphosphate	C10H16N5O13P3	105.0	HMDB0000538	C00002	0.00392	0.00494	0.00452	0.00491	0.00460	0.00433	0.68725	1.03369	0.04781
Ornithine	Ornithine	C5H12N2O2	226.1	HMDB0000214	C00077	0.00601	0.00543	0.00565	0.00411	0.00712	0.00622	0.90335	1.02172	0.03100
Glutathione	Glutathione	C10H17N3O6S	131.1	HMDB0000125	C02471	0.04519	0.05300	0.04088	0.05827	0.04358	0.03959	0.91276	1.01705	0.02439
Uridine	Uridine	C9H12N2O6	115.1	HMDB0000296	C00299	0.00011	0.00012	0.00014	0.00013	0.00012	0.00013	0.89949	1.01067	0.01531
Creatinine	Creatinine	C4H7N3O	168.0	HMDB0000562	C00791	0.00603	0.00468	0.00362	0.00530	0.00376	0.00528	0.99668	1.00080	0.00116
Methionine	L-Methionine	C5H11NO2S	181.1	HMDB0000696	C00073	0.00089	0.00072	0.00066	0.00077	0.00076	0.00070	0.91362	0.98873	-0.01635
Fructose-1,6-diphosphate	Fructose 1,6-bisphosphate	C6H14O12P2	260.0	HMDB0001058	C00354	0.00231	0.00127	0.00162	0.00217	0.00159	0.00132	0.91743	0.97481	-0.03681
Glycerate	Glyceric acid	C3H6O4	260.0	HMDB0000139	C00258	0.00114	0.00090	0.00083	0.00098	0.00086	0.00093	0.74503	0.96232	-0.05541
Allantoin	Allantoin	C4H6N4O3	260.0	HMDB0000462	C01551	0.00248	0.00223	0.00196	0.00190	0.00201	0.00246	0.67815	0.95456	-0.06710
Isoleucine	L-Isoleucine	C6H13NO2	260.0	HMDB0000172	C00407	0.00306	0.00251	0.00244	0.00249	0.00244	0.00259	0.50007	0.93984	-0.08951
Serine	L-Serine	C3H7NO3	155.1	HMDB0000187	C00065	0.00931	0.00831	0.00785	0.00668	0.00926	0.00792	0.57684	0.93729	-0.09344
Carnosine	Carnosine	C9H14N4O3	260.0	HMDB0000033	C00386	0.00002	0.00004	0.00006	0.00003	0.00003	0.00005	0.86188	0.93723	-0.09352
Leucine	L-Leucine	C6H13NO2	180.1	HMDB0000687	C00123	0.00172	0.00151	0.00169	0.00141	0.00166	0.00147	0.26295	0.92103	-0.11868
Proline	L-Proline	C5H9NO2	297.1	HMDB0000162	C00148	0.00306	0.00282	0.00318	0.00278	0.00260	0.00294	0.16792	0.91951	-0.12106
Phosphoenolpyruvate	Phosphoenolpyruvic acid	C3H5O6P	175.1	HMDB0000263	C00074	0.00604	0.00277	0.00261	0.00429	0.00275	0.00342	0.80861	0.91546	-0.12744
Tyrosine	L-Tyrosine	C9H11NO3	165.1	HMDB0000158	C00082	0.00190	0.00174	0.00167	0.00146	0.00180	0.00158	0.26685	0.91006	-0.13597
Hexose-P	Galactose 1-phosphate	C6H13O9P	446.1	HMDB0000645	C00446	0.00129	0.00095	0.00084	0.00112	0.00066	0.00100	0.62522	0.90191	-0.14894
Hexose-P	Mannose 6-phosphate	C6H13O9P	204.1	HMDB0001078	C00275	0.00129	0.00095	0.00084	0.00112	0.00066	0.00100	0.62522	0.90191	-0.14894
Hexose-P	Glucose 1-phosphate	C6H13O9P	257.1	HMDB0001586	C00103	0.00129	0.00095	0.00084	0.00112	0.00066	0.00100	0.62522	0.90191	-0.14894
Hexose-P	D-Mannose 1-phosphate	C6H13O9P	172.0	HMDB0006330	C00636	0.00129	0.00095	0.00084	0.00112	0.00066	0.00100	0.62522	0.90191	-0.14894
Histidine	L-Histidine	C6H9N3O2	146.1	HMDB0000177	C00135	0.00376	0.00322	0.00289	0.00275	0.00339	0.00265	0.35696	0.89056	-0.16721
Glucose-6P	Glucose 6-phosphate	C6H13O9P	334.1	HMDB0001401	C00092	0.00200	0.00147	0.00133	0.00169	0.00119	0.00136	0.51077	0.88593	-0.17474
Glucose	D-Glucose	C6H12O6	172.0	HMDB0000122	C00031	0.00052	0.00035	0.00047	0.00033	0.00040	0.00044	0.40569	0.87056	-0.19998
Adenylthiomethylpentose	5'-Methylthioadenosine	C11H15N5O3S	290.0	HMDB0001173	C00170	0.00265	0.00259	0.00279	0.00216	0.00222	0.00256	0.08532	0.86545	-0.20848
Citrulline	Citrulline	C6H13N3O3	203.1	HMDB0000904	C00327	0.00304	0.00227	0.00257	0.00233	0.00234	0.00211	0.23772	0.86072	-0.21638
Phenylalanine	L-Phenylalanine	C9H11NO2	192.0	HMDB0000159	C00079	0.00068	0.00068	0.00073	0.00043	0.00057	0.00078	0.42135	0.85375	-0.22812
CDP-ethanolamine	CDP-Ethanolamine	C11H20N4O11P2	118.0	HMDB0001564	C00570	0.00265	0.00392	0.00315	0.00307	0.00258	0.00252	0.30302	0.84153	-0.24891
Tryptophan	Tryptophan	C11H12N2O2	130.0	HMDB0030396	C00806	0.00022	0.00019	0.00013	0.00012	0.00016	0.00017	0.41483	0.83925	-0.25283
Glycerophosphocholine	Glycerophosphocholine	C8H20NO6P	257.1	HMDB0000086	C00670	0.04377	0.06182	0.06618	0.04372	0.04924	0.04805	0.27101	0.82097	-0.28460
Glycerol-3P	Glycerol 3-phosphate	C3H9O6P	172.0	HMDB0000126	C00093	0.00188	0.00164	0.00142	0.00139	0.00114	0.00143	0.12131	0.80179	-0.31870
Glutamine	L-Glutamine	C5H10N2O3	146.1	HMDB0000641	C00064	0.01153	0.01321	0.01438	0.00841	0.00921	0.01109	0.03897	0.73379	-0.44656
Glycerophosphoinositol	1-(sn-Glycero-3-phospho)-1D-myo-inositol	C9H19O11P	334.1	HMDB0011649	C01225	0.00005	0.00005	0.00005	0.00003	0.00004	0.00004	0.00868	0.72723	-0.45952
Glycerol-2P	Beta-Glycerophosphoric acid	C3H9O6P	172.0	HMDB0002520	C02979	0.00059	0.00043	0.00040	0.00030	0.00027	0.00037	0.10136	0.66695	-0.58434
Sedoheptulose-7P	D-Sedoheptulose 7-phosphate	C7H15O10P	290.0	HMDB0001068	C00281	0.00208	0.00113	0.00096	0.00096	0.00077	0.00092	0.28167	0.63465	-0.65597
Carnitine (C2:0)	L-Acetylcarnitine	C9H17NO4	203.1	HMDB0000201	C02571	0.00028	0.00033	0.00034	0.00015	0.00016	0.00019	0.00395	0.52331	-0.93426
Citric acid	Citric acid	C6H8O7	192.0	HMDB0000094	C00158	0.05796	0.04311	0.09725	0.02789	0.03700	0.02658	0.15351	0.46128	-1.11628
Succinate	Succinic acid	C4H6O4	118.0	HMDB0000254	C00042	0.01874	0.02596	0.02024	0.00691	0.00784	0.00856	0.02025	0.35913	-1.47741
Itaconic acid	Itaconic acid	C5H6O4	130.0	HMDB0002092	C00490	0.06848	0.08037	0.07017	0.00020	0.00012	0.00020	0.00259	0.00240	-8.70139

Supplemental Table 2. Antibody and dye list

Target	Conjugation	Supplier	Catalgoue Number	Host	Target Species
CD16/32	-	eBioscience/ Thermo Fisher	14-0161	rat	mouse
CD11b	FITC	eBioscience/ Thermo Fisher	11-0112	rat	mouse/human
Siglec-F	PE	BD bioscience	562068/552126	rat	mouse
Ly6G	PerCP-Cy5.5	BD bioscience	560602	rat	mouse
CD115	PE-Cy7	eBioscience/ Thermo Fisher	25-1152	rat	mouse
Ly6C	Alexa Fluor 647	AbD serotec	MCA2389A647	rat	mouse
CD45	APC-Cy7	BioLegend	103115/103116	rat	mouse
CD3e	FITC	eBioscience/ Thermo Fisher	11-0031	Armenian hamster	mouse
CD8a	PE	eBioscience/ Thermo Fisher	12-0081	rat	mouse
CD19	PerCP-Cy5.5	eBioscience/ Thermo Fisher	45-0193	rat	mouse
CD11b	PE-Cy7	BD bioscience	552850	rat	mouse/human
CD4	APC	eBioscience/ Thermo Fisher	17-0041	rat	mouse
CD115	Alexa Fluor 488	BioLegend	135512	rat	mouse
CD11b	PE	eBioscience/ Thermo Fisher	12-0112	rat	mouse/human
MHCII	Brilliant Violet 510	BioLegend	107635	rat	mouse
CD11c	PE-Cy7	eBioscience/ Thermo Fisher	25-0114	Armenian hamster	mouse
CCR2	Alexa Fluor 700	R&D systems	FAB5538N	rat	mouse
CD62L, L-Selectin	PE-Cy7	eBioscience/ Thermo Fisher	25-0621	rat	mouse
CD44	APC	eBioscience/ Thermo Fisher	17-0441	rat	human/mouse
CD4	APC-H7	BD bioscience	560181	rat	mouse
F4/80	FITC	Biolegend	123108	rat	mouse
MHCII (MHC I-A/I-E)	PerCP-Cy5.5	BD bioscience	562363	rat	mouse
F4/80	APC-eFluor 780	eBioscience/ Thermo Fisher	47-4801	rat	mouse
CD68	Alexa Fluor 488	AbD serotec	MCA1957A488	rat	mouse
CD11b	PerCP-Cy5.5	BD bioscience	550993	rat	mouse/human
F4/80	Brilliant Violet 711	BioLegend	123147	rat	mouse
CX3CR1	Brilliant Violet 421	Biolegend	149023	Mouse	Mouse
CD16/32	APC-Cy7	BD bioscience	560541	rat	mouse
CD43	FITC	BD bioscience	561856	rat	mouse
CXCR4	Alexa Fluor 488	eBioscience/ Thermo Fisher	53-9991	rat	mouse
CD117, c-Kit	PE	Biolegend	105807/105808	rat	mouse
CD115	PE-Cy7	BioLegend	135523/135524	rat	mouse
CD135	APC	BioLegend	135309/135310	rat	mouse
Ly-6G	Pacific Blue	Biolegend	127611/127612	rat	mouse
Ly6C	Brilliant Violet 510	BioLegend	128033	rat	mouse
FVD	e780	Thermo Fisher	65-0865		all
7AAD	-	Molecular Probes	A1310		
Annexin V	FITC	Biolegend	640905		all
ER-MP58	-	AbD serotec	MCA2391	rat	mouse
Rabbit anti-Rat 2nd	biotin	Dako	E0468	rabbit	rat

Supplemental Table 3. List of primers

Target	Sequence
Acod1-FW	AGTTTTCTGGCCTCGACCTG
Acod1-RV	AGAGGGAGGGTGGAATCTCT
Nos2-FW	GCAAACCCAAGGTCTACGTTCA
Nos2-RV	CCTCATTGGCCAGCTGCTT
Il1b-FW	AAAGAATCTATACCTGTCCTGTGTAATGAAA
Il1b-RV	GGTATTGCTTGGGATCCACACT
Ldlr-FW	GCATCAGCTTGGACAAGGTGT
Ldlr-RV	GGGAACAGCCACCATTGTTG
Nr4a1-FW	TTGAGTTCGGCAAGCCTACC
Nr4a1-RV	GTGTACCCGTCCATGAAGGTG
Abca1-FW	CCCAGAGCAAAAAGCGACTC
Abca1-RV	GGTCATCATCACTTTGGTCCTTG
Abcg1-FW	TCGGACGCTGTGCGTTTT
Abcg1-RV	CCCACAAATGTCGCAACCT
Apoe-FW	GCCTAGCCGAGGGAGAGCCG
Apoe-RV	CATAGTGTCCTCCATCAGTGC
Cd36-FW	GCCAAGCTATTGCGACATGA
Cd36-RV	AAAAGAATCTCAATGTCCGAGACTTT
Pparg-FW	GAAGTTCAATGCACTGGAATTAGATG
Pparg-RV	CCTCGATGGGCTTCACGTT
Nr1h3-FW	GCTCTGCTCATTGCCATCAG
Nr1h3-RV	TGTTGCAGCCTCTCTACTTGGA

7



General Discussion

General Discussion

Immunometabolism has revolutionised our understanding of how immune cells shape inflammatory responses; through an intricate network of metabolic pathways and signals that control immune cell function [1-4]. Macrophages, orchestrators of both inflammatory responses and tissue homeostasis, have been under the spotlight in this field [5-7]. Their dysregulation is responsible for driving numerous inflammatory diseases, yet therapeutic strategies to redirect aberrant macrophages towards protective phenotypes remain elusive [8, 9]. The discovery that metabolites function beyond their classical roles of energy production and biosynthesis has opened new avenues for therapeutic intervention, particularly in diseases where macrophages are key drivers of pathology such as atherosclerosis, cancer, and rheumatoid arthritis [10-13].

Main outcomes of this thesis

This thesis researched both new and established macrophage immunometabolites with the goal of uncovering their therapeutic potential in the treatment of atherosclerosis. After defining what exactly constitutes an "immunometabolite" (**chapter 2)**, the first part of this thesis focuses on the identification of novel macrophage immunometabolites through use of liquid chromatography-mass spectrometry (LC-MS) based metabolomics. We identified adenine (**chapter 3**) and 2-hydroxyglutarate (2HG) (**chapter 4**) as macrophage immunometabolites that are upregulated during macrophage inflammation. By combining both functional and metabolic assays we discovered that they both possess anti-inflammatory properties and the capacity to control core metabolic processes, such as oxidative phosphorylation (OXPHOS) and glycolysis.

The second part of this thesis revisits well-characterised macrophage immunometabolites, succinate and itaconate, with the latter investigated in the context of atherosclerosis. Our analysis revealed an anti-inflammatory role for succinate (**chapter 5**) by suppressing IL-6, tumour necrosis factor alpha (TNFα) and nitric oxide (NO) secretion and expression of CD40, CD86 and inducible nitric oxide synthase (iNOS). These findings challenge the dogma that placed succinate as a core immunometabolite, accumulating in pro-inflammatory macrophages and exacerbating inflammation through hypoxia-inducible factor 1-alpha (HIF-1α) signalling and IL-1β secretion [14]. In **chapter 6**, we demonstrate that ablation of ACOD1, the enzyme responsible for itaconate synthesis, results in the formation of more stable atherosclerotic plaques [15]. *Acod1*-deficient foam cells showed enhanced survival and lipid handling without exacerbating plaque size development, indicating that ACOD1 inhibition could be a promising therapeutic strategy to limit cardiovascular disease progression. These findings highlight the context-dependent nature of immunometabolism and emphasises the importance of further unravelling

how immunometabolites interact with and impact macrophage inflammation and metabolism.

In this discussion I will consolidate the main findings of this thesis and highlight the contrasting roles that immunometabolites play in facilitating macrophage inflammatory responses. I will also discuss how selection of the appropriate model is critical when answering research questions related to mechanistic insight versus therapeutic potential. Finally, I will explain how the results from this thesis provide a starting point for the generation of both systemic and targeted immunometabolic based therapies for the treatment of atherosclerosis and suggesting methods of implementation into the clinic.

An evolutionary view on immunometabolism

Glycolysis and OXPHOS are highly conserved metabolic pathways that are present in almost all living organisms [16]. It is widely accepted that glycolysis was present on earth before photosynthesis gave rise to oxygen [16]. Once oxygen became a part of glycolysis as we know it today, the anaerobic side of glycolysis was retained, and could act as a fundamental defence mechanism for early organisms without an immune system [17]. By rapidly converting glucose into lactic acid, cells simultaneously starve the system of energy sources and reduce the surrounding pH, generating an inhospitable environment that can inhibit pathogen expansion [17]. Just as these metabolic pathways are highly conserved, so are the existence of nucleotides.

On an evolutionary standpoint, adenine is likely to have existed on earth since the start of the biotic era [18]. With this in mind, a mechanism was proposed for adenine generation outside of an organism, solely synthesised through thermochemical reactions [19, 20]. This provides a foundation for the existence of adenine even predating the biotic era. Similar to glycolysis existing as both a set of catabolic reactions and a defence mechanism, we could hypothesise that adenine plays a major role in the function of organisms beyond that of forming the basis of genetic material and energy production. Using LC-MS, we identified adenine (**chapter 3**) as an immunometabolite that is elevated 2- to 3-fold in M-CSF macrophages when compared to GM-CSF differentiated macrophages [21]. Exogenously adding adenine to inflammatory macrophages resulted in reduced secretion of cytokines IL-10, TNFα and IL-12p40 as well as expression of surface markers CD40 and CD38. This increased abundance of adenine drove M-CSF macrophages towards a quiescent state, preventing the accumulation of metabolites typically seen during inflammation and lowering ATP production from both glycolytic and OXPHOS pathways. We show that adenine is not inducing quiescence through NF-κB, the adenine salvage pathway or metabolic signalling pathways AMPK, AKT and p38 MAPK, and thus there are alternative mechanisms that could be worth investigating.

Immunometabolites are known to act as protein modifiers, by interacting with and altering the function of proteins [22, 23]. The citric acid (TCA) cycle derivative succinyl-CoA, the metabolite prior to succinate, is involved in the post translational modification of proteins, by adding a succinyl group to lysine residues and thereby affecting the overall net charge of the protein, affecting protein function [22]. Narunsky et al. investigated the possibility for adenine to interact with proteins, showing that interactions may occur from angles of the adenine molecular structure other than that of the DNA binding side [18]. However, it was discussed that adenine itself is unlikely to bind to proteins, and instead, the adenine component of cofactors such a FAD, ATP and NAD is what can affect protein binding affinity. An alternative signalling mechanism that could explain the inflammatory mediating effects of adenine observed in **chapter 3** is the existence of adenine receptors. Similar to the succinate binding G protein-coupled receptor 91 (GPR91/SUCNR1), that we investigated in **chapter 5**, and the newly discovered itaconate receptor OXGR1, there is the possibility for a cell surface adenine receptor to exist in humans [24]. In the investigation of purinergic receptors, a family of G protein-coupled receptors were discovered in mouse, hamster and rats, named P0 receptors, that possess an affinity for binding adenine [25-27]. Upon analysis of gene expression within rats, it was identified that these receptors were mostly expressed in dorsal root ganglia, however peripheral blood leukocyte expression of the adenine receptors was amongst the top tissues analysed [27]. Whilst expression of these adenine receptors has not been recognised yet in human tissue, the presence of other purinergic receptors, named P1 and P2 receptors, are expressed in humans and other species and function in a similar manor to P0 receptors [28]. Moreover, P1 and P2 receptors have been described to be stress response receptors in human macrophages and have major immunomodulatory properties when binding adenosine and ATP, respectively [29, 30]. Therefore, the hypothesis that humans express P0 receptors has not been excluded. These receptors have been shown to induce both pro- and anti-inflammatory effects due to coupling with either Gi/o or Gs proteins, and upon activation, inhibit or stimulate the synthesis of cAMP, respectively [31, 32]. It is well described that accumulation of intracellular cAMP correlates with resolution of inflammation, however interestingly adenine binding P0 receptors have thus far only been shown to reduce intracellular cAMP and therefore would be bound to a Gi/o protein [33]. It is possible that the presence of Gs-coupled P0 receptors exist and could be a possible explanation for the anti-inflammatory responses we see in adenine treated human macrophages.

Context is key

This thesis demonstrates that immunometabolites function in more complex ways than initially thought; their immunomodulatory effects are highly context dependent. In **chapter 5**, we showed that succinate, originally considered pro-inflammatory through its interaction with the SUCNR1 receptor, instead suppressed inflammation in our experiments

[34]. The structurally modified derivative of succinate, diethyl succinate, was used to show succinate's pro-inflammatory inducing function [14]. However, these modifications can induce strong electrophilic stress responses in cells that aren't present with the unmodified forms of the metabolite [35]. This phenomenon is observed with itaconate. Modified derivatives like dimethyl itaconate (DMI) and 4-octylester itaconate (4-OI) reduce secretion of cytokines such as secretion of IL-6, IL-10, and interferon beta (IFN-β) from inflammatory macrophages, while natural itaconate increases IFN-β production [35]. This highlights an important methodological consideration that researchers must contemplate when studying mechanisms of immunometabolism; are modified immunometabolites the correct model for this research question? We suggest that derivatives of cellular metabolites are not suitable candidates for fundamental research that aims to uncover the immunomodulatory properties of endogenous immunometabolites. Moreover, it is important to always refer to these derivatives by their compound name rather than their endogenous name to avoid misleading readers. This led us to an approach in **chapter 6** that refrained from the use of modified immunometabolites, using only natural, unmodified itaconate and *Acod1*$^{-/-}$ macrophages to study the immunomodulatory mechanisms of itaconate in atherosclerosis [36].

This does not mean however, that investigating the mechanisms behind diethyl succinate, and other structurally modified immunometabolite derivatives, is redundant. The potent immune-regulating properties of metabolite derivatives make them ideal therapeutic candidates for clinical management of inflammatory diseases. The compound dimethyl fumarate (DMF), a derivative of the TCA cycle metabolite fumarate, is used in the management of the inflammatory disease multiple sclerosis (MS) [37]. DMF controls anti-inflammatory responses through activation of the transcription factor nuclear factor erythroid 2-related factor 2 (NRF2). Due to its electrophilic properties, DMF modifies the NRF2 inhibitor Kelch-like ECH-associated protein 1 (KEAP1) through a Michael addition reaction which covalently bonds DMF to a thiol group on KEAP1 [38]. The uninhibited NRF2 allows transcription of antioxidant enzymes such as NADPH quinone oxidoreductase 1 (NQO1) and thus reduces synthesis of reactive oxygen species (ROS) and induces anti-inflammatory responses in macrophages [9, 38, 39]. This is a very similar mechanism to the more novel immunometabolite, 4-OI, which has been proposed as a promising treatment against inflammation and coagulation [40, 41]. Diethyl succinate, in contrast to DMF and 4-OI, is unlikely to induce such reactions due to the absence of a Michael acceptor site; a carbon-to-carbon double bond with a carbonyl group attached. However, as we observed in our study, diethyl succinate indeed exhibited anti-inflammatory properties which were independent of the SUCNR1 receptor. Since diethyl succinate freely enters the cell, it is uncertain whether this is an intra- or extracellular mechanism. The addition of diethyl succinate to microglia, the resident macrophage of the brain, similarly suppresses the secretion of pro-inflammatory cytokine TNFα through a SUCNR1 independent manner

[42]. Microglia are suppressed in their ability to elicit mitochondrial fission during an inflammatory response, in the presence of diethyl succinate, due to its capacity to increase phosphorylation of serine 637 in dynamin-related protein (DRP1), a protein known to control mitochondrial fission [42]. This leads to a marked decrease in ROS synthesis and dampens microglial immune responses. The direct mechanism behind diethyl succinates mitochondrial regulation is still unknown and whether this also occurs in inflammatory macrophages is an interesting avenue to investigate further.

Navigating mechanistic heterogeneity in atherogenic mouse models

Aside from the duality of immunometabolism function on a cellular level, studying the role of immunometabolism on inflammatory disease progression in the context of a disease model can also create contrasting outcomes [43]. The generation of atherogenic mouse models in 1992 revolutionised the field by providing more accessible experimental tools and has since resulted in a variety of models to work with [43-45]. This proliferation of available mouse models to study atherosclerosis presents researchers with a critical decision regarding model selection: which model is most suitable for this research question, and to what extent can the results be generalised across different models or more importantly, translated to human pathology? *Apoe*$^{-/-}$ and *Ldlr*$^{-/-}$ knockout mice have emerged as the primary models over the past three decades, with the latter utilised in our **chapter 6** investigation [44, 45]. These models function through distinct mechanisms: *Apoe*$^{-/-}$ mice lack apolipoprotein E (ApoE), a glycoprotein that facilitates receptor-mediated clearance of very low-density lipoproteins (VLDL) and chylomicrons, resulting in elevated circulating levels of these lipids [43, 46, 47]. Conversely, *Ldlr*$^{-/-}$ mice are deficient in the low-density lipoprotein (LDL) receptor, leading to increased circulating LDL [43, 47]. While both models develop atherosclerotic plaques when fed high-fat diets, *Ldlr*$^{-/-}$ mice more closely mirror human pathophysiology, as LDL represents the primary cholesterol carrier in human atherosclerosis progression [48]. An important consideration when selecting between these models is that the ApoE glycoprotein possesses immunomodulatory properties beyond lipid transport, including enhancement of systemic inflammation [47, 49]. This dual functionality makes *Apoe*$^{-/-}$ mice particularly suitable for studying atherosclerosis in systemic inflammatory contexts such as smoking or obesity [50].

ApoE3-Leiden mice carry an *ApoE3* mutation that induces hyperlipidaemia while retaining ApoE's immunological functions, thereby addressing the altered systemic inflammatory state of *Apoe*$^{-/-}$ mice [43, 51]. More recently, models utilising proprotein convertase subtilisin/kexin type 9 (PCSK9) gain-of-function mutations delivered via adeno-associated virus vectors (AAVs) have gained prominence [52,53]. PCSK9, an enzyme secreted by the liver, binds to cell surface LDL receptors, triggering their internalisation and degradation, thus reducing the availability of receptors for LDL clearance [52, 53]. While these AAV-PCSK9 models develop atherosclerosis effectively, the lesion burden is somewhat lower

compared to *Ldlr*$^{-/-}$ mice and predominantly elevates VLDL rather than LDL cholesterol, creating a distinct metabolic profile [54]. These differences illustrate that model selection for studying immunometabolism in atherosclerosis requires careful consideration as each model generates lesions with unique lipid profiles and inflammatory signatures, potentially influencing immunometabolic pathways [43].

The ACOD1-itaconate axis in atherosclerosis

Our findings in **chapter 6** reveal a striking contrast with recent literature regarding the role of ACOD1 and itaconate in atherosclerosis progression. While we demonstrated that *Acod1* deficiency leads to more stable atherosclerotic plaques with smaller necrotic cores in *Ldlr*$^{-/-}$ mice, other recent investigations by Song et al. (2023), Cyr et al. (2024), and Hong et al. (2024) report exacerbated atherosclerotic burden, including necrotic core development, under *Acod1* deficiency, or protection from atherosclerosis progression in the presence of 4-OI or nanoparticle-delivered itaconate (Table 1) [55-57]. This apparent contradiction warrants careful examination, as it highlights the context-dependent nature of immunometabolic regulation in complex disease models.

A critical factor potentially explaining these divergent outcomes is the choice of atherosclerosis model. Our study utilised bone marrow transplantation into *Ldlr*$^{-/-}$ mice, whereas Song et al. implemented an AAV-PCSK9 approach [55]. As discussed earlier, these models generate distinctly different lipid profiles: *Ldlr*$^{-/-}$ mice primarily accumulate LDL cholesterol, while AAV-PCSK9 models show greater VLDL elevation [54]. These lipoprotein differences could significantly impact macrophage inflammatory responses and metabolic pathways, as LDL and VLDL particles interact with different cell surface receptors and have different ratios of cholesterol and triglyceride content [58]. Furthermore, the mechanisms of disease progression differ between models; *Ldlr*$^{-/-}$ mice are chronically defective in the removal of circulating LDL, compared to the acute rapid-onset of lipid accumulation in the AAV-PCSK9 model [52]. This chronic LDL handling deficiency in *Ldlr*$^{-/-}$ mice may result in a more robust compensatory antioxidant response compared to the acute nature of the AAV-PCSK9 model and therefore, could determine whether macrophages are able to withstand enhanced lipid accumulation.

Among the studies presented in Table 1, Cyr et al.'s 2024 investigation using *Ldlr*$^{-/-}$ male and female mice transplanted with *Acod1*$^{-/-}$ bone marrow on a western diet most closely parallels our experimental design in **chapter 6** [56]. Sex-specific effects could contribute to the discrepancies between the two studies, as female and male mice exhibit markedly different inflammatory responses to hyperlipidaemia [59]. Estrogen, produced by females, have been shown to significantly lower atherosclerosis burden in comparison to male mice, and female mice with estrogen inhibitors [60, 61]. Cyr and colleagues however highlighted that ACOD1 still protected mice from excessive plaque progression, regardless of sex

Supplemental Table 1. Studies on the role of ACOD1 and itaconate in different atherosclerotic murine models

Author	Atherosclerosis Model	ACOD1-Itaconate axis intervention	Observation
Harber et al., 2024 [36]	*Ldlr*$^{-/-}$ female mice fed HFD for 9 weeks	*Acod1*$^{-/-}$ vs control bone marrow transplantation 6 weeks prior to HFD initiation	**ACOD1 is atherogenic:** *Acod1*$^{-/-}$ transplanted mice displayed more stable plaques by decreased apoptosis and necrosis, and higher lipid content in foam cells
Song et al., 2023 [55]	AAV-PCSK9 injection in male mice fed WD for 10 weeks	*Acod1*$^{-/-}$ vs control mice	**ACOD1 is atheroprotective:** 1.5-fold larger lesions and 3-fold larger necrotic cores in *Acod1*$^{-/-}$ mice
		Acod1$^{fl/fl}$ *LysM*^{cre} vs control mice	**ACOD1 is atheroprotective:** 2-fold larger lesions and 3-fold larger necrotic cores in *Acod1*$^{fl/fl}$ *LysM*^{cre} mice with increased macrophage infiltration
		Twice weekly *i.p.* injection of 4-OI in WT atherogenic mice after WD initiation	**4-OI is atheroprotective:** Lesion area, necrotic core area and macrophage content of 4OI treated atherogenic mice were lower than control mice. 4OI treatment prevented mitochondrial dysfunction in plaque macrophages
Cyr et al., 2024 [56]	*Ldlr*$^{-/-}$ male mice fed WD for 34 weeks	Thrice weekly *i.p.* injection of 4-OI for 4 weeks in WT mice after 30 weeks of WD	**4-OI is atheroprotective:** 2-fold higher macrophage content and necrotic core area in control mice vs 4-OI treated mice. IL-1β staining reduced in 4-OI treated mice
	Ldlr$^{-/-}$ male and female mice fed WD for 12 weeks	*Acod1*$^{-/-}$ vs control bone marrow transplantation 6 weeks prior to WD initiation	**ACOD1 is atheroprotective:** Significantly larger plaques in both male and female mice transplanted with *Acod1*$^{-/-}$ bone marrow. Macrophage and lipid content also increased in these mice

	AAV-PCSK9 injection in male mice fed WD for 12-16 weeks	*Acod1*$^{-/-}$ vs control mice	**ACOD1 is atheroprotective:** Plaque size, as well as macrophage and lipid content are significantly higher in *Acod1* deficient atherosclerotic mice
Hong et al., 2024 [57]	*Ldlr*$^{-/-}$ male mice fed HCHFD for 16 weeks	Twice weekly *i.v.* injection of itaconate vs control lipid nanoparticles for 8 weeks after 16 weeks of HCHFD	**Itaconate-containing nanoparticles are atheroprotective:** Plaque size, necrotic core size and plaque lipid content are decreased in atherogenic mice treated with itaconate-containing nanoparticles. Smooth muscle cell to macrophage ratio is increased in the mice.

High fat diet (HFD) consists of 15% fat and 0.15% cholesterol. Western diet (WD) consists of 21% fat and 0.2% cholesterol. High cholesterol high fat diet (HCHFD) consists of 20% fat and 1.25% cholesterol.

[56]. The use of female mice in our study is consequently an unlikely explanation for the discrepancies between these 4 studies. Intriguingly, intracellular lipid content in Acod1 deficient macrophages in this study was increased, similar to what we reported in our atherosclerotic mice. This shared observation suggests a fundamental role for the ACOD1-itaconate axis in regulating lipid metabolism. Despite their observation of increased plaque and macrophage lipid content, the proportion of necrotic core burden remained similar between control and Acod1 deficient mice [56]. Acod1 deficiency in macrophages may therefore enhance macrophage lipid tolerance, potentially raising the threshold at which lipid accumulation triggers cell death pathways. Our multi-omics approach revealed that Acod1 deficiency redirects glycolytic flux toward glycerol-3-phosphate synthesis, which is used in de novo triglyceride formation within macrophages. Rather than contributing to plaque instability, this metabolic shift appears to improve cell survival in our model, reducing apoptosis and necrotic core formation.

These contrasting results emphasise the importance of model selection when investigating immunometabolic mechanisms in complex diseases. Collectively, these studies reveal the context-dependent nature of the ACOD1-itaconate axis in atherosclerosis, simultaneously influencing lipid metabolism and cell survival. Future investigations should directly compare these models under identical experimental conditions to elucidate the model specific factors determining whether Acod1 deficiency stabilises or exacerbates atherosclerotic lesions, and as such, gain a better understanding of the therapeutic potential of the ACOD1-itaconate axis.

Future directions: advancing clinical translation of atherosclerosis immunometabolism

The insights gained from the studies in this thesis show the complex and context-dependent nature of immunometabolism yet underscores the variety of metabolic targets that could be exploited to control aberrant macrophages in inflammatory disease. The future of treating atherosclerosis may lie in modulating macrophage immunometabolism to shift the balance from pro-inflammatory, plaque-destabilising states towards resolution and repair. However, that requires translation of these complex pre-clinical findings into effective and safe clinical interventions.

The most well established immunometabolic pathways, some of which are described in this thesis, happen to be essential pathways that are regulated in almost all cell types. Succinate for example, is part of the TCA cycle and its associated enzyme SDH is crucial in both the TCA cycle and the electron transport chain. Adenine forms the basis of genetic material and therefore is ubiquitously present in all cell types. Intervening with such vital immunometabolic pathways with non-specific treatment options to combat atherosclerosis progression could result in undesirable off target side-effects due to the heterogenic nature of metabolic pathways in different immune cells [2]. However, drugs

such as DMF and metformin, which are already used to treat complex inflammatory diseases, are evidence that modulating essential metabolic pathways will not necessarily result in systemic adverse events [9]. DMF as described earlier is a suppressor of the ubiquitously expressed NRF2 protein, whilst metformin is a suppresser of gluconeogenesis. In diseases like MS for DMF, or potentially atherosclerosis, where multiple cell types can contribute to pathology, a broader immunometabolic intervention could re-wire the overall immune environment towards a less inflammatory state [2, 62]. Whilst substantial new mechanistic insight into the immunomodulating properties of adenine and succinate is needed before considering its potential in treating atherosclerosis, DMF and metformin provide a positive prospect for non-specific immunometabolic-based treatments. Nevertheless, treatments that target immunometabolic pathways that are specifically regulated in atherosclerosis or techniques that deliver drugs in a localised manner would be a safer approach for treating atherosclerosis in the clinic [13, 63].

The specific regulation of the ACOD1-itaconate axis in macrophages makes it an ideal pathway to target without the risk of altering the activity of the immune system on a systemic level. Our demonstration of *Acod1* ablation leading to more stable atherosclerotic plaques provides evidence that generation of ACOD1 inhibitors could be a promising therapeutic [36]. However, given the contrasting outcomes in different studies, it may be necessary to determine the patient populations or specific plaque environments where ACOD1 inhibition would be most beneficial. Human plaques appear to vary in their expression of ACOD1. As seen in the results from Song et al., 2023, ACOD1 expression is depleted in larger, occluding plaques, whilst Hong et al., 2024 observe a heightened expression of ACOD1 in more vulnerable plaques [55, 57]. Therefore, not all patients may benefit from ACOD1 inhibitors and prior characterisation of plaques from procedures such as carotid endarterectomy could help identify patients who could respond to ACOD1 inhibition.

While our work highlights the potential benefits of ACOD1 inhibition, the therapeutic effectiveness of itaconate derivatives like 4-OI, as explored by others, also warrants consideration in the clinic, particularly for patients who may not be susceptible to ACOD1 inhibition [40, 55, 56, 64, 65]. Since these are potent anti-inflammatory mediators, techniques with targeted delivery to the plaque may be necessary to avoid compromising the patients' immune system. The development of nanoparticle-based drug delivery systems offers a possible solution. Nanoparticles, which can be made from an array of lipoproteins like high-density lipoproteins (HDL), LDL and VLDL, could be engineered to specifically deliver itaconate, 4-OI, adenine receptor modulators, or agents that regulate succinate or 2HG pathways directly to atherosclerotic plaque macrophages [57, 66, 67]. Since plaque macrophages are abundantly taking up LDL and VLDL, these make ideal carriers of non-specific treatments. Moreover, nanoparticles can be formulated with

ligands on their surface that bind to receptors expressed on inflammatory macrophages, like CD86 and CD40 [66, 67]. Such targeted delivery would not only enhance efficacy at the site of disease, but also minimise systemic exposure and potential side effects, an important consideration given the broad effects of these metabolites on cellular function.

Recently, a new polymer was designed that contains itaconate in its structural backbone, which releases itaconate over time in its local environment, supressing the growth of bacteria [68]. Similar to the anti-inflammatory properties of itaconate reported in **chapter 6** and other papers, this polymer also suppressed inflammation of macrophages, by reducing secretion of inflammatory mediators IL-1β, CCL2 and NO [68]. The protective effect of nanoparticle implants containing a fraction of DMI was also shown in mice and rats, which promoted expression of anti-oxidant genes to combat inflammation, whilst also protecting against damage from myocardial infarction [69]. Building stents from these new itaconate containing biomaterials could be an alternative approach to delivering localised itaconate to vulnerable plaques in patients. Since it is a degradable polyester, the effectiveness of the diffused itaconate on driving atherosclerosis regression would need to be considered to determine whether the patient is no longer at risk without the structural support of the stent.

Future work in this field should aim at bridging immunometabolism research from animal to human context, by focusing on designing and testing these nanotherapeutics and polymer stents in advanced, human-relevant pre-clinical models of atherosclerosis. With technologies such as vessel-on-a-chip emerging in the cardiovascular disease space and its potential to mimic human plaques, binding and endocytosis efficacy of nanoparticles, as well as release of itaconate from polymer-based stents, can be tested in a fully human environment that also models vascular flow [70]. *Ex vivo* culturing of human atherosclerotic plaques also provides a method of testing immunometabolism mediating nanoparticles and stents in the context of preserved human plaques and observing their effect on immune cell activity [71].

Concluding remarks

In this thesis we delved in to the dense network and vastly regulated world of macrophage immunometabolism, contributing to the field by both identifying novel regulatory metabolites and re-evaluating the functions of established ones within the specific context of atherosclerosis. Our identification of adenine and 2HG as anti-inflammatory immunometabolites in macrophages, in addition to the validation of a protective role for succinate and the plaque-stabilising effect of Acod1 deficiency, together highlights an essential theme in immunometabolism: context is key. The findings presented here provide a more nuanced understanding where the function of an immunometabolite is shaped by the cellular environment, the specific disease model, and the molecular form in

which it is presented. By uncovering the complexity and the extensive immunomodulating therapeutic options that exist within immunometabolism, we hope that the work discussed in this thesis will support the step towards developing novel immunometabolic treatments that not only halt the progression of atherosclerosis, but may also promote regression, ultimately reducing the global burden of cardiovascular disease.

References

1. Xu, R., He, X., Xu, J., Yu, G., Wu, Y., Immunometabolism: signaling pathways, homeostasis, and therapeutic targets. . MedComm, 2024. 5(11): p. e789.
2. Hu, T., et al., Metabolic regulation of the immune system in health and diseases: mechanisms and interventions. Signal Transduct Target Ther, 2024. 9(1): p. 268.
3. O'Neill, L.A., R.J. Kishton, and J. Rathmell, A guide to immunometabolism for immunologists. Nat Rev Immunol, 2016. 16(9): p. 553-65.
4. Ryan, D.G., et al., Coupling Krebs cycle metabolites to signalling in immunity and cancer. Nat Metab, 2019. 1: p. 16-33.
5. Ryan, D.G. and L.A.J. O'Neill, Krebs Cycle Reborn in Macrophage Immunometabolism. Annu Rev Immunol, 2020. 38: p. 289-313.
6. Viola, A., et al., The Metabolic Signature of Macrophage Responses. Front Immunol, 2019. 10: p. 1462.
7. Jha, A.K., et al., Network integration of parallel metabolic and transcriptional data reveals metabolic modules that regulate macrophage polarization. Immunity, 2015. 42(3): p. 419-30.
8. Van den Bossche, J., et al., Mitochondrial Dysfunction Prevents Repolarization of Inflammatory Macrophages. Cell Rep, 2016. 17(3): p. 684-696.
9. Palsson-McDermott, E.M. and L.A.J. O'Neill, Targeting immunometabolism as an anti-inflammatory strategy. Cell Res, 2020. 30(4): p. 300-314.
10. Dussold, C., et al., Modulation of macrophage metabolism as an emerging immunotherapy strategy for cancer. J Clin Invest, 2024. 134(2).
11. Su, R., et al., Immunometabolism in cancer: basic mechanisms and new targeting strategy. Cell Death Discov, 2024. 10(1): p. 236.
12. Dang, Q., et al., Cancer immunometabolism: advent, challenges, and perspective. Mol Cancer, 2024. 23(1): p. 72.
13. Certo, M., M. Rahimzadeh, and C. Mauro, Immunometabolism in atherosclerosis: a new understanding of an old disease. Trends Biochem Sci, 2024. 49(9): p. 791-803.
14. Tannahill, G.M., et al., Succinate is an inflammatory signal that induces IL-1beta through HIF-1alpha. Nature, 2013. 496(7444): p. 238-42.
15. Michelucci, A., et al., Immune-responsive gene 1 protein links metabolism to immunity by catalyzing itaconic acid production. Proc Natl Acad Sci U S A, 2013. 110(19): p. 7820-5.
16. Chandel, N.S., Glycolysis. Cold Spring Harb Perspect Biol, 2021. 13(5).
17. LeGrand, E.K., Beyond nutritional immunity: immune-stressing challenges basic paradigms of immunometabolism and immunology. Front Nutr, 2025. 12: p. 1508767.

18. Narunsky, A., et al., On the evolution of protein-adenine binding. Proc Natl Acad Sci U S A, 2020. 117(9): p. 4701-4709.
19. Roy, D., K. Najafian, and P. von Ragué Schleyer, Chemical evolution: the mechanism of the formation of adenine under prebiotic conditions. Proc Natl Acad Sci U S A, 2007. 104(44).
20. Oró, J., Synthesis of adenine from ammonium cyanide. Biochemical and Biophysical Research Communications, 1960. 2(6): p. 407-412.
21. Harber, K.J., et al., Adenine is an anti-inflammatory metabolite found to be more abundant in M-CSF over GM-CSF-differentiated human macrophages. Immunol Lett, 2024. 265: p. 23-30.
22. Park, J., et al., SIRT5-mediated lysine desuccinylation impacts diverse metabolic pathways. Mol Cell, 2013. 50(6): p. 919-30.
23. Qin, W., et al., Chemoproteomic Profiling of Itaconation by Bioorthogonal Probes in Inflammatory Macrophages. J Am Chem Soc, 2020. 142(25): p. 10894-10898.
24. Zeng, Y.R., et al., The immunometabolite itaconate stimulates OXGR1 to promote mucociliary clearance during the pulmonary innate immune response. J Clin Invest, 2023. 133(6).
25. Thimm, D., et al., Characterization of new G protein-coupled adenine receptors in mouse and hamster. Purinergic Signal, 2013. 9(3): p. 415-26.
26. Gorzalka, S., et al., Evidence for the functional expression and pharmacological characterization of adenine receptors in native cells and tissues. Mol Pharmacol, 2005. 67(3): p. 955-64.
27. Bender, E., et al., Characterization of an orphan G protein-coupled receptor localized in the dorsal root ganglia reveals adenine as a signaling molecule. Proc Natl Acad Sci U S A, 2002. 99(13).
28. von Kugelgen, I., et al., Cloning and functional expression of a novel Gi protein-coupled receptor for adenine from mouse brain. Mol Pharmacol, 2008. 73(2): p. 469-77.
29. Ferrari, D., et al., Purinergic Signaling in Controlling Macrophage and T Cell Functions During Atherosclerosis Development. Front Immunol, 2020. 11: p. 617804.
30. Hasko, G., et al., Shaping of monocyte and macrophage function by adenosine receptors. Pharmacol Ther, 2007. 113(2): p. 264-75.
31. Burnstock, G., Purine and purinergic receptors. Brain Neurosci Adv, 2018. 2: p. 2398212818817494.
32. Huang, Z., et al., From purines to purinergic signalling: molecular functions and human diseases. Signal Transduct Target Ther, 2021. 6(1): p. 162.
33. Tavares, L.P., et al., Blame the signaling: Role of cAMP for the resolution of inflammation. Pharmacol Res, 2020. 159: p. 105030.
34. Harber, K.J., et al., Succinate Is an Inflammation-Induced Immunoregulatory Metabolite in Macrophages. Metabolites, 2020. 10(9).
35. Swain, A., et al., Comparative evaluation of itaconate and its derivatives reveals divergent inflammasome and type I interferon regulation in macrophages. Nat Metab, 2020. 2(7): p. 594-602.
36. Harber, K.J., et al., Targeting the ACOD1-itaconate axis stabilizes atherosclerotic plaques. Redox Biol, 2024. 70: p. 103054.
37. Montes Diaz, G., et al., Dimethyl fumarate treatment in multiple sclerosis: Recent advances in clinical and immunological studies. Autoimmun Rev, 2018. 17(12): p. 1240-1250.

38. Brennan, M.S., et al., Dimethyl fumarate and monoethyl fumarate exhibit differential effects on KEAP1, NRF2 activation, and glutathione depletion in vitro. PLoS One, 2015. 10(3): p. e0120254.
39. Chen, H., et al., Hydroxycarboxylic acid receptor 2 mediates dimethyl fumarate's protective effect in EAE. J Clin Invest, 2014. 124(5): p. 2188-92.
40. Mills, E.L., et al., Itaconate is an anti-inflammatory metabolite that activates Nrf2 via alkylation of KEAP1. Nature, 2018. 556(7699): p. 113-117.
41. Ryan, T.A.J., et al., Dimethyl fumarate and 4-octyl itaconate are anticoagulants that suppress Tissue Factor in macrophages via inhibition of Type I Interferon. Nat Commun, 2023. 14(1): p. 3513.
42. Wang, L., et al., Diethyl Succinate Modulates Microglial Polarization and Activation by Reducing Mitochondrial Fission and Cellular ROS. Metabolites, 2021. 11(12).
43. Emini Veseli, B., et al., Animal models of atherosclerosis. Eur J Pharmacol, 2017. 816: p. 3-13.
44. Piedrahita, J.A., et al., Generation of mice carrying a mutant apolipoprotein E gene inactivated by gene targeting in embryonic stem cells. Proc Natl Acad Sci U S A, 1992. 89(10): p. 4471-4475.
45. Plump, A.S., Smith, J. D., Hayek, T., Aalto-Setälä, K., Walsh, A., Verstuyft, J. G., Rubin, E. M., & Breslow, J. L., Severe hypercholesterolemia and atherosclerosis in apolipoprotein E-deficient mice created by homologous recombination in ES cells. Cell, 1992. 71(2): p. 343–353.
46. Pendse, A.A., et al., Apolipoprotein E knock-out and knock-in mice: atherosclerosis, metabolic syndrome, and beyond. J Lipid Res, 2009. 50 Suppl(Suppl): p. S178-82.
47. Getz, G.S. and C.A. Reardon, Do the Apoe-/- and Ldlr-/- Mice Yield the Same Insight on Atherogenesis? Arterioscler Thromb Vasc Biol, 2016. 36(9): p. 1734-41.
48. Boren, J., et al., Low-density lipoproteins cause atherosclerotic cardiovascular disease: pathophysiological, genetic, and therapeutic insights: a consensus statement from the European Atherosclerosis Society Consensus Panel. Eur Heart J, 2020. 41(24): p. 2313-2330.
49. Liu, B., et al., Apoe-knockout induces strong vascular oxidative stress and significant changes in the gene expression profile related to the pathways implicated in redox, inflammation, and endothelial function. Cell Signal, 2023. 108: p. 110696.
50. Lo Sasso, G., et al., The Apoe(-/-) mouse model: a suitable model to study cardiovascular and respiratory diseases in the context of cigarette smoke exposure and harm reduction. J Transl Med, 2016. 14(1): p. 146.
51. M., v.d.M.A., et al., Transgenic mice carrying the apolipoprotein E3-Leiden gene exhibit hyperlipoproteinemia. J Biol Chem. , 1993. 268(14).
52. Keeter, W.C., et al., The AAV-PCSK9 murine model of atherosclerosis and metabolic dysfunction. Eur Heart J Open, 2022. 2(3): p. oeac028.
53. Roche-Molina, M., et al., Induction of sustained hypercholesterolemia by single adeno-associated virus-mediated gene transfer of mutant hPCSK9. Arterioscler Thromb Vasc Biol, 2015. 35(1): p. 50-9.
54. Bjorklund, M.M., et al., Induction of atherosclerosis in mice and hamsters without germline genetic engineering. Circ Res, 2014. 114(11): p. 1684-9.

55. Song, J., et al., Itaconate suppresses atherosclerosis by activating a Nrf2-dependent antiinflammatory response in macrophages in mice. J Clin Invest, 2023. 134(3).
56. Cyr, Y., et al., The IRG1-itaconate axis protects from cholesterol-induced inflammation and atherosclerosis. Proc Natl Acad Sci U S A, 2024. 121(15): p. e2400675121.
57. Hong, N.E., et al., Nanoparticle-based itaconate treatment recapitulates low-cholesterol/low-fat diet-induced atherosclerotic plaque resolution. Cell Rep, 2024. 43(11): p. 114911.
58. Ares, M.P. and M.M. Stollenwerk, Inflammatory effects of very low-density lipoprotein and fatty acids. Future Cardiol, 2006. 2(3): p. 315-323.
59. Smit, V., et al., Sexual dimorphism in atherosclerotic plaques of aged Ldlr(-/-) mice. Immun Ageing, 2024. 21(1): p. 27.
60. Fairweather, D., Sex differences in inflammation during atherosclerosis. Clin Med Insights Cardiol, 2014. 8(Suppl 3): p. 49-59.
61. Marsh, M.M., et al., Protection against atherosclerosis by estrogen is independent of plasma cholesterol levels in LDL receptor-deficient mice. Journal of Lipid Research, 1999. 40(5): p. 893-900.
62. Lercher, A., H. Baazim, and A. Bergthaler, Systemic Immunometabolism: Challenges and Opportunities. Immunity, 2020. 53(3): p. 496-509.
63. Ketelhuth, D.F.J., et al., Immunometabolism and atherosclerosis: perspectives and clinical significance: a position paper from the Working Group on Atherosclerosis and Vascular Biology of the European Society of Cardiology. Cardiovasc Res, 2019. 115(9): p. 1385-1392.
64. Diotallevi, M., et al., Itaconate as an inflammatory mediator and therapeutic target in cardiovascular medicine. Biochem Soc Trans, 2021. 49(5): p. 2189-2198.
65. Tang, C., et al., Activation of Keap1-Nrf2 signaling by 4-octyl itaconate protects human umbilical vein endothelial cells from high glucose. Biochem Biophys Res Commun, 2019. 508(3): p. 921-927.
66. Yaghmur, A., J. Ostergaard, and H. Mu, Lipid nanoparticles for targeted delivery of anticancer therapeutics: Recent advances in development of siRNA and lipoprotein-mimicking nanocarriers. Adv Drug Deliv Rev, 2023. 203: p. 115136.
67. Chen, W., et al., Macrophage-targeted nanomedicine for the diagnosis and treatment of atherosclerosis. Nature Reviews Cardiology, 2022. 19(4): p. 228-249.
68. Huyer, L.D., et al., Macrophage immunomodulation through new polymers that recapitulate functional effects of itaconate as a power house of innate immunity. Adv Funct Mater, 2021. 31(6).
69. Nakkala, J.R., et al., Dimethyl Itaconate-Loaded Nanofibers Rewrite Macrophage Polarization, Reduce Inflammation, and Enhance Repair of Myocardic Infarction. Small, 2021. 17(17): p. e2006992.
70. Maringanti, R., et al., Atherosclerosis on a Chip: A 3-Dimensional Microfluidic Model of Early Arterial Events in Human Plaques. Arterioscler Thromb Vasc Biol, 2024. 44(12): p. 2453-2472.
71. Lebedeva, A., et al., Ex vivo culture of human atherosclerotic plaques: A model to study immune cells in atherogenesis. Atherosclerosis, 2017. 267: p. 90-98.


A

Appendices

English Summary

Inflammatory diseases are amongst the most prevalent health complications, with neurodegenerative, cancer, cardiovascular and respiratory diseases making up part of the top-10 causes of death worldwide. The innate immune system constitutes the body's first line of defence against invading pathogens and aberrant cell activity. Central to this system are macrophages, highly plastic myeloid cells that reside in every tissue, or differentiate from circulating monocytes. They perform an array of essential functions, including phagocytosis of cell debris and pathogens, activating the adaptive immune system, and repairing damaged tissue. However, when these macrophages are unable to mount a sufficient inflammatory response, diseases such as cancer can progress. Vice versa, when macrophages become overly inflammatory, diseases such as atherosclerosis can develop. Whilst there are numerous drugs currently prescribed to patients suffering from such inflammatory diseases, they often lack the specificity of reversing the aberrant immune cells to a healthy state whilst keeping the rest of the immune system intact.

Immunometabolism, one of the key fields of research that we focus on in this thesis, has fundamentally shifted our understanding of how metabolism and the immune system are intertwined. Beyond metabolisms' role in producing the energy necessary to carry out of specific cell functions, metabolites can also act as signalling molecules that regulate immune cell function. During inflammation, macrophages rewire their core metabolic activity from oxidative phosphorylation (OXPHOS) to a highly glycolytic state, driving rapid ATP production. When doing so, the metabolic profile of these macrophages vastly changes, leading to accumulation of metabolites such as succinate and itaconate, which have been shown to mediate pro-inflammatory and anti-inflammatory responses in macrophages, respectively. These are just two examples of immunometabolites, and in **chapter 2** of this thesis, we define what constitutes as an immunometabolite. In addition to acting as direct signalling molecules, immunometabolites also function as cofactors, allosteric regulators, or substrates for epigenetic modifications such as histone methylation or acetylation. By carrying out these different functions, immunometabolites can drive macrophage inflammatory phenotype.

Atherosclerosis is a chronic inflammatory disease of the arterial wall. Macrophages are pivotal in the development of this disease, migrating over the endothelium and phagocytosing oxidised low-density lipoprotein (oxLDL), leading to the development of foam cells. These cells then become apoptotic and release cytokines, oxLDL and cell debris, due to a failure in orchestrating apoptosis correctly with a fully intact membrane, further exacerbating the recruitment and migration of inflammatory macrophages. The formation of a necrotic core, containing dead and dying macrophages, as well as fibrous cap thinning, are characteristic of vulnerable plaques which can rupture and lead

to thrombus formation and a myocardial infarction. Statins, which target cholesterol metabolism, have proven beneficial for patients with atherosclerosis, however they fail to address the residual inflammation that remains in these patients. Immunosuppressive drugs, such as canakinumab which is an anti-interleukin (IL)-1β antibody, have also been tested in patients with atherosclerosis to prevent further macrophage activation in the plaque, however due to its systemic suppression, undesirable adverse events occurred. This creates an unmet need for treatments that can specifically target inflammatory macrophages within the plaque to return to a homeostatic state, whilst retaining the activity of the rest of the immune system. Understanding the metabolic programs that govern macrophage function and survival within atherosclerosis are essential for developing these types of immunometabolic-based therapies.

In the first part of this thesis, we applied a discovery-based liquid chromatography-mass spectrometry (LC-MS) metabolomics approach to identify new immunometabolic regulators of human macrophage activation. In **chapter 3**, we compared the metabolic profiles of granulocyte-macrophage colony-stimulating factor (GM-CSF) differentiated macrophages, which more frequently contribute towards inflammatory disease progression, with macrophage colony-stimulating factor (M-CSF) differentiated macrophages, which tend to be more homeostatic. This screen revealed that the purine nucleotide base adenine was significantly more abundant in M-CSF differentiated human macrophages. We investigated the functional relevance of adenine in inflammatory human macrophages, highlighting its suppressive effect on cytokines IL-10, TNF and IL-12p40 and expression of cell surface markers CD40 and CD38. Adenine treatment also induced a state of metabolic quiescence, simultaneously suppressing both glycolysis and OXPHOS, resulting in significantly reduced ATP production. This chapter describes adenine as a novel endogenous signal upregulated during macrophage inflammation with anti-inflammatory function, establishing a new role for purine metabolism in the control of macrophage inflammation.

In another metabolomics study, we identified 2-hydroxyglutarate (2HG) as one of the most accumulating metabolites in lipopolysaccharide (LPS)-stimulated mouse and human macrophages, with D-2-hydroxyglutarate (D-2HG) representing the most abundant enantiomer. Known primarily for its role as an oncometabolite in IDH1 and IDH2 mutated cancers, its function in macrophages was not explored. Therefore, in **chapter 4**, we aimed to characterise its role in the context of inflammation. Metabolomics revealed that D-2HG accumulation, as well as the other 2HG enantiomer L-2-hydroxyglutarate (L-2HG), occurs later in the inflammatory response, reaching levels higher than basal measurements mainly 24 hours after the initial stimulus. The suppression of inflammatory genes *Il6*, *Tnf*, *Nos2* and *Il1b* before the accumulation of 2HG started indicated a possible anti-inflammatory role for 2HG. Functional experiments indeed showed that treatment

with D-2HG significantly dampened the secretion of inflammatory cytokines IL-6 and TNF in both mouse and human macrophages. D-2HG also suppressed the expression of cell surface marker CD40 and intracellular inducible nitric oxide synthase in mouse macrophages and surface markers CD197 and CD274 in human macrophages. This effect was similarly seen *in vivo* where mice undergoing peritoneal macrophage migration were injected with D-2HG and LPS, but with the additional effect of increased secretion of IL-10 in plasma and the peritoneal cavity. **Chapter 4** thus establishes D-2HG as an endogenous immunometabolite that functions as a delayed brake on the immune response.

After identifying novel macrophage immunometabolites, we focused on clarifying the immunomodulatory role of the already established immunometabolite succinate. Succinate, when first identified as a metabolite that accumulated in pro-inflammatory macrophages, was described as driving pro-inflammatory responses, increasing the secretion of IL-1β. However, succinate was later shown to induce anti-inflammatory responses in macrophages through binding of the succinate receptor SUCNR1. In **chapter 5**, we aimed to identify how succinate truly affects inflammatory macrophage function. By systematically comparing the impact that cell-permeable diethyl succinate, non-permeable extracellular succinate, and the receptor SUCNR1 have on macrophage function, we examined the context-dependent nature of succinate signalling. We found that diethyl succinate actively suppressed the secretion of pro-inflammatory cytokines IL-6 and TNF. Furthermore, macrophages deficient in the cell surface receptor SUCNR1 exhibited a hyper-inflammatory response to LPS, suggesting that extracellular succinate signalling, contrary to some reports, contributes to an anti-inflammatory feedback loop. These findings add a layer of nuance to the field, demonstrating that the ultimate function of diethyl succinate and SUCNR1 in an isolated, homogenous setting is anti-inflammatory. However, it is likely that within an organism, the presence of other secretory factors and signalling pathways could alter how the succinate-SUCNR1 axis behaves. This work serves as a cautionary reminder that the role of immunometabolism should not be oversimplified.

The final experimental chapter of this thesis aimed to highlight the impact of immunometabolic pathways on the development of atherosclerosis in an *in vivo* setting. We investigated the ACOD1-itaconate axis, a highly macrophage-specific immunometabolic pathway upregulated during inflammation. A comparative study of itaconate derivatives highlighted the diverse effects these molecules have on macrophage inflammatory signalling and concluded that these effects are due to the derivatives' structural modifications. To avoid misinterpreting the effect of itaconate on atherosclerosis with the use of these derivatives, in **chapter 6** we performed a transplantation of *Acod1*$^{-/-}$ bone marrow into *Ldlr*$^{-/-}$ atherogenic mice, depleting the inflammation-induced synthesis of endogenous itaconate in macrophages. These *Ldlr*$^{-/-}$ mice were then fed a high-fat western diet to induce atherosclerosis. Given itaconate's well-documented anti-

inflammatory and antioxidant properties in vitro, we hypothesized that its absence would exacerbate atherosclerosis.

In a contradictory finding to our hypothesis, *Acod1*$^{-/-}$ bone marrow significantly improved plaque stability by reducing the necrotic core area, a key feature of plaque vulnerability. Interestingly, this was not due to smaller plaques or a reduction in macrophage content. Mice transplanted with *Acod1*$^{-/-}$ bone marrow instead had an increase in circulating monocytes, more recruitment of macrophages to the plaque, and increased lipid content and cell size of plaque foam cells, compared with mice transplanted with *Acod1*$^{+/+}$ bone marrow. We revealed that *Acod1*$^{-/-}$ foam cells and inflammatory macrophages were in fact more viable, undergoing apoptosis less frequently and potentially explaining how necrosis was reduced despite the increased macrophage recruitment. By using transcriptomics data and stable isotope tracer-based metabolomics we identified that the absence of itaconate improved the flexibility of *Acod1*$^{-/-}$ macrophage lipid handling. This work uncovers the potential of ACOD1 inhibition as a novel therapeutic strategy to promote plaque stability.

The findings in this thesis presents the complex and highly contextual nature of macrophage immunometabolism, whilst highlighting the therapeutic potential of numerous immunometabolites in the treatment of aberrant macrophages within inflammatory diseases.

Nederlandse Samenvatting

Inflammatoire ziekten behoren tot de meest prevalente gezondheidscomplicaties wereldwijd; neurodegeneratieve, cardiovasculaire en respiratoire aandoeningen, evenals kanker, maken deel uit van de top-10 doodsoorzaken. Het aangeboren immuunsysteem vormt de eerste verdedigingslinie van het lichaam tegen binnendringende pathogenen en afwijkende celactiviteit. Centraal in dit systeem staan macrofagen: zeer plastische myeloïde cellen die in elk weefsel terug te vinden zijn of differentiëren uit circulerende monocyten. Zij vervullen een reeks essentiële functies, waaronder de fagocytose van celresten en pathogenen, het activeren van het adaptieve immuunsysteem en het herstellen van beschadigd weefsel. Wanneer deze macrofagen echter geen adequate ontstekingsreactie kunnen genereren, kunnen ziekten zoals kanker zich ontwikkelen. Omgekeerd, wanneer macrofagen overmatig inflammatoir worden, kunnen ziekten zoals atherosclerose ontstaan. Hoewel er talrijke medicijnen worden voorgeschreven aan patiënten met dergelijke inflammatoire ziekten, missen deze vaak de specificiteit om enkel de afwijkende immuuncellen naar een gezonde staat terug te brengen, terwijl de rest van het immuunsysteem intact blijft.

Immunometabolisme, een van de voornaamste onderzoeksgebieden in dit proefschrift, heeft ons begrip van de verwevenheid tussen het metabolisme en het immuunsysteem fundamenteel veranderd. Naast de rol van het metabolisme in de productie van energie die nodig is voor specifieke celfuncties, kunnen metabolieten ook fungeren als signaalmoleculen die de functie van immuuncellen reguleren. Tijdens een ontsteking herprogrammeren macrofagen hun centrale metabole activiteit van oxidatieve fosforylering (OXPHOS) naar een sterk glycolytische staat, wat leidt tot snelle ATP-productie. Hierdoor verandert het metabole profiel van deze macrofagen drastisch, resulterend in de accumulatie van metabolieten zoals succinaat en itaconaat, waarvan is aangetoond dat ze respectievelijk pro- en anti-inflammatoire reacties in macrofagen mediëren. Dit zijn slechts twee voorbeelden van immunometabolieten; in **hoofdstuk 2** van dit proefschrift definiëren we wat een immunometaboliet kenmerkt. Naast hun functie als directe signaalmoleculen, fungeren immunometabolieten ook als cofactoren, allosterische regulatoren of substraten voor epigenetische modificaties, zoals histon-methylering of -acetylering. Door deze verschillende functies uit te voeren, kunnen immunometabolieten het inflammatoire fenotype van macrofagen sturen.

Atherosclerose is een chronische inflammatoire ziekte van de arteriële wand. Macrofagen spelen een cruciale rol in de ontwikkeling van deze ziekte. Ze migreren over het endotheel en fagocyteren geoxideerd lage-densiteit lipoproteïne (oxLDL), wat leidt tot de vorming van schuimcellen. Deze cellen worden vervolgens apoptotisch en scheiden cytokinen, oxLDL en celresten uit, wat de rekrutering en migratie van inflammatoire macrofagen

verder verergert. De vorming van een necrotische kern met dode en stervende macrofagen, evenals het dunner worden van de fibreuze kap, zijn kenmerken van kwetsbare plaques die kunnen barsten en tot trombusvorming en een myocardinfarct kunnen leiden. Statines, gericht op het cholesterolmetabolisme, zijn gunstig gebleken voor patiënten met atherosclerose, maar ze slagen er niet in de residuele ontsteking aan te pakken die bij deze patiënten achterblijft. Immuunsuppressieve geneesmiddelen, zoals canakinumab, een anti-interleukine (IL)-1β antilichaam, zijn ook getest bij patiënten met atherosclerose om verdere macrofaagactivatie in de plaque te voorkomen. Vanwege de systemische onderdrukking traden er echter ongewenste bijwerkingen op. Dit creëert een onvervulde behoefte aan behandelingen die specifiek inflammatoire macrofagen in de plaque kunnen beïnvloeden om terug te keren naar een homeostatische toestand, met behoud van de activiteit van de rest van het immuunsysteem. Inzicht in de metabole programma's die de functie en overleving van macrofagen binnen atherosclerose reguleren, is essentieel voor de ontwikkeling van dit soort op immunometabolisme gebaseerde therapieën.

In het eerste deel van dit proefschrift pasten we een op ontdekking gerichte metabolomics benadering toe om nieuwe immunometabole regulatoren van humane macrofaagactivatie te identificeren. In **hoofdstuk 3** vergeleken we de metabole profielen van met granulocyt-macrofaag koloniestimulerende factor (GM-CSF) gedifferentieerde macrofagen, die vaker bijdragen aan de progressie van inflammatoire ziekten, met macrofaag koloniestimulerende factor (M-CSF) gedifferentieerde macrofagen, die doorgaans meer homeostatisch zijn. Deze screening onthulde dat de purinenucleotidebase adenine significant overvloediger was in M-CSF-gedifferentieerde humane macrofagen. We onderzochten de functionele relevantie van adenine in inflammatoire humane macrofagen en benadrukten het onderdrukkende effect op de cytokinen IL-10, TNF en IL-12p40 en de expressie van de celoppervlaktemarkers CD40 en CD38. Adeninebehandeling induceerde ook een staat van metabole onderdrukking, waarbij zowel glycolyse als OXPHOS gelijktijdig werden verlaagd, resulterend in een significant lagere ATP-productie. Dit hoofdstuk beschrijft adenine als een nieuw endogeen signaal dat wordt opgereguleerd tijdens macrofaagontsteking met een anti-inflammatoire functie, en vestigt daarmee een nieuwe rol voor het purinemetabolisme in de controle van macrofaagontsteking.

In een andere metabolomics-studie identificeerden we 2-hydroxyglutaraat (2HG) als een van de meest geïnduceerde metabolieten in met lipopolysacharide (LPS)-gestimuleerde muizen- en humane macrofagen, waarbij D-2-hydroxyglutaraat (D-2HG) het meest voorkomende enantiomeer was. Hoofdzakelijk bekend om zijn rol als oncometaboliet in kankers met een IDH1- en IDH2-mutatie, was de functie ervan in macrofagen nog niet onderzocht. Daarom was het doel van **hoofdstuk 4** om de rol ervan in de context van ontsteking te karakteriseren. Metabolomics onthulde dat de accumulatie van 2HG

laat in de ontstekingsrespons optreedt en pas 24 uur na de initiële stimulus niveaus bereikt die hoger zijn dan de basale metingen. Deze kinetiek van 2HG inductie na de inductie van de inflammatoire genen *Il6*, *Tnf*, *Nos2* en *Il1b* suggereerde een mogelijke anti-inflammatoire rol voor 2-HG. Functionele experimenten toonden inderdaad aan dat behandeling met D-2HG de secretie van de inflammatoire cytokinen IL-6 en TNF in zowel muizen- als humane macrofagen significant remde. D-2HG onderdrukte ook de expressie van de celoppervlaktemarker CD40 en induceerbaar stikstofoxidesynthase in muizenmacrofagen, en de oppervlaktemarkers CD197 en CD274 in humane macrofagen. Dit effect werd ook *in vivo* waargenomen, waar muizen werden geïnjecteerd met D-2HG en LPS, met als bijkomend effect een verhoogde secretie van IL-10 in plasma en de peritoneale holte. **Hoofdstuk 4** vestigt D-2HG dus als een endogene immunometaboliet die functioneert als een vertraagde rem op de immuunrespons.

Na het identificeren van nieuwe immunometabolieten in macrofagen, richtten we ons op het verhelderen van de immunomodulerende rol van de reeds bekende immunometaboliet succinaat. Toen succinaat voor het eerst werd geïdentificeerd als een metaboliet dat accumuleert in pro-inflammatoire macrofagen, werd het beschreven als een aanjager van pro-inflammatoire reacties, via een verhoogde secretie van IL-1β. Later werd echter aangetoond dat succinaat anti-inflammatoire reacties in macrofagen induceert door binding aan de succinaatreceptor SUCNR1. In **hoofdstuk 5** was ons doel om te bepalen hoe succinaat de functie van inflammatoire macrofagen daadwerkelijk beïnvloedt. Door systematisch de impact van cel-permeabel diëthylsuccinaat, niet-permeabel extracellulair succinaat en de receptor SUCNR1 op de macrofaagfunctie te vergelijken, onderzochten we de contextafhankelijke aard van succinaatsignalering. We vonden dat diëthylsuccinaat de secretie van de pro-inflammatoire cytokinen IL-6 en TNF actief onderdrukte. Bovendien vertoonden macrofagen zonder de celoppervlaktereceptor SUCNR1 een hyper-inflammatoire respons op LPS, wat suggereert dat extracellulaire succinaatsignalering, in tegenstelling tot sommige rapporten, bijdraagt aan een anti-inflammatoire feedback-loop. Deze bevindingen voegen een laag van nuance toe aan het veld en tonen aan dat de uiteindelijke functie van diëthylsuccinaat en SUCNR1 in een geïsoleerde, homogene setting anti-inflammatoir is. Dit werk dient als een waarschuwing dat de rol van immunometabolisme niet te simplistisch moet worden voorgesteld.

Het laatste experimentele hoofdstuk van dit proefschrift had tot doel de impact van immunometabole routes op de ontwikkeling van atherosclerose in een *in vivo*-setting te belichten. We onderzochten de ACOD1-itaconaat-as, een sterk macrofaag-specifieke immunometabole route die wordt opgereguleerd tijdens ontsteking. Een vergelijkende studie van itaconaatderivaten benadrukte de diverse effecten die deze moleculen hebben op de inflammatoire signalering van macrofagen en concludeerde dat deze effecten te wijten zijn aan de structurele modificaties van de derivaten. Om een misinterpretatie

van het effect van itaconaat op atherosclerose door het gebruik van deze derivaten te vermijden, voerden we in **hoofdstuk 6** een transplantatie uit van *Acod1*$^{-/-}$ beenmerg in *Ldlr*$^{-/-}$ atherogene muizen, waardoor de door ontsteking geïnduceerde synthese van endogeen itaconaat in macrofagen werd geëlimineerd. Deze *Ldlr*$^{-/-}$ muizen kregen vervolgens een westers dieet met een hoog vetgehalte om atherosclerose te induceren. Gezien de goed gedocumenteerde anti-inflammatoire en anti-oxidatieve eigenschappen van itaconaat in vitro, veronderstelden we dat de afwezigheid ervan de atherosclerose zou verergeren.

In tegenstelling tot onze hypothese, verbeterde *Acod1*$^{-/-}$ beenmerg de plaquestabiliteit significant door de necrotische kern te verkleinen, een belangrijk kenmerk van plaque-kwetsbaarheid. Interessant is dat dit niet te wijten was aan kleinere plaques of een vermindering van het macrofaaggehalte. Muizen getransplanteerd met *Acod1*$^{-/-}$ beenmerg hadden juist een toename van circulerende monocyten, meer rekrutering van macrofagen naar de plaque en een verhoogd lipidegehalte en celgrootte van schuimcellen in de plaque. We onthulden dat *Acod1*$^{-/-}$ schuimcellen en inflammatoire macrofagen levensvatbaarder waren, minder vaak apoptose ondergingen, wat mogelijk verklaart hoe de necrose werd verminderd ondanks de verhoogde macrofaagrekrutering. Met behulp van transcriptomics-data en op stabiele isotopen gebaseerde tracer-metabolomics, identificeerden we dat de afwezigheid van itaconaat de flexibiliteit van de lipidehuishouding van *Acod1*$^{-/-}$ macrofagen verbeterde. Dit werk onthult het potentieel van ACOD1-remming als een nieuwe therapeutische strategie om plaquestabiliteit te bevorderen.

De bevindingen in dit proefschrift presenteren de complexe en zeer contextafhankelijke aard van het immunometabolisme van macrofagen, en belichten tegelijkertijd het therapeutisch potentieel van talrijke immunometabolieten bij de behandeling van afwijkende macrofagen binnen inflammatoire ziekten.

List of Publications

1. **Harber KJ,** Verberk S, Van den Bossche J. Going -omics to identify novel therapeutic targets for cardiovascular disease. *eBioMedicine*, 2019; 41, 7-8

2. de Goede KE, **Harber KJ**, Van den Bossche J. Let's Enter the Wonderful World of Immunometabolites. *Trends Endocrinol Metab.* 2019;30(6):329-331.

3. **Harber KJ**, de Goede KE, Verberk SGS, Meinster E, de Vries HE, van Weeghel M, de Winther MPJ, Van den Bossche J. Succinate Is an Inflammation-Induced Immunoregulatory Metabolite in Macrophages. *Metabolites*. 2020;10(9):372.

4. Verberk SGS, van der Zande HJP, Baardman J, de Goede KE, **Harber KJ**, Keuning ED, Lambooij JM, Otto F, Zawistowska-Deniziak A, de Vries HE, de Winther MPJ, Guigas B, Van den Bossche J.Myeloid ATP Citrate Lyase Regulates Macrophage Inflammatory Responses In Vitro Without Altering Inflammatory Disease Outcomes. *Front Immunol*. 2021;12:669920.

5. de Goede KE, Verberk SGS, Baardman J, **Harber KJ**, van Kooyk Y, de Winther MPJ, Schetters STT, Van den Bossche J. Myeloid-Specific Acly Deletion Alters Macrophage Phenotype In Vitro and In Vivo without Affecting Tumor Growth. *Cancers* (Basel). 2021;13(12):3054.

6. van der Lee DI, Koutsoumpli G, Reijmers RM, Honders MW, de Jong RCM, Remst DFG, Wachsmann TLA, Hagedoorn RS, Franken KLMC, Kester MGD, **Harber KJ**, Roelofsen LM, Schouten AM, Mulder A, Drijfhout JW, Veelken H, van Veelen PA, Heemskerk MHM, Falkenburg JHF, Griffioen M. An HLA-A*11:01-Binding Neoantigen from Mutated NPM1 as Target for TCR Gene Therapy in AML. *Cancers* (Basel). 2021;13(21):5390.

7. de Goede KE, **Harber KJ**, Gorki FS, Verberk SGS, Groh LA, Keuning ED, Struys EA, van Weeghel M, Haschemi A, de Winther MPJ, van Dierendonck XAMH, Van den Bossche J. d-2-Hydroxyglutarate is an anti-inflammatory immunometabolite that accumulates in macrophages after TLR4 activation. *Biochim Biophys Acta Mol Basis Dis*. 2022;1868(9):166427.

8. Maassen S, Coenen B, Ioannidis M, **Harber KJ**, Grijpstra P, Van den Bossche J, van den Bogaart G. Itaconate promotes a wound resolving phenotype in pro-inflammatory macrophages. *Redox Biol*. 2023;59:102591.

9. Juni RP, Phelp PG, Bink DI, Kremer V, van Bergen AS, Espinosa Gonzalez P, Rombouts KB, **Harber KJ**, Heister DAF, Yeung KK, Van den Bossche J, Kuster DWD; Amsterdam UMC COVID-19 Biobank Study Group; Krijnen PAJ, Niessen HWM, Boon RA. COVID19 Impairs

Cardiac Function via Endothelial H19 and IL6 Signaling. *Circ Res.* 2023;132(5):648-651.

10. **Harber KJ**, Nguyen TA, Schomakers BV, Heister DAF, de Vries HE, van Weeghel M, Van den Bossche J, de Winther MPJ. Adenine is an anti-inflammatory metabolite found to be more abundant in M-CSF over GM-CSF-differentiated human macrophages. *Immunol Lett*. 2024;265:23-30.

11. **Harber KJ**, Neele AE, van Roomen CP, Gijbels MJ, Beckers L, Toom MD, Schomakers BV, Heister DA, Willemsen L, Griffith GR, de Goede KE, van Dierendonck XA, Reiche ME, Poli A, L-H Mogensen F, Michelucci A, Verberk SG, de Vries H, van Weeghel M, Van den Bossche J, de Winther MP. Targeting the ACOD1-itaconate axis stabilizes atherosclerotic plaques. *Redox Biol*. 2024;70:103054.

Portfolio of Education

Conferences and symposia

Event	Date	ECTS
ACS PhD Retreat	March 2019	1,00
Annual AII Retreat 2019	June 2019	0,30
Immunometnet 2019	June 2019	0,29
Immunometnet 2020	November 2020	0,29
Rembrandt Symposium 2020	November 2020	1,00
ACS Annual Symposium 2021	October 2021	1,00
AII PhD Retreat 2021	November 2021	1,50
Rembrandt Symposium 2021	November 2021	1,00
Immunometnet 2022	May 2022	1,00
NVVI Annual Meeting 2022	May 2022	1,50
ACS PhD Retreat 2022	May 2022	1,50
DAS 2022	June 2022	1,00
AII Annual Symposium 2022	June 2022	1,00
European Myeloid and Dendritic Cell Annual Symposium 2022	September 2022	1,00
AII PhD Retreat 2022	November 2022	0,61

Courses and meetings

Course or meeting	Date	ECTS
TRIM, EVB, MB2 & group meetings	Throughout PhD	6,00
Advanced Immunology Course	February 2019	3,00
R2-Introduction	April 2019	0,30
Organising ACS PhD Retreat 2020	June 2019-March 2020	1,50
Using R for data anlysis	June 2019	1,50
Hartstichting Papendal Course	October 2019	2,50
Basic Microscopy	November 2019	1,50
ONLINE Research Integrity Course 2023	April 2023	2,00

Teaching and education

Activity	Date	ECTS
Medical Biochemistry Lab and Workgroups	Throughout PhD	1,14
BETA Inform - Bachelor/Master Thesis Supervision	November 2020-June 2021	3,00
Immunometabolism workgroups	November 2022	0,21

Prizes

Award	Date	Event
Best poster prize	October 2019	Hartstichting Papendal Course
Third place TedMed talk	October 2019	Hartstichting Papendal Course
Best poster prize	October 2021	ACS Annual Symposium 2021
Best oral presentation	May 2022	ACS PhD Retreat 2022
Best oral presentation	June 2022	DAS 2022
Best Abstract/runner-up oral presentation	November 2022	AII PhD Retreat 2022

Acknowledgements

Wow, what a journey this PhD has been! It feels surreal that I am now writing the last couple of pages of this book that has culminated from 4 years of experiments, reading, presentations, courses and of course publishing articles, and this is an accomplishment that I honestly cannot believe I've reached. Without all the people I have met on the way, both before and during the PhD, with all your support and all the fun we've had together, I might not have made it this far.

First of all, **Jan**, I want to thank you for giving me the opportunity to join your group and do a PhD with you in the Molecular Cell Biology and Immunology department! People have always told me that I have plenty of enthusiasm and optimism in life, and perhaps that is one of the main reasons that we clicked during the interview and during my time in your research group. You were always coming up with fresh new ideas with great confidence and that definitely rubbed off on me and kept me going through each year of the PhD. The results I got at the end of an experiment were always what I looked forward to the most, and because of your enthusiasm it was a pleasure to come and share them with you, even when they weren't going in the direction I had hoped for! Maybe I came into your office a few times too many completely unannounced just to show you the latest results, whoops! But outside of the MCBI I have also had some great times with you, from inviting the group to your house for BBQs, to enjoying some laughs together during lab days out. I also may not have discovered the wonderful world of Lambic and Geuze beer without you and damn I am so grateful for that! The rhubarb Nath from Cantillon we had at your house after a day of working together is still my favourite beer I've ever had! Thank you for all the help and guidance you have given me over the years.

I also know that my PhD would not have been the same without the support of **Menno**. I remember that moving to your group in the Medical Biochemistry department at the end of my first year I was slightly nervous and intimidated to now start regularly reporting my results to you, however I could not have got you more wrong. Not only did you give me great direction with my projects, but most importantly you really got me to think much more independently and asked me the right questions during our meetings to help me realise I could steer these projects myself. In your office, not long after me joining the department, you said something along the lines of "Okay you've shown me the results now, but if you had to pick one of these metabolites to study further, what are you going to pick, and why?". Well, that ended up being Adenine and so a new project was born. It was certainly difficult moving away from all the friends and connections I had made at the Molecular Cell Biology and Immunology department, but you made me feel very welcome there! You threw me straight in to the group before meeting all of them by asking me to present my TedMed talk from the Hartstichting course, comparing atherosclerosis to the

houses of parlement during Brexit. I don't know if everyone got it, but they certainly got a good sense of who I was, I guess. Thank you for being a great supervisor and helping me get to the end.

From macrophages and atherosclerosis with Menno, to metabolomics with **Michel**. During my first year, relatively inexperienced with omics, you already got me my own workspace in the Genetic Metabolic Diseases department to work on the mass spec data myself which I was very excited to do. Thank you for throwing me straight in to it and getting me immediately interested in the omics world! You always said yes to the samples I wanted to bring for metabolomics and lipidomics, and the data that I got from those experiments were some of the most exciting datasets I got to work with. Thankfully I had your endless knowledge in chemistry, omics and mass spectrometry to guide me through it.

Elga, I'm very grateful for your support during our meetings where we would meet with all the promoters to look at my PhD progress holistically and helped me with focusing on what else was needed to get the PhD complete. This really helped me get all my publications! But I also cannot forget that you were always a happy, smiling, friendly face to have pop into the open office area in the MCBI where I was sitting, every now and then checking in on me to see how it's all going.

Group Jan, we had such a nice research team, and it was great having you all there during my PhD! **Sanne** and **Kyra**, you were there from the start and you both made me feel settled in immediately. Sanne I can only ever remember you laughing and smiling your way through the PhD and it was crazy to see how easy you made the whole journey look, you definitely made me realise that the PhD doesn't need to be stressful. Kyra, we practically spent our entire PhD together and I really appreciated the support we gave each other through some of the struggles we faced in the lab. Having some nights out with some of the other people from work was a great way to destress. **Xanthe**, you only joined us for a year, but you were such a nice addition to the group, and I was sad to see you leave, your experience as a new post doc really added to our team meetings. **Nico**, you joined towards the end of my PhD, but it didn't stop us from forming a formidable submarine crew! **Laszlo**, thanks for bringing your knowledge from the Radboud to our team meetings during the end of my projects, it was great to have some fresh ideas, and **Daan** you really helped me get so much data when I needed it the most, I'm very grateful for your dedication to understand my not so straightforward plate layouts. **Rike**, you already were in our group as a guest PhD for maybe around a year before we realised our joint love for music. Once we found that out, something just clicked and we got on so well, and I've enjoyed the times we've spent together over the last years so much! Our writing retreat to France was such a fun trip, getting our coffee and chocolates every day, going to the fromagerie and boulangerie where I tried to practice my French, and heading up

the mountain together at the end of the retreat. I've really appreciated all the time we've spent sharing our ups and downs with each other, and our friendship is one of the things I'm most grateful for to come out of my time as a PhD. I'm certain we are going to go see Eris Drew and Octo Octa together many more times, I can't wait. To group Jan, a massive thank you to you all for everything you did both inside and outside of my PhD journey.

There were of course some amazing people on both the 12th, 11th and 10th floor of the MCBI who I cannot forget about. **Kelly**, I remember you were one of the first PhDs I met during the MCBI Christmas party before I had even started my PhD and your personality alone made me realise I had joined the right department and it was bound to be a fun 4 years ahead of me. **Aram** and **Dennis**, we started our PhDs roughly around the same time which unfortunately meant we had to endure the Corona period during our 2nd year and part of our 3rd. It was a real blow to our research, but at least we had memorable borrels after work, the PhD weekend, and Lab Day out together in our first year. Once corona was over, it didn't take us long to get the whole 10th and 12th floor together regularly in the offices for some much-needed social healing. **Parand, Sabela, Carla, Merel** and **Inge** I loved the time we spent together having some drinks after work at in the open office, at the Mahler, going swimming in the Amstel, going to the Efteling or heading out to the Exit. **Henrique, Julia, Fabio, Lelly,** and **Victor,** we've had countless amazing nights out together and they really helped me get through both the hard days at the lab, but also the endless writing of my thesis. Our joint love for music brought us close and I've cherished the time we've spent with each other, either having dinner at each other's houses, celebrating my birthday with you, camping at Draaimolen, or even going all the way to Croatia. **Davide, Caddy, Loet, Sem,** and **Jelle,** thank you also for all the wonderful times and welcome distractions in the open office on the 12th floor. Also thank you to **Celine, Irene, Shalmalee, Britt, Katarina,** and **Eveline** for making my regular journeys down to the 11th and 10th floors a lot of fun! A big thank you to everyone from the MCBI for making my time there unforgettable, it truly was difficult when it came to an end. Without you all, the legendary cocktail nights wouldn't have been such a success!

Once I moved to the Medical Biochemistry department I also met some wonderful people, despite it being broken up by Corona. **Guillermo** thank you for all the conversations we had in the lab during my experiments, talking about trying to learn how to produce music, and discussing different artists and music genres. You always had a smile on your face and brought a calming atmosphere to the lab which really helped me settle into the new department. **Oliver**, thank you for sharing all your crazy stories about your dedication to your research, and answering the endless number of questions I asked you in our office; I apologise for distracting you a bit with them! **Cindy** and **Marion**, without your expertise in the animal lab and in histology I wouldn't have completed my Itaconate/ACOD1 paper which is the work I am the proudest of! I really appreciated that both of you always asked

me about how I was progressing through my PhD; your kindness towards me never went unnoticed. **Rosalie**, your enthusiasm was infectious and you were always a joy to have a chat with, you certainly brought some light-heartedness to the group! **Annette, Maarten, Lisa** and **Koen,** thank you for your knowledge and support during presentations in the department or at congresses, you definitely imparted some wisdom throughout the years and helped me to consider alternative experiments that I had not done yet. **Anh**, you were a fantastic student to supervise, and it gave me a lot of joy to see that you decided to carry on your academic career and do a PhD of your own, you certainly showed you were capable of it! I hope that you look back on your internship fondly. Thank you to the whole Medical Biochemistry department for all the help, support and opportunities you gave me during my PhD.

Whilst I have had an amazing journey through the PhD, I can't help but miss everyone who I had to leave behind to come to The Netherlands. **Jon**, we became friends so quickly during French class in high school that somehow, we ended up going on a 3-week holiday to America together in that same year, crazy when I think about it. You've always been my closest friend and not being able to share these last 10 years with you fully is such a shame because we are always in hysterics when we are with each other. I have to thank you so much for the countless times you came to visit me in The Netherlands, 7 times in 1 year even which is insane, and our trip to Croatia was unforgettable. I hope you keep making trips over to The Netherlands; no matter how long it is in between each visit, I always know we fall right back into our teenage selves as soon as you arrive. I miss you loads man. **Nicola**, thank you for all the funny memories growing up in school, and letting me stay with you guys when I come over to visit. I am wishing you and Jon all the best in your hunt for a house together! I hope you'll make it over to Amsterdam with Jon one year. **Kate**, thank you for all the many attempts to keep contacting me despite my terrible skills in keeping in contact with people. I will make sure to always find time to visit you when you are over from Australia and just know you are always welcome to stay with us as well! I wish we could see each other more often. **Morgan, Suzanne, Dan, Claire, Katie, James, Crabb, Hwee, Mark, Tom** and **Ewan,** meeting up with you all when I am back home in the UK is always like stepping back in to school and it sucks that I cannot spend as much time with you all as I would like. Thank you for always inviting me everywhere still and not forgetting about me after these 10 years that I´ve not been living in the UK. **Campbell** we were neighbours growing up and spent so much time together, from playing and painting Warhammer, to going to theme parks, playing PlayStation games and building a treehouse in your back garden. I´m very grateful for our friendship and that we have been meeting up more and more lately, you always had a lot of supportive things to say when I would tell you about my PhD.

The PhD journey was certainly a difficult one, with a lot of perseverance, stress and failure,

but perhaps leaving behind my **Mum** and my sister **Kirsten** was one of the hardest things I have had to do and is something that I still struggle with today. **Mum** and **Kirsten**, it took me a very long time to get used to only seeing you a few weeks a year, and once I felt like I had got to grips with it, **Kirsten** you decided to start a family with your wonderful husband **George**. Not being there to support you through the challenges you faced, as well as being an uncle to my adorable niece **Sienna**, and now my new nephew **Ruben**, would have me in tears when I would be travelling back to The Netherlands. Sometimes I have had to ask myself, "why have I left all these people I love behind". I´ve never really had a clear answer for that one. **Kirsten**, we have always been very close as brother and sister! you´ve certainly been there for me when I had some difficult times over the last years and I have not forgotten about that. I have loved coming over and staying at your house, having trips into London together, playing some board games at home with the family and having good long catchups with each other about everything that's going on in our lives. I will never stop sharing everything with you. It has been a delight seeing what a fantastic loving and caring mum you have become! I promise that I will keep coming over regularly to visit you all, cook you extravagant dinners and be the best uncle to Sienna and Ruben, and best brother to you! **George**, I couldn't ask for a better brother-in-law: cracking painfully bad dad jokes (of which some I'll admit do make me giggle), having a beer ready in the fridge for me every time I come over, trying your hardest at Dutch blitz, but most importantly just being a supportive husband, father, son-in-law and brother-in-law. I know my family is in good hands with such a rockstar around. I'm so grateful that you have never made a problem about me coming over and staying with you all, and I really hope that someday in the near future when we get a bigger place, we can return the favour and have you regularly stay with us. **Mum**, you are such a special person in my life. I may have been a difficult teenager growing up, but damn I am so grateful for how close we are and the effort we make to see each other! Every time I am home you make each day I am there seem so valuable and that our time together should not be taken for granted or wasted. I love to see your joy when I take you out to London, partly because we go to some lovely places, but also because I see that you are happy to be with your son again; and I'm very happy to be with you. I cherish all of the memories we made on our holidays together and I still hope we will make some more on new holidays. It gives me so much pleasure when you tell me all about the social activities you get up to these days, that you have found so many different things to do that give you happiness, so never feel shy to give me a call and tell me all about them! Some of the best times I spend with you lately is just being back at home, playing some games, and feeling like I've gone a decade back in time. let's make sure we keep doing that.

Dad, it is crazy that its now over 10 years ago since I moved to The Netherlands and started this journey. I still have very clear memories of us going on a beer tour (not much has changed eh!) where we went to De Bieb, Huppel and then to Grote Markt and we discussed

the idea of me coming over to do a masters. Not long after that, I got accepted and I suddenly had to move. I'm so thankful for being able to spend so much time together over these years; Enjoying some beer festivals, our trip to Brussels, going to concerts, and the trip to Italy! Sometimes I think it's quite crazy how similar we can be in our mannerisms and our optimistic view on life and how we spend it. Thank you for giving me the opportunity to go on this journey and be able to make all of these wonderful memories with you! **Meg**, had you not thought about my future more than I did myself before moving to The Netherlands and suggest that I study here, who knows where I would be right now and what I would be doing. The fact this idea became a reality and that I have got to spend so much time with you, Dad, Louie and Juliette is something I will always be grateful for. I know you have looked out for me, supported me in my endeavours and wanted the best for me since I moved here, and I want to thank you for that! I look forward to all the times we will spend all together in the future! **Louie**, my god we spent so much time together when you were growing up. I loved the mornings when I was living at the house and you would come up the stairs, at 5 years old, and come and wake me up for breakfast (i think you were also secretly hoping you could play some games on my computer). Going skiing, playing board games, introducing you to some of the things that I enjoyed when I was young, playing lots of video games together and going out the front to play some football are just some of the most cherished memories I have with you. Whenever I was at the house, we were practically inseparable! I'm so grateful that I could be a part of your childhood at such a young age and watch you grow up into the cheeky brother you are now who just wants to spend all his time with his friends. I see a lot of my younger self in you that's for sure! **Juliette**, what an amazing sister you are! I feel like I've seen you change sooo much over the last 10 years and through that time we have become so close. I know you struggled a lot with studying in your final years of school, but I was such a proud brother to see you power through and graduate and start your adult life! I hope you realise how funny you are, because you are always making me crack up when we see each other. I love that you have always felt so comfortable sharing everything that's on your mind and everything you've been up to with me, it's always great to get a full "what's going on in Juliette's life" update. Let's promise to keep sharing things and looking out for each other!

To my entire family I want to thank you for all for always expressing your support towards me and that you look forward to the day that I will get my PhD, for that I am utterly grateful! I love you all very much.

Thomas, my first friend in The Netherlands, you have been instrumental to my integration into this country, I hope you realise that. Thanks to you I found my life in Leiden, you took me to my first ever festival and you introduced me to Minerva at a rugby event. Beyond all that, you then offered for me to move in with you when I was in desperate need of a new home. Absolutely one of the most supportive friends I have, which I'm very grateful

for. Not grateful enough to take you to my hometown in Essex which we spoke about for 10 years, but I think our trip to London was a perfect alternative. You showed me how to be a tourist in London! You are also the only friend outside of the PhD who has seen how chaotic I work in the lab, but you can keep the details to yourself during my defence. Thanks for always being there when I needed it and making me laugh with our Peaky Blinders impersonations, internet historian quotes and simple Dutch conversations!

Pieter, we have spent an insane amount time together over the last 10 years, starting with Minerva, to playing GameCube at the Pieterskerkstraat, learning how to DJ in your room, festivals, beer tochts and more. I've always really appreciated that we've both been fully open with each other about things going on in our life with no concern for judgement. Some of my favourite times have just been playing chess at the Kerkstraat blasting Pink Floyd and chatting about everything that's been going on lately. We also managed to find our ways to keep ourselves entertained during corona which was certainly necessary during that time. Thanks for always making our time together extraordinary, I definitely learnt a thing or two from you over the years on how to let your hair down. **Reinder, Lucas, Max, Pieter, Bob, Jeroen, Thijs** and **Bas,** thanks for all the amazing times whilst I lived in Leiden; nights at the tent, the skiing trips, going to Crete and all of the stories we made along the way. I barely spent any of my student time in Leiden with anyone else except you guys, and I don't regret a thing!

And now my beloved paranymphs. **Dimi**, somehow we only got to know each other in my final year of the PhD, where a quick trip to the coffee machine turned into an hour-long chat about music. Immediately after that, we were hanging out so regularly, practicing our DJing and sharing music with each other. You even came to join me and Jon in Croatia that same year which was such a fun trip. You kept on asking me the right questions when I was doubting myself, and some of the decisions I made in that first year we got to know each other, I might not have made without your encouragement. The impact you've had on my life is immeasurable and I'm so thankful that we have become so close. Whatever you need, whenever you need it, I'll be there as much as possible just as you have been for me. I'm very much looking forward to all the hiking trips, Gamescom trips, holidays, sleeping gods, video gaming, biking and festivals we will inevitably be doing in the years to come. Love you loads man!

Hannah, it's going to be difficult to try and write in moderation for your part of the acknowledgements! But before I do I want to thank some wonderful people I now know because of you. **Anna** and **Noor**, thank you both for being so kind and welcoming to me every time I came over to the Concertgebouw! The 3 of you have such a lovely friendship and I'm very grateful that I could join you for dinner at the house when me and Hannah started dating, and to DTRH with the rest of the group. You're always welcome at ours for your weekly meet up, and I'll happily cook a nice dinner and join you sometimes! **Hans**,

Mirella, and **Thijs**, you welcomed me into the family immediately and have been so supportive of me and Hannah. I love to see how close the 4 of you are and being a part of that is wonderful. **Hans**, joining the VJTV for a few hikes now has been a lot of fun, and I'm very excited to plan the England hike with you! Also seeing Nick Cave with Hannah and Thijs was a really special day. **Mirella**, it is such a joy to have a good chat with you, hearing your funny stories and what movies I need to go see. I love to see you in your element when you're in the garden at home! Thank you both for all the help you have given me and Hannah with the house, those weekends working there together were very special and I hope that I can return the favour to you all when you need it! **Thijs**, you're such an easy guy to talk to and have really enjoyed chatting with you about Magic, League, WoW and music I used to listen to when I was younger. It's also really nice that I joined you and your friend group a few times for drinks, playing pool, or helping you move to your new apartment, which meant i got to know a bit more about your life and who you spend your time with. We definitely should go and play some more pool! I had such a great time going on holiday to Switzerland with you all, and I'm very much looking forward to everything we will do together in the years to come.

Hannah, you are the ultimate support in my life, not only for helping me get the PhD done but also in many other ways, for which I cannot begin to describe how grateful I am. You so quickly became my best friend and the person I trust the most in my life, and because of that we have had some crazy years together. I have never met someone that I can so easily have endless conversations with and be 100% unapologetically myself. In fact, spending time with you is so enjoyable that to get this thesis finalised it took for you to go on 2 holidays so that I wouldn't find myself being distracted by just hanging out with you at home. Thank you for accepting my chaoticness and even telling me that it is one of the things you love about me! luckily, we are quite similar in that regard, and it makes for wonderfully unexpected situations and experiences together. Our holiday to the Balkans was the perfect holiday, with so many hikes and going on adventures and discovering new cities! But I also love that we plan so many little weekend trips together and find so many opportunities to have fun with each other. I can never get enough of you! I know you are always going to look out for me and support me in everything I do, and I will absolutely do the same for you. Our future is going to be amazing! Love you so much Hannah!

Everyone in these acknowledgements have helped me in one way or another to get me to where I am today. Having them in my life means the world to me.

About the Author



Karl Jorgen Harber was born in Romford, Essex, in the United Kingdom on the 22nd of June 1993. He grew up in a small village called Doddinghurst until he graduated from high school in 2011 and moved to Nottingham to do his BSc in Biomedical Sciences at Nottingham Trent University.

Following his graduation, he moved to The Netherlands to do an MSc in Biomedical Research at Leiden University, where his interest in immunology and research exponentially grew. He did 3 internships, all within the LUMC, one in the department of Paediatrics researching the effect of anti-thymocyte globulin serotherapy in children after stem cell transplantation, a second in the department of Haematology investigating HLA-class 1 restricted neoantigens in acute myeloid leukaemia, and a final one in the department of Infectious Diseases looking into the antimicrobial effects of tyrothricin on human skin. Having spent much of his master's degree in the hospital he knew he wanted to continue doing research and therefore he looked to start a PhD.

In 2019 Karl started his PhD in the research group of Jan Van den Bossche, in the department of Molecular Cell Biology and Immunology in the Amsterdam UMC, location VUMC. He also joined the group of Menno de Winther in the Medical Biochemistry department of the Amsterdam UMC, location AMC. Karl spent 50% of his PhD at each location and was additionally supervised by Michel van Weeghel and Elga de Vries. Here he studied the immunometabolic networks involved in macrophage inflammation, particularly within atherosclerosis, which resulted in this thesis.

After his PhD, Karl joined the company Excerpta Medica in Amsterdam, now part of OHMC, working as a publications manager and medical writer. Here, he is involved in writing and publishing articles focused on clinical trials in COPD and bronchiectasis for the drugs dupilumab and itepekimab.

